The requirement and regulation of the glutamine transporter, ASCT2 in mammary gland tumorigenesis

Emma Still

University College London

and

The Francis Crick Institute

PhD Supervisor: Mariia Yuneva

A thesis submitted for the degree of

Doctor of Philosophy

University College London

November 2017

Declaration

I, Emma Still, confirm that the work presented in this thesis is my own. Where information has been derived from other sources, I confirm that this has been indicated in the thesis.

Abstract

In order to survive and proliferate within the challenging tumour microenvironment, cancer cells adapt their metabolism to meet their increased energetic and biosynthetic requirements, whilst also maintaining the redox balance. These changes in metabolism are dependent on both the genetic alterations driving tumorigenesis and the tissue of tumour origin.

The first aim of this project was to determine whether metabolic changes in mammary gland tumours are determined by the initiating genetic event. To do this, this project compared the metabolic remodelling associated with the transformation of the mammary gland by two major oncogenes involved in breast cancer, MYC and ErbB2. This analysis revealed metabolic differences between both tumours and the normal mammary gland and between the two tumour types. Having confirmed that metabolic changes in tumours are determined by the initiating genetic event, this project then wanted to determine whether these metabolic differences could be exploited to develop new therapeutic strategies against either type of tumour. One of the major differences observed between these two tumour types was the increased glutamine catabolism in MYC-induced tumours compared to ErbB2 induced tumours. This was associated with the increased expression and N-glycosylation of the glutamine transporter, ASCT2. The regulation of ASCT2 by MYC in MYC-induced tumour cells was confirmed. Knockdown of ASCT2 revealed that the transporter is required for the proliferation and survival of cells isolated from MYC-induced tumours. This suggests that ASCT2 may be a good therapeutic target against tumours with high MYC activity.

Previous work has demonstrated the difficulties in directly targeting ASCT2, due to its similarity with other amino-acid transporters. By understanding more about how ASCT2 is regulated, it is believed that more specific therapeutic strategies could be developed that indirectly target ASCT2 through one of its regulatory pathways. Thus, this study also investigated the link between the hexosamine biosynthesis pathway (HBP), glycosylation and glutamine metabolism, demonstrating that glutamine is required for the N-glycosylation of ASCT2. This confirmed that ASCT2 stability is

regulated by glutamine, suggesting that glutamine availability may alter the transporter's activity.

Impact Statement

This project compared the metabolic remodelling associated with the transformation of the mammary gland by two major oncogenes involved in breast cancer, MYC and ErbB2. This analysis revealed metabolic differences between both tumours and the normal mammary gland and between the two tumour types, confirming that metabolic changes in tumours are determined by the initiating genetic event.

This study demonstrated that mammary gland tumours induced by MYC have significantly higher glutamine catabolism than normal mammary gland tissue and tumours induced by ErbB2. This comparison identified other altered pathways in MYC and ErbB2-induced mammary gland tumours compared to the normal mammary gland, including glycolysis, glutaminolysis and amino acid synthesis, suggesting that studies into the enzymes involved in these altered metabolic pathways could reveal new therapeutic strategies against one or both tumour types.

The increased glutamine catabolism in MYC-induced tumours was associated with increased expression and N-glycosylation of the glutamine transporter, ASCT2, compared to ErbB2-induced tumours. Knockdown of ASCT2 revealed that the transporter is required for the proliferation and survival of cells isolated from MYC-induced tumours. This supports previous work in the field suggesting that ASCT2 is a good therapeutic target against tumours dependent on ASCT2 activity.

Where previous work suggested that inhibiting ASCT2 would be a good therapeutic strategy against triple negative breast cancer, this work demonstrates the requirement for ASCT2 in an ER+ tumour model, increasing the potential application of future ASCT2 inhibitors. This work confirms that MYC regulates ASCT2 expression and demonstrates the suitability of MYC as a biomarker for some ASCT2-expressing breast cancers. However, not all tumours with high expression of ASCT2 overexpress MYC and thus, other biomarkers need to be described.

Previous work demonstrates the regulation of the hexosamine biosynthesis pathway (HBP) by downstream glutamine catabolism, through the regulation of GFAT1

expression by αKG. This study investigates this link between the HBP, glycosylation and glutamine metabolism, demonstrating that glutamine concentration regulates the N-glycosylation of ASCT2. This confirms that tumours can alter their metabolic profiles to adapt to their changing tumour microenvironment.

The majority of metabolic studies currently performed take a single snapshot of the tumour at a particular stage of development. Here, I have demonstrated that bigger ErbB2-induced tumours have higher total concentrations of lactate and TCA cycle intermediates as well as higher levels of these metabolites derived from both glucose and glutamine. This suggests that the metabolic requirements of the cells in bigger tumours are different from those in smaller tumours, potentially due to the increased proliferative or metastatic abilities of the cells, or due to changes in the overall tumour composition. This should be taken into account in future *in vivo* metabolic studies, as comparisons between different tumours could be influenced by the different size and stage of the tumours. This study also provides the first evidence that the metabolism of the normal mammary gland changes at different stages of development, which may be determined by the changing metabolism of different cells composing the normal mammary gland. Again, future studies are required to determine why the metabolic profile of the mammary gland changes as it goes through each stage of development.

Acknowledgement

First and foremost, I would like to thank my supervisor, Dr. Mariia Yuneva, for giving me the opportunity to be a PhD student in her lab. Thank you for all of your help, advice and patience over the past four years.

I would also like to thank all of the past and present members of the Oncogenes and Metabolism laboratory at the Francis Crick Institute, for sharing their expert technical knowledge and continuous support. I would especially like to thank both Dr. Mariia Yuneva and Dr. Andres Mendez Lucas for performing all of the tail vein injections of the mice in this project.

I would like to thank Dr. Dimitrios Anastasiou for his useful feedback and for allowing me to use his MMTV-ErbB2 mice in this project. I would also like to thank his lab, the Cancer Metabolism laboratory at the Francis Crick Institute, for their helpful technical and scientific advice, often shared over cake and coffee.

I would like to acknowledge the members of my thesis committee, Dr. Alex Gould, Dr. Iris Salecker and Dr. Antonella Spinazzola, for their advice and support during this project.

I was very fortunate to work at the National Institute for Medical Research and the Francis Crick Institute during my PhD, which had a number of science technology platforms (STP) that I could use. I would especially like to thank Dr. James MacRae, the head of the Metabolomics STP, who gave expert metabolomics and glycosylation advice during this project and whose facility maintained the GC-MS equipment used. I would also like to thank Dr. Paul Driscoll for running my NMR samples.

I would also like to thank the Experimental Histopathology STP at the Francis Crick Institute, who prepared many of my tissue slices. I would also like to thank the High Throughput STP, headed by Dr. Mike Howell, for their generous use of the Incucyte.

I would also like to thank Professor Carlos Caldas, for kindly donating human patient-derived xenograft samples for use in this project. I would especially like to thank Dr. Alejandra Bruna and Wendy Greenwood in his laboratory, for their help with this.

I would like to end by acknowledging my family: parents, David and Janet, and siblings, Chris and Nicki, for their constant encouragement and support. If they had not encouraged my curiosity, I would never have pursued a career in science.

Finally, I would like to thank James, who has been unfailingly supportive, understanding and patient throughout this process, and who has learnt more about cancer metabolism than a dentist needs to know.

Table of Contents

Table of Figures

List of Tables

Abbreviations

^{18}F-FDG-PET	Fludeoxyglucose (^{18}F) – Positron Emission Tomography
αKG	αKetoglutarate
2DG	2-deoxyglucose
4OHT	4-hydroxytamoxifen
Akt	Ak strain transforming
Ala	Alanine
ALL	Acute Lymphoblastic Leukaemia
AMPK	5' Adenosine monophosphate-activated protein kinase
ANCOVA	Analysis of covariance
ANOVA	Analysis of Variance
AOA	Aminooxyacetate
APS	Ammonium persulfate
ASCT2	Alanine Serine Cysteine Transporter 2
Asn	Asparagine
ASNS	Asparagine Synthetase
Asp	Aspartate
ATCC	American Type Culture Collection
ATF4	Activating Transcription Factor 4
ATP	Adenosine Triphosphate
BCA	Bicinchoninic Acid Assay
BPTES	Bis-2-(5-phenylacetamido-1,3,4-thiadiazol-2-yl) ethyl sulphide
BSA	Bovine Serum Albumin
BSTFA	N,O-Bis(trimethylsilyl)trifluoroacetamide
CAFs	Cancer Associated Fibroblasts
cDNA	Complementary DNA
Cit	Citrate
CoA	Co-enzyme A
Conc	Concentration
D$_2$O	Deuterium Oxide
DAPI	4',6-Diamidino-2-Phenylindole
DESI-MS	Desorption electrospray ionization mass spectrometry

DMEM	Dulbecco's Modified Eagle's Medium
DMSO	Dimethyl sulfoxide
DNA	Deoxyribonucleic acid
DSS	4,4-dimethyl-4-silapentane-1-sulfonic acid
E1a	Adenovirus early region 1a
E2F3	E2F Transcription Factor 3
ECL	Enhanced chemiluminescence
ECM	Extra Cellular Matrix
EGF	Epithelial Growth Factor
EGFR	Epithelial Growth Factor Receptor
eIF2a	Eukaryotic Translation Initiation Factor 2A
EMT	Epithelial-Mesenchymal Transition
EpCAM	Epithelial Cell Adhesion Molecule
ER	Estrogen receptor
ER-stress	Endoplasmic Reticulum stress
ErbB2	Erythroblastosis oncogene B
ETC	Electron Transport Chain
FAD	Flavin adenine dinucleotide
FALGPA	N-(3-[2-Furyl]acryloyl)-Leu-Gly-Pro-Ala
FASN	Fatty Acid Synthase
Fum	Fumarate
GAB	Glutaminase B
GAC	Glutaminase C
GC-MS	Gas Chromatography Mass Spectrometry
GC-MSD	Gas Chromatography Mass Selective Detector
GDH	Glutamate Dehydrogenase
GFAT1/2	Glucosamine:fructose-6-phosphate aminotransferase 1/2
GlcNAc	N-Acetylglucosamine
Gls1/2	Glutaminase 1/2
Gly	Glycine
GnT	N-acetylglucosaminyltransferase

GOT1/2	Glutamate oxaloacetate transaminase (aspartate aminotransferase) 1/2
GPNA	γ-L-Glutamyl-p-nitroanilide
GPT1/2	Glutamate-pyruvate transaminase (alanine aminotransferase) 1/2
GS	Glutamine Synthetase
GTP	Guanosine triphosphate
H&E	Hematoxylin & Eosin
HBP	Hexosamine Biosynthesis Pathway
HEPES	4-(2-hydroxyethyl)-1-piperazineethanesulfonic acid
FBS	Foetal Bovine Serum
HER2	Human Epidermal Growth Factor Receptor 2
HIF	Hypoxia Inducible Factor
HK1/2	Hexokinase 1/2
HPLC	High Performance Liquid Chromatography
HRP	Horse Radish Peroxidase
Hygro	Hygromycin
IF	Immunofluorescence
IGF	Insulin-like Growth Factor
IGFR	Insulin-like Growth Factor Receptor
IgG	Immunoglobulin G
IHC	Immunohistochemical
Ile	Isoleucine
iMMEC	Immortalised Mouse Mammary Epithelial Cells
kDa	kilo-Dalton
KGA	Kidney Glutaminase
KRas	Kirsten rat sarcoma virus proto-oncogene gene
Lac	Lactate
LAT1	Large Neutral Amino Acid Transporter
LC-MS	Liquid Chromatography Mass Spectrometry
LDHA	Lactate Dehydrogenase A
Leu	Leucine
LGA	Liver Glutaminase

lncRNA	Long Non-coding RNA
Mal	Malate
MALDI	Matrix Assisted Laser Desorption/Ionisation
MAPK	Mitogen-activated protein kinase
MAX	MYC-associated factor X
MCT	Monocarboxylate Transporter
MDH	Malate Dehydrogenase
ME	Malic Enzyme
MEFs	Mouse Embryonic Fibroblasts
Met	Methionine
METABRIC	Molecular Taxonomy of Breast Cancer International Consortium
Mins	Minutes
miRNA	Micro RNA
MMEC	Mouse Mammary Epithelial Cells
MMTV	Mouse Mammary Tumour Virus Promoter
MSI	Mass Spectrometry Imaging
mTOR	Mammalian Target of Rapamycin
mTORC	Mammalian Target of Rapamycin Complex
MWCO	Molecular Weight Cut-Off
MYC	Myelocytomatosis viral oncogene
NADH	Nicotinamide adenine dinucleotide
NADPH	Nicotinamide adenine dinucleotide phosphate
NMR	Nuclear Magnetic Resonance
O-GlcNAc	O-Linked beta-N-acetylglucosamine
p53	Tumour Protein 53
P5C	Pyrroline-5-carboxylate
PAM50	Prosigna Breast Cancer Prognostic Gene Signature Assay
PAS	Periodic Acid-Schiff
PBS	Phospho-Buffered Saline
PBS-CMF	Phospho-Buffered Saline – Calcium/Magnesium Free
PBS-T	Phospho-Buffered Saline with 0.05% Tween
PCR	Polymerase Chain Reaction

PDX	Patient Derived Xenograft
Pen/Strep	Penicillin/ Streptomycin
PFA	Paraformaldehyde
PHGDH	Phosphoglycerate dehydrogenase
PI3K	Phosphoinositide 3-kinase
PKM1/2	Pyruvate Kinase Muscle Isozyme 1/2
PNGase F	Peptide :N-Glycosidase F
PPP	Pentose Phosphate Pathway
PR	Progesterone Receptor
Pro	Proline
PRPP	Phosphoribosyl pyrophosphate
PSAT	Phosphoserine aminotransferase
PTEN	Phosphatase and tensin homolog
Puro	Puromycin
PyMT	Polyoma virus Middle T
qPCR	Quantitative PCR
Ras	Rat sarcoma virus proto-oncogene gene
Rb	Retinoblastoma protein
RNA	Ribonucleic Acid
RNAi	RNA interference
RNF5	Ring Finger Protein 5
ROS	Reactive Oxygen Species
Rpm	Revolutions per minute
RT-PCR	Real Time PCR
SDS	Sodium Dodecyl Sulphate
SDS-PAGE	Sodium Dodecyl Sulphate – Polyacrylamide Gel Electrophoresis
Secs	Seconds
Ser	Serine
SGK	Serum and glucocorticoid-inducible kinase
SHMT1	Serine hydroxymethyltransferase 1
shRNA	Short Hairpin RNA
siASCT2	siRNA targeting ASCT2

siGLS1	siRNA targeting Gls1
siRNA	Small Interfering RNA
SLC	Solute Carrier Family Transporter
SNAT	Sodium-coupled Neutral Amino Acid Transporter
Src	Sarcoma protein
Succ	Succinate
TCA cycle	Tricarboxcylic Acid Cycle
TCMS	Trichloromethylsilane
TDG	Thymine DNA glycosylase
TEMED	N,N,N',N'-Tetramethylethylenediamine
TET	Ten-eleven Translocation
Thr	Threonine
TNBC	Triple Negative Breast Cancer
U.K.	United Kingdom
UDP-GlcNAc	Uridine disphosphate N-acetylglucosamine
UT	Untreated
v/v	volume/volume
Val	Valine
VEGF	Vascular Endothelial Growth Factor
WB	Western Blotting
Zeo	Zeocin

Chapter 1.   Introduction

1.1 Cancer

Cancer is defined as not one, but an array of diseases within the body caused by the uncontrolled growth of abnormal cells, with over 200 types of the disease depending of the cell type and tissue of origin. Between 2003-2014, U.K. cancer incidence rates increased by 7% (Cancer Research UK, 2017), and in 2014, 163,444 people in the U.K. died from cancer (Cancer Research UK, 2017). This makes cancer one of the most significant causes of mortality not only in the U.K. but throughout the developed world; highlighting the need for continued efforts to gain a better understanding of how cancer initiates and progresses, in order to develop improved therapeutic strategies against the disease.

The progression from a normal cell to a cancer cell is a complex multi-step process, where cells accumulate several genetic and epigenetic changes, altering their dependencies on particular genes and pathways. When tumour cells become dependent on a single oncogene, this is known as oncogene-addiction (Weinstein and Joe, 2006), and many current therapeutic strategies aim to exploit this addiction by targeting that particular gene or pathway. However, in order to fully develop into a tumour, cells must simultaneously sustain proliferative signals and overcome replicative immortality whilst evading growth suppressors and resisting cell death (Weinstein and Joe, 2006). Because of the complex combination of factors required for tumour survival, it is becoming increasingly difficult to rationalise this complex neoplastic disease, which differs based on the cell and tissue of origin, as well as the complex mutational background of the tumour.

1.1.1 Breast Cancer

Breast cancer is the second most common cancer in the world, the fifth most common cause of cancer death and the leading cause of cancer deaths in women (Hutchinson, 2010). In 2015, breast cancer was the most common cancer in the U.K. accounting for

15% of all new cancer cases (Cancer Research UK, 2017). However, the prognosis for early stage breast cancer is positive, with a 99% and 90% survival rate after 5 years for those diagnosed with stage 1 or 2 breast cancer respectively, in the U.K. (Cancer Research UK, 2017). This is due to improved early detection and drastic surgical approaches such as mastectomies that are effective before the disease has spread beyond the breast. However, the prognosis for the latter stages of the disease decreases rapidly, to a 60% 5-year survival rate for those with stage 3 disease and a 15% 5-year survival rate for those with stage 4 disease (Cancer Research UK, 2017). Once the disease has spread beyond the breast and lymph nodes to other organs, it can no longer be cured and current therapies can only control disease progression. Thus, while work to improve the early detection of the disease is vital, so that early stage breast cancer can be successfully cured through surgical intervention, there is still a need to develop new therapeutic strategies against breast cancer to be able to effectively treat late-stage disease.

Breast cancer is currently divided into multiple subtypes based on the distinct morphologies and clinical implications of the different tumours. These include the luminal A subtype, which is hormone receptor positive (ER+/PR+) and HER2 negative; the luminal B subtype which is hormone receptor positive (ER+/PR+) and can be either HER2 positive or negative; the triple negative subtype, which is hormone receptor and HER2 negative, the HER2-enriched subtype, which is hormone receptor negative and HER2 positive and the normal-like subtype, which is hormone receptor positive and HER2 negative.

Accurate grouping of breast cancer into clinically relevant subtypes is important for therapeutic decision making. Currently, traditional variables, such as tumour size, tumour grade and nodal involvement are the foundations of patient prognosis and management decisions. These are used alongside classical immunohistochemical (IHC) markers, such as the estrogen receptor (ER), the progesterone receptor (PR) and the HER2 receptor when deciding therapeutic strategies. However, the development of high-throughput platforms for gene expression analysis has revealed complex molecular characteristics that can change how breast cancer patients are stratified and treated.

Predictive biomarkers, such as the expression of the ER, PR and HER2 receptor have proven clinically useful as many therapeutic strategies target the tumour's dependence on the downstream signalling pathways from these receptors. For instance, anti-estrogen therapies, including tamoxifen, fulvestrant and anastrozole are effective against ER+ tumours, as they block downstream signalling from the ER that promotes cell proliferation. Similarly, HER2 overexpressing tumours respond well to trastuzumab (Herceptin), which is a monoclonal antibody against HER2. Thus, traditional breast cancer classification based on the expression of these receptors has been useful at dictating therapeutic strategy. However, the incidence of resistance against both anti-estrogen and trastuzumab therapies is increasing (Clarke et al., 2003; Ahmad et al., 2014), with up to 70% of women becoming resistant to trastuzumab within a year of starting the treatment (Pohlmann et al., 2009).

The triple-negative subtype of breast cancer (TNBC) is somewhat poorly defined by the absence of ER, PR and HER2, rather than the presence of a particular driving or targetable feature. These tumours, which make up roughly 15% of all breast cancer cases (Sharma, 2016), have the worst prognosis and rely on traditional chemotherapy and radiotherapy if surgery is no longer a viable treatment option.

With the development of new techniques, such as microarrays, which perform gene expression profiling, distinctive molecular portraits of breast cancer have been defined. In the first study of its kind, Sorlie et al. (2003) used 456 cDNA clones to classify 5 breast cancer subtypes with distinct clinical outcomes (Sorlie et al., 2003). These subtypes map to the IHC-defined subtypes based on their molecular profiles. Likewise, the PAM50 gene classifier defines tumour subtypes based on the expression of 50 genes related to hormone receptors, proliferation genes, and myoepithelial and basal markers (Parker et al., 2009). Further to this, increasing information is being gained regarding miRNA, lncRNA and epigenetic changes in breast cancer to help describe these molecular subtypes further. The identification of the particular pathways that are altered in different subtypes could allow the response to pathway-targeted therapies to be predicted. Gatza et al. (2010) described 17 subgroups within the 5 classical subtypes of

breast cancer, which differentiate tumours with similar clinical and biological properties based on their altered pathway activity (Gatza et al., 2010). By improving the way tumours are currently classified, more specific biomarkers against breast cancer can be described and new therapeutic targets could be identified. Likewise, the prediction of patient response to particular therapies will improve.

Current therapeutic approaches have expanded beyond these classical IHC-defined subtypes, and increasing research is being done to identify and target specific oncogenes or tumour suppressor genes and their downstream signalling pathways. A number of oncogenes have been shown to regulate the enzymes involved in cell metabolism, supporting tumour development as the tumour's metabolic needs change. Thus, current work aims to identify metabolic dependencies and weaknesses of different tumours, in order to find new therapeutic targets.

1.1.1.1 The MYC proto-oncogene and Breast Cancer

The proto-oncogene, MYC, is a transcription factor that dimerises with MAX to bind DNA and regulate gene expression (Amati and Land, 1994). MYC regulates many genes involved in cell growth, proliferation, metabolism, differentiation and apoptosis. MYC is deregulated in many types of cancer, either through gene amplification, altered transcriptional regulation, and mRNA and protein stabilisation, causing the loss of tumour suppressors and activation of tumour-promoting pathways (Camarda et al., 2017). In breast cancer, not only can the MYC oncogene itself be deregulated, but its activation can be altered by deregulated upstream signalling pathways. For instance, MYC is downstream of Ras, Wnt, Notch, ERα and HER2, all of which are frequently deregulated in breast cancer (Liao and Dickson, 2000).

MYC is amplified in approximately 15% of breast cancers and is associated with poor clinical outcome (Deming et al., 2000). MYC expression, phosphorylation and downstream gene activation are elevated in human triple negative breast cancer patients compared to receptor positive tumours (Horiuchi et al., 2012). However, MYC is also a downstream target of ERα, and its overexpression has been implicated in hormone

independence in ER+ breast cancer cells and tumour models (Wang et al., 2011; Shajahan-Haq et al., 2014; Chen et al., 2015). Likewise, MYC overexpression in human tumours has been linked to resistance to endocrine therapies (Miller et al., 2011). A recent study using the METABRIC breast cancer cohort evaluated the correlation between MYC and other genes within the different subtypes of breast cancer, and found that MYC downstream signalling changed dependent on the tumour subtype (Green et al., 2016).

The triple negative subtype of breast cancer is associated with the most aggressive form of the disease (Cancer Genome Atlas, 2012) and the worst prognosis, as currently, there are no targeted therapeutic strategies against this form of the disease. As MYC overexpression is frequently observed in breast cancer (Deming et al., 2000), and is associated with endocrine therapy resistant ER+ breast cancer (Wang et al., 2011; Shajahan-Haq et al., 2014; Chen et al., 2015) and triple negative breast cancer (Horiuchi et al., 2012), both of which currently lack specific therapeutic strategies, studying the role of MYC is these tumours might enable new therapeutic targets downstream of MYC to be identified.

1.1.1.2   The ErbB2 proto-oncogene and Breast Cancer

The receptor tyrosine kinase ErbB2, also known as Neu or HER2, is an epidermal growth factor receptor that is frequently amplified or overexpressed in cancer, specifically in the HER2-enriched and luminal B subtypes of the disease. It is a member of the ErbB family of plasma membrane bound receptors, which can form homo- or heterodimers as well as higher-order oligomers, upon activation by growth factor ligands. After ligand binding and dimerization, the receptors regulate a series of downstream signalling pathways, which control cell cycle progression, cell proliferation and cell survival, as summarised in Figure 1.1. The downstream signalling effects of ErbB2 are complex dependent on the differential effects of the different ErbB2-containing heterodimers. For example, EGFR/ErbB2 heterodimers preferentially stimulate the MAPK pathway, whereas the ErbB2/ErbB3 heterodimer activates both the MAPK and PI3K/AKT pathway. One of the major effects of increased ErbB2 signalling,

is the activation of the oncogene, Src, a non-receptor tyrosine kinase that activates downstream pathways including the MAP kinase pathway. This pathway can regulate several transcription factors, as well as activating genes that induce cell cycle entry, such as Cdk4 and Cdk6. Downstream ErbB2 signalling can also activate the PI3K signalling pathway, which is also important in regulating the cell cycle, and thus, is directly related to cell proliferation.
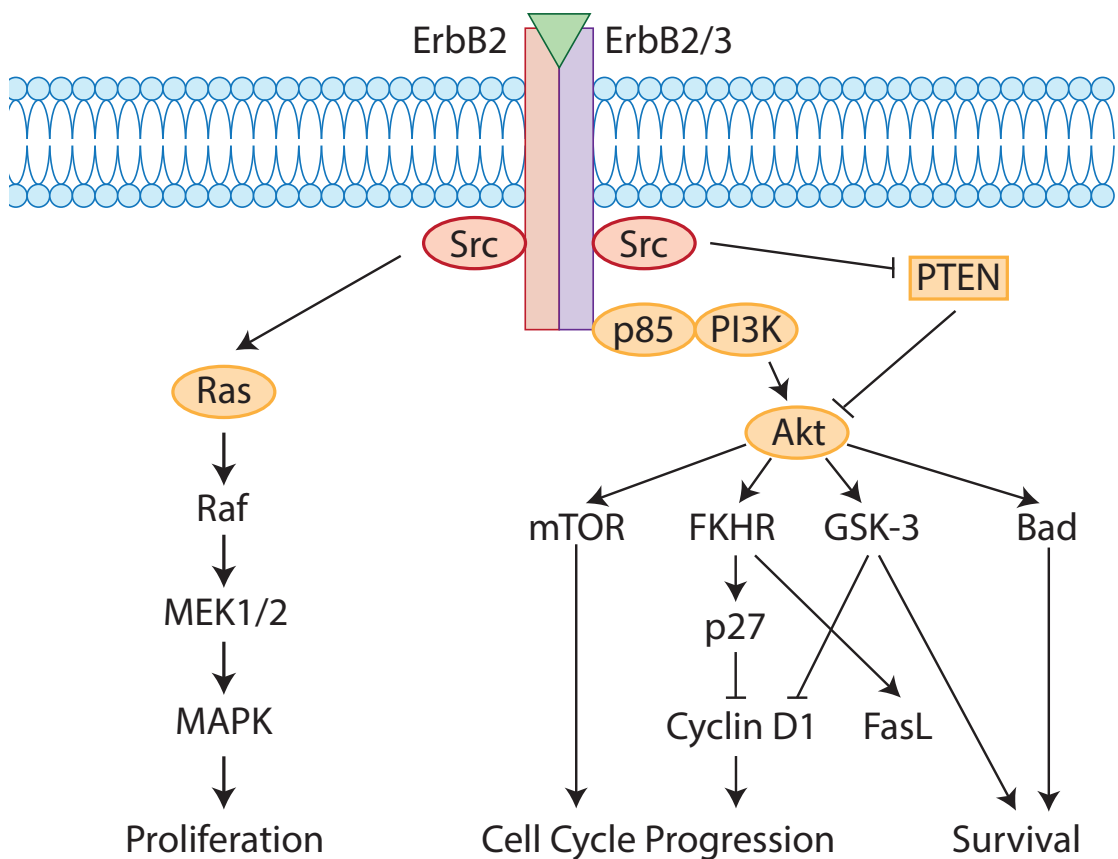
Figure 1-1 Downstream ErbB2 signalling

ErbB2 forms homo- and hetero-dimers at the plasma membrane to activate downstream signalling pathways that regulate cellular proliferation, cell cycle progression and cell survival.

ErbB2 is overexpressed or amplified in 20-30% of primary human breast cancer, and correlates to poor patient outcome (Slamon et al., 1989). Traditionally, ErbB2-deregulated tumours, known as HER2+ tumours, are treated with the monoclonal antibody, Trastuzumab (Herceptin) (Moja et al., 2012). Trastuzumab has multiple

mechanisms of action, where is can attract immune cells to tumour sites to induce antibody-dependent cellular cytotoxicity, whilst also interfering with the MAPK and PI3K/Akt pathways, causing cell cycle arrest and suppressing growth and proliferation (Vu and Claret, 2012). It also interferes with the dimerization of ErbB2, preventing its downstream activation (Vu and Claret, 2012). Another monoclonal antibody, Pertuzumab, which inhibits ErbB2 and ErbB3 dimerisation is also used alongside Trastuzumab (Squires et al., 2017). Unfortunately, most patients treated with Trastuzumab become resistant to the drug within a year (Vogel et al., 2002; Pohlmann et al., 2009), causing further disease progression. Mechanisms of Trastuzumab resistance include signalling from other ErbB receptors or other receptors such as the IGF receptor, activation of other oncogenes such as c-MET and src, activation of PI3k/Akt/mTOR, loss of PTEN or increased VEGF expression (Luque-Cabal et al., 2016). Due to the high prevalence of HER2 in breast cancer, combined with the difficulty in long-term treatment of these tumours, there is still a considerable need to find new therapeutic strategies against HER2+ breast cancer.

1.1.1.3   ErbB2 and MYC co-expression in Breast Cancer

ErbB2 downstream signalling has been shown to increase MYC translation through activation of the PI3K/Akt/mTOR pathway (Galmozzi et al., 2004). MYC and ErbB2 co-expression has been shown in many human tumour samples (Park et al., 2005) and is associated with increased cell proliferation. Similarly, co-expression of both MYC and ErbB2 in breast cancer cells led to the acquisition of a self-renewing phenotype due to the increased expression of lipoprotein lipase (Nair et al., 2014). The co-expression of both oncogenes is associated with a more aggressive clinical phenotype (Nair et al., 2014). However, fewer than half of HER2+ breast tumours also have MYC deregulation (Xu et al., 2010).

1.2   Cancer Metabolism

Cellular metabolism refers to all of the life-sustaining chemical reactions that occur within cells. In normal cells, these pathways provide the energy and biosynthetic

intermediates required for growth and proliferation. Cell metabolism demonstrates a high level of plasticity, adapting to changes in the microenvironment and the metabolic demands of the cell as tissues undergo periods of growth, development, damage and repair.

In order to sustain the increased proliferation associated with tumorigenesis, cancer cells simultaneously increase their energy production as well as the production of biosynthetic intermediates. Altered metabolic pathways are commonly observed in almost all tumour types, resulting in different dependencies for specific nutrients or enzymes. The development of stable isotope labelling coupled to mass spectrometry and NMR detection techniques for the study of metabolic pathways *in vitro* and *in vivo* has greatly advanced our understanding of the metabolic changes that occur in tumours (Boros et al., 2003; Miccheli et al., 2006; Fan et al., 2009).

Although tumour metabolism has long been considered a promising discipline in the development of cancer therapeutics, the majority of work has focused on changes in glucose metabolism, specifically the increased conversion of glucose to lactate observed in many tumours (Warburg et al., 1927). The observation that mammalian cells rely on both glucose and glutamine (Reitzer et al., 1978; Moreadith and Lehninger, 1984; Board et al., 1990; Yuneva et al., 2007) shifted the focus to the more diverse range of pathways that are rewired in many tumours. More recently, tumours have also been demonstrated to utilise lactate and acetate as a carbon source (Mashimo et al., 2014; Hui et al., 2017).

However, the majority of work studying tumour metabolism has utilised *in vitro* cell systems or *in vivo* mouse models of the disease, which have been shown to perturb the metabolic phenotype of the tumour cells being studied (Davidson et al., 2016). A recent study by Sellers et al. performed stable isotope labelling in human patients, confirming that these tumours utilise glucose *in situ* (Sellers et al., 2015). Similar studies using alternative carbon sources in patients are yet to be performed in order to confirm the utilisation of other carbon sources such as glutamine and acetate *in situ.* However, radioactive probes, such as ^{18}F-fluoroglutamine have been used in patients to confirm

that specific tumours consume more glutamine that their normal tissue counterparts (Hassanein et al., 2016), which confirms many of the results observed in other models, that specific tumours consume more glutamine.

1.2.1   Glucose Metabolism

Glucose is a key component of cellular metabolism, allowing for energy to be harnessed in the form of ATP through the oxidation of its carbon bonds. This can occur during either glycolysis or mitochondrial respiration. Glucose uptake coupled to lactate production dramatically increases in many developing and proliferating cells, including tumour cells (Warburg et al., 1927; Milman and Yurowitzki, 1967; Hommes and Wilmink, 1968; Wang et al., 1976). The conversion of glucose to lactate, which occurs even in the presence of oxygen, is known as aerobic glycolysis. Using aerobic glycolysis to produce ATP is inefficient compared to ATP production through mitochondrial respiration. However, computational modelling combined with metabolomics data revealed that the rate of glucose catabolism increases so that the amount of ATP produced in a similar time is comparable by either pathway (Shestov et al., 2014).

Glucose is not just required for the production of ATP. Several anabolic pathways that are upregulated in tumours, require glycolytic intermediates. These include the pentose phosphate pathway (PPP), which generates pentose phosphates for ribonucleotide synthesis and NADPH; the hexosamine biosynthesis pathway, which is required for the glycosylation of proteins; the serine biosynthesis pathway, which generates amino acids; and is followed by the one-carbon metabolism cycle, which generates NADPH required for purine and glutathione synthesis. Glycolytic intermediates are also required for lipid biosynthesis and the production of acetyl-CoA, which is required for protein acetylation. (Figure 1.2).

Increased glucose uptake coupled to lactate production is commonly observed in many tumour cells (Warburg, 1925; Warburg et al., 1927; Milman and Yurowitzki, 1967; Hommes and Wilmink, 1968; Wang et al., 1976). As well as producing ATP through

aerobic glycolysis, lactate production also produces NADH, a co-factor required for the production of nucleotides and lipids. NADH is also involved in protection from reactive oxygen species (ROS) through the regeneration of glutathione. Thus, increased aerobic glycolysis can also help supply the increased need for NADH. Similarly, it is believed that the acidification of the tumour microenvironment through the excretion of lactate is beneficial for tumour cells. This has been shown to aid tumour invasion (Kato et al., 2007) and promote angiogenesis (Fukumura et al., 2001; Xu et al., 2002) as well as affecting infiltrating macrophages (Colegio et al., 2014). However, changes in glucose metabolism are frequently an early event during tumorigenesis occurring a long time before the tumour becomes invasive (Ying et al., 2012; Shain et al., 2015). As metabolism has a high level of plasticity, it is likely that the observed changes in glucose metabolism in tumours are required for different processes at different times to meet the changing needs of the tumour as it develops.
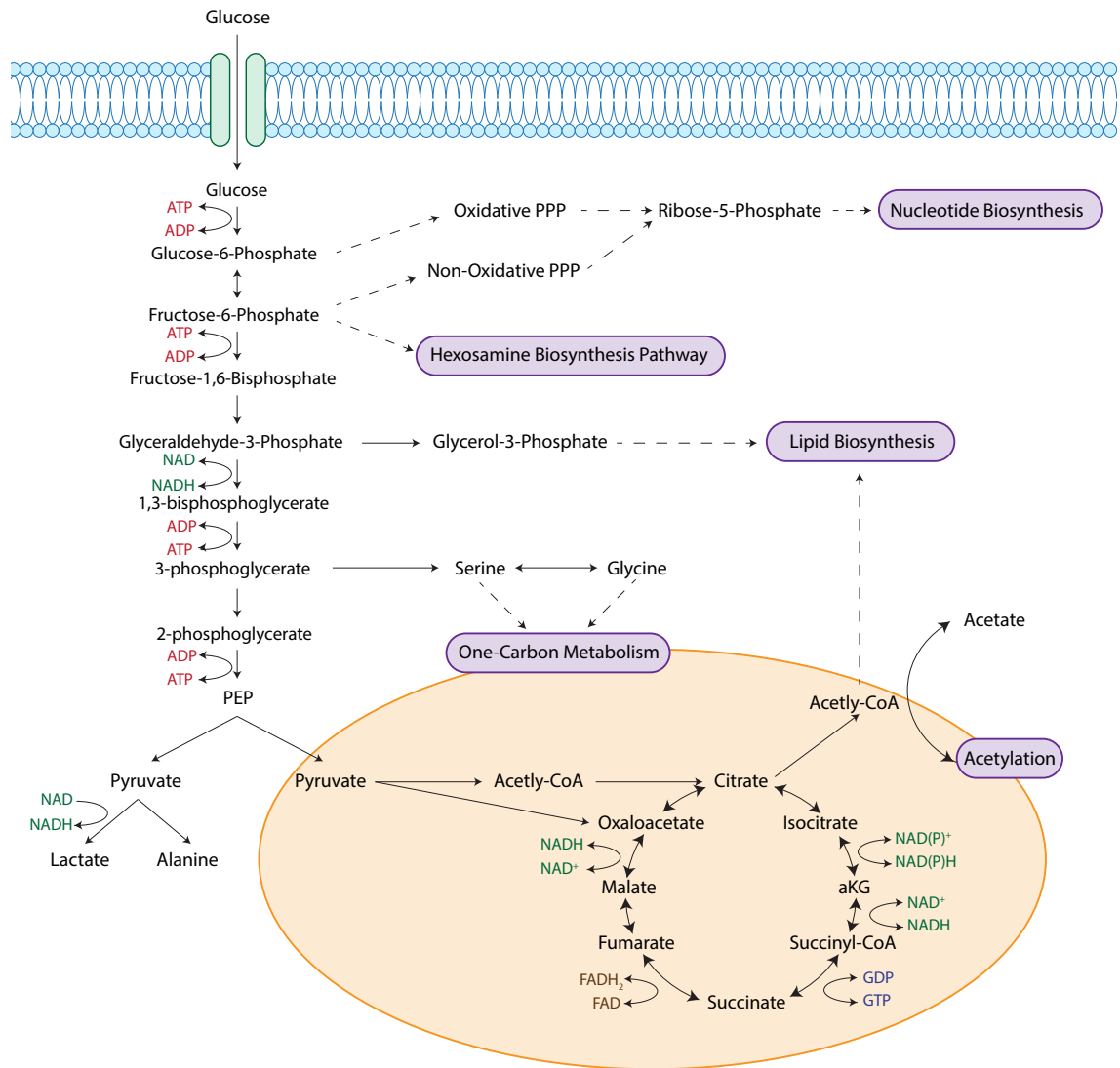
Figure 1-2 Glucose Catabolism

Glucose catabolism supports nucleotide biosynthesis, the hexosamine biosynthesis pathway, lipid biosynthesis, one carbon metabolism and protein acetylation. It also replenishes NAD(P)H to maintain the redox balance. Glucose can produce energy in the form of ATP through glycolysis and aerobic respiration in the mitochondria (orange oval), where electrons from the NAD(P)H and $FADH_2$ produced in the TCA cycle, pass through the Electron Transport Chain (ETC) to produce the electrochemical proton gradient required for ATP synthesis.

1.2.2   Glutamine Metabolism

Glutamine belongs to a unique class of amino acids that are thought of as 'conditionally essential.' Under normal conditions, glutamine is non-essential, as it can be synthesised through the metabolism of other amino acids. However, under certain catabolically stressed conditions such as sepsis, glutamine consumption rapidly increases (Noguchi et al., 1996). Cells that are especially dependent on glutamine, such as those in the intestinal mucosa, rapidly undergo necrosis during glutamine deprivation (Lacey and Wilmore, 1990). Similarly, specific cancer and oncogene-transformed cells are dependent on glutamine and undergo apoptosis during glutamine deprivation (Petronini et al., 1996; Yuneva et al., 2007; Weinberg et al., 2010). In these rapidly dividing cells, glutamine is rapidly consumed and acts as a source for energy production, a nitrogen and carbon source for biomass accumulation, as well as being important in wider cell signalling.

Glutamine enters into cells via a number of different glutamine transporters. It is then catabolised into glutamate via a glutaminase enzyme (Figure 1.3). There are two different tissue-specific glutaminase genes in mammals: kidney-type glutaminase (Gls1) and liver-type glutaminase (Gls2). Gls1 is more widely expressed in normal tissues than Gls2, although some co-expression of the two isoforms occurs in the brain (Olalla et al., 2002) and in cancer cells (Perez-Gomez et al., 2005). There are two isoforms of Gls1 generated through alternative splicing: KGA and GAC, which share exons 1-14 and have unique C-terminals (Elgadi et al., 1999). Likewise, there are two isoforms of Gls2, which have different N-terminals, producing a long and a short form, known as GAB and LGA respectively (Martin-Rufian et al., 2012). Changes in the expression of glutaminase isoforms have been shown in various cancer types, dependant on their tissue specificity and oncogenic driver (Wang et al., 2010; Yuneva et al., 2012; Qie et al., 2014; Xiao et al., 2015). Expression of the more active isoform of Gls1, GAC, is more frequently observed in several cancer types, suggesting that alternative splicing may play a role in the increased glutaminolytic flux seen in some cancers (Van Den Heuvel et al., 2012).

Glutamine synthetase (GS) performs the reverse reaction to glutaminase, producing glutamine from glutamate and ammonia. Recent studies have shown that GS activity supports proliferation in transformed and cancer cell lines, as increased glutamine production enhances nucleotide synthesis and amino acid transport (Bott et al., 2015). While co-expression of both glutaminase and GS has been demonstrated (Svenneby and Torgner, 1987), it is unknown how both glutamine synthesis and glutamine catabolism are co-ordinated within cells. Likewise, it remains to be elucidated why newly synthesised glutamine is preferred over an ample exogenous supply in some tumours.

1.2.2.1 Glutamine as a carbon source

During glutaminolysis, glutamine is catabolised losing both its amino and amido nitrogen groups to produce αKetoglutarate (αKG) from its carbon backbone (Figure 1.3). This αKG enters into the TCA cycle where it can be metabolised by oxidative decarboxylation, which is required for energy production. Alternatively, this αKG can be catabolised by reductive carboxylation, where αKG is converted to citrate through the reverse direction of the TCA cycle, to support lipogenesis, which is required for cell membranes and cell signalling. This pathway is favoured in some cancer cells, and is promoted when cells experience hypoxia (Le et al., 2012; Sun and Denko, 2014) or when mitochondrial respiration is impaired (Fendt et al., 2013). These forward and reverse TCA cycle fluxes are not necessarily exclusive, which is frequently seen in cancer (Mcguirk et al., 2013). Although the direction of these fluxes is determined by the ratio of αKG to citrate (Fendt et al., 2013), the upstream determinants of this ratio are yet to be fully described. Thus, increased glutamine catabolism in cancer cells is an important carbon source for energy production through the TCA cycle. Glutamine also donates carbons for amino acid synthesis, where intermediates downstream of glutamine catabolism, such as oxaloacetate and pyruvate, are converted to amino acids by the addition of an amino group (Figure 1.3).

1.2.2.2   Glutamine as a nitrogen source

Glutamine is also an important source of nitrogen in cells, donating both its amino and amido nitrogen for the production of amino acids. The conversion of glutamate to αKG can be performed through a number of enzymes. When glutamate dehydrogenase (GDH) catalyses this reaction, the amino nitrogen is released in the form of ammonia. However, when this reaction is performed by an aminotransferase, the amino nitrogen is passed onto a carbon backbone to produce amino acids, including serine, alanine and aspartate (Figure 1.3). A recent study by Coloff et al. (2016) demonstrated differences in glutamate metabolism between proliferating and quiescent mammary gland cells (Coloff et al., 2016). While quiescent cells favoured glutamate dehydrogenase (GDH) activity to convert glutamate to αKG, in order to fuel the TCA cycle, proliferating cells shifted from GDH activity to transaminase activity to simultaneously synthesise non-essential amino acids, such as serine, aspartate and alanine, while also producing αKG for the TCA cycle.

The alanine aminotransferases (cytosolic GPT1 and mitochondrial GPT2) catalyse the production of αKG and alanine from the transfer of the amino nitrogen from glutamate onto pyruvate. In the liver, this reaction plays an important role in the glucose-alanine cycle required to support gluconeogenesis. In colon cancer cells, GPT2 was shown to co-ordinate increased pyruvate production with increased glutamine catabolism, to feed carbons from glutamine into the TCA cycle (Smith et al., 2016).

Glutamine can donate both carbons and the amino nitrogen for the production of aspartate through the cytosolic aspartate aminotransferase, GOT1. After αKG enters into the TCA cycle, it can be metabolised into oxaloacetate, which receives the amino nitrogen from glutamate to produce aspartate. Aspartate is required for purine and pyrimidine synthesis, as well as for protein synthesis. Recently, aspartate production was shown to be required for cell proliferation in the presence of electron transport chain (ETC) inhibition (Birsoy et al., 2015). GOT1 operates with GOT2, the mitochondrial isoform, in the Malate-Aspartate shuttle, which is required to shuttle electrons into the mitochondria for the ETC and the restoration of NAD+ pools required for glycolytic flux (Son et al., 2013).

Glutamine can also donate its amido nitrogen to convert aspartate into asparagine, in a reaction catalysed by asparagine synthetase (ASNS). Asparagine is required for protein synthesis. Recently, it was shown in liposarcoma and breast cancer cells that intracellular asparagine levels regulate the uptake of other amino acids, enabling it to play an exchange factor role, and consequently regulate mTOR activity and protein synthesis (Krall et al., 2016).

The *de novo* synthesis of the amino acid serine also requires the amino-nitrogen from glutamine, which is transferred onto 3-phosphohydroxypyruvate by the aminotransferase, PSAT. Serine is required for the synthesis of several other metabolites, including glycine, cysteine, folate, sphingolipids, purines and pyrimidines. Serine is a major donor of one-carbon units to the folate cycle, through one-carbon metabolism. It can also act as an allosteric activator of several different enzymes, such as pyruvate kinase isoform 2 (PKM2) (Chaneton et al., 2012). In breast cancer cell lines, half of the αKG feeding into the TCA cycle was derived from PSAT activity, showing that serine biosynthesis can also supplement energy production in tumour cells (Possemato et al., 2011).

Both carbon and nitrogen from glutamate can be used to produce proline. Proline is a non-essential amino acid required for protein biosynthesis, especially the production of the extracellular matrix protein, collagen. Proline production also provides a mechanism for redox homeostasis, through the transfer of reducing potential from NADH or NADPH to pyrroline-5-carboxylate (P5C).

As well as transferring nitrogen to amino acids, glutamine also donates nitrogen for the *de novo* synthesis of purines and pyrimidines, the nucleotide bases of DNA and RNA. In the first step of purine and pyrimidine synthesis, the amido group of glutamine is used to activate the ribose backbone using PRPP amidotransferase during purine synthesis, and to produce carbamoyl phosphate in the first step of pyrimidine metabolism. Likewise, the amino-nitrogen is required to produce nucleotide precursors for the synthesis of both purines and pyrimidines.

1.2.2.3   The Hexosamine Biosynthesis Pathway

Both glucose and glutamine are required for the hexosamine biosynthesis pathway (HBP), where glutamine donates an amino group to the glycolytic intermediate, glucose-6-phosphate, in a reaction catalysed by GFAT1/2. This pathway produces Uridine diphosphate N-acetylglucosamine (UDP-GlcNAc), the precursor required for both O-linked and N-linked glycosylation, which is required for the stability and function of many proteins. Deregulated glycosylation is a common feature of many tumour types (Stowell et al., 2015), occurring at both early and late stages of tumour progression. It can result from changes in O- and N-glycan core structure or changes in glycosyltransferase expression. Aberrant glycosylation has been shown to affect several oncogenes during tumorigenesis. For instance, increased glycan branching of EGFR has been shown to increase its residency at the plasma membrane, thus, increasing its period of activity to promote cell growth (Lajoie et al., 2007).

Changes in HBP are associated with more aggressive disease states in cancer (Yang et al., 2016; Li et al., 2017). For example, increased expression of the rate-limiting enzyme, GFAT1, predicts poor prognosis in both hepatocellular carcinoma and pancreatic cancer patients (Yang et al., 2016; Li et al., 2017). Whereas loss of GFAT1 in gastric cancer promotes EMT and predicts more advance disease staging (Duan et al., 2016). Increased glucose uptake during EMT was shown to be utilised for increased HBP, opposed to increased glycolysis and pentose phosphate pathway (PPP) activity. The increased O-GlcNAc produced resulted in aberrant cell surface glycosylation (Lucena et al., 2016).

While glucose deprivation has been shown to decrease UDP-GlcNAc production via the HBP in cancer cell lines, the same was not observed with glutamine deprivation. Instead increasing glutamine concentrations were shown to increase HBP activity (Abdel Rahman et al., 2013). A study by Wellen et al. (2010), demonstrated that supplementing glucose-deprived media with GlcNAc preserved interleukin-3 receptor glycosylation and localisation at the plasma membrane and rescued cell growth in B lymphoma cells (Wellen et al., 2010). This was dependent on glutamine uptake and catabolism. Thus, the HBP links altered tumour metabolism with aberrant glycosylation, providing a

mechanism for cancer cells to respond to changes in the microenvironment and their
metabolic requirements.
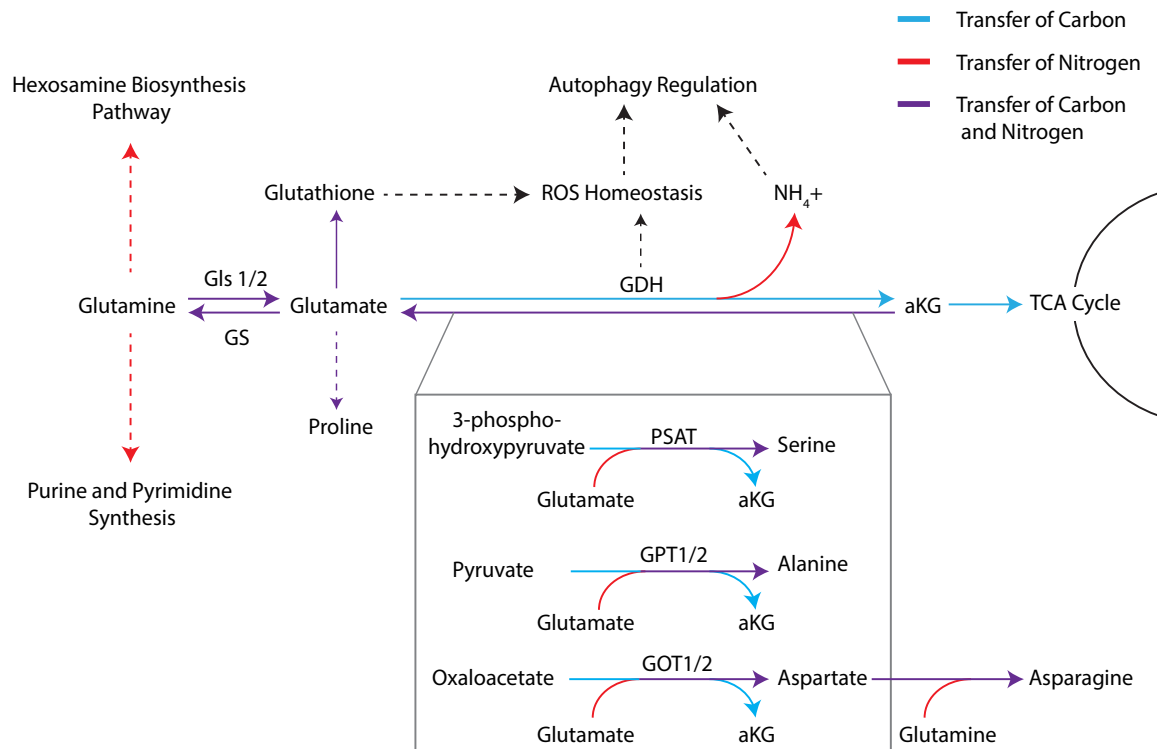
Figure 1-3 Glutamine acts as both a carbon and nitrogen donor

By donating carbon to αKG to fuel the TCA cycle, glutamine supports energy
production through mitochondrial respiration. Glutamine donates both carbon and
nitrogen for amino acid synthesis, and donates its amino nitrogen for purine and
pyrimidine synthesis and the hexosamine biosynthesis pathway. Glutamine also helps
maintain the redox balance and regulate autophagy.
Gls 1/2 - Glutaminase 1 and 2, GS – Glutamine synthetase, GDH – Glutamate
Dehydrogenase, αKG – α-Ketoglutarate, PSAT – Phosphoserine aminotransferase, GPT
1/2 – Alanine aminotransferase 1 and 2, GOT 1/2 – Glutamate oxaloacetate
transaminase 1 and 2, ROS – Reactive Oxygen Species,
Image adapted from Still and Yuneva, 2017.

1.2.2.4   Other uses of glutamine

Glutamine metabolism has also been shown to regulate ROS homeostasis and effect

wider cell signalling through mTORC activation and by regulating epigenetic

mechanisms. Elevated levels of reactive oxygen species (ROS) have been detected in

almost all tumours (Liou and Storz, 2010), causing oxidative stress, which can damage

cellular biomolecules, including DNA, proteins and lipids. Increased glutamine

catabolism into the TCA cycle could increase ROS levels, by fuelling the ETC, which can leak electrons to generate superoxide. However, there are a number of ways that glutamine can help regulate ROS levels. For instance, glutamine is required for glutathione synthesis, which neutralises peroxide free radicals by acting as an electron donor. Glutamine metabolism also aids the production of NADPH and NADH through GDH and malic enzyme 1 respectively (Son et al., 2013; Jin et al., 2015).

Glutamine metabolism has also been shown to regulate mTOR activity, and thus, regulates cell growth, proliferation, motility and survival. mTOR can form two functionally distinct complexes, mTORC1 and mTORC2, where both complexes are regulated by changes in glutamine metabolism. When glutamine concentrations are low during amino acid starvation, mTORC1 upregulates autophagy. Glutamine in combination with leucine has been shown to activate mTORC1 through increased glutaminolysis and αKG production (Duran et al., 2012). mTORC2 has also been shown to be regulated by the changing levels of glutamine catabolites (Moloughney et al., 2016). Conversely, mTORC1 signalling also regulates glutamine metabolism by promoting glutamine entry into the TCA cycle by GDH (Csibi et al., 2013), and through the activation of MYC translation (Csibi et al., 2014). Likewise, mTORC2 also regulates glutamine metabolism by regulating the expression of the amino acid transporters, SNAT2 and LAT1 (Boehmer et al., 2003; Rosario et al., 2013) and the oncogenes MYC (Masui et al., 2013) and Akt, which in turn regulate the expression of several genes involved in glutamine metabolism (Gottlob et al., 2001; Wise et al., 2008; Gao et al., 2009; Hagiwara et al., 2012).

As well as regulating autophagy through mTORC1 activity, glutamine has also been shown to supress autophagy through the production of NADPH and glutathione, which prevent the activation of autophagy by limiting ROS levels. However, glutamine can also promote autophagy through the production of ammonia during glutamine catabolism by GDH (Cheong et al., 2011).

Glutamine metabolism has also been shown to regulate many of the epigenetic changes observed in tumours. For example, TET proteins, the dioxygenases that play a key role

41

in cytosine demethylation, are dependent on αKG, produced downstream of glutamine. This enables them to reverse DNA methylation when αKG concentrations are low (Ito et al., 2011). Glutamine also promotes histone acetylation, as citrate produced from the catabolism of glutamine in the TCA cycle can be used to produce acetyl-CoA, the precursor of acetylation (Metallo et al., 2011; Mullen et al., 2011; Wise et al., 2011).

1.2.3   Glutamine Transport

Given the diverse roles that glutamine plays in a number of different pathways to support tumour cells, it is hardly surprising that glutamine uptake and the expression of glutamine transporters are also altered in many tumour types. Glutamine is hydrophilic and soluble in water, and so cannot diffuse across the plasma membrane into cells, requiring transporters to facilitate its uptake. Currently, there are fourteen identified mammalian transporters that can transport glutamine, amongst other substrates. These transporters fall within four distinct gene families: SLC1, SLC6, SLC7 and SLC38.

The SLC6 gene family transports several amino acids as well as a variety of neurotransmitters. SLC6A14 is upregulated in a number of different cancers, including colon (Gupta et al., 2006), cervical (Gupta et al., 2006), breast (Babu et al., 2015) and pancreatic (Penheiter et al., 2015). While the whole-body knockout of SLC6A14 has no observable physical or metabolic phenotype, it demonstrates delayed onset and progression of mammary gland tumours in MMTV-PyMT mice (Babu et al., 2015), suggesting that SLC6A14 could be a good therapeutic target against breast cancer.

The members of the SLC7 family of amino acid transporters are unique as many of them function of heterodimers, consisting of a transporter subunit and a chaperone subunit that interacts with the transporter during biosynthesis and localises the transporter to the plasma membrane. Each of these heterodimeric transporters functions as obligatory exchangers, where the influx of amino acid substrates is coupled to the efflux of other amino acid substrates. SLC7A5 and SLC7A8 are known as LAT1 and LAT2. The expression of LAT1 increases in many cancers, including melanoma, lung and colon cancer (Yanagida et al., 2001; Kaira et al., 2008; Wang et al., 2014; Shimizu et al., 2015). As LAT1 is an obligatory exchanger, it is unlikely that its main role in

promoting tumorigenesis is through the supply of amino acids. Recently, LAT1 was shown to co-operate with ASCT2, a member of the SLC1 family of amino acid transporters, to regulate amino acid concentrations within cells and thus, activate mTOR (Nicklin et al., 2009; Cormerais et al., 2016) (Figure 1.4). The whole-body knockout of LAT1 is embryonic lethal due to the requirement for LAT1 to transport most of the essential amino acids to the brain (Poncet et al., 2014). This lethality limits the potential of LAT1 as a therapeutic strategy against cancer, as high-affinity inhibitors of LAT1 are likely to interfere with amino acid delivery to the brain.

All members of the SLC38 family of amino acid transporters are sodium-coupled neutral amino acid transporters (SNATs). SNAT2 (SLC38A2) is a transcriptional target of the tumour suppressor gene, p53, where SNAT2 is active when p53 is lost. Similarly, SNAT3 (SLC38A3) and SNAT5 (SLC38A5) are thought to be beneficial to tumour cells, due to the intracellular alkalisation that occurs alongside their sodium-mediated glutamine transport. This is thought to neutralise intracellular acidification due to the production of lactate from increased glycolysis.

The final family of glutamine transporters are the most heavily described, due to their frequent overexpression in cancer. The SLC1 family transports both neutral and anionic amino acids. SLC1A5, otherwise known as ASCT2 is the only member of this family to transport glutamine, and can coordinate the influx and efflux of glutamine depending on the concentration gradients of various amino acids across the plasma membrane. Therefore, in normal tissues, ASCT2 contributes to the homeostasis of neutral amino acids inside cells. Under normal conditions, ASCT2 is expressed in the intestine, lung, testis, skeletal muscle and adipose tissue.
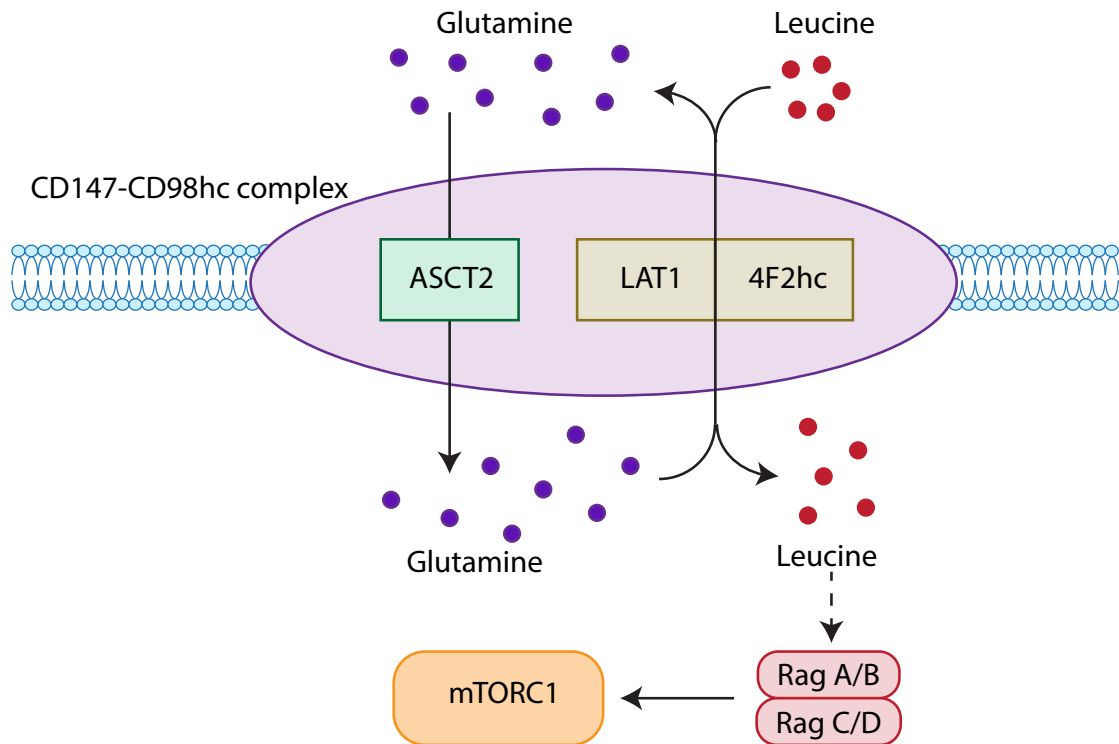
Figure 1-4 ASCT2 and LAT1 co-operation

ASCT2 and LAT1 co-operate to regulate internal amino acid concentrations, regulating mTORC1 activation by Rag GTPases.
Image adapted from Zheng et al., 2016.

1.2.3.1 ASCT2 and cancer

The neutral amino acid transporter, ASCT2, is receiving increasing attention for its potential requirement in cancer due to its increased expression in many different types of cancer, including breast cancer (Kim et al., 2014; Van Geldermalsen et al., 2016; Bernhardt et al., 2017), colon cancer (Huang et al., 2014; Toda et al., 2017), endometrial cancer (Marshall et al., 2017), hepatocellular carcinoma (Namikawa et al., 2014; Sun et al., 2016), lung cancer (Shimizu et al., 2014; Hassanein et al., 2015), melanoma (Wang et al., 2014), myeloma (Bolzoni et al., 2016), neuroblastoma (Ren et al., 2015; Xiao et al., 2015), ovarian cancer (Hudson et al., 2016), glioblastoma (Wise et al., 2008), renal cell carcinoma (Liu et al., 2015) and prostate cancer (Ono et al., 2015; Wang et al., 2015).

The activity of ASCT2 is also thought to couple to two other amino acid transporters. Firstly, it has been suggested that the influx of glutamine by ASCT2, could fuel the transport function of SLC7A11 (xCT) (Bhutia et al., 2015), which imports cystine required for the synthesis of glutathione to support redox homeostasis. This coupling between glutamine uptake and SLC7A11 antiporter activity was demonstrated to be required for the growth of triple negative breast cancer cells *in vivo* (Timmerman et al., 2013).

Likewise, ASCT2 activity is believed to couple with the activity of LAT1 to co-ordinate intracellular amino acid concentrations, and thus, regulate mTORC1 activation (Wasa et al., 1996; Crespo et al., 2002; Peng et al., 2002; Nicklin et al., 2009) (Figure 1.4). This exchange mechanism serves to equilibrate cytoplasmic amino acid pools, without expending any energy from the sodium electrochemical gradient. As obligatory amino acid exchangers, LAT1 and ASCT2 cannot mediate the net uptake of amino acids, but can maintain the concentrations of particular substrates.

LAT1 and ASCT2 have been shown to form part of the same CD147-CD98 complex (Xu and Hemler, 2005). Using a combination of covalent cross-linking, protein identification by mass spectrometry and co-immunoprecipitation, CD147 was shown to be associated with the regulator of cell proliferation, EpCAM, as well as the transporters, LAT1, ASCT2 and monocarboxylate transporters (MCTs) (Xu and Hemler, 2005). The association of these transporters within this complex is being exploited to create more potent MCT inhibitors attached to glutamine or tyrosine residues (Nair et al., 2016). Knockdown experiments demonstrated that loss of the CD147-CD98 complex activated AMP-activated protein kinase (AMPK), resulting in changes in energy metabolism. Disruption of this complex demonstrated that it is required for the import of amino acids and activation of mTORC1 (Cormerais et al., 2016). Interestingly, LAT1 activity was required to promote tumorigenesis, opposed to the β-integrin signalling from the CD98 subunit (Cormerais et al., 2016) in human colon, kidney and lung cancer cell lines. Due to their cooperativity and function within the same complex, the patterns of overexpression of LAT1 and ASCT2 in cancer are almost identical

(Fuchs and Bode, 2005; Namikawa et al., 2014; Kaira et al., 2015; Nikkuni et al., 2015; Honjo et al., 2016), and often correlate with tumour growth and poor prognosis.

1.2.3.2 Regulation of ASCT2

ASCT2 is regulated at multiple stages, where both its protein expression and post-transcriptional modification need to occur before the transporter localises to the plasma membrane. The N-linked glycosylation of ASCT2 was shown to be required for the localisation of the protein at the membrane (Console et al., 2015). This is thought to be because the N-glycosylation increases the stability of the protein, increasing its latency opposed to providing a localisation signal for the protein (Console et al., 2015). Several mechanisms regarding how ASCT2 is regulated have been described, mainly focusing on the increase in protein expression in tumours, while the regulation of ASCT2 N-glycosylation remains, as yet, undescribed.

The proto-oncogene, MYC, was shown to regulate the transcription of ASCT2 in a glioma cell line, where knockdown of MYC decreased ASCT2 expression and MYC was found to selectively bind the promoter region of ASCT2 (Wise et al., 2008). This is part of a transcriptional programme activated by MYC that increases several of the genes required for glutaminolysis in tumours (Wise et al., 2008; Gao et al., 2009; Bott et al., 2015; Camarda et al., 2017). In neuroblastoma, N-MYC activation of ASCT2 was shown to be regulated by the transcription factor, ATF4 (Qing et al., 2012; Ren et al., 2015). ATF4 is activated by eIF2a, which becomes phosphorylated as part of an endoplasmic reticulum stress (ER-stress) response, during amino acid starvation or during oxidative stress (Harding et al., 2003). Thus, through ATF4 regulation of MYC, tumour cells can modulate ASCT2 expression in response to amino acid concentrations and ER-stress. Similarly, stabilisation of hypoxia-inducible factor 2α (HIF-2α) has been shown to activate MYC in oxidative cancer cells, increasing the expression of ASCT2 and Gls1 (Perez-Escuredo et al., 2016).

A second mechanism of ASCT2 regulation during ER-stress has been described. ASCT2 expression was shown to be regulated by the ubiquitin ligase, RNF5, as part of

an ER-stress response (Jeon et al., 2015). Using breast cancer cell lines, ER-stress was shown to increase RNF5 association with ASCT2, promoting its ubiquitination and degradation.

A recent study found ASCT2 to be physically associated in a molecular complex with the epithelial growth factor receptor (EGFR), in head and neck squamous cell carcinoma (Lu et al., 2016). By using a monoclonal antibody against EGFR, Cetuximab, ASCT2 was degraded through EGFR endocytosis (Tao et al., 2017). A study evaluating glutamine uptake by ASCT2 in enterocytes, found that ASCT2 localisation to the plasma membrane was induced by EGF treatment (Avissar et al., 2008). Interestingly, total ASCT2 expression did not change with EGF treatment, but the proportion of ASCT2 localised to the plasma membrane increased instead, suggesting that EGF treatment does not affect the transcription of ASCT2. This study did not observe co-localisation of ASCT2 and EGFR. Instead, they demonstrate that in enterocytes ASCT2 regulation by EGF is through downstream EGFR signalling by MAPK, PI3K and Rho signalling (Avissar et al., 2008).

As well as being regulated by oncogenes, ASCT2 expression was observed to be negatively regulated by the tumour suppressor RNA gene, miRNA-137 (Dong et al., 2017). The expression of miRNA-137 is frequently lost in many tumours, resulting in increased ASCT2 expression. However, at present, little is understood about how miRNA-137 targets ASCT2 or how the expression of miRNA-137 is lost in tumours. Similarly, the tumour suppressor gene, Rb was also shown to regulate ASCT2 expression via the Rb-regulated transcription factor E2F-3 (Reynolds et al., 2014). When Rb is lost, E2F-3 binds directly to the ASCT2 promoter to increase its transcription.

ASCT2 activity is also induced through the kinase activity of the serine/threonine kinases, SGK1-3 and protein kinase B. The constitutive activation of these kinases was shown to increase the abundance of ASCT2 at the plasma membrane. However, it is unknown if these kinases regulate ASCT2 expression or N-glycosylation. These kinases

are activated by insulin and IGF1, suggesting that they could alter ASCT2 localisation in response to changes in the tumour microenvironment (Palmada et al., 2005).

ASCT2 expression was shown to be more directly regulated by the tumour microenvironment, as the expression of the transporter was observed to be directly regulated by changing glutamine concentrations (Bungard and Mcgivan, 2004). This study used hepatocellular carcinoma cells to demonstrate decreased ASCT2 promoter activity in the absence of glutamine, suggesting that ASCT2 expression is dependent on glutamine. However, this study was performed before the requirement for the N-glycosylation of ASCT2 for membrane localisation was described, and thus, they do not address the requirement for glutamine for the HBP, and thus, glycosylation. While the requirement for glutamine for the HBP has been demonstrated (Wellen et al., 2010; Abdel Rahman et al., 2013), precisely how glutamine regulates ASCT2 expression and localisation is yet to be fully described. Interestingly, N-glycosylation of ASCT2 decreased during glucose deprivation or glycolytic inhibition in leukaemia cells, demonstrating that inhibition of the HBP prevents ASCT2 localisation to the plasma membrane (Polet et al., 2016).

Interestingly, the observation that selective estrogen receptor modulator therapies are effective against cancers in non-estrogen sensitive tissues led to the observation that the estrogen receptor modulators, Tamoxifen and Raloxifene decrease ASCT2 expression in ER- breast cancer cell lines (Todorova et al., 2011). Treatment with increasing concentrations of Tamoxifen and Raloxifene resulted in decreasing glutamine uptake and ASCT2 expression (Todorova et al., 2011). However, it is yet to be demonstrated how these estrogen-receptor modulating compounds regulate ASCT2, whether it is through direct regulation of its expression or due to off-target effects of the treatment.

The mechanism regulating the N-glycosylation of ASCT2 is still unknown. While changes in global N-glycosylation are frequently observed in cancer, many of the mechanisms regulating these processes remain to be fully elucidated.

During the first step of N-glycosylation, GlcNAc-P, from the UDP-GlcNAc produced from the HBP, is transferred to the lipid precursor, dolichol phosphate on the cytoplasmic face of the endoplasmic reticulum membrane. Fourteen sugars are sequentially added to the dolichol phosphate before bloc transfer of the entire glycan structure to an Asn-X-Ser/Thr sequence in a protein that is currently being synthesised and translocated through the endoplasmic reticulum membrane. The protein-bound N-glycan is then remodelled in the endoplasmic reticulum and Golgi by a series of enzymes, known as glycosidases and glycosyltransferases. Tumour cells display a range of glycosylation alterations, where aberrant glycan modifications are added to proteins and different protein sites become glycosylated (Pinho and Reis, 2015). This could be due to changes in the expression or localisation of glycosyltransferases and glycosidases (Buckhaults et al., 1997; Gill et al., 2010; Hatano et al., 2011) and changes in substrate availability (Kumamoto et al., 2001; Wellen et al., 2010).

1.2.3.3   Therapeutic targeting of ASCT2 in cancer

Due to the dependence of many cancer cells on glutamine metabolism, combined with the increased expression of ASCT2 in many tumours, recent studies have focused on inhibiting ASCT2 as a potential therapeutic target against different forms of cancer. Recently, knockdown of ASCT2 by shRNA in human triple-negative breast cancer cell lines was shown to be effective against both tumour initiation and progression *in vivo* (Van Geldermalsen et al., 2016). This study shows that MYC overexpression correlates to ASCT2 expression in human breast cancer patients, but does not specifically discuss the regulation of ASCT2 and specific patient selection for ASCT2 inhibition therapy, ignoring the variation in ASCT2 expression and N-glycosylation between the different human breast cancer cell lines in their study (Van Geldermalsen et al., 2016).

Similarly, knockdown of ASCT2 by shRNA decreased glutamine uptake and proliferation in human myeloma cells both *in vivo* and *in vitro* (Bolzoni et al., 2016). Likewise, knockdown of ASCT2 expression in human hepatoma cells induced apoptosis (Fuchs et al., 2004) and decreased tumour growth *in vivo* in human small cell lung cancer xenografts (Hassanein et al., 2015). Similar results were observed in

prostate cancer cell lines, where shRNA-mediated inhibition of ASCT2 decreased glutamine uptake, cell cycle progression, mTORC1 pathway activation and cell growth (Wang et al., 2015). Thus, these studies provide evidence for the suitability of inhibiting ASCT2 as a targeted therapeutic strategy against glutamine-dependent ASCT2-overexpressing tumours.

Similarly, targeting the mechanisms regulating ASCT2 expression has also been demonstrated to be effective against tumour growth. For instance, treating MMTV-PyMT tumours with Paclitaxel decreased tumour growth by inducing an ER-stress response that degraded ASCT2 expression through RNF5-mediated ubiquitination (Jeon et al., 2015). Thus, this demonstrates that inhibition of ASCT2, either directly or indirectly could be a successful therapeutic approach against glutamine-dependent tumorigenesis.

However, two recent studies have shown that when ASCT2 is inhibited, other transporters can compensate for this lost glutamine uptake. Polet and colleagues (2016) demonstrated that when ASCT2 activity was diminished due to inhibition of the HBP by glucose deprivation or inhibition of glycolysis by 2-deoxyglucose (2DG) treatment, the amino acid antiporter, LAT1, was upregulated in human leukaemia cell lines (Polet et al., 2016). This increase in LAT1 activity could counteract the effects of ASCT2 downregulation, suggesting that inhibiting both ASCT2 and LAT1 in combination may prove a more effective therapeutic strategy against glutamine-dependent leukaemia. Similarly, Broer et al. (2016) also demonstrated that other amino acid transporters could compensate for lost ASCT2 activity (Broer et al., 2016). Using epithelial cervical cancer cells and osteosarcoma cells, they observed an amino acid starvation response during the deletion of ASCT2. However, this did not reduce cell growth. Instead they observed increased SNAT1 expression to replace ASCT2 function. Again, this study proposed the suitability of a combination approach to targeting glutamine uptake in cancer.

Considerable work has been done to develop compounds that specifically inhibit ASCT2. One of the most frequently used ASCT2 inhibitors developed is γ-L-Glutamyl-

p-nitroanilide (GPNA), which acts as a glutamine mimic that binds to the active site of glutamine transporters to competitively inhibit transporter activity (Esslinger et al., 2005). It has been demonstrated that GPNA binds through specific hydrogen bonding and a lipophilic binding interaction to the active site of ASCT2 (Esslinger et al., 2005). However, recent work by Broer et al. (2016) and Chiu et al. (2017) describe the broader range of GPNA activity, as a general inhibitor of sodium-independent amino acid transporters (Broer et al., 2016; Chiu et al., 2017). Considerable work has been done to modify the existing backbone of GPNA in order to make the compound more specific (Colas et al., 2015; Schulte et al., 2015; Schulte et al., 2016). Likewise, benzylserine and benzylproline derivatives are being modified to improve their specificity and potency against ASCT2 (Grewer and Grabsch, 2004; Singh et al., 2017). A synthetic polymer has recently been described that binds to cells with a high density of ASCT2 at the plasma membrane (Yamada et al., 2017). It is believed that polymers such as this could be exploited to efficiently deliver inhibitory compounds to cancer cells. More recently, monoclonal antibodies have been created that specifically bind ASCT2, resulting in decreased growth in colorectal cells, demonstrating an alternative approach to inhibiting ASCT2 (Kasai et al., 2017; Suzuki et al., 2017).

A whole-body ASCT2-deficent mouse has been produced that does not appear to have any observable phenotypes, especially demonstrating normal B and T cell populations (Masle-Farquhar et al., 2017). This is important as it suggests that any therapies inhibiting ASCT2 should be tolerated well by the rest of the body, especially by the immune system. While creating specific ASCT2 targeting therapies is proving difficult due to the similarities between amino acid transporters, it has been shown that targeting the mechanisms regulating ASCT2 expression can be effective (Jeon et al., 2015), thus, by understanding more about how ASCT2 is regulated, more specific methods of targeting ASCT2 activity may be developed.

1.3   Factors affecting tumour metabolism

While all tumours need to alter their metabolic phenotypes to adjust to their increased energetic and biosynthetic needs, not all tumours alter their metabolism in the same way,

with different tumours depending on different nutrients and pathways. Differences in metabolism between tumours have been shown to be regulated by a number of different mechanisms, enabling tumours to adapt to their changing microenvironment. This makes it difficult to predict the metabolic phenotype of a particular tumour and how that tumour might respond to a therapeutic strategy targeting altered metabolic pathways.

The tissue of tumour origin has been demonstrated to affect tumour metabolism (Yuneva et al., 2012). This is thought to be partly due to the metabolic features of the tissue of origin as well as due to the differences in tumour microenvironment the tissue of origin provides. A number of normal organs within the body have specialised metabolic adaptations that allow them to perform their functions correctly, and it is likely that these metabolic adaptations influence tumorigenesis in different ways. The importance of studying tumour metabolism in the full context of the surrounding tumour microenvironment was recently demonstrated by Davidson and colleagues (2016), who demonstrated that the metabolic profiles of KRas-driven lung cancer cells changed dependent on whether the cells were grown *in vitro* or *in vivo* (Davidson et al., 2016).

Tumour cells have been shown to interact with infiltrating cancer-associated fibroblasts (CAFs) in order to support their increased energetic requirements (Yang et al., 2016). Likewise, metabolic interplay between tumour cells and immune cells has been observed, where both cell types compete for nutrients (Chang et al., 2015). Tumour cells have also been shown to interact with their neighbouring tumour cells in order to support their altered metabolic requirements. It is thought that a symbiotic relationship exists between aerobic and hypoxic cancer cells, where tumour cells shift their preference for lactate-fuelled respiration and aerobic glycolysis (Sonveaux et al., 2008).

As well as the surrounding microenvironment effecting tumour metabolism, the internal tumour environment would also effect individual cells. While tumours promote the growth of new blood vessels through VEGF signalling (Jakeman et al., 1993; Shweiki et al., 1993) as tumours become larger, regions develop that are distant from blood vessels, and thus, these regions receive fewer nutrients and experience lower oxygen

concentrations (Helmlinger et al., 1997). It has been demonstrated that the metabolism of tumour cells changes based on proximity to blood vessels, ischemia and infiltrating tumour-associated macrophages, resulting in defined gradients of extracellular metabolites (Carmona-Fontaine et al., 2017).

Likewise, when oxygen concentrations are low, the HIF transcription factors are stabilised. HIF1 regulates most of the enzymes required for glycolysis, promoting increased glucose catabolism under hypoxic conditions (Kress et al., 1998; Airley et al., 2001; Graven et al., 2003; Minchenko et al., 2004; Jean et al., 2006). The effect of HIF stabilisation on tumour metabolism also appears to be context dependent, as the effect of hypoxia varies dependent on the system being studied (Wiesener et al., 2003; Hutchison et al., 2004; Mayer et al., 2004).

Many oncogenes have been described to regulate specific metabolic changes observed in tumours. In many cases, this is due to direct regulation of metabolic enzymes by the oncogene or tumour suppressor gene.

1.3.1   The MYC oncogene and metabolism

MYC-transformed cells have been observed to increase glutamine utilisation and increase the expression of key metabolic enzymes, including those involved in glycolysis (Shim et al., 1997; Kim et al., 2004; Kim et al., 2007) and glutaminolysis (Wise et al., 2008; Gao et al., 2009; Wang et al., 2011; Bott et al., 2015). Not only does MYC regulate the expression of these genes, but it also appears to favour particular splice variants, such as PKM2 over PKM1 (David et al., 2010). MYC also increases the shuttling of glucose into the pentose phosphate pathway (PPP), to replenish the reducing equivalent NADPH and produce ribose required for nucleotide synthesis (Morrish et al., 2009; Wang et al., 2011). However, the metabolic phenotype of MYC-deregulated cancer cells is dependent on the cancer context (Yuneva et al., 2012).

In breast cancer, the regulation of metabolism by MYC has been shown to be context dependent. For instance, in human triple negative breast cancer, MYC expression

correlates with ASCT2 expression (Van Geldermalsen et al., 2016), and triple negative breast cancer cell lines are more sensitive to Gls1 inhibition than ER+ cell lines (Gross et al., 2014), although this study does not consider the MYC status of the cell lines. However, induction of MYC expression in the mammary epithelial cell line, MCF10A, caused TDG promoter demethylation, resulting in increased glutamine synthetase, (GS) expression (Bott et al., 2015). Loss of GS in these cells and triple negative breast cancer cell lines decreased cell proliferation and *in vivo* tumour growth (Bott et al., 2015). Metabolic analysis of a MYC-driven model of triple negative breast cancer revealed deregulated glycolysis and TCA cycle metabolism (Camarda et al., 2016), but did not explore the cause of this deregulation further. Fatty acid oxidation intermediates are also upregulated in a MYC-driven model of triple negative breast cancer (Camarda et al., 2016). Inhibition of fatty acid oxidation decreased energy metabolism and decreased tumour growth in this model.

1.3.2   The ErbB2 oncogene and metabolism

HER2+ tumours were shown to have the highest expression of the enzymes and transporters involved in glutaminolysis of the breast cancer subtypes (Kim et al., 2013). Both murine and human ErbB2-positive tumour cells have been shown to be glutamine dependent (Mcguirk et al., 2013), although the regulation of glutamine catabolising enzymes is believed to be regulated by the transcriptional co-activator, PGC-1α in ErbB2-positive cells (Mcguirk et al., 2013). Similarly, ErbB2 has been shown to induce Gls1 expression in MCF10A mammary epithelial cells, through a MYC-independent mechanism (Qie et al., 2014). Knockdown or inhibition of Gls1 decreased the proliferation of these cells and HER2+ human breast cancer cell lines.

HER2+ tumours also show strong correlations with the proteins involved in lipid biosynthesis compared to other breast cancer subtypes (Kim et al., 2015). ErbB2 is closely correlated with fatty acid synthase (FASN) and acetyl-CoA expression, and is believed to regulate their protein expression at a translational level (Yoon et al., 2007).

ErbB2 has also been shown to affect glycolysis. For instance, ErbB2 is linked to lactate dehydrogenase A (LDHA) expression via the activation of PI3K/Akt, resulting in HIF-1α activation (Zhao et al., 2009). Similarly, ErbB2 mammary gland tumours express high levels of hexokinase 2 (HK2), an isoform of glucokinase, the enzyme regulating the first step in glycolysis. HK2 was demonstrated to be required for tumour initiation and maintenance in ErbB2-driven mammary gland tumours in mice (Patra et al., 2013). Likewise, knockout of the glucose transporter, GLUT1 decreased tumour development in ErbB2-induced mammary gland tumours (Wellberg et al., 2016), again demonstrating the requirement for glucose catabolism in ErbB2-driven tumours.

1.4 Clinical approaches using altered tumour metabolism

Current understanding regarding how metabolic pathways are altered in cancer have led to the development on new therapeutic targets and diagnostic tools. It is believed that by expanding our knowledge of how tumours regulate these pathways, more effective therapeutic targets as well as improved diagnostic tools could be developed.

One of the most frequently used clinical tools to utilise altered tumour metabolism is ^{18}F-FDG-PET. This technique uses radio-labelled glucose (^{18}F-FDG) to detect glucose-consuming tissues within the body using a PET scan, and is used to identify tumours, and monitor their size during treatment. While this technique can identify glucose consuming tumours, it fails to identify tumours that do not heavily consume glucose (Sato et al., 2017). Likewise, it also cannot differentiate tumours in organs that normally consume a lot of glucose, such as the brain and bladder. However, within different types of breast cancer, ^{18}F-FDG uptake strongly correlates to the oncogenic driver of the tumour, when several different tumour types were compared (Alvarez et al., 2014), demonstrating that ^{18}F-FDG-PET alongside tumour profiling can be used to predict therapeutic outcome as well as track tumour progression.

Current work aims to expand the applications of ^{18}F-FDG-PET by using a different substrate, ^{18}F-Glutamine. By looking at the uptake of ^{18}F-glutamine in lung tumour xenografts, not only could tumours be identified, but also by comparing ^{18}F-FDG to ^{18}F-

glutamine uptake, the tumour's metabolic profile could be predicted, influencing potential therapeutic strategies (Hassanein et al., 2016). ^{18}F-glutamine uptake correlated to ASCT2 expression, potentially indicating which tumours would respond well to ASCT2 inhibition (Hassanein et al., 2016). Similarly, comparison of ^{18}F-FDG to ^{18}F-glutamine uptake, revealed that ^{18}F-glutamine uptake was a more specific predictive marker for the response of colon cancer patients to BRAF-targeting therapy (Schulte et al., 2017). Similarly, differential uptake of ^{11}C-acetate, ^{11}C-choline and ^{11}C-methionine have also been demonstrated by some human cancers (Groves et al., 2007; Grassi et al., 2012).

A similar strategy uses tethered amino acids, where selected amino acids such as glutamine and tyrosine have been used to direct molecular imaging agents to tumour cells. This causes the accumulation of both transporters and the imaging agent in cells that are overexpressing certain transporters, enabling ASCT2 and LAT1 overexpressing tumours to be identified (Makrides et al., 2007; Stefania et al., 2009). Thus, the potential to exploit altered tumour metabolism as a diagnostic and clinical tool remains to be fully explored.

Cancer metabolism is also being exploited for new therapies. This has been demonstrated by the successful use of the enzyme L-asparaginase to treat acute lymphoblastic leukaemia (ALL) and other related lymphomas (Gutierrez et al., 2006). As ALL cancer cells consume asparagine, L-asparaginase deaminates asparagine in the blood to aspartate so that it can no longer be consumed by ALL cancer cells.

Currently, our ability to effectively treat tumours is inhibited by the inability to target many common driver mutations, such as overexpressed MYC or mutant KRas. It is believed that targeting their downstream effector pathways, such as increased aerobic glycolysis or glutaminolysis will weaken these tumours, either proving effective as a single therapy or in combination with current chemotherapy approaches. Pre-clinical models targeting downstream metabolic enzymes that are activated by these genetic changes appear to be effective. For instance, small molecule inhibitors of the glycolytic enzyme, 6-phosphofructo-2-kinase in KRas-mutant Lewis lung carcinoma xenografts

were shown to suppress tumour growth in mice (Clem et al., 2008). Similar results were observed when lactate dehydrogenase A was inhibited by a small molecule inhibitor in MYC-overexpressing lymphoma and pancreatic cancer xenografts (Le et al., 2010). These studies demonstrated that targeting metabolism as an effector of altered signalling pathways might be an effective way to target cancer. As all cancer cells rely on changes in metabolic pathways to support their growth and survival, targeting metabolism has the potential to affect a wide range of tumour types with a single compound.

Many recent studies suggest that inhibiting glutamine catabolism in tumours would be an effective therapeutic approach (Wang et al., 2010; Yuneva et al., 2012; Xiang et al., 2015; Van Geldermalsen et al., 2016). The Calithera Gls1 inhibitor, CB-839 was shown to be effective against triple-negative breast tumour xenografts (Gross et al., 2014) and has been taken into phase I clinical trials as a single agent against renal cell carcinoma and acute myeloid leukaemia, and in combination with Paclitaxel, a cytoskeletal drug that stabilises microtubule polymers, in triple negative breast cancer (Calithera-Biosciences, 2017).

Current work on tumour metabolism has revealed several important features of altered tumour metabolism that remain to be explored therapeutically. Frequently, tumours have been shown to express particular isoforms of metabolic enzymes over others (Wang et al., 2010; Van Den Heuvel et al., 2012; Gershon et al., 2013; Patra et al., 2013), revealing a potential therapeutic window if that particular isoform can be targeted. Some enzyme isoforms are particularly attractive therapeutic targets, as in the case of HK2, which is the embryonic isoform of the glucokinase enzyme, and so has limited expression in normal adult tissues. Thus, therapeutic strategies specifically targeting HK2 should have limited off-target effects.

Cancer therapies are moving towards an increasingly personalised approach. Ideally all tumours would be sequenced to gain a full understanding of their mutagenic background and altered signalling and metabolic pathways. However, this is currently too costly and inefficient to be applied to every cancer patient. While in some cases,

tumour subtypes have been effective at classifying tumours based on their suitability for certain treatments, as in the receptor-based subtypes applied to breast cancer, frequently these subtypes do not fully describe the tumours sufficiently to predict and understand therapeutic outcomes. By understanding more about how different metabolic phenotypes correlate with specific tumour subtypes or with particular oncogenes, within each tissue, better therapeutic predictions could be developed. Likewise, new biomarkers for particular metabolic changes could be described that might result in improved patient selection for specific treatments. Recently, metabolic heterogeneity was observed within TNBC cell lines resulting in differential sensitivity to tyrosine kinase inhibition (Lanning et al., 2017), demonstrating that understanding different metabolic profiles is valuable when targeting specific breast cancer subtypes.

Therefore, this project aims to analyse the metabolic phenotypes of two different types of mammary gland tumours, induced by different oncogenes, with the hope of identifying new therapeutic targets against either type of tumour. Tumours driven by the MYC and ErbB2 oncogenes were selected due to their high cancer incidence (Slamon et al., 1989; Deming et al., 2000), known interactions with metabolic enzymes (Kim et al., 2007; Wise et al., 2008; Gao et al., 2009; Wang et al., 2011; Qie et al., 2014; Bott et al., 2015) and the current difficulties associated with treating breast cancers expressing either oncogene (Miller et al., 2011; Horiuchi et al., 2012).

1.5   Thesis Aims

The initial aim of this thesis is to compare the metabolism of mammary gland tumours induced by two different oncogenes, ErbB2 and MYC. By comparing central carbon metabolism within these tumours using stable isotope labelling analysed by GC-MS, key metabolic similarities and differences between these tumours and normal mammary gland tissue can be observed. By describing any metabolic dependencies in these tumours, potential therapeutic targets against ErbB2 or MYC-induced tumours could be identified.

The following chapters will outline efforts to address the following aims of the thesis:

- To characterise the metabolic phenotypes of MMTV-ErbB2 and MMTV-MYC mammary gland tumours compared to normal mammary gland tissue,

- To identify differences in the expression of glutamine transporters and glutaminolytic enzymes between the tumour models,

- To analyse the requirement for glutamine and the glutamine transporter, ASCT2 in MYC-induced mammary gland tumour cells,

- To explore how ASCT2 is regulated in MYC and ErbB2-induced tumours and derived cells,

- To explore how glutamine metabolism affects ASCT2 expression and post-translational modification in both tumour models.

Chapter 2.   Materials & Methods

2.1 Reagents and Chemicals

2.1.1 Mice

All mouse procedures followed United Kingdom Home Office regulations and were approved by the Animal Welfare and Ethical Review panel of the Francis Crick Institute.

The following mice were used during this project:
FVB/NJ – internal stock at the Francis Crick Institute.

MMTV-MYC (Tg(MMTV-MYC)141-3Led) bought from the Jackson Laboratory, MGI ID: 2447500.

MMTV-ErbB2 (Tg(MMTV-Erbb2)NL1Mul/J) were kindly donated by Dimitrios Anastasiou (The Francis Crick Institute) for this project, who bought them from the Jackson Laboratory, MGI ID: 3050871.

2.1.2 Cell Lines

The following commercial cell line was used during this project. All other cell lines were created by Emma Still using the MMEC and tumour cell isolation protocols described in Chapter 2.2.

BOSC 23 cell line – a modified version of 293T-based human kidney cell line, used as a retroviral producer cell line. ATCC number: CRL-11270.

2.1.3   Plasmids

The following plasmids were used for the generation of stably transfected cell lines.

Table 2-1 Plasmids

Plasmid	Backbone	Supplier
pCL-ECO	CMV-LXSN	A gift from Inder Verma (Addgene plasmid 12371) (Naviaux et al., 1996)
pBabe-12S E1a	pBabe-puro	A gift from Scott Lowe (Addgene plasmid 18742) (Samuelson and Lowe, 1997)
pBabe-hygroER	pBabe-hygro	A gift from William Tansey (Cold Spring Harbour Laboratory) (Eilers et al., 1989)
HER2 CA V659E	pcDNA3	A gift from Mein-Chie Hung (Addgene plasmid 16259) (Li et al., 2004)
pBabe-Puro-KRas*G12V	pBabe-puro	A gift from Christopher Counter (Addgene plasmid 46746) (Lampson et al., 2013)
pBabe-c- MYC-zeo	pBabe-zeo	A gift from Susan Linquist (Addgene plasmid 17758) (Dai et al., 2007)
pBabe-hygroER-MYC	pBabe-hygro	A gift from William Tansey (Cold Spring Harbour Laboratory) (Eilers et al., 1989)
pBabe-hygro-p53 DD	pBabe-hygro	A gift from Bob Weinburg (Addgene plasmid 9058) (Hahn et al., 2002)

2.1.4 Antibiotics

The plasmids used for cell transduction contained antibiotic resistance markers, so that after cell transduction, the cells could be treated with antibiotics in order to select for the cells expressing the added plasmid.

Table 2-2 Antibiotics used for cell selection

Antibiotic	Supplier	Catalogue Number	Final Conc.
Hygromycin B	Sigma	H9773	50 µg/mL
Neomycin (G418)	Sigma	A1720	100 µg/mL
Puromycin	Sigma	P8833	0.5 µg/mL
Zeocin	Thermo Fisher Scientific	12821610	100 µg/mL

2.1.5 Cell Media and Isolation Buffers

The following cell culture medias were used for the adherent culture of cells or for the isolation of cells as described in the protocols outlined in Chapter 2.2.

Table 2-3 MMEC Media

Component	Supplier	Catalogue Number	Final Conc.
DMEM/F12	Life Technologies	21331-046	-
HEPES	Gibco	15630-056	10 mM
FBS	Gibco	10270	10%
Glutamine	Gibco	25030-024	2 mM
Insulin	Sigma	I1882	5 µg/mL
Hydrocortisone	Sigma	H0888	1 µg/mL
EGF	Life Technologies	PMG8043	10 ng/mL
Pen/Strep	Gibco	15140-122	100 µg/mL

Table 2-4 HBEC Media

Component	Supplier	Catalogue Number	Final Conc.
DMEM/F12	Life Technologies	21331-046	-
HEPES	Gibco	15630-056	10 mM
FBS	Gibco	10270	10 %
Glutamine	Gibco	25030-034	2 mM
Insulin	Sigma	I1882	1 μg/mL
BSA	Sigma	A2058	1 mg/mL
Hydrocortisone	Sigma	H0888	0.5 μg/mL
Gentamycin	Calbiochem	1405-41-0	50 μg/mL
Pen/Strep	Gibco	15140-122	100 μg/mL

Table 2-5 BOSC cell Media

Component	Supplier	Catalogue Number	Final Conc.
DMEM	Life Technologies	31053	-
FCS	Gibco	10270	10 %
Glutamine	Gibco	25030-024	2 mM
Pen/Strep	Gibco	15140-122	100 μg/mL

Table 2-6 Estrogen-depleted media for pBabe-MYCER studies

Component	Supplier	Catalogue Number	Final Conc.
DMEM/F12 (no phenol red)	Gibco	21041-033	-
HEPES	Gibco	15630-056	10 mM
Dialysed FBS	Gibco	10270	10 %
Glutamine	Gibco	25030-034	2 mM
Insulin	Sigma	I1882	1 μg/mL
EGF	Life Technologies	PMG8043	10 ng/mL
Hydrocortisone	Sigma	H0888	0.5 μg/mL
Pen/Strep	Gibco	15140-122	100 μg/mL

Table 2-7 13C5-glutamine labelled media for metabolomics studies

Component	Supplier	Catalogue Number	Final Conc.
DMEM/F12	Gibco	21331-046	-
HEPES	Gibco	15630-056	10 mM
Dialysed FBS	Gibco	10270	10 %
$^{13}C_5$-Glutamine	Cambridge Isotopes Laboratories	184161-19-1	2 mM
Insulin	Sigma	I1882	1 µg/mL
EGF	Life Technologies	PMG8043	10 ng/mL
Hydrocortisone	Sigma	H0888	0.5 µg/mL
Pen/Strep	Gibco	15140-122	100 µg/mL

Table 2-8 Tumour cell isolation collagenase buffer

Component	Supplier	Catalogue Number	Final Conc.
DMEM/F12	Gibco	21331-046	-
HEPES	Gibco	15630-056	10 mM
BSA	Sigma	A2058	2 %
Insulin	Sigma	I1882	1 µg/mL
Hydrocortisone	Sigma	H0888	0.5 µg/mL
Collagenase (Type L)	Sigma	C8176	1 mg/mL
Gentamycin	Calbiochem	1405-41-0	50 µg/mL

Table 2-9 MMEC isolation collagenase buffer

Component	Supplier	Catalogue Number	Final Conc.
RPMI-1640	Gibco	31870-082	-
HEPES	Gibco	15630-056	10 mM
BSA	Sigma	A2058	2.5 %
Collagenase (Type L)	Sigma	C8176	1 mg/mL

2.1.6 Inhibitors and activators

The following compounds were used during this project. All solutions were filtered before use.

Table 2-10 MMEC isolation collagenase buffer

Compound	Supplier	Catalogue Number	Solvent
4-hydroytamoxifen (4OHT)	Sigma	H7904	Ethanol
L-glutamic acid γ-(p-nitroanilide) (GPNA)	Sigma	G6133	Water
N,N'-[thiobis(2,1-ethanediyl-. 1,3,4-thiadiazole-5,2-diyl)]bis-benzeneacetamide (BPTES)	Sigma	SML0601	DMSO

2.1.7 Enzymes

The following enzymes were used during this project, as described in the procedures outlined in Chapter 2.2.

Table 2-11 Enzymes

Enzyme	Supplier	Catalogue Number	Activity
Collagenase (Type L)	Sigma	C8176	< 1.0 FALGPA units/mg solid
PNGase F	Sigma	G5160	> 5,000 units/mL

2.1.8 Stable Isotope labelled substrates

The following stable isotope labelled substrates were used for bolus injections and *in vitro* metabolomics experiments. For bolus injections, stable isotope labelled substrates were dissolved in sterile saline. For cell culture experiments, stable isotope labelled substrates were dissolved in water. All solutions were filtered before use.

Table 2-12 Stable Isotope labelled substrates

Compound	Supplier	Catalogue Number	Conc: bolus injections	Conc: cells
$^{13}C_6$-glucose	Cambridge Isotope Laboratories	110187-42-3	200 mg/mL	-
$^{13}C_5$-glutamine	Cambridge Isotope Laboratories	184161-19-1	40 mg/mL	2 mM
$\alpha^{15}N$-glutamine	Cambridge Isotope Laboratories	80143-53-3	40 mg/mL	-

2.1.9 Antibodies

Antibodies for immunoblotting and immunofluorescence were stored according to the manufacturers' instructions. For immunoblotting, primary antibodies were diluted into 5% BSA /0.05% sodium azide/ PBS-T (0.05% Tween in PBS). Secondary antibodies were diluted into 5% milk/PBS-T.

For immunofluorescence, primary and secondary antibodies were diluted into 1% BSA/ 0.05% sodium azide / PBS-T.

Table 2-13 Secondary antibodies

Antibody	Supplier	Catalogue Number	WB dilution	IF dilution
Goat anti-rabbit IgG-HRP	Santa Cruz	sc-2301	1:4000	-
Goat anti-mouse IgG-HRP	Invitrogen	62-6520	1:4000	-
Alexa-Fluor 555 goat anti rabbit IgG	Life Technologies	A21428	-	1:1000
Alexa-Fluor 488 goat anti mouse IgG	Life Technologies	A11015	-	1:1000

Table 2-14 Primary antibodies

Antibody	Supplier	Catalogue Number	WB dilution	IF dilution
Actin	Sigma	A5228	1:100,000	-
ASCT2	Santa Cruz	sc-99002	1:1000	1:100
ERα	Abcam	ab75635	1:1000	-
ErbB2	Abcam	ab16901	1:1000	1:250
GS	Abcam	ab93439	1:1000	-
HK1	Cell Signalling	C35C4	1:1000	-
HK2	Cell Signalling	C64G5	1:1000	-
MYC	Abcam	ab32072	1:1000	1:100
O-GlcNAc	Thermo Fisher Scientific	MA1-072	1:500	-
PHGDH	Santa Cruz	sc-292792	1:1000	-
SNAT2	Santa Cruz	sc-67081	1:1000	-

2.1.10 Taqman Probes

The following Taqman probes were used for quantitative RT-PCR.

Table 2-15 Taqman probes

Probe	Supplier	Catalogue Number	Exons spanned	Species
ASCT2	Thermo Fisher Scientific	Mm00436603_m1	4 – 5	Mouse
GDH	Thermo Fisher Scientific	Mm00492353_m1	3 – 4	Mouse
Gls1	Thermo Fisher Scientific	Mm01257301_m1	17 – 18	Mouse
Gls2	Thermo Fisher Scientific	Mm01164860_mH	15 – 16	Mouse
GLUL	Thermo Fisher Scientific	Mm00725701_s1	7	Mouse
18S	Thermo Fisher Scientific	Mm04277571_s1	-	Mouse
KRas	Thermo Fisher Scientific	Hs00364284_g1	3 – 4	Human
ErbB2	Thermo Fisher Scientific	Hs01001586_m1	1 – 2	Human
MYC	Thermo Fisher Scientific	Hs00153408_m1	2 – 3	Human

2.1.11 RNAi Oligonucleotides

For the transfection of cells with siRNA, DharmaFECT 1 transfection reagent was used (Dharmacon T-2001-03).

Table 2-16 RNAi Oligonucleotides

siRNA	Supplier	Catalogue Number
siASCT2	Sigma	EMU060451
siGLS1	Santa Cruz	sc-145431
siMYC	Sigma	EMU075291
ON-TARGET plus non-targeting siRNA	Dharmacon	D-001810-10-05

2.1.12 Other Chemicals

The following chemicals were used during this project:
- 2-mercaptoethanol – BioRad, 161-0710
- 4,4-trimethyl-1-propanesulfonic acid (DSS) – Sigma, 178837
- 40% Acrylamide-Bis – BioRad, 161-0148
- 4X Laemmli Buffer – BioRad, 161-0747
- Acetonitrile – Acros Organics, 32573
- Ammonium Persulfate – Sigma, A3678
- BCA protein quantification kit – Thermo Fisher Scientific, 23227
- Bradford reagent – BioRad, 500-0205
- BSA – Sigma, A2058
- BSTFA + TMCS – Supelco, 33148
- Chloroform – Sigma, 372978
- Coomassie: Instant blue - Expedeon, Prod 15BIL
- Crystal Violet powder – Sigma, C0775
- Deuterium Oxide (D_2O) – Sigma, 1.03428
- DTT – Sigma, D0632

- EDTA – Sigma, E6758

- Effectene transfection reagent – Qiagen, 301427

- Ethanol – Thermo Fisher Scientific, E0650DF/17

- Glycerol – Sigma, G5516

- High capacity cDNA reverse transcriptase kit – Thermo Fisher Scientific, 4368814

- HPLC-grade Methanol – Honeywell Research Chemicals, 34966

- L-Norleucine – Sigma, N8513

- Matrigel growth factor reduced basement membrane matrix – Corning, 356230

- Methanol – Sigma, 34966

- Methoxyamine hydrochloride – Sigma, 226904

- N,N,N',N',-Tetramethylethylenediamine (TEMED) – Sigma, T9281

- NucView 488 Caspase-3 substrate – Biotium, 10402

- Phosphatase inhibitor cocktail – Roche, 04906837001

- Pierce Glycoprotein Staining Kit - Thermo Fisher Scientific, 24562

- PMSF – Sigma, P7626

- Polybrene – Sigma, TR-1003

- Precision plus protein standard – BioRad, 161-0374

- Protease inhibitor cocktail – Roche, 11836170001

- Pyridine – Sigma, 270970

- Scyllo-Inositol – Sigma, I8132

- SDS – Sigma, 1614363

- Sodium Azide – Sigma, S2002

- Taqman master mix – Thermo Fisher Scientific, 4369016

- TRI reagent – Sigma, T9424

- Triton X-100 – Sigma, T8787

- Tween – VWR, 66368413

- Vectashield with DAPI – Vector Labs, H-1200

- Xylenes – Sigma, 214736

2.2   Experimental Procedures

2.2.1   Cell culture, isolation and manipulation

2.2.1.1   Isolation of mouse mammary epithelial cells (MMECs)

Mammary glands 3, 4 and 5 without the inguinal lymph nodes were collected from 8-10-week-old virgin female mice and placed into 10 mL MMEC collagenase buffer. The glands were weighed before being mashed with sterile blades until creamy (roughly 10 minutes). The glands were put into 5 mL MMEC collagenase buffer per gram of flesh with a final concentration of 1 mg/mL collagenase L. The glands were shaken for 30 minutes at 37°C at 200 rpm. The glands were spun for 5 minutes at 1800 rpm and the top layer of fat was removed. The remaining cell pellet was washed with DMEM/F12 and then resuspended in MMEC media and redistributed into 6 well plates, approximately 2 wells for every mouse harvested.

2.2.1.2   Isolation of mammary gland tumour cells

The protocol for the isolation of tumour cells was adapted from (Derose et al., 2013).

The tumours were dissected and weighed. They were mashed for five minutes with sterile blades and transferred to a new falcon tube. 10 mL collagenase buffer per gram of tissue was added and the tissue was shaken at 37°C for 1 hour at 200 rpm. The tissue was spun at 530 xg for 5 mins. If the cell pellet was visibly red or topped by a ring of red blood cells, the tissue was resuspended in TAC solution (170 mM Tris Buffer, 150 mM ammonium chloride, pH 7.4), to lyse the red blood cells, incubated at 37°C for 5 mins and spun again. This step was repeated until all the blood was gone. The remaining tumour cells were spun at 530 xg for 5 mins and then resuspended in DMEM/F12 and filtered through a 70 µM filter. Cells were plated into HBEC media (Table 2.4). After one day, cells were transferred into MMEC media (Table 2.3) for normal cell growth.

2.2.1.3 Generation of stably transfected cell lines using retroviral transduction

For the transduction of MMECs and isolated mammary gland tumour cells, the Qiagen Effectene transfection reagent was used (Qiagen, 301427).

BOSC cells were used for virus production and were only used at early passages. BOSC cells were seeded to be 70-80% confluent the following day, and were allowed to stick down overnight. The following day, BOSC cell media was changed 1 hour before transfection.

For each plate of BOSC cells to be transfected: 150 µL EC reagent, 1 µg pCL-ECO, 2 µg plasmid, and 8 µL Enhancer reagent were mixed and incubated at room temperature for 5 mins. After this, 25 µL Effectene reagent was added and the solution was incubated for a further 15 mins at room temperature. 1 mL of BOSC media was added and the solution was added dropwise to the BOSC cells. The BOSC cells were incubated at 37°C overnight and the media was changed to fresh BOSC media the following day. The BOSC cells were incubated at 37°C for 60 hours.

The day before transduction, the cells being transduced were seeded into 6-well plates.

On the day of transduction, the media from the BOSC cells was collected and filtered through a 0.2 µM filter. Polybrene was added to give a final concentration of 1 µg/mL and the media was added to the cells being transduced. The cells were spun at 1350 rpm for 70 mins. After centrifugation, the cell media was changed to fresh MMEC media. The transduction process was repeated the following day.

When transduced cells reached 70% confluent, antibiotic selection was started using the concentrations of antibiotic described in Table 2.2. Non-transduced cells were also treated with antibiotics to indicate when the cells were fully selected for the presence of the added plasmid.

2.2.1.4 siRNA transfection of isolated tumour cells using DharmaFECT reagent

siRNA transfection was performed according to the protocol specified by Dharmacon, using the quantities suggested.

Briefly, the day before siRNA transfection, the cells being transfected were seeded so that they were approximately 70% confluent the following day. On the day of transfection two solutions were prepared. In tube one, the siRNA stock solution was diluted into serum-free media to give a final concentration of 25 nM. In tube two, DharmaFECT reagent was added to serum-free media. Each tube was incubated for 5 mins at room temperature. After this, tube one was added to tube two, and the solution was incubated at room temperature for a further 20 mins. The siRNA solution was added to MMEC media (Table 2.3) and added to the cells. To reduce toxicity, cell media was changed to following day to MMEC media.

2.2.1.5 Preparation of dialysed serum

In specific cases where estrogen-free media was required or during metabolomics studies, when the concentration of small molecules needs to be controlled for, dialysed serum was used in the cell media. To do this, 100 mL serum was sealed in Snakeskin dialysis tubing (3.5K MWCO, Life Technologies, 68035) and incubated in 6 L PBS-CMF for 72 hours at 4°C. The PBS-CMF was changed every 12 hours.

This procedure reduces the concentration of any small molecules such as amino acids, hormones and cytokines.

2.2.2 Cell enumeration and apoptosis assays

2.2.2.1 Cell mass detection by crystal violet staining

Cells were washed with PBS and fixed and stained with crystal violet staining solution (5% crystal violet powder in 20% methanol). Fixed cells were incubated for 30 mins at room temperature and then excess staining solution washed away with water.

To quantify crystal violet staining, the stained wells were lysed in crystal violet lysis buffer (Sorenson's buffer: 5M sodium chloride in 50% Ethanol, pH 4.2) on a rocker for 30 mins. A plate reader (Tecan Infinite M1000 Pro) was used to read the absorbance of the crystal violet stain at 570 nm.

2.2.2.2   Cell confluency detection by the Incucyte FLR imaging system

Cells were plated at a low density into black, clear-bottomed 96-well plates and incubated in an incucyte FLR imaging system, to gain an initial reading. The cells were allowed to stick down overnight. Fresh media containing any treatment was added to the cells carefully to prevent too much disruption of the cells. Cell confluency was recorded by the incucyte FLR imaging system. Images were taken every 3 hours for 72 hours.

2.2.2.3   Cell apoptosis quantification by Caspase-3 fluorescent staining

Cells were plated at a low density into black, clear-bottomed 96-well plates and incubated in an incucyte FLR imaging system, to gain an initial reading. The cells were allowed to stick down overnight. To detect apoptosis, NucView 488 Caspase-3 substrate was added to the media. This dye enters the cytoplasm and is cleaved by Caspase-3/7 during apoptosis, releasing the high affinity DNA dye, which then migrates to the cell nucleus and stains DNA with green fluorescence (Cen et al., 2008). Fluorescence was detected by the incucyte FLR imaging system. Images were captured every 3 hours for 72 hours. The number of apoptotic cells detected was normalised to the cell confluence at each time point.

2.2.3 Molecular Biology Techniques

2.2.3.1 Protein quantification

Bradford Assay

Protein lysates were prepared in RIPA buffer (150 mM sodium chloride, 30 mM Tris pH 7.5, 1 mM EDTA, 1% Triton-X, 10% glycerol, 0.1 mM PMSF, 0.5 mM DTT, protease inhibitor cocktail, phosphatase inhibitor cocktail).

To ensure that the samples used for western blotting were the same concentration for equal protein loading, protein samples were quantified using a Bradford assay. Tissue and cell samples were collected in RIPA buffer and kept on ice throughout. Samples were spun at 4°C at 1000 rpm for 5 mins to remove cell debris and the supernatant was transferred to a fresh tube. 2 μL of protein sample was added to 198 μL Bradford reagent. Absorbance at 595 nm was recorded and used to calculate the concentration of protein in each sample.

BCA Assay

In order to quantify protein concentration after metabolite extraction, a BCA assay was used. Dried protein pellets were dissolved in Tris-SDS buffer (62.5 mM Tris, 2% SDS, pH6.8). If samples did not dissolve when incubated at 90°C for an hour, they were briefly sonicated, in a sonicating water bath. Samples were incubated at 90°C for a further 10 mins. The BCA protein quantification kit was used. Reagent A was mixed with reagent B at a ratio of 50:1. 4 μL of protein solution was added to 70 μL of BCA reagent. The samples were incubated at 37°C for 30 mins and absorbance at 562 nm was measured and used to calculate the concentration of protein in each sample.

2.2.3.2 Western Blotting

Sample Preparation

Quantified protein samples were diluted to 1 μg/μL into 4X Laemli buffer and water and heated at 90°C for 10 mins.

SDS-PAGE

8% and 10 % SDS-PAGE gels were prepared using the following solutions.

Table 2-17 Solution for 4x 8% ad 10% Running gels

	8% Running gels	10% Running gels
Water (mL)	16.5	15
40% Acrylamide-Bis (mL)	6	7.5
1.5 M Tris pH 8.8, 0.4% SDS (mL)	7.5	7.5
10% APS (µL)	300	300
TEMED (µL)	20	20
Final Volume (mL)	30	30

Table 2-18 Solution for 4X 4% Stacking gels

	4% Stacking gels
Water (mL)	12.9
40% Acrylamide-Bis (mL)	2.1
0.5 M Tris pH 6.8, 0.4% SDS (mL)	5
10% APS (µL)	100
TEMED (µL)	20
Final Volume (mL)	20

15-20 µg of protein was loaded into each column of the gels. A precision plus protein standard was also loaded to identify protein molecular weights. Gels were run in 1X protein running buffer at 100V and 140 mA for 90 mins. 10 X protein running buffer was prepared by the Media kitchen at the Francis Crick Institute using 25 mM Tris, 192 mM glycine and 0.1% SDS, pH 8.5.

Immunoblotting

To transfer proteins from an SDS-PAGE gel to a nitrocellulose membrane, an electrophoretic transfer cell was used. The SDS-PAGE gel was removed from the glass

and rinsed in 1X transfer buffer. The gel was loaded onto the membrane and the transfer was performed at 400 mA for 120 mins at 4°C. 10 X protein transfer buffer was prepared by the Media kitchen at the Francis Crick Institute using 25 mM Tris, 192 mM glycine, 0.2% SDS and 20% methanol, pH 8.3.

To prevent non-specific binding of antibodies, the membrane was blocked in 5% milk for 60 mins at room temperature. Primary antibodies were diluted in 1% BSA/ 0.05% sodium azide / PBS-T at the dilutions given in Table 2.13. The membranes were incubated in primary antibody at 4°C overnight.

A secondary antibody conjugated to horseradish-peroxidase (HRP) was used to visualise the primary antibody bound to the protein of interest on the membrane. Secondary antibodies were diluted into 1% BSA/ 0.05% sodium azide / PBS-T at the dilutions given in Table 2.14. After the washing steps, membranes were incubated in secondary antibody for 60 mins at room temperature. The secondary antibody was visualised by chemiluminescence using the Amersham ECL detection kit (GE Healthcare, RPN2236) and detected by medical X-ray film (SLS, MOL7016). The film was developed with an automatic X-ray film processor.

2.2.3.3   PNGase F enzyme assay for protein de-glycosylation

400 μg of protein lysate (ground tumour in RIPA protein lysis buffer quantified by a Bradford assay) was made up to a final volume of 70 μL in water. 20 μL PBS and 5 μL 2% SDS with 1M 2-mercaptoethanol was added. The samples were incubated at 100°C for 5 mins. After being cooled to room temperature, 5 μL of 15% Triton X-100 was added. 4 μL PNGase F was added and the solution was incubated for 6 hours at 37°C. Cleavage was confirmed by western blotting.

2.2.3.4   Glycoprotein staining

The Pierce Glycoprotein Staining Kit was used for the visualisation of glycoproteins.

Protein samples were lysed in RIPA buffer and quantified using a Bradford assay. Samples were diluted in PBS and 4X Laemmli buffer to give samples of the same protein concentration and were boiled at 90°C for 5 mins. 20 μg of protein sample were loaded onto a 10% SDS gel and separated using SDS-PAGE based on molecular weight. A horseradish peroxidase positive control and a soybean trypsin inhibitor negative control were also loaded.

After electrophoresis, gels were fixed in 50% methanol for 30 mins. Gels were washed in 3% acetic acid for 20 mins. The gels were agitated in oxidising solution for 15 mins. They were then washed with 3% acetic acid for 15 mins before being incubated in glycoprotein staining reagent for 15 mins. Gels were transferred to reducing solution for 5 mins before being washed extensively in 3% acetic acid for 16 hours.

After imaging, the gels were incubated in coomassie for an hour to visualise total protein loading on each gel.

2.2.3.5 Fixed tissue preparation

Tissue pieces were incubated in 4% PFA overnight and then stored in 70% ethanol. The samples were embedded in wax and sliced at 5 μM and stuck onto slides. The Experimental Histopathology Platform at the Francis Crick Institute performed the embedding and cutting procedures.

2.2.3.6 Immunofluorescence in fixed tissue

Tissues samples were dewaxed in Xylenes for 20 mins, and then rehydrated in decreasing concentrations of ethanol as follows:
- 100% Ethanol, 10 mins,
- 95% Ethanol, 5 mins,
- 70% Ethanol, 5 mins,
- 50% Ethanol, 5 mins,

Slides were submerged in 10 mM sodium citrate buffer, pH 6.0 and boiled for 17 mins. The slides were cooled to room temperature and washed in PBS. Slides were blocked for 10 mins in blocking solution (1% BSA in PBS-T, 0.05% sodium azide). Primary antibody was diluted into blocking solution and added to slides. Slides were incubated in a humidified chamber at 4°C overnight. The following day, slides were washed with PBS and then incubated in secondary antibody diluted in blocking solution, in the dark. Slides were washed in PBS and then vectashield containing DAPI was added and a coverslip placed over the slides.

2.2.3.7 Immunofluorescence in fixed cells

Cells were plated into chamber slides (1000 cells/well). After the experiment, the cells were fixed in 4% PFA for 10 mins at room temperature. The cells were washed with PBS and then permeabilised in 1% Triton X-100 for 10 mins. The cells were blocked for 1 hour at room temperature in blocking solution (1% BSA in PBS-T, 0.05% sodium azide). Cells were incubated overnight in primary antibody in blocking solution at 4°C in a humidified chamber. The following day, slides were washed with PBS and then incubated in secondary antibody diluted in blocking solution, in the dark. Slides were washed in PBS and then vectashield containing DAPI was added and a coverslip placed over the slides.

2.2.3.8 RNA isolation from tissue and cell samples

Tissue and cell samples were collected in 500 μL TRIzol reagent and kept on ice. 100 μL chloroform was added and the samples were shaken vigorously by hand for 15 secs. The samples were incubated for 3 mins at room temperature. The samples were spun at 12 000 xg for 25 mins at 4°C. After centrifugation, the aqueous phase was transferred into a new tube.

250 μL 100% isopropanol was added to each sample and the samples were incubated at room temperature for 10 mins. The samples were spun at 12 000 xg for 10 mins at 4°C. After centrifugation, the supernatant was removed to leave the RNA pellet. The pellet

was washed with 1 mL 75% ethanol and vortexed briefly. The samples were spun at 7500 xg for 5 min at 4°C. The wash was discarded and the pellet was left to air-dry for 10 mins in a fume hood. The dry pellet was resuspended in RNAse-free water and incubated at 55°C for 15 mins.

RNA concentration was measured using a NanoDrop spectrophotometer.

2.2.3.9   Complementary DNA synthesis

Total RNA was used to generate its complementary DNA (cDNA) with MultiScribe Reverse Transcriptase, using the high capacity cDNA reverse transcriptase kit (Thermo Fisher Scientific, 4368814). 1 µg of RNA was added to 2 µL 10X RT buffer, 0.8 µL 25X dNTP mix (100 mM), 2 µL 10X RT random primers and 1 µL MultiScribe Reverse Transcriptase. The final volume was made up to 20 µL using RNAse-free water.

The PCR conditions were as follows
-   25°C for 10 mins,
-   37°C for 120 mins,
-   85°C for 5 secs,
-   4°C indefinitely,

2.2.3.10 Quantitative Real-Time PCR

Quantitative Real-time PCR was used to quantify gene expression, using Taqman gene expression assays.

Each reaction included 1 µL of cDNA, 1 µL Taqman probe, 10 µL Master Mix and 8 µL RNAse-free water. Negative controls such as non-template controls were included in every run. Samples were run on an Applied Biosystems ViiA 7. Data were analysed using the delta-delta Ct method.

2.2.4   Metabolomics techniques

2.2.4.1   Bolus injections

Mice were administered a bolus of stable isotope labelled substrates via tail-vein injections. The labelled substrates were administered at the concentrations and injection regimens in the table below (Table 2.19). 15 minutes after the final injection, mice were terminally anaesthetised. Blood samples were collected by cardiac puncture, incubated at 4°C for 15 minutes, and spun at 2000 xg for 15 mins. The supernatant (serum) was collected and snap frozen in liquid nitrogen. After cardiac puncture, the mice were culled via cervical dislocation and tissue samples were quickly dissected and snap frozen. Samples used for metabolomics analyses were clamped in liquid nitrogen to ensure rapid quenching of metabolism.

All of the mice injected in this project were injected by Andres Mendez Lucas and Mariia Yuneva.

Table 2-19 Bolus injection regimens

Compound	Conc: bolus injections	Number injections	Time between injections	Time between last injection and sample collection
$^{13}C_6$-glucose	200 mg/mL	1	-	15 mins
$^{13}C_5$-glutamine	40 mg/mL	2	15 mins	15 mins
$\alpha^{15}N$-glutamine	40 mg/mL	2	15 mins	15 mins

2.2.4.2   Polar Metabolite Extraction

<u>Cells</u>

Cell metabolite samples were kept on ice for all stages of extraction. Cells were cultured in 6-well plates and incubated in $^{13}C_5$-glutamine media (Table 2.7).

After labelling, cell plates were put on ice and washed twice with ice-cold PBS. Cell metabolism was quenched using 500 µL cold methanol containing 1 µL of 1 mM scylloinositol (1 nmole per sample) added directly to the cells in the 6-well plate. Cells were scraped into 2 mL Eppendorf tubes. A further 250 µL methanol was used to wash the well and scrape any remaining cells into the same tube. 250 µL ultrapure water and 250 µL chloroform were added to cell pellet to give 1:3:1 chloroform: methanol: water. Cell samples were vortexed for 15 mins and incubated for 1 hour at 4°C with periodic sonication. The samples were spun for 20 mins at 4°C at 16 000 rpm. The supernatant was transferred into new 2 mL Eppendorf and dried in a speed vacs.

The remaining cell pellet was re-extracted using 200 µL methanol and 100 µL ultrapure water. The samples were vortexed for 15 mins and incubated for 1 hour at 4°C with periodic sonication. The samples were spun for 20 mins at 4°C at 16 000 rpm. The supernatant was transferred into the same tube as the previous dried supernatant and dried in a speed vacs. Once dry, the dried supernatant was resuspended in 50 µL chloroform, 150 µL methanol and 150 µL ultrapure water (1:3:3), vortexed and spun at 4°C for 20 mins at 16 000 rpm. The polar phase was transferred into GC vial inserts and dried in a speed vacs, the lower lipid phase was discarded. Cell metabolites were derivatised before GC-MS analysis using the protocol described below (Chapter 2.2.4.3).

Remaining cell pellets were dried briefly in the speed vacs. The protein content of the protein pellets was measured using a BCA protein assay described above (Chapter 2.2.3.1).

Serum

300 µL methanol containing 1 µL of 1 mM scylloinositol (1 nmole per sample) and 100 µL chloroform were added to 5 µL serum. The sample was vortexed and spun. The supernatant was transferred to a GC vial insert and dried in a speed vacs. Serum metabolites were derivatised before GC-MS analysis using the protocol described below (Chapter 2.2.4.3).

<u>Tissue</u>

After snap freezing, tissue samples were ground into a fine powder using a pestle and mortar in liquid nitrogen. Ground samples were stored at -80°C.

Approximately 5 mg of tissue was added to 15 mL falcon tubes, stored on ice. 1 mL chloroform: acetonitrile (1:1, v/v) containing 1 µL of 1 mM scylloinositol (1 nmole per sample) was added and the tubes were vortexed for 15 s. The samples were incubated for 1 hour at 4°C with periodic sonication. 1.5 mL chloroform, 0.5 mL acetonitrile and 1.5 mL ultrapure water were added and each sample was vortexed for a further 15s and then spun at 4000 xg for 20 mins at 4°C. The phases were separated into fresh 2 mL Eppendorf tubes. The lipid phase was discarded and the polar phase was used for all subsequent steps.

The remaining tissue pellet was re-extracted using 0.5 mL chloroform: acetonitrile (2:1, v/v), 0.5 mL chloroform and 0.5 mL ultrapure water. The samples were vortexed for 15s, incubated for 1 hour at 4°C with periodic sonication. They were spun at 4 000 xg for 20 mins at 4°C. The phases were separated into the same tubes as before, combining both polar phases. The polar phases were dried in a speed vac. Dried samples were resuspended in 100 µL methanol and transferred into a GC vial insert and then dried again. Dried samples were derivatised before GC-MS analysis using the protocol described below (Chapter 2.2.4.3).

The remaining tissue pellets were dried at 50°C overnight and weighed to calculate the dried weight of tissue used for the extraction.

2.2.4.3   Derivatisation for GC-MS analysis of polar metabolites

The protocol for derivatisation is the same for cell, serum and tissue samples.

GC vial inserts containing extracted metabolites were washed with 60 µL methanol containing 1 µL 5 mM L-Norleucine and dried in a speed vacs. The vial inserts were washed again with 60 µL methanol and dried. 20 µL 20 mg/mL methoxyamine

hydrochloride in pyridine was added to each insert using a glass positive displacement pipette. The samples were vortexed briefly and incubated at room temperature overnight. 20 µL fresh BSTFA with TMChS was added to each sample and the samples were incubated at room temperature for an hour.

Samples were run by GS-MS using an Agilent GC-MSD (7890A-5975C). Data analysis was performed using Agilent MassHunter Quantitative Analysis software.

2.2.4.4 Sample preparation for 1D-NMR

Media

100 µL cell media was spun at 16 000 rpm for 20 mins at 4°C. The supernatant was transferred to a fresh 1.5 mL Eppendorf tube. 300 mL methanol containing 3.12 µL 50 mM DSS and 100 µL chloroform was added to the media supernatant and the samples were vortexed and spun at 16 000 rpm for 20 mins at 4°C. The supernatant was transferred into a fresh tube and dried using a speed vacs. The dried supernatant was resuspended in 160 µL Deuterium Oxide (D_2O) and transferred into an NMR vial.

Cells

To extract the polar metabolites for 1D-NMR analysis, cell samples were collected and extracted in the same way as for GC-MS analysis (Chapter 2.2.5.3), except 3.12 µL 50 mM DSS was added to the samples instead of 1 µL of 1 mM scylloinositol. Once the polar phase was dry, the samples were resuspended in 160 µL D_2O and transferred into an NMR vial.

Samples were run by 1D-NMR using a Brucker 700 mHz instrument by Paul Driscoll in the Metabolomics Platform at the Francis Crick Instrument. Sample preparation and data analysis were performed by Emma Still. Data analysis was performed using the MestReNova software for NMR.

Chapter 3.   Characterisation and metabolic profiling of ErbB2 and MYC-induced mammary gland tumours

3.1   Introduction

In order to simultaneously meet the increased energetic and synthetic needs associated with increased proliferation and survival, tumours rewire their metabolic networks. These changes in tumour metabolism have been shown to depend on both the genetic driver of the tumour as well as the tissue of tumour origin (Wise et al., 2008; Gaglio et al., 2011; Yuneva et al., 2012). Tumour cells are also known to interact with their surrounding stromal cells (Pavlides et al., 2009; Fiaschi et al., 2012; Yang et al., 2016), as well as inducing the growth of new blood vessels so they can meet their altered energetic and anabolic needs (Hanahan and Folkman, 1996). It has been shown that knocking down some of the enzymes whose expression is altered in tumours, prevents tumour growth (Wang et al., 2010; Patra et al., 2013; Xiang et al., 2015), suggesting that these enzymes might be good therapeutic targets against cancer. However, while targeting certain metabolic pathways has been shown to be effective against some tumour types, not all tumours respond in the same way. This was recently demonstrated by Maddocks et al. (2017), who observed that a serine and glycine deprivation diet reduced tumour growth in genetically engineered models of intestinal cancer, driven by APC inactivation and lymphoma driven by MYC activation, but did not alter tumour formation in KRas-driven models of pancreatic and intestinal cancers (Maddocks et al., 2017). Thus, this project aims to compare the metabolic phenotypes of two different models of mammary gland tumorigenesis, induced by different oncogenes, with the hope of identifying potential therapeutic targets against either model.

Stable isotope tracers have been widely used to map metabolic pathways and quantify fluxes in cells, tissues and organisms (Bak et al., 2007; Deberardinis et al., 2007; Fan et al., 2011). Because many metabolites are required for multiple pathways, and total metabolite concentration does not distinguish between metabolite production and consumption; quantification of metabolite concentration alone is not enough to determine how metabolites are used to fuel specific pathways. Thus, stable isotope

labelling is required to enable the flux of metabolites to be traced through specific pathways. In order to compare the metabolic phenotypes of different models of mammary gland tumorigenesis, control and tumour-bearing mice were given bolus injections of stable isotope labelled compounds through the tail vein. Metabolites were extracted and run by Gas-Chromatography Mass Spectrometry (GC-MS).

In this project, I decided to focus on changes in central carbon metabolism between the two types of tumour, as these pathways connect energy production to the generation of biosynthetic intermediates and the maintenance of the redox balance. Thus, by identifying any changes in these critical pathways, the most potent therapeutic targets could be identified. GC-MS was chosen to analyse tissue metabolites as it has a good detection sensitivity for many of the intermediates of central carbon metabolism, due to its high-chromatographic resolution. However, identifying metabolites by GC-MS in tissue extracts, requires a sample preparation step that involves several hours of drying the samples in a speed vacs at 45°C, which can result in metabolite losses. Similarly, the sample introduction system and the ionisation step can also affect specific metabolites causing their poor detection or degradation. Thus, the application of parallel techniques, such as GC-MS and LC-MS in parallel, would give a more comprehensive study of the tumour metabolome. However, in this study, GC-MS analysis alone could sufficiently detect the desired metabolites.

3.2 Chapter 3 Aims

- Optimise stable isotope labelling techniques in *in vivo* mammary gland and mammary gland tumours,
- Determine whether the metabolic profile of the mammary gland changes as the mammary gland develops,
- Characterise the phenotypic features of the MMTV-ErbB2 and MMTV-MYC models of mammary gland tumours,
- Compare the metabolic profiles of ErbB2 and MYC-induced mammary gland tumours,
- Identify differences in glutamine transporter expression between ErbB2 and MYC-induced mammary gland tumours,
- Identify if overall glycosylation changes in ErbB2 and MYC-induced tumours,

3.3 Optimisation of stable isotope labelling for mammary gland tumours and normal mammary gland controls

Before comparing the metabolic phenotypes of normal and tumour tissues, a number of factors in the study needed to be controlled for. This included confirming the injection efficiency of the administered bolus injections and determining whether tumour size effects tumour metabolism. All mice were given either one bolus of $^{13}C_6$-glucose or two boluses of $^{13}C_5$-glutamine or $\alpha^{15}N$-glutamine. 15 minutes after the last injection, mice were culled and tissue samples were snap frozen. The extracted metabolites were analysed by GC-MS.

3.3.1 Efficiency of bolus injections of stable isotope labelled substrates

The injection of labelled substrates might affect the global metabolism of the mice. To this end, I did not have tissues or serum from control animals that were not injected with any of the stable isotope labelled compounds. Nevertheless, comparison of metabolite concentration in serum from mice injected with $^{13}C_6$-glucose, $^{13}C_5$-glutamine or $\alpha^{15}N$-glutamine allowed us to conclude that a bolus injection of glucose does not

trigger a global change in metabolism (Figure 3.1). If the glucose injections were inducing an insulin-like response in the mice, I would expect their metabolic profiles to be different to the mice injected with glutamine. Moreover, I cannot detect stress signals, such as cortisone by GC-MS, and so this study does not look at the effect any stress induced by the injection is having on the metabolism of the mice.

The injection efficiency can also vary between mice and may cause differences in the amount of labelled substrate the tissues receive. To evaluate the injection efficiency, the percent labelling from each injection into metabolites in the serum was studied as this would identify any outliers with consistently high or low labelling. The individual values from each mouse are displayed in Figures 3.2-4, showing the concentration and percent labelling of serum metabolites after $^{13}C_6$-glucose, $^{13}C_5$-glutamine or $\alpha^{15}N$-glutamine bolus injections. Representative metabolites are shown.

These data were analysed using the ROUT method to detect outliers by fitting the data to a curve with non-linear regression (Motulsky and Brown, 2006). Q, the maximum desired false discovery rate was set to 1%. This analysis did not reveal any outliers from the concentration or percent labelling of serum metabolites and so no tumour samples were disregarded during this study, as all the injections were determined to have been at a similar efficiency. Any identified outliers would have been removed from the study as it would be difficult to determine if the metabolic features identified in the tissues were due to the tissue or the injection efficiency.
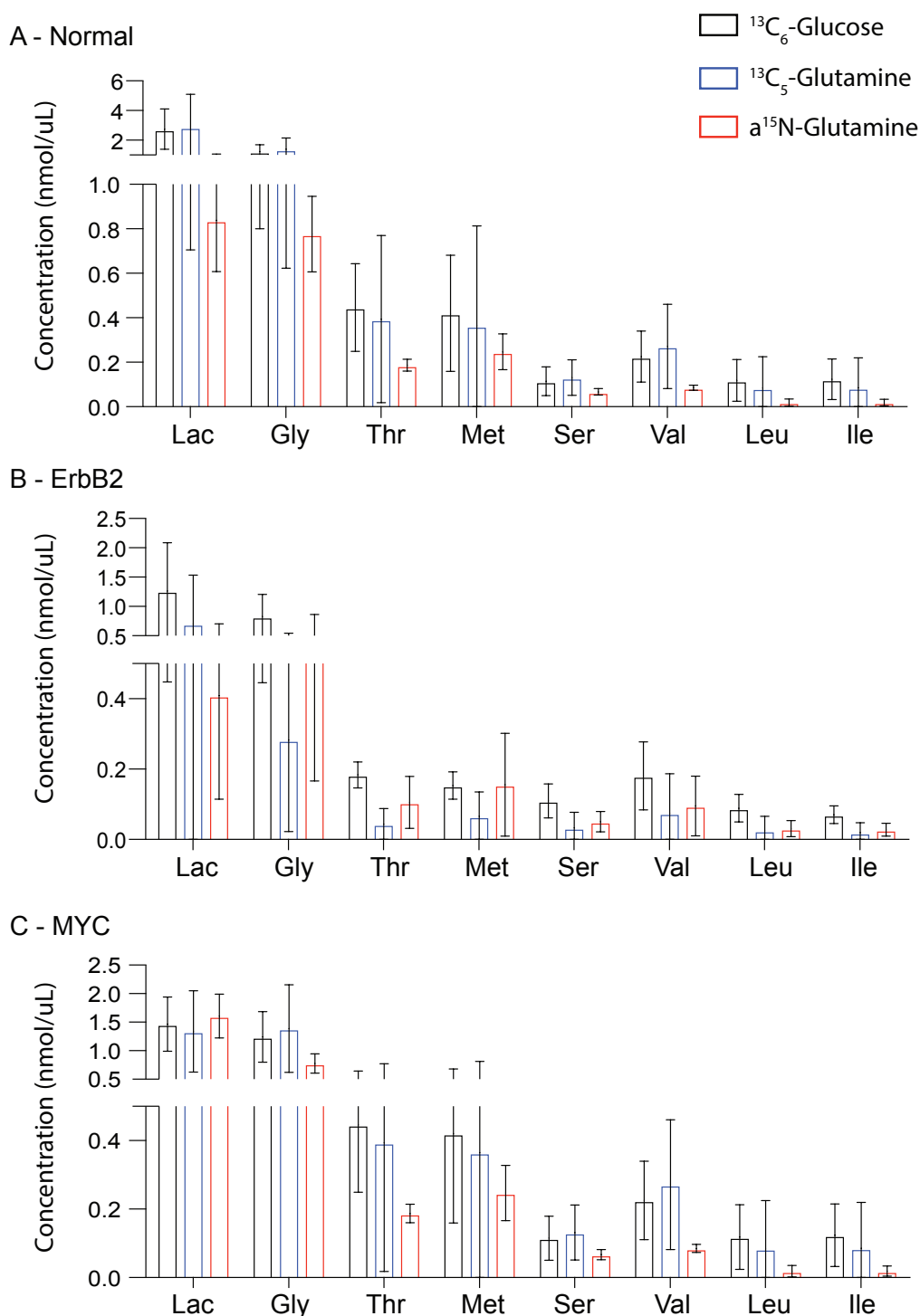
Figure 3-1 The injection of different stable isotope labelled substrates does not affect the concentration of serum metabolites

Total concentration of serum metabolites in healthy mice (A) and mice bearing ErbB2 (B) and MYC (C) –induced tumours. Concentration is expressed as nmol of metabolite per μL serum. n = 4-6 mice per group. Error bars denote standard deviation. Lac = lactate, Gly = glycine, Thr = threonine, Met = methionine, Ser = serine, Val = valine, Leu = leucine, Ile = isoleucine,
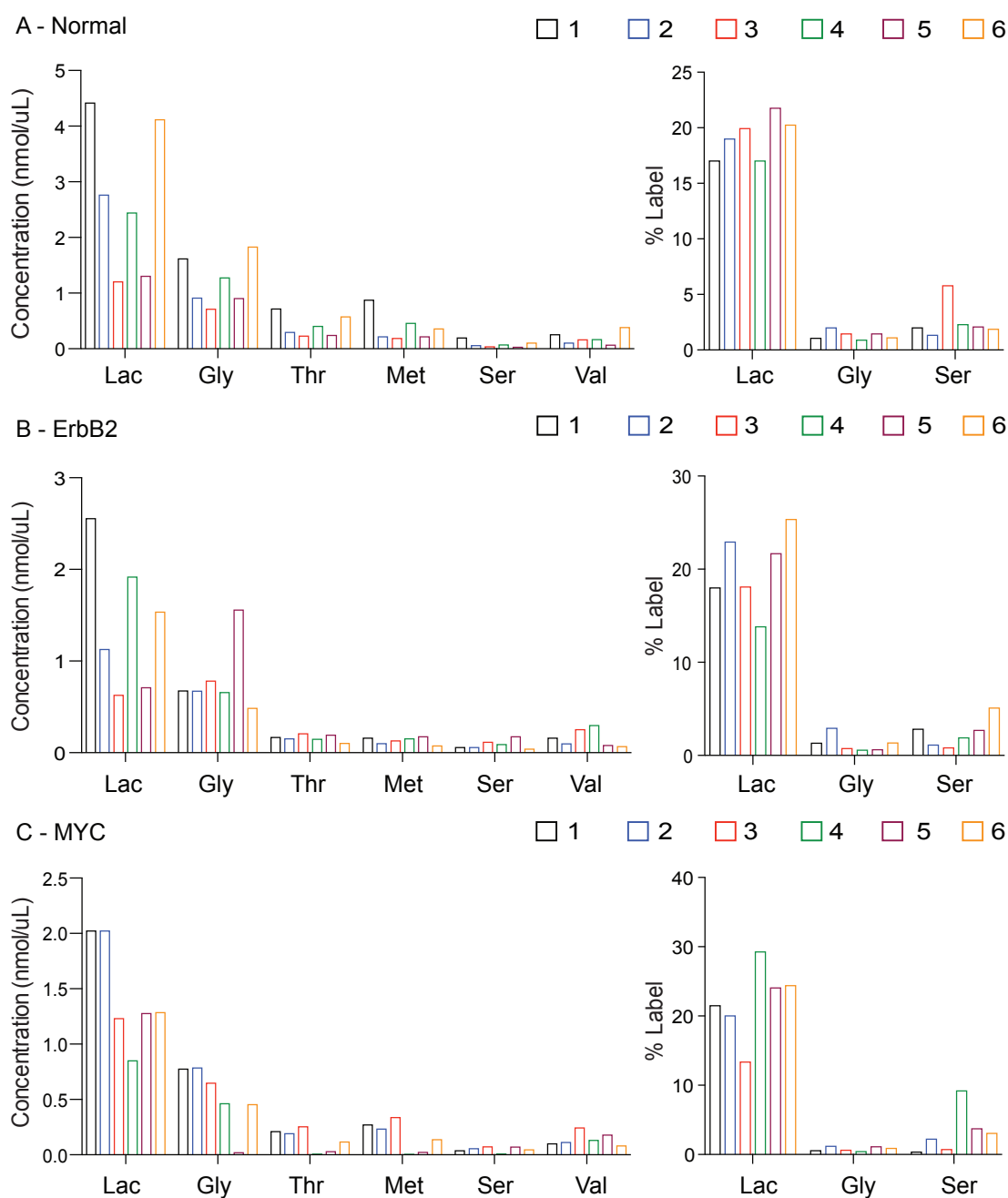
Figure 3-2 The efficiency of the $^{13}C_6$-glucose bolus injections was consistent between mice

Total concentration and percent label from $^{13}C_6$-glucose of serum metabolites in healthy mice (A) and mice bearing ErbB2 (B) and MYC (C) –induced tumours. 1-6 represents each individual mouse. Concentration is expressed as nmol of metabolite per μL serum. Percent label represents the sum of all isotopomers except M+0.

Lac = lactate, Gly = glycine, Thr = threonine, Met = methionine, Ser = serine, Val = valine,
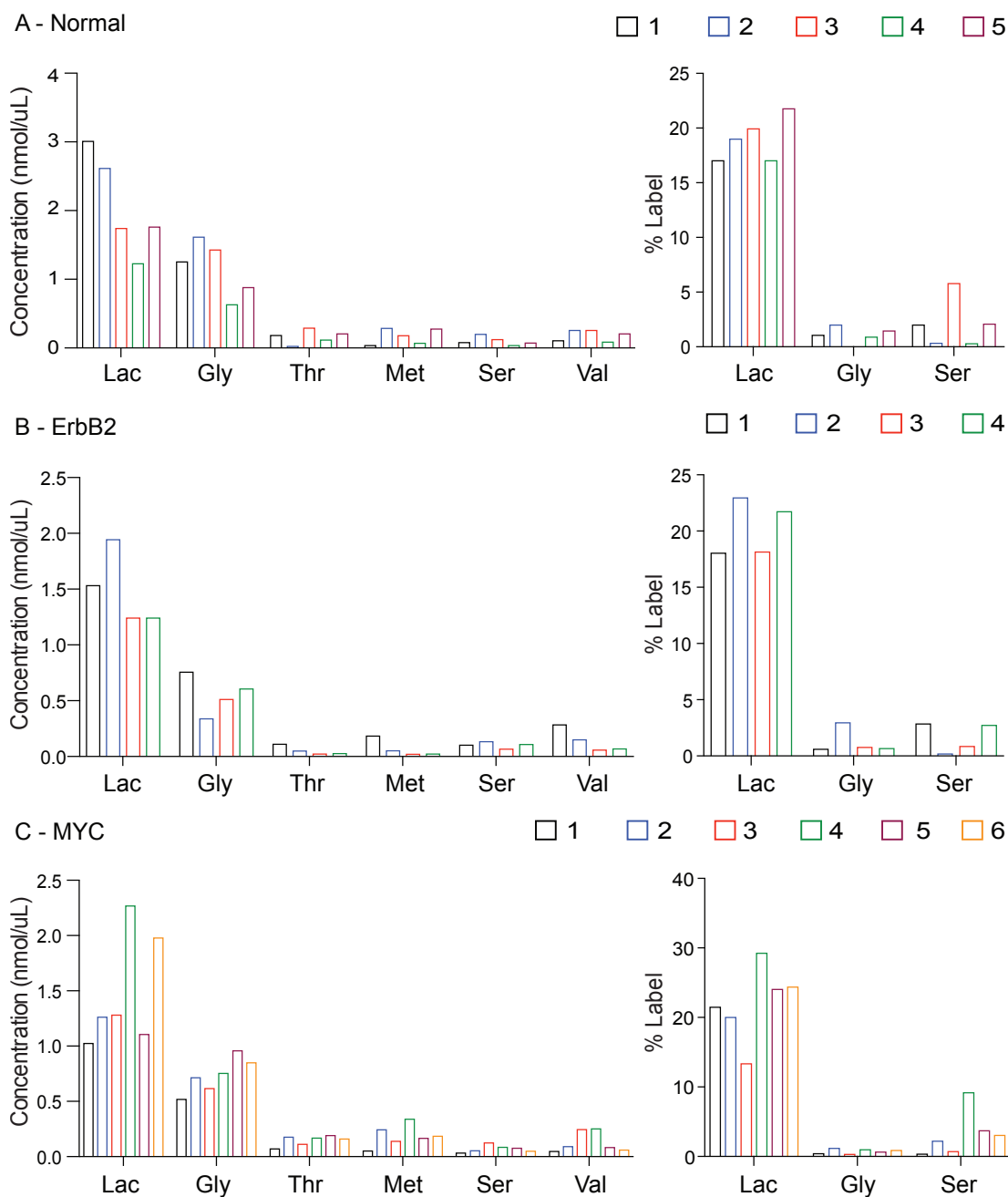
Figure 3-3 The efficiency of the ^{13}C$_5$-glutamine bolus injections was consistent between mice

Total concentration and percent label from ^{13}C$_5$-glutamine of serum metabolites in individual healthy mice (A) and mice bearing ErbB2 (B) and MYC (C) –induced tumours. 1-5 represents each individual mouse. Concentration is expressed as nmol of metabolite per µL serum. Percent label represents the sum of all isotopomers except M+0.

Lac = lactate, Gly = glycine, Thr = threonine, Met = methionine, Ser = serine, Val = valine,
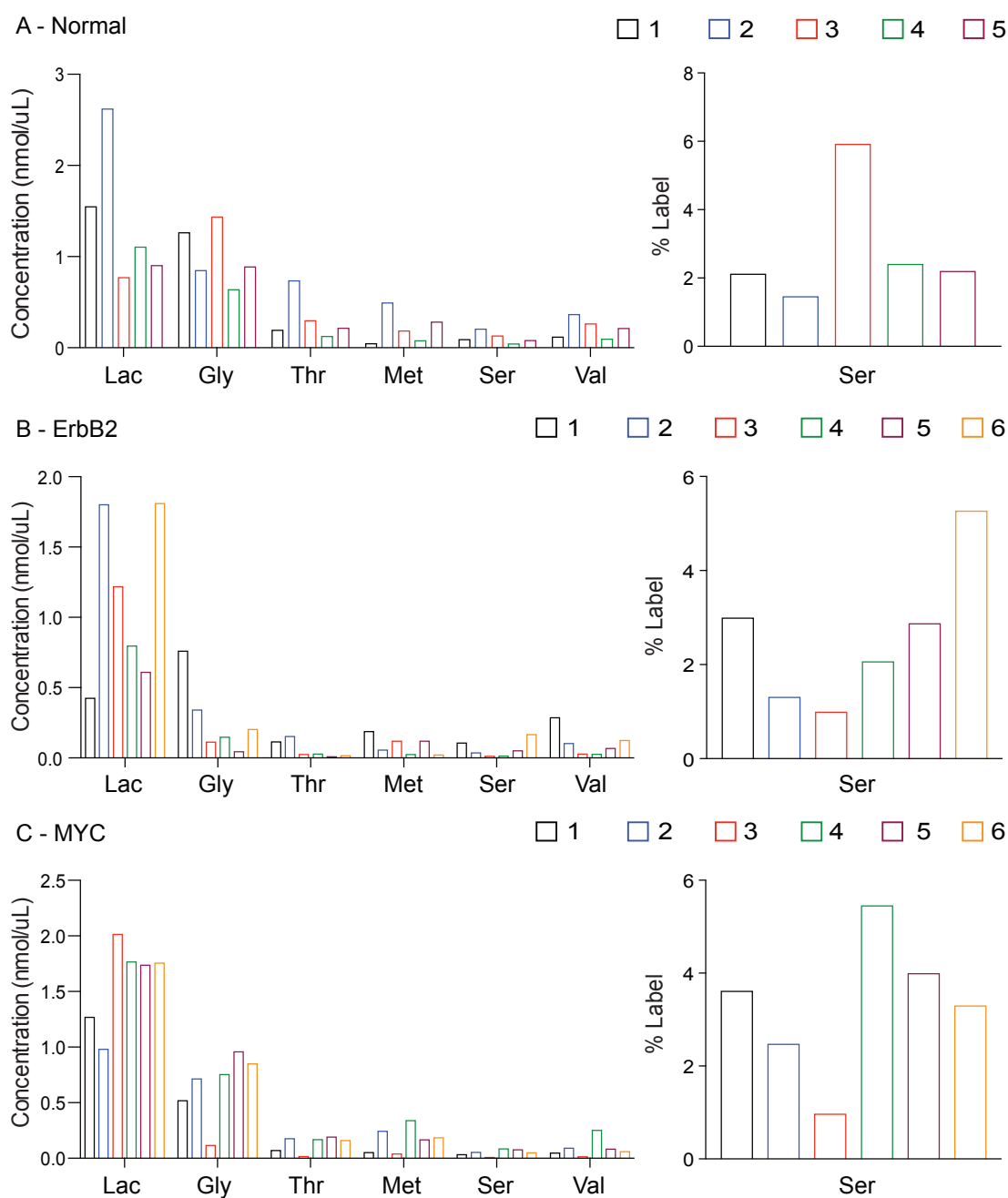
Figure 3-4 The efficiency of the α^{15}N-glutamine bolus injections was consistent between mice

Total concentration and percent label from α^{15}N-glutamine of serum metabolites in healthy mice (A) and mice bearing ErbB2 (B) and MYC (C) –induced tumours. 1-5 represents each individual mouse. Concentration is expressed as nmol of metabolite per μL serum. Percent label represents the sum of all isotopomers except M+0.
Lac = lactate, Gly = glycine, Thr = threonine, Met = methionine, Ser = serine, Val = valine,

3.3.2 Tumour size affects the metabolic profile of MMTV-ErbB2 tumours

Another factor to consider before comparing the metabolic phenotype of both tumour types was if the size of the tumour would affect their metabolic profiles. The ability of the labelled compound to penetrate the tumour may be altered in larger tumours. As tumours grow, parts of the tumour may develop away from blood vessels, creating regions within the tissue with different oxygen and nutrient availability or the cellular composition of a tumour may change (Helmlinger et al., 1997; Carmona-Fontaine et al., 2017). To determine if the metabolic profile of a tumour depends on its size, MMTV-ErbB2 mice bearing tumours measuring either 1 cm or 1.5 cm in diameter were given bolus injections of either $^{13}C_6$-glucose or $^{13}C_5$-glutamine. Data was normalised to the dry weight of the tissue extracted to account for any differences in loading.

The concentration of several metabolites, including succinate, fumarate, alanine, proline and serine was lower in the smaller tumours compared to the bigger ones, demonstrating that size can impact the metabolic profile of the tumour (Figure 3.5A). The percent labelling from $^{13}C_6$-glucose and $^{13}C_5$-glutamine was consistent between the different sizes of tumours, showing that while the overall concentration of these metabolites had changed, the proportion being produced from glucose and glutamine remained the same. These results demonstrate that the catabolism of glucose and glutamine increases as tumours get larger. This might indicate that in larger tumours, the tumour cells themselves are different, where the cells could have accumulated more mutations due to genetic instability or could be more proliferative or metastatic, increasing their energetic and biosynthetic requirements. However, as this study takes an average of the whole tumour, the metabolic differences observed between small and larger tumours might also indicate a change in the quality and composition of the tumours at different sizes. These changes could reflect a shift in the ratio of well vascularised cells to hypoxic and necrotic cells. Current work is being done using mass spectrometry imaging (MSI) techniques, to study how cell metabolism and the metabolic interactions between different cell types changes across tumour slices (Randall et al., 2016; Tillner et al., 2017).

In order to study how metabolism changes as a tumour develops, tumours taken at several different stages could be studied. This would identify at which stage the tumours would be most sensitive to a therapeutic strategy against a particular metabolic enzyme or could identify enzymes that are required at all stages of tumour development. Based on the data in Figure 3.5, all future experiments were performed on mice bearing tumours 1 cm in diameter, to ensure that any differences in the metabolic profile observed are due to the different oncogenic drivers and not the size of the tumours.
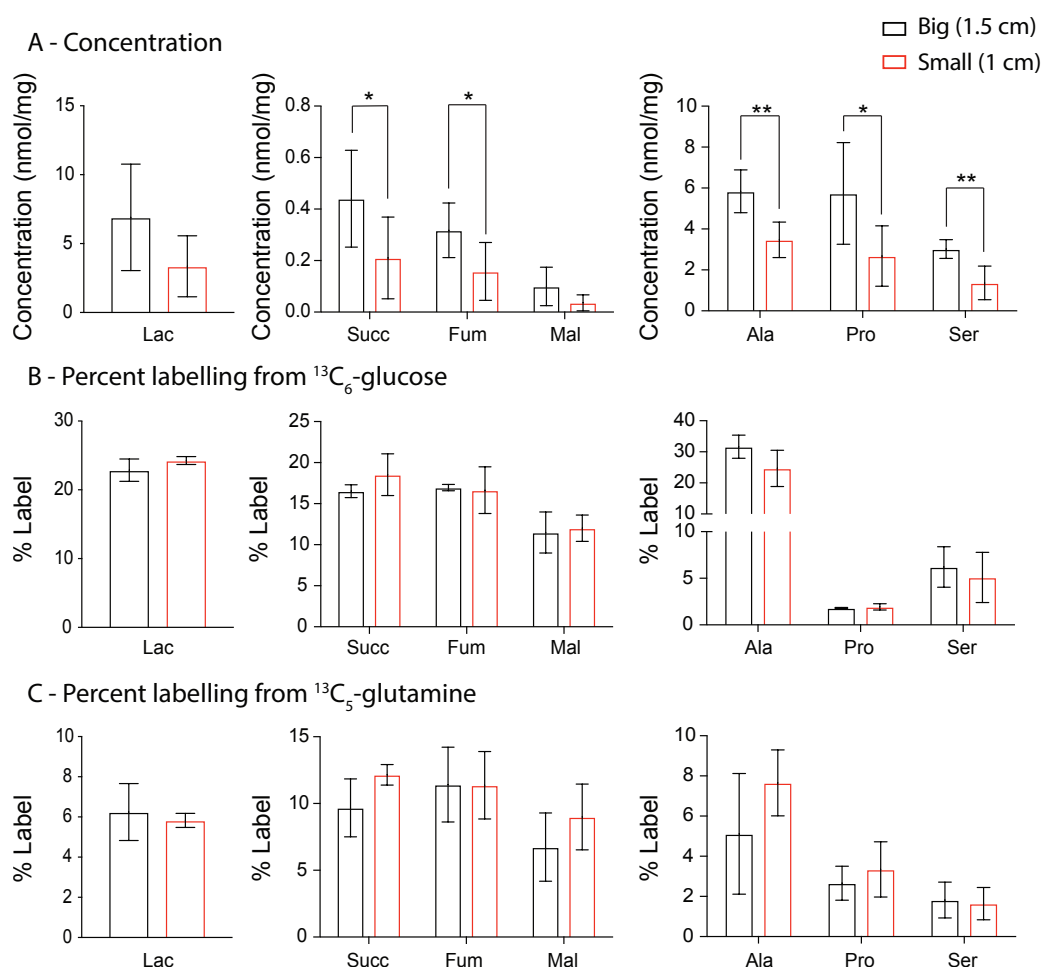
Figure 3-5 Bigger tumours have altered metabolic profiles compared to smaller tumours

A – Total concentration of metabolites in big (1.5 cm) and small (1 cm) ErbB2-induced mammary gland tumours. Concentration is expressed as nmol of metabolite per mg of cell protein.
B + C – Percent ^{13}C labelling from $^{13}C_6$-glucose (B) and $^{13}C_5$-glutamine (C) (sum of all isotopomers except M+0).
Lac = lactate, Succ = succinate, Fum = fumarate, Mal = malate, Ala = alanine,
Pro = proline, Ser = serine,
n = 3 mice per group. Unpaired t-test * $P < 0.05$, ** $P< 0.01$, Error bars denote standard deviation.

3.4 The metabolic phenotype of the normal mammary gland changes with age

While evaluating the metabolic remodelling that occurs during transformation, the metabolism of a tumour is compared to the metabolism of a normal tissue counterpart. However, it is not always clear what the appropriate control tissue is. The normal mammary gland, for example, is a complex tissue consisting of several different cell types, including basal and luminal epithelial cells and adipose cells. The mammary gland goes through several stages of development, during puberty, pregnancy and lactation. Prior to puberty, the mammary gland develops in line with the rest of the body in a stage of hormone-independent growth, but during puberty, the mammary gland enters a phase of rapid growth and proliferation to form a branched network of epithelial ducts. After puberty, the growth of the mammary gland becomes hormone-dependent, undergoing further ductal elongation and branching with recurrent estrous cycles.

In the ErbB2 and MYC-induced mammary gland tumours compared in this project, the oncogene of interest is under the control of the MMTV promoter. This promoter contains response elements to glucocorticoids, androgens and progesterone, which are regulated by the estrous cycle in virgin mammary glands (Menezes et al., 2014). The promoter has its highest expression during pregnancy and lactation, but is also expressed during mammary gland development and is potentially activated during embryonic development (Wagner et al., 2001). The activity of the promotor increases during puberty, with the rapid changes in hormone levels, and remains active in adult, virgin mice (Otten et al., 1988; Aupperlee et al., 2013). Puberty in the wild-type mice used in this project begins when the mice are approximately 6 weeks old (Maclennan et al., 2011).
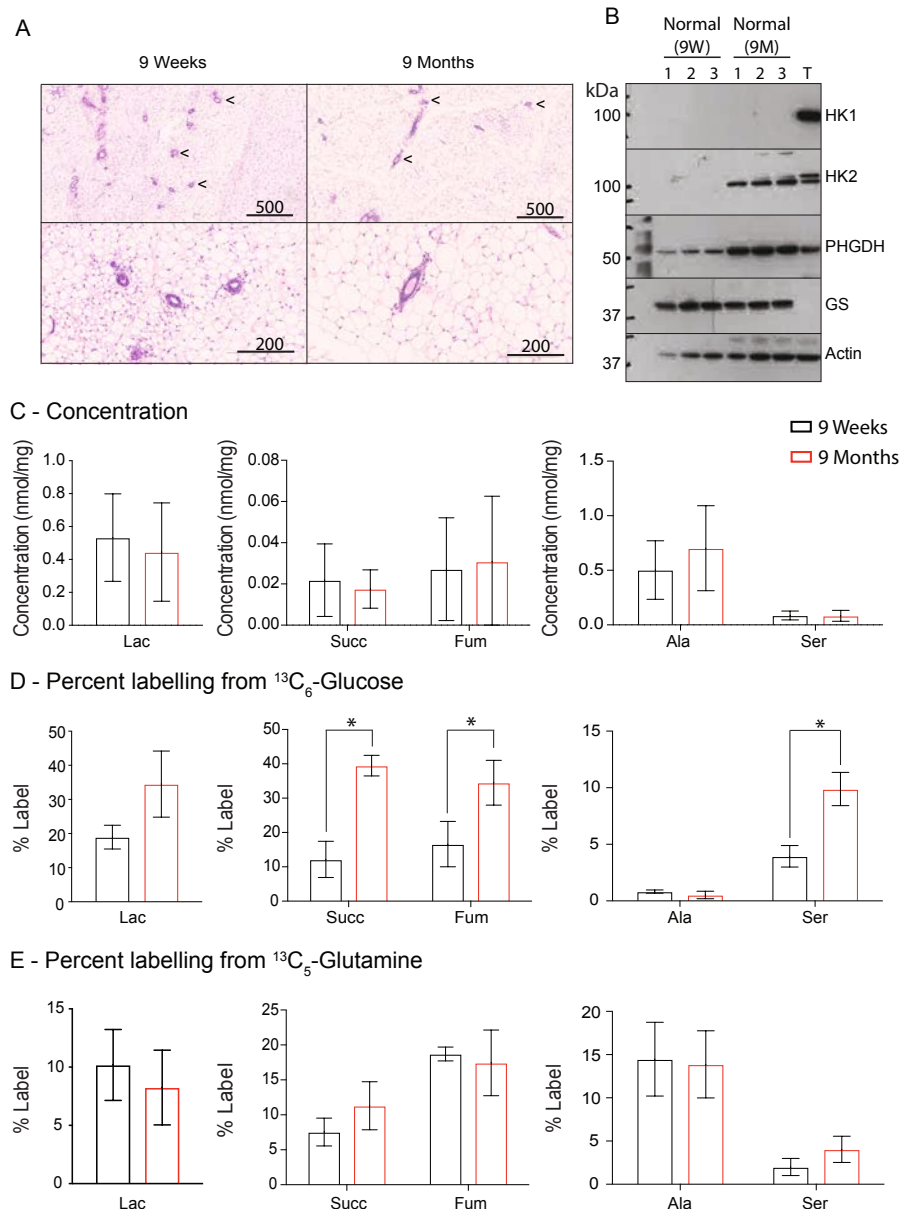
Figure 3-6 The mammary gland in 9-month old mice is histologically and metabolically different to the mammary gland in 9-week old mice

A – H&E stained slices of mammary glands from 9-week and 9-month old mice. Scale bars: top: 500 µM, bottom: 200 µM. Images representative of 3 different tissues taken from 3 different mice. Epithelial ducts indicated by <.

B – Protein expression of metabolic enzymes in mammary glands from 9-week (9 W) and 9-month (9 M) old mice. An ErbB2-induced tumour sample (T) is included as a positive control for the antibodies. Replicates are three different tissues taken from three different mice.

C – Total concentration of metabolites in mammary glands from 9-week and 9-month old mice. Concentration is expressed as nmol of metabolite per mg of cell protein.

D – Percent ^{13}C labelling from $^{13}C_6$-glucose (sum of all isotopomers except M+0).

E – Percent ^{13}C labelling from $^{13}C_5$-glutamine (sum of all isotopomers except M+0).

Lac = lactate, Succ = succinate, Fum = fumarate, Ala = alanine, Ser = serine,

n = 3 mice per group. Unpaired t-test * $P < 0.05$, Error bars denote standard deviation.

In order to identify whether the metabolism of the normal mammary gland changes between the time of tumour initiation to the time when the tumours have developed, mammary gland samples were collected from mice going through puberty (9 weeks), when the activity of the MMTV promoter is first initiated by progesterone, and mice age-matched to the tumour-bearing mice (9 months).

The histology of the mammary gland shows that between 9 weeks and 9 months, the epithelial ducts (indicated by <) elongate and the surrounding adipose cells increase in size (Figure 3.6A). To determine the metabolic profiles of these tissues, 9-week and 9-month old mice were given bolus injections of $^{13}C_6$-glucose and $^{13}C_5$-glutamine, and the mammary gland samples were analysed by GC-MS.

Glucose catabolism via glycolysis produces pyruvate, which can be used for acetyl-CoA synthesis, which feeds carbons into the TCA cycle, alanine synthesis and lactate production. Serine is produced from the oxidation of the glycolytic intermediate 3-phosphoglycerate, and so also receives carbons from glucose. Increased lactate production from glucose via aerobic glycolysis is frequently observed in tumours (Liberti and Locasale, 2016). Glutamine can also donate carbons to the TCA cycle, through the production of αKG. Cycling of malate in the TCA cycle using malic enzymes enables the production of pyruvate from malate, enabling the carbons donated to the TCA cycle from glutamine to feed into pyruvate, and thus, produce alanine.

The concentration of lactate, succinate, fumarate, alanine and serine did not change between the different ages of mammary gland (Figure 3.6C). However, the percent labelling into lactate from $^{13}C_6$-glucose increased in the older mammary glands. Likewise, the labelling into succinate and fumarate from $^{13}C_6$-glucose is higher in the older mammary glands (Figure 3.6D). This correlates to the increased HK2 protein expression observed in this tissue (Figure 3.6B), demonstrating that glucose catabolism into the TCA cycle increases in the mammary gland from the older mice. While the percent labelling into alanine from $^{13}C_6$-glucose does not change, the percent labelling into serine from $^{13}C_6$-glucose is higher in the tissue from the older mice. This correlates with the increased PHGDH expression observed, suggesting that serine biosynthesis

increases in older mammary gland tissue. The labelling from $^{13}C_5$-glutamine was not significantly altered between the two tissues (Figure 3.6E), suggesting that glutamine catabolism does not change in older mice. The expression of glutamine synthetase (GS) in both ages of mammary gland tissue is also approximately equal, suggesting that glutamine production is fairly similar in the mammary gland at both ages. However, to confirm this, the labelling of $^{13}C_6$-glucose into glutamine would need to be studied.

These data demonstrate that while mammary glands from 9-month old mice have similar glutamine metabolism to those in 9-week old mice, their glucose metabolism is different. These metabolic differences could be due to the change in the composition of the tissue at the different ages, where the epithelial ducts are larger in the adult mice. Adipose cells have a unique metabolism as they store energy in the form of lipids, and so these changes could reflect a change in the size and development of the adipocytes. This increased glycolysis might also reflect differences in the proliferation of the different cells composing the normal mammary glands. However, it is difficult without Ki67 staining, to identify which cells are more proliferative. Thus, it is difficult to understand these changes in the metabolic profiles of the mammary gland at different ages without further studies. To identify if there are common metabolic features associated with mammary gland proliferation, opposed to tumorigenesis, the activity of metabolic pathways can be studied when mammary gland proliferation is induced through pregnancy and lactation.

The mammary gland is not unique in its multicellular composition. Thus, more work needs to be done within the field, to identify and study the specific cell of tumour origin, in order to identify how these cells alter their metabolic profiles as they become tumorigenic.

3.5 ErbB2 and MYC-induced mammary gland tumours are phenotypically distinct

The metabolic phenotype of tumours is dependent on the genetic alterations driving the tumour and the tissue of tumour origin (Yuneva et al., 2012), as well as the interaction of the tumour with the stroma and its nutrient supply (Pavlides et al., 2009; Fiaschi et al., 2012; Yang et al., 2016). In order to determine how different oncogenes regulate the metabolism of mammary gland tumours, two mouse models of mammary gland tumorigenesis induced by different oncogenes were selected. These oncogenes were determined based on their known interactions with a number of metabolic enzymes (Yoon et al., 2007; Wise et al., 2008; Liu et al., 2012), their high incidence in breast cancer (Slamon et al., 1989; Deming et al., 2000) and the difficulties associated with treating tumours with high ErbB2 and MYC activity (discussed in Chapter 1) (Pohlmann et al., 2009; Miller et al., 2011; Horiuchi et al., 2012). In both models, the oncogene of interest was under the control of the MMTV promoter, which is expressed in mammary epithelial cells, as well as having some off-target expression in the salivary glands and intestine (Ahmed et al., 2002; Taneja et al., 2009). The MMTV-ErbB2 mammary gland tumour model expresses a mutant form of human ErbB2, V664D. This mutant is constitutively active and so no longer needs ligand binding and receptor dimerisation to activate downstream signalling pathways (Ursini-Siegel et al., 2007). The MMTV-MYC model of mammary gland tumorigenesis overexpresses the mouse MYC oncogene.
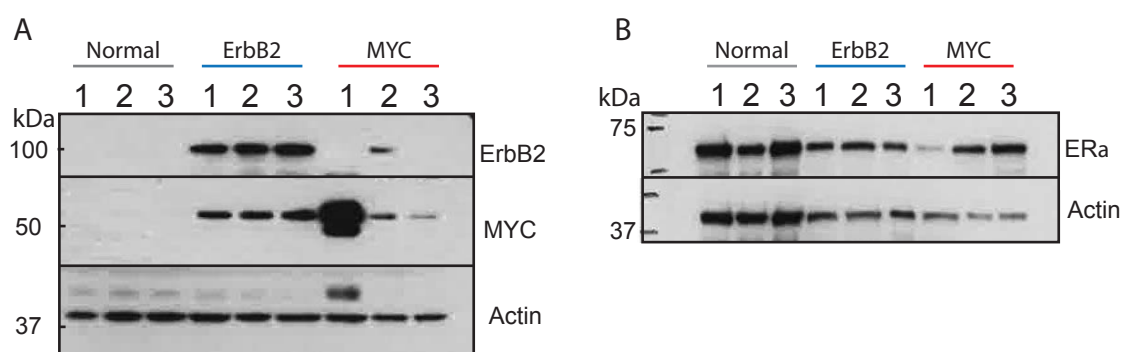
Figure 3-7 Protein expression of ErbB2, MYC and ERα in ErbB2 and MYC-induced mammary gland tumours

Protein expression of ErbB2 (A), MYC (A), and ERα (B) in normal mammary gland tissue from wild-type mice (9 months) and ErbB2 and MYC-induced mammary gland tumours (ErbB2/MYC). Biological triplicates are shown (tissues from three different mice per group).

ErbB2 protein expression was confirmed in the ErbB2-induced tumour model, and was absent or lower in MYC-induced tumours (Figure 3.7A). This ErbB2 expression was localised to the cytoplasm and plasma membrane (Figure 3.9), consistent with ErbB2 being a receptor tyrosine kinase and functional at the plasma membrane (Gusterson et al., 1987). Increased MYC protein expression compared to the normal mammary gland was observed in both ErbB2 and MYC-induced tumours (Figure 3.7A), consistent with MYC being a downstream target of ErbB2 (Hynes and Lane, 2001). While MYC was localised to the nucleus in the MYC-induced tumours, consistent with its function as a transcription factor, MYC did not demonstrate the same nuclear localisation in ErbB2-induced tumours (Figure 3.8). It is unknown if MYC is active in the ErbB2-induced tumours, and if it is active, whether this is in the traditional transcriptional factor role. Understanding if MYC is active in ErbB2-induced tumours would help to interpret results observed in this model, especially in comparison with the MMTV-MYC model.
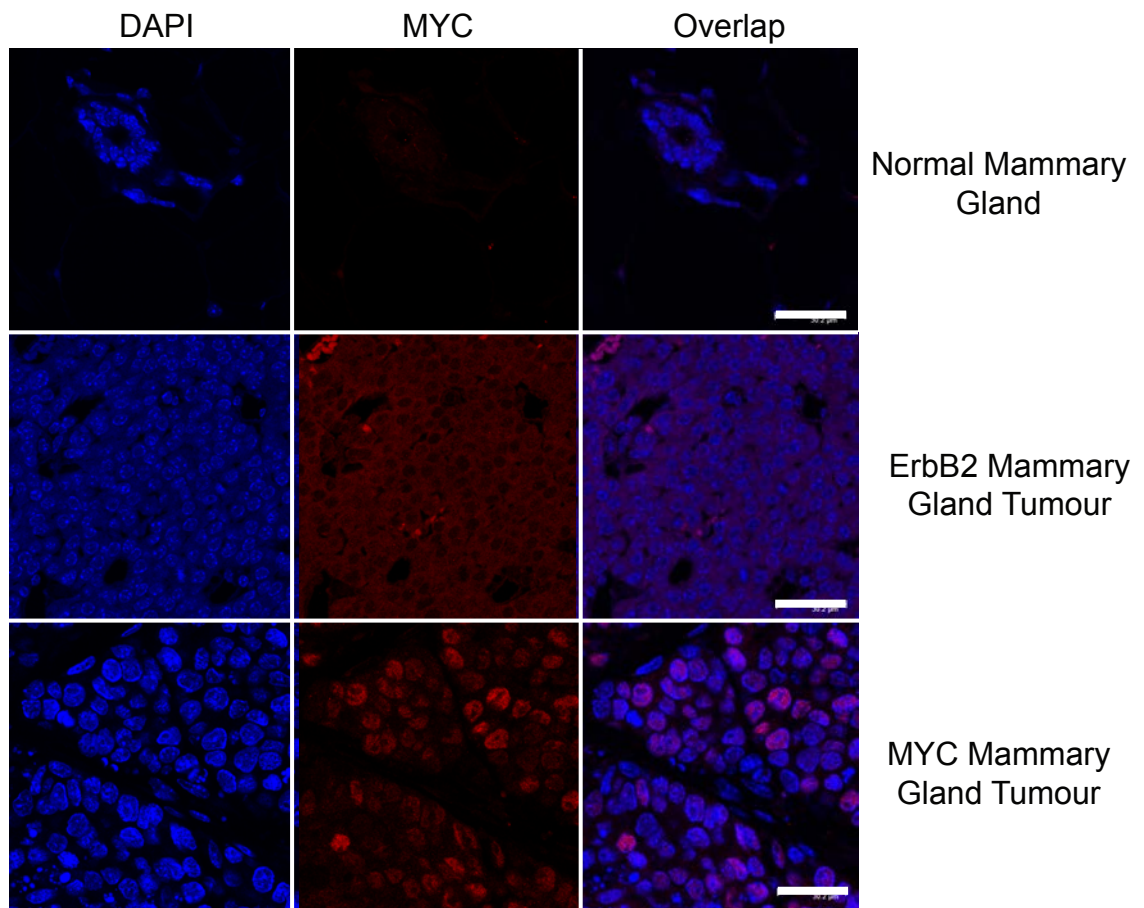
Figure 3-8 Localisation of MYC in ErbB2 and MYC-induced mammary gland tumours

MYC (red) and DAPI (blue) staining of normal mammary gland tissue (9 months), and ErbB2 and MYC-induced mammary gland tumours. Scale bar: 50 µM.

of 3 different tissue s[...] mice.

DAPI	ErbB2	Overlap	

Normal Mammary Gland

ErbB2 Mammary Gland Tumour

MYC Mammary Gland Tumour

Figure 3-9 Localisation of ErbB2 in ErbB2 and MYC-induced mammary gland tumours

ErbB2 (green) and DAPI (blue) staining of normal mammary gland tissue (9 months), and ErbB2 and MYC-induced mammary gland tumours. Scale bar: 50 µM.
Images representative of 3 different tissue samples from 3 different mice.

The expression of the estrogen receptor (ERα) was also studied in both tumour types compared to the normal mammary gland (Figure 3.7B). While it was slightly decreased in both tumour types compared to the normal mammary gland, it was still expressed. This is important to remember when trying to correlate any results seen in these tumours to human patients.

ErbB2 and MYC-induced tumours develop and grow at similar rates, developing between 6 and 10 months in both models (Figure 3.10A and B). Mice were culled when the largest tumour reached 1.2-1.5 cm in diameter, which is the humane endpoint for this model. Figure 3.10B shows that there is no significant difference in tumour growth once tumours were detected. However, it is important to note that while mice with MYC-induced tumours tended to only develop one tumour, the majority of mice with ErbB2-induced tumours developed multiple tumours, with some mice having as many as 6-8 tumours (Figure 3.10C). This could alter the metabolic phenotypes of the tumours as it is unknown how these tumours interact with each other or affect the overall nutrient supply and metabolism of the whole mouse. For this reason, mice with only one tumour were used for the remainder of this project.

The development of multifocal tumours in the MMTV-ErbB2 model infers that overexpression of activated ErbB2 is sufficient to efficiently transform mammary epithelial cells in transgenic mice (Ursini-Siegel et al., 2007). Whereas MMTV-MYC mice have been shown to require additional Ras mutations in order to become fully tumorigenic (D'cruz et al., 2001). This requirement for additional mutations partly explains why MMTV-MYC mice develop 1-2 tumours per mouse, where the MMTV-ErbB2 mice frequently develop >2 tumours per mouse.

Both mice with MYC and ErbB2-induced tumours developed metastatic nodules in the lungs. This was quantified by analysing hematoxylin and eosin (H&E) stained slices of lungs taken from tumour-bearing mice. This suggests that both tumour models are equally as metastatic, although the metastasis of these tumours to other tissues was not studied.

Figure 3-10 MMTV-ErbB2 and MMTV-MYC mice develop tumours at the same rate

A – Percent survival of mice with ErbB2 and MYC-induced tumours. Mice were culled when the biggest tumour reached 1.2 – 1.5 cm in diameter. n = 30 mice per group.
B – Tumour growth of MMTV-ErbB2 and MMTV-MYC tumours. n = 10 mice per group. Error bars denote standard deviation.
C – Number of mammary gland tumours per mouse in MMTV-ErbB2 and MMTV-MYC mice. n = 25 mice per group.
D – Number of metastatic nodules in the lungs of MMTV-ErbB2 and MMTV-MYC mice. Lung metastasis were identified in H&E stained slices of lungs taken from mice with 1 cm mammary gland tumours. n = 7 mice per group.

The tumours driven by a mutated ErbB2 oncogene appear to be physically very different to those driven by the MYC oncogene (Figure 3.11, images are representative of 'normal' tumours). At an observational level, MYC-induced tumours were usually connected to large visible blood vessels, whereas these were not observed in ErbB2-induced tumours. ErbB2 tumours, however, frequently contained large deposits of blood within them, compared to the more solid tissue structure of the MYC-induced tumours (Figure 3.11). This was also observed by H&E staining of the ErbB2-induced tumours (Figure 3.12), which shows intense eosin staining of red blood cells in slices taken from ErbB2-induced tumours, but not in MYC-induced tumours. These differences could suggest that despite developing at similar rates, these tumours might receive different oxygen and metabolite concentrations, and thus, could be metabolically different. However, to determine this, ultrasound imaging of the tumours could be used to detect blood flow in and around the tumours (Yao et al., 2012). The oxygen partial pressure in these tumours could also be detected using electron paramagnetic resonance imaging (EPRI) of pre-internalised oxygen sensing nanoprobes, inserted into the tumour (Bratasz et al., 2007). Tissue slices could also be stained with pimonidazole, to identify the levels of hypoxia between the two types of tumour (Varia et al., 1998).
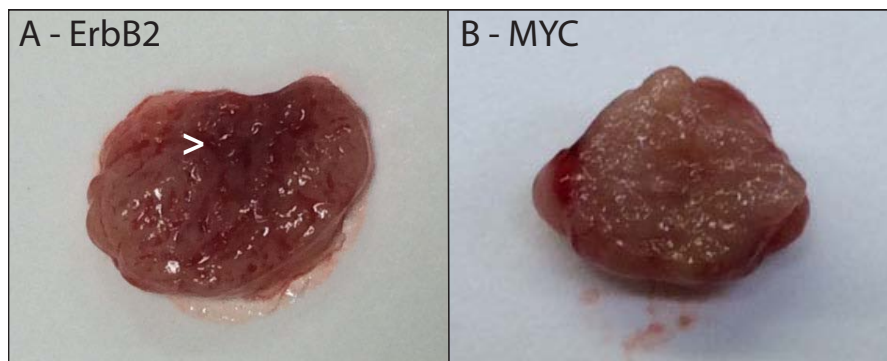
Figure 3-11 Photographs of ErbB2 (A) and MYC (B) -induced mammary gland tumours showing different physical structures

ErbB2 tumours usually contained blood whereas MYC tumours were more solid.
> shows deposit of blood.
Tumours were taken when they reached 1 cm in diameter.

Although, both MYC and ErbB2 have been shown regulate VEGF signalling (Mezquita et al., 2005; Klos et al., 2006), it is unknown if this has the same effect on angiogenesis. This could cause the two tumours to have altered blood vessel growth and blood flow and thus, receive different oxygen and nutrient concentrations.

H&E staining of tumour slices also revealed that MYC-induced tumours have greater structural heterogeneity between samples compared to ErbB2-induced tumours, which had more consistent cellular arrangements. Each of the ErbB2-induced tumours displayed similar cellular structures where the cells formed nodular, solid patterns, which is typical of mammary tumours driven by the ErbB2 oncogene (Figure 3.12) (Cardiff and Wellings, 1999). However, the MYC-induced tumours demonstrated a more diverse range of cellular structures, where different MYC-induced tumours had different patterns of cell structures. Some MYC-induced tumours, such as in Figure 3.12G had a similar nodular pattern of cells to that observed in the ErbB2-induced tumours, whereas in other MYC-induced tumours, such as those in Figure 3.12H, I and J, the cells formed more ductal structures, where the cells formed irregular glands. Likewise, the amount of stromal infiltration also seemed to vary more between MYC-induced tumours compared to ErbB2-induced tumours, as seen in Figure 3.12K which has high levels of stroma compared to Figure 3.12L.

MYC-driven tumours were previously shown to demonstrate substantial histological heterogeneity (Andrechek et al., 2009). This histological heterogeneity corresponded to genetic heterogeneity and in some cases, was linked to the acquisition of secondary Ras mutations. The heterogeneity in the MYC-induced tumours might correlate to distinct subgroups within MYC-driven tumours, dependent on their acquired secondary mutations. Thus, it is important to consider these differences in tumour heterogeneity when interpreting the results from MYC-induced tumours, as they might display more variability than the ErbB2-induced tumours

MMTV-ErbB2 mammary gland tumours
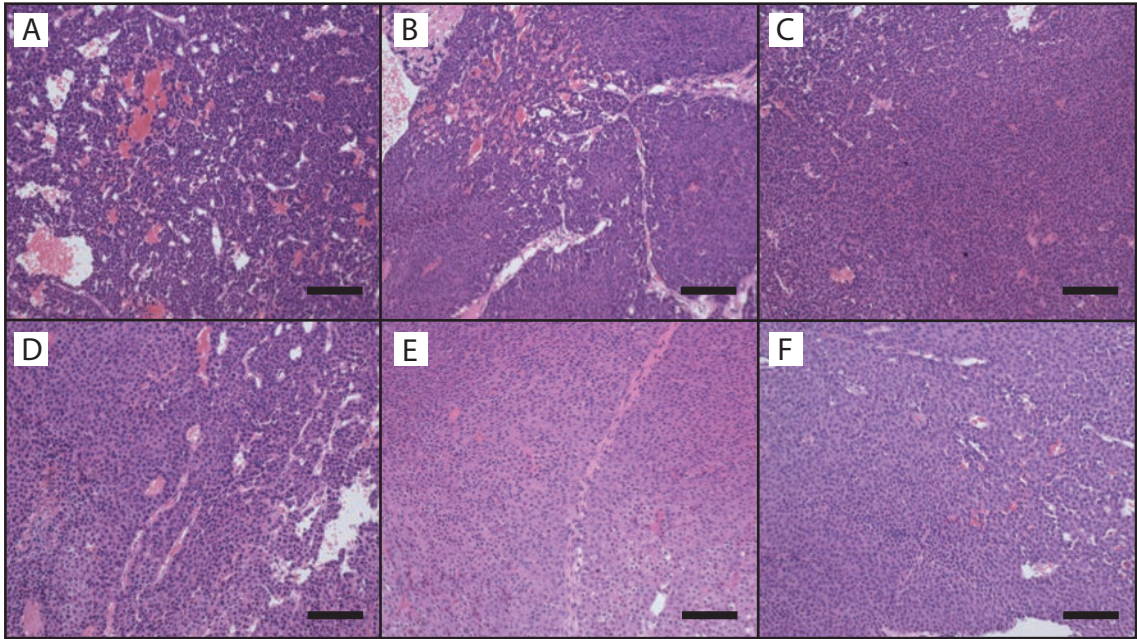
MMTV-MYC mammary gland tumours
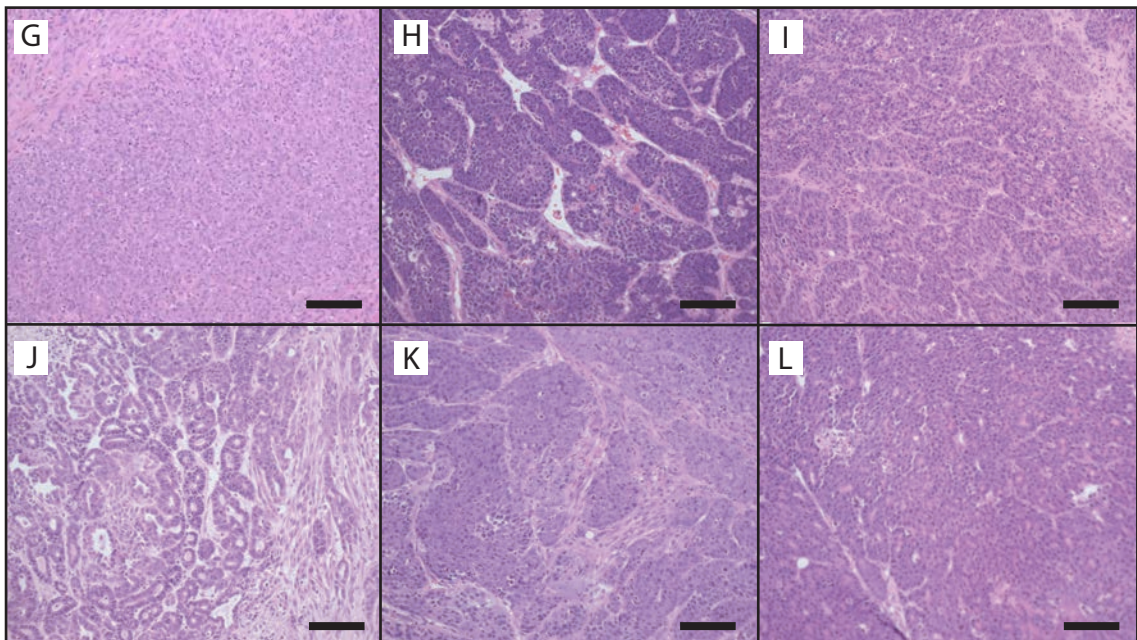
Figure 3-12 MMTV-MYC tumours have greater histological diversity than MMTV-ErbB2 tumours

H&E stained slices from MMTV-ErbB2 and MMTV-MYC tumours. A – L represent different tumours taken from different mice. Each tumour was taken when it reached 1 cm in diameter. Images are representative of the histological subtypes observed in several different tumours. Scale bar: 100 μM.

3.6   Metabolic profiling of ErbB2 and MYC-induced mammary gland tumours

In order to compare the metabolism of normal mammary gland tissue and ErbB2 and MYC-induced mammary gland tumours, 9-month old wild-type mice and mice bearing one 1 cm diameter tumour were given either one bolus of $^{13}C_6$-glucose, or two boluses of $^{13}C_5$-glutamine or $\alpha^{15}N$-glutamine.

It is important when considering these data to remember that the normal mammary gland tissue contains a variety of different cell types, including adipose and epithelial cells. Adipose cells have unique metabolic features within the body as they are designed to store lipids. Thus, the comparisons made here do not compare tumours to their specific cell of origin alone, but also include the surrounding tissue. Thus, the changes observed may be acquired during tumorigenesis or could be due to a change in the proportion of cells studied with specific metabolic features.

This technique uses ground powder from the whole tumour, and so the results are an average of the metabolic features across the tumour. Tumours are known to have different regions of hypoxia and necrosis based on their nutrient and oxygen supply and so the metabolism of the tumour should change in these different regions. Currently, MSI techniques, such as DESI-MSI and MALDI-MSI are being employed to study the metabolism of individual regions preserved in tissue slices (Randall et al., 2016; Tillner et al., 2017). This will allow the metabolism of mammary epithelial cells to be studied in context to their surrounding adipose cells and will allow different regions within tumours to be compared.

Increased lactate production as a result of increased glycolytic flux is commonly observed in many tumours (Liberti and Locasale, 2016). The concentration of lactate increased in both tumour types compared to normal mammary gland tissue (Figure 3.13), demonstrating that like many tumours, these tumours have increased lactate accumulation. The percent labelling of lactate from $^{13}C_6$-glucose was similar for each tissue type, but the concentration of ^{13}C-labelled lactate was higher in the tumours,

especially MYC-induced tumours, suggesting that the catabolism of glucose through glycolysis into lactate is increased in both tumours compared to normal mammary gland tissue.

The concentration of the TCA cycle intermediates, succinate, fumarate and malate increased in both tumour types compared to normal mammary gland tissue (Figure 3.13). The concentration of these intermediates that was labelled from $^{13}C_6$-glucose also increased in both tumour types compared to normal mammary gland. This suggests that catabolism of glucose into the TCA cycle increased in both types of tumour. Combined with the lactate data, this suggests that ErbB2 and MYC-induced tumours have increased catabolism of glucose into both lactate and the TCA cycle.

The expression of two of the isoforms of glucokinase, HK1 and HK2, which are frequently increased in tumours, including ErbB2 and MYC-driven tumours (Kim et al., 2007; Patra et al., 2013), was studied (Figure 3.13B). HK1 expression increased in both tumour types compared to normal mammary gland tissue, but was higher in ErbB2-induced tumours compared to MYC-induced ones. HK2 expression altered from a single band in the normal adult mammary gland to the appearance of a doublet in both tumour types. This might suggest that HK2 is modified in these tumours, which alters its molecular weight. PI3K and Akt have been shown to phosphorylate HK2, which increases its association with the mitochondria, providing a protective mechanism that protects the mitochondria against oxidants or calcium ion stimulated permeability transition pore opening (Miyamoto et al., 2008). However, I cannot exclude that the antibody binds to a non-specific protein that is present in the tumours but not in the normal mammary gland tissue. However, the expression level of this doublet is consistent between the ErbB2 and MYC-induced tumours, suggesting that they have similar HK2 expression. The increase in HK1 expression and possible modification of HK2, correlate to the observed increase in glucose catabolism, suggesting that the increased glycolytic flux could be due to the activities of HK1 and HK2. HK2 was shown to be required for the development and maintenance of ErbB2-induced mammary gland tumours (Patra et al., 2013), demonstrating that targeting glycolytic enzymes in these tumours represents a good therapeutic strategy.
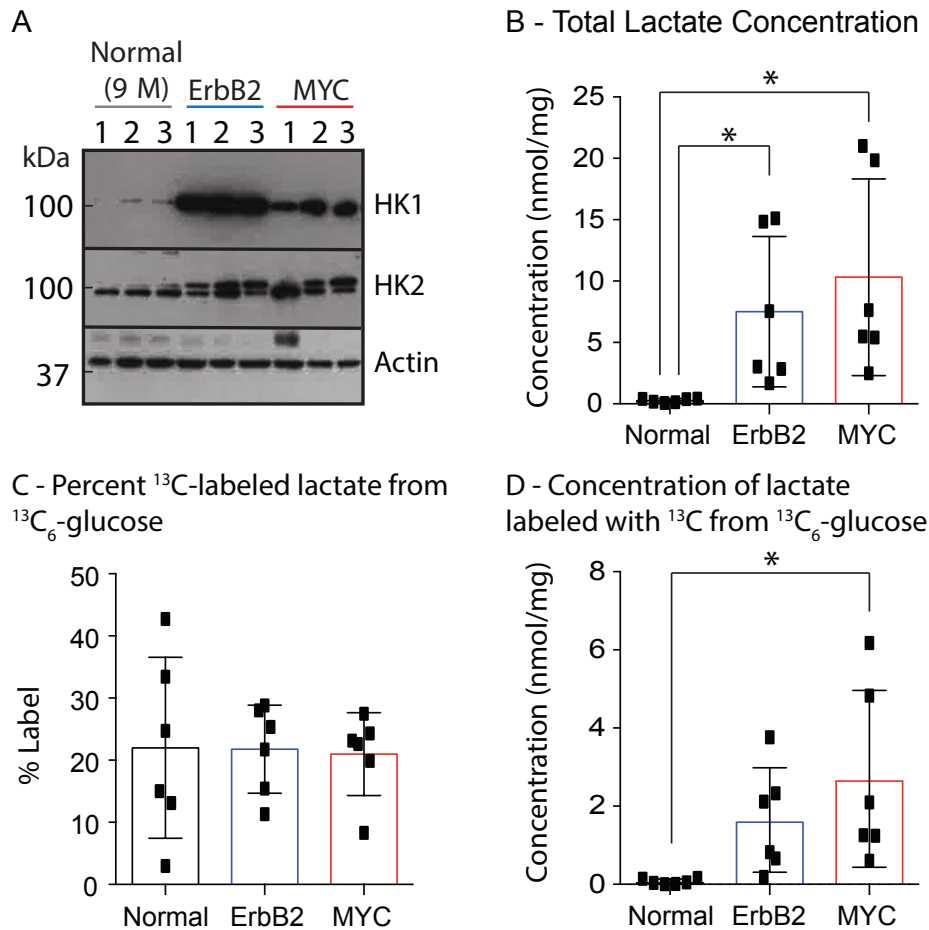
Figure 3-13 Glucose flux to lactate is increased in ErbB2 and MYC-induced tumours compared to the normal mammary gland

A – HK1 and HK2 protein expression in normal mammary gland tissue from 9 month (9 M) old mice and ErbB2 and MYC-induced mammary gland tumours (ErbB2/MYC). Biological triplicates are shown (tissues from three different mice per group).
B - D – Total concentration (B), percent label (C), and concentration of ^{13}C from $^{13}C_6$-glucose (D) into lactate in normal mammary gland tissue (Normal) and ErbB2 and MYC–induced tumours (ErbB2/MYC) after a $^{13}C_6$-glucose bolus injection. Concentration is expressed as nmol of metabolite per mg of dried tissue. Percent label represents the sum of all isotopomers except M+0. n = 6 mice per group.
One-way ANOVA with Tukey's multiple comparisons test, *P < 0.05, Error bars denote standard deviation.
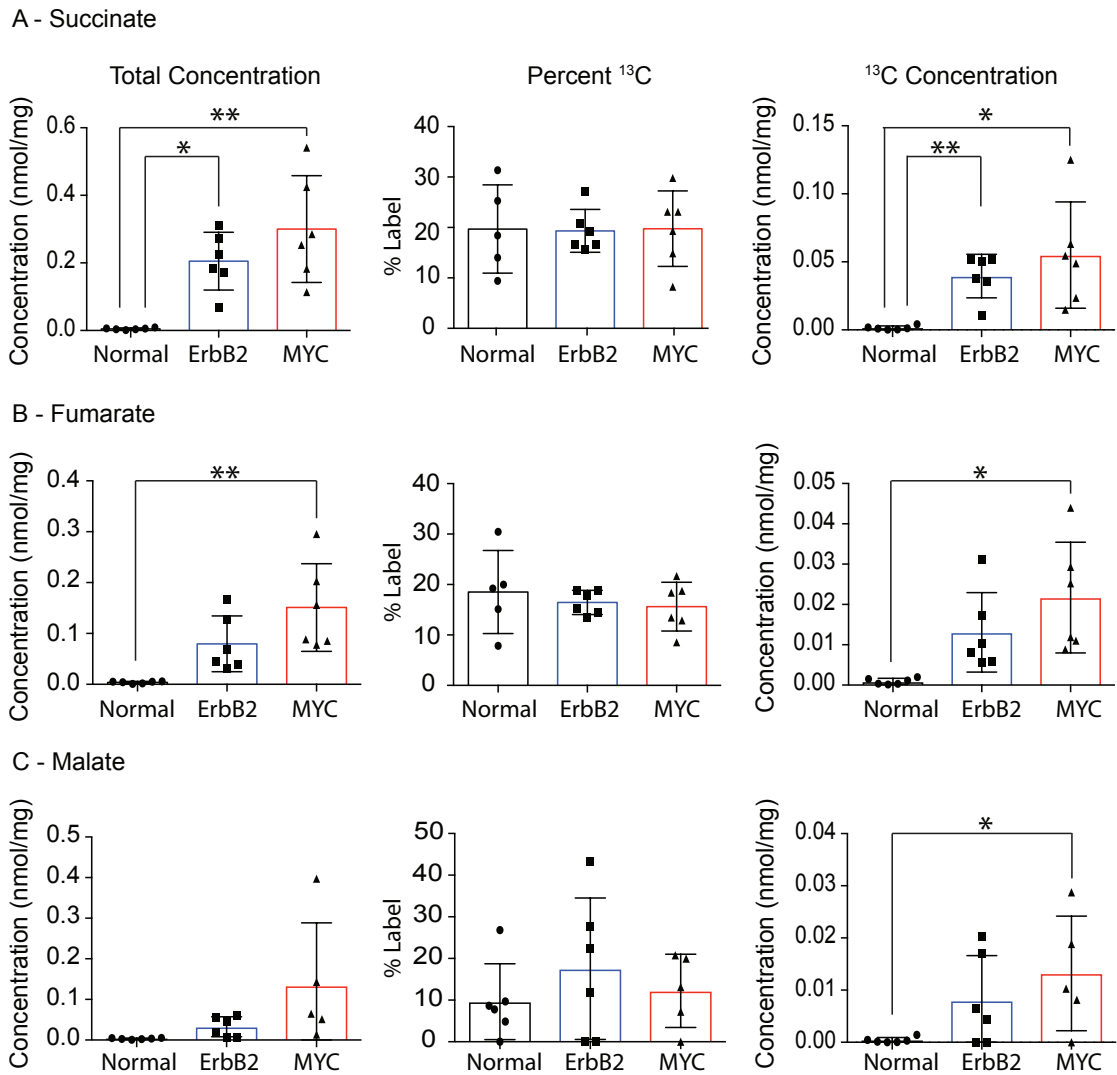
Figure 3-14 Glucose catabolism into the TCA cycle is increased in ErbB2 and MYC-induced tumours compared to the normal mammary gland

A, B + C – Total concentration, percent label and concentration of ^{13}C from ^{13}C$_6$-glucose of succinate (A), fumarate (B) and malate (C) in normal mammary gland tissue (Normal) and ErbB2 and MYC–induced tumours (ErbB2/MYC). Concentration is expressed as nmol of metabolite per mg of dried tissue. Percent label represents the sum of all isotopomers except M+0. n = 5-6 mice per group.
One-way ANOVA with Tukey's multiple comparisons test, *P < 0.05, **P < 0.01, Error bars denote standard deviation.
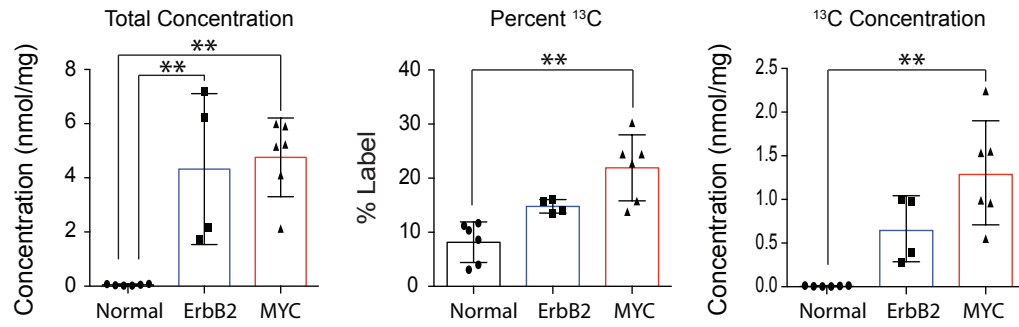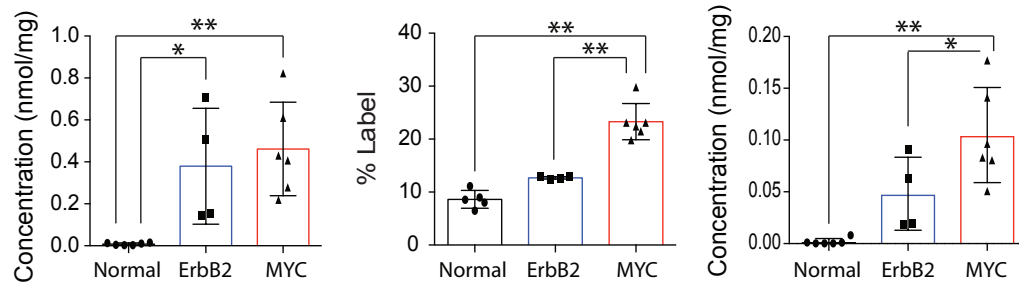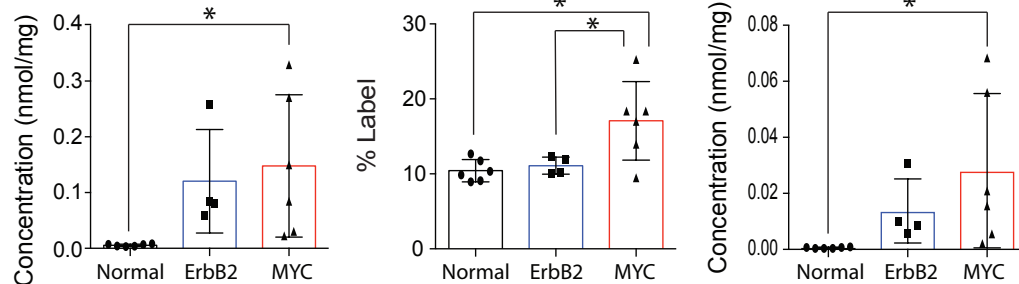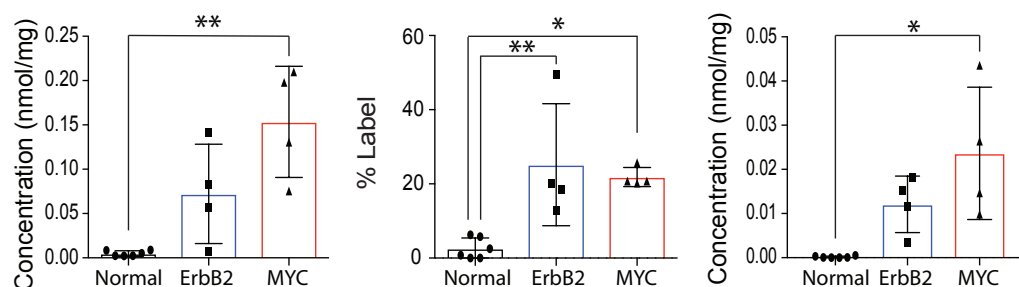
Figure 3-15 Glutamine catabolism into the TCA cycle is increased in MYC-induced tumours compared to the normal mammary gland and ErbB2-induced tumours

A, B, C + D – Total concentration, percent label and ^{13}C concentration from $^{13}C_5$-glutamine of glutamate (A), succinate (B), fumarate (C) and malate (D) in normal mammary gland tissue (Normal) and ErbB2 and MYC–induced tumours (ErbB2/MYC). Concentration is expressed as nmol of metabolite per mg of dried tissue. Percent label represents the sum of all isotopomers except M+0. n = 4 – 6 mice per group. One way ANOVA with Tukey's multiple comparisons test, *P < 0.01, **P < 0.001, Error bars denote standard deviation.

Normal mammary gland and tumour samples from mice injected with $^{13}C_5$-glutamine showed that both tumours have higher concentrations of glutamate, succinate, fumarate and malate than normal mammary gland tissues (Figure 3.15), similar to the concentrations observed in tumours from $^{13}C_6$-glucose injected mice (Figure 3.14). The concentration of ^{13}C-labelled glutamate, succinate, fumarate and malate increases in both tumours, demonstrating that both tumour types have increased flux of glutamine into the TCA cycle compared to the normal mammary gland. However, the percent ^{13}C-labelling from glutamine into glutamate (albeit not reaching statistical significance), succinate and fumarate is higher in MYC-induced tumours compared to ErbB2-induced tumours, demonstrating that the catabolism of glutamine into the TCA cycle is higher in MYC-induced tumours compared to ErbB2-induced tumours.

3.7 Differential use of glutamine in ErbB2 and MYC-induced mammary gland tumours

$^{13}C_6$-glucose and $^{13}C_5$-glutamine labelling revealed that both ErbB2 and MYC-induced mammary gland tumours have increased glucose and glutamine catabolism compared to the normal mammary gland. The increase in glucose catabolism into lactate and the TCA cycle was comparable between the two tumour types, whereas glutamine catabolism was significantly higher in MYC-induced tumours compared to ErbB2-induced tumours.

During glutaminolysis, glutamine is converted to glutamate, which can then be converted to αKG, which feeds into the TCA cycle. The production of αKG from glutamate can occur through a number of different pathways, where the carbons from glutamate are donated to αKG. If this reaction is performed by glutamate dehydrogenase (GDH), the amino group from glutamate is used to produce ammonia. Whereas if this reaction is performed by an aminotransferase, the amino nitrogen passes onto a carbon backbone to produce either alanine, aspartate or serine.

To produce alanine and aspartate, the carbon backbones required, pyruvate and oxaloacetate respectively, can contain carbons from glucose or glutamine catabolism

(Figure 3.16). Whereas the carbons in the backbone required to produce serine, 3-phosphohydroxypyruvate, predominantly comes from the oxidation of the glycolytic intermediate, 3-phosphopyruvate. Thus, the amino acids produced receive a nitrogen from glutamine and carbons from glucose or glutamine. Proline is also synthesised from glutamine, receiving both carbons and nitrogen (Figure 3.16). Therefore, I evaluated the contribution of either glutamine-derived carbon or nitrogen to the synthesis of alanine, aspartate, proline and serine.
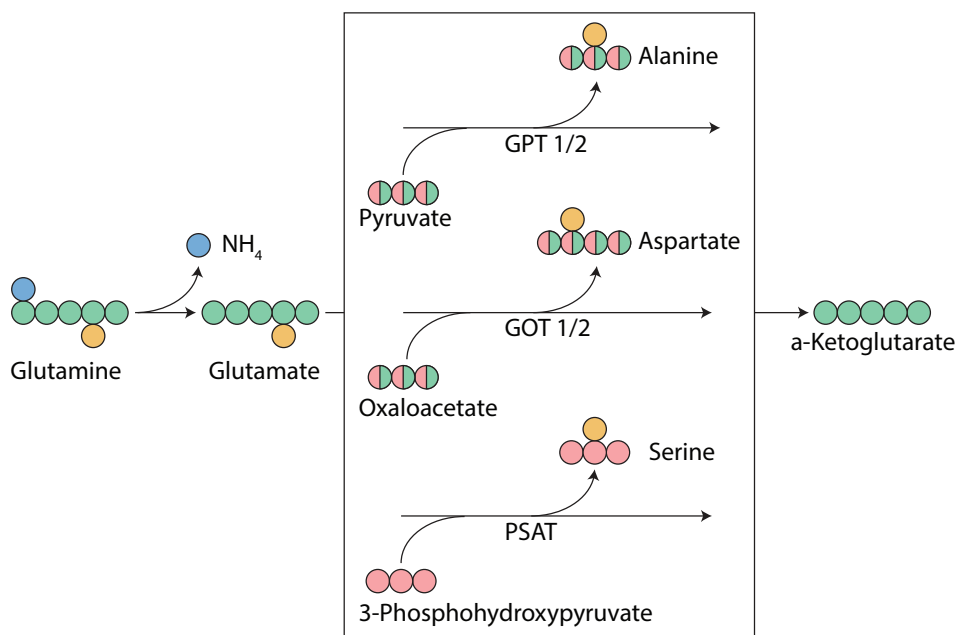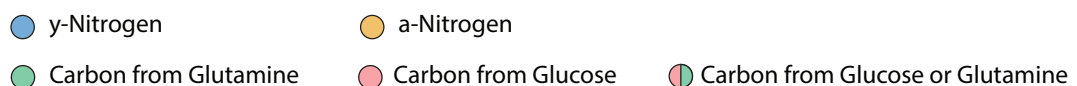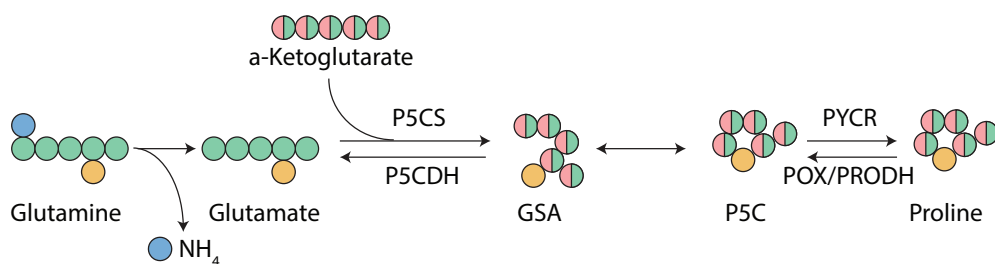
Figure 3-16 The synthesis of alanine, aspartate, proline and serine requires the amino nitrogen from glutamine, as well as carbons from glucose and glutamine
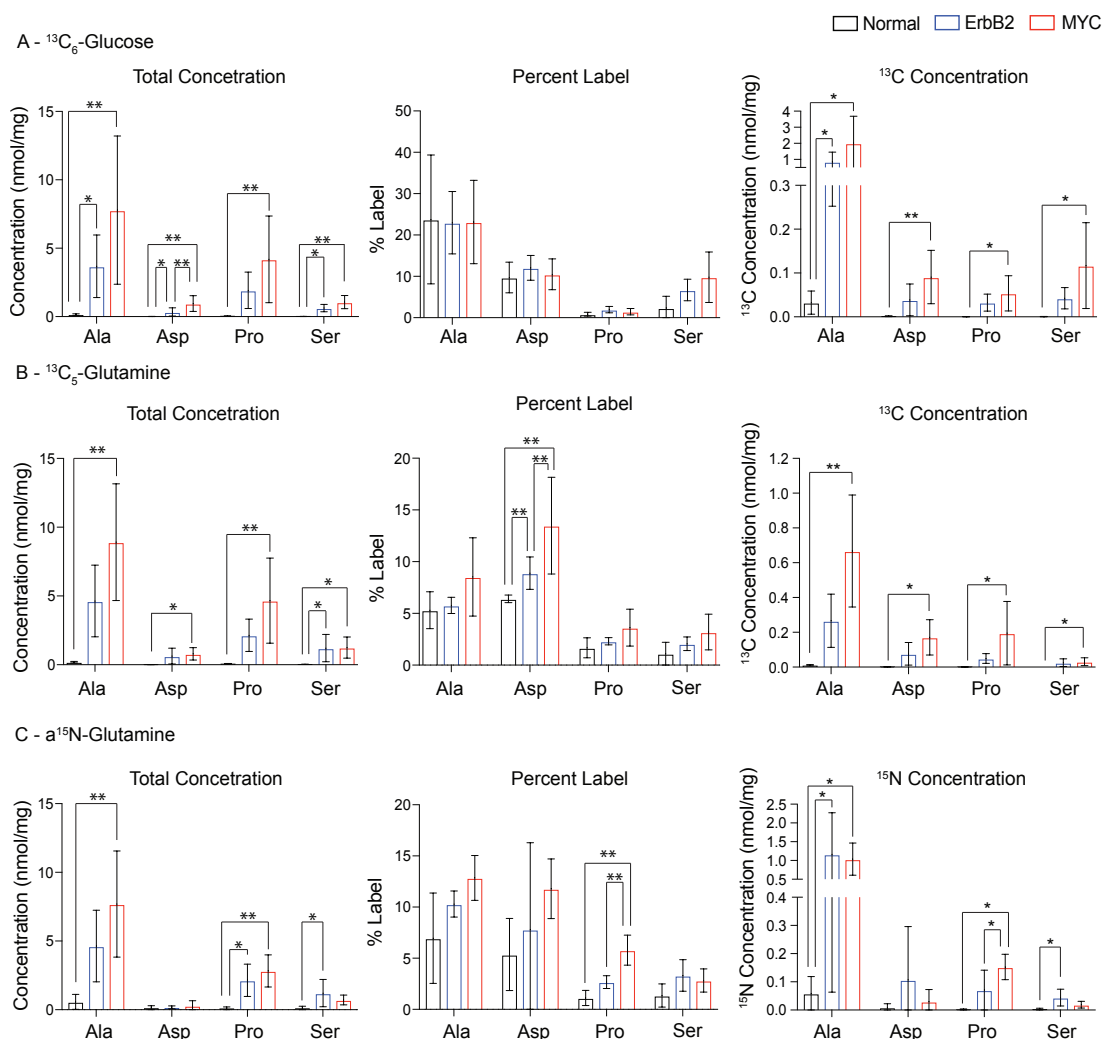
Figure 3-17 Glutamine flux to proline and aspartate is increased in MYC-induced tumours compared to ErbB2-induced tumours

A, B + C – Total concentration, concentration of labelled intermediate and percent label from $^{13}C_6$-glucose (A), $^{13}C_5$-glutamine (B) and α^{15}N-glutamine (C) of alanine, aspartate, proline and serine in normal mammary gland tissue (Normal) and ErbB2 and MYC–induced tumours (ErbB2/MYC). Concentration is expressed as nmol of metabolite per mg of dried tissue. Percent label represents the sum of all isotopomers except M+0. n = 4 – 6 mice per group.
Ala = alanine, Asp = aspartate, Pro = proline, Ser = serine,
One way ANOVA with Tukey's multiple comparisons test, *P < 0.01, **P < 0.001,
Error bars denote standard deviation.

The concentration of glutamine-derived amino acids, alanine, aspartate, proline and serine were similar regardless of the injection the mice received (Figure 3.17). The concentration of all of these amino acids increased in the tumours compared to normal mammary gland tissue. However, there were no consistently significant differences in the concentrations of the amino acids between ErbB2 and MYC-induced tumours.

These amino acids play an important role in cellular metabolism, as they are required for protein synthesis, purine and pyrimidine synthesis and the production of other amino acids, including asparagine and glycine. Alanine, aspartate, proline and serine also have a number of additional roles, which are required to support tumour cell growth.

The incorporation of $^{13}C_6$-glucose, $^{13}C_5$-glutamine and $\alpha^{15}N$-glutamine into alanine increased in both ErbB2 and MYC-induced tumours compared to the normal mammary gland tissue suggests that alanine aminotransferase (GPT1/2) activity may be higher in these tumours. Recently, GPT2 was shown to couple increased pyruvate production to glutamine catabolism to drive TCA cycle anaplerosis in colon cancer cells (Smith et al., 2016). GPT2 activity was shown to be required in the cancer cells, but not in non-transformed cells, thus, suggesting that inhibiting alanine aminotransferases could be a good therapeutic target against specific cancers. However, the role of alanine aminotransferases in breast cancer and specifically MYC or ErbB2-induced breast cancers remains to be elucidated.

While the levels of alanine synthesis appear to be comparable between the two tumour types, the concentration of ^{13}C-labelled aspartate, proline and serine from $^{13}C_6$-glucose and $^{13}C_5$-glutamine was higher in MYC-induced tumours compared to ErbB2-induced tumours and normal mammary gland tissue, demonstrating that the production of these amino acids from glucose and glutamine was greater in MYC-induced tumours (Figure 3.17). This demonstrates that as well as having increased glutamine catabolism into the TCA cycle compared to ErbB2-induced tumours, MYC-induced tumours also catabolise more glutamine into aspartate, proline and serine.

The higher incorporation $^{13}C_6$-glucose and $^{13}C_5$-glutamine into aspartate in MYC-induced tumours compared to ErbB2-induced tumours could suggest that the requirement for aspartate synthesis and the activity of the aspartate aminotransferases (GOT1/2) is greater in these tumours. Increased aspartate synthesis could be required for protein and nucleotide synthesis, as well as fuelling the aspartate-malate shuttle, which transports electrons across the inner mitochondrial membrane for oxidative phosphorylation. Aspartate produced from glutamine catabolism has previously been shown to be utilised in a pathway that produces pyruvate from aspartate via the enzymes, aspartate aminotransferase 1 (GOT1), malate dehydrogenase 1 (MDH1) and malic enzyme 1 (ME1). This pathway regenerates NADPH, and was shown to be required to maintain redox homeostasis and support tumour cell growth (Son et al., 2013). Thus, the increased aspartate production observed in MYC-induced tumours could also be required to maintain the redox balance. The role and requirement of aspartate and aspartate aminotransferases in MYC-induced tumours is yet to be described.

MYC-induced tumours also demonstrated increased incorporation of $^{13}C_6$-glucose and $^{13}C_5$-glutamine into serine than ErbB2-induced tumours. Serine plays a number of different roles in tumours. As well as being required for the synthesis of many intermediates, serine also contributes carbon to one-carbon metabolism and can allosterically regulate metabolic enzymes, such as PKM2 (Chaneton et al., 2012). Through this, serine can regulate glycolytic flux. Given the increase in serine biosynthesis in both tumour types (Figure 3.17), the expression of two of the enzymes involved in the serine biosynthesis pathway, PHGDH and PSAT was studied (Figure 3.18). PHGDH is expressed at a similar level in both tumours and mammary gland tissue from 9-month old mice. PSAT expression was higher in both tumour types compared to normal mammary gland, but was expressed at a similar level in both tumours. This supports the finding that serine biosynthesis is increased in both tumours.
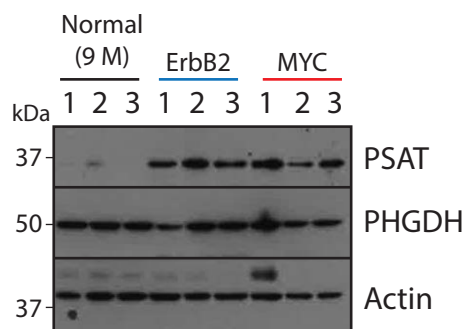
Figure 3-18 PSAT and PHGDH protein expression
PSAT protein expression increases in ErbB2 and MYC-induced tumours compared to normal mammary gland tissue from 9-month (9 M) old mice. Biological triplicates are shown (tissues taken from three different mice per group).

It was recently shown in thyroid cancer that the enzymes of the serine biosynthesis pathway do not increase in the same way in each type of thyroid cancer, where the tumours that express high levels of PHGDH do not necessarily express high levels of SHMT1 (Sun et al., 2016). It has also been demonstrated in human breast cancer cell lines and patient tumour samples that the expression of PSAT and PHGDH does not always change in the same way (Kim et al., 2014). While PHGDH is traditionally believed to be the rate-limiting enzyme of the serine biosynthesis pathway and is upstream of PSAT activity, the increase in serine biosynthesis (Figure 3.17) coupled to the increase in PSAT expression suggests that in both these systems, PSAT is the limiting enzyme for serine biosynthesis and might suggest that targeting PSAT opposed to PHGDH in these tumours would represent a suitable therapeutic target, if these tumours are found to be dependent on serine biosynthesis.

Previous work using the pan-transaminase inhibitor, aminooxyacetate (AOA), demonstrated that targeting aminotransferases decreased the growth of breast cancer cells, xenografts and tumours in a transgenic MMTV-rTtA-TetO-MYC model of tumorigenesis (Thornburg et al., 2008). Aminotransferase reactions could be required to fuel the TCA cycle, as it has been shown that 50% of the αKG feeding into the TCA cycle in breast cancer cells was derived from PSAT activity (Possemato et al., 2011).

117

Alternatively, the increased biosynthesis of these amino acids could be required for alternative functions such as the maintenance of the redox balance, in the case of aspartate or to regulate other metabolic pathways, in the case of serine. Thus, further work on the roles of specific aminotransferases and the amino acids produced by them will help elucidate if any are specifically required for MYC-induced tumours.

The amino acid, proline, can also be synthesised using both carbon and nitrogen from glutamine. While proline synthesis increases in both tumours types compared to the normal mammary gland, the catabolism of glucose and glutamine into proline was greater in MYC-induced tumours compared to ErbB2-induced tumours (Figure 3.17). Increased proline synthesis was previously described with MYC activation, where MYC increased the expression of the genes involved in proline synthesis, while simultaneously decreasing the expression of the genes involved in proline catabolism (Liu et al., 2012). Proline catabolism by proline oxidase generates electrons to produce ROS and initiates several downstream effects including blocking the cell cycle and initiating apoptosis (Donald et al., 2001). Thus, increased proline synthesis reverses this to promote cell survival. Proline is required for the production of proteins, especially the extracellular matrix (ECM) protein, collagen. The ECM is frequently deregulated in cancer, altering its structure and composition, to create a pro-tumorigenic microenvironment (Sangaletti et al., 2017). Increased collagen production from proline has been shown to encase breast cancer cells (Zhu et al., 2014). Similarly, increased proline production in ovarian cancer provides a protective mechanism against chemotherapy as the cells are wrapped in collagen (Choi et al., 2006). Thus, the increased proline production observed in MMTV-MYC tumours could contribute to ECM remodelling through increased collagen production. Inhibiting proline production in these tumours might induce cell death by altering the redox balance and could increase the sensitivity of these tumours to existing chemotherapies by decreasing their collagen production.

3.8 Altered expression of glutaminolysis genes in ErbB2 and MYC-induced mammary gland tumours

As both tumours demonstrated increased glutamine catabolism compared to normal mammary gland tissue, the RNA and protein expression of the genes involved in glutaminolysis was studied in order to determine if these are differentially expressed in the tissues. Glutamine is produced from glutamate by glutamine synthetase (GS). GS RNA and protein expression was significantly decreased in both tumour types compared to normal mammary gland tissue (Figure 3.19A and B), suggesting that glutamine synthesis is reduced in both tumours. This demonstrates that in this model, MYC does not increase GS expression as previously observed in a different model of MYC-induced breast cancer (Bott et al., 2015).

Glutaminase (Gls) performs the first step of glutaminolysis, the catabolism of glutamine to glutamate. Glutaminase has two major isoforms: Gls1 and Gls2, where Gls1 has two splice variants, KGA and GAC, both of which were detected but not distinguished by the Taqman probe used in Figure 3.19. The RNA expression of Gls1 was not significantly increased in either tumour type compared to normal mammary gland tissue (Figure 3.19). However, Gls2 RNA expression was significantly higher in MYC-induced tumours compared to normal mammary gland and ErbB2-induced tumours. However, the expression levels of Gls2 were lower than Gls1, suggesting that Gls1 is mostly likely the predominant isoform in both tumours. MYC has been shown to regulate Gls1 protein expression through miR-23a/b suppression (Gao et al., 2009), and increased Gls1 protein expression has been demonstrated in MYC-induced tumours (Yuneva et al., 2012). Thus, while there was no significant increase in the mRNA expression of Gls1, this does not mean that the protein expression is not increased and so the protein expression of Gls1 and Gls2 in these tumours needs to be determined.

The second step of glutaminolysis, the conversion of glutamate to αKG, can be performed by the enzyme glutamate dehydrogenase (GDH). The RNA expression of GDH is significantly increased in ErbB2-induced tumours compared to normal mammary gland and MYC-induced mammary gland tumours. This suggests that the

increased catabolism of glutamine observed in both tumours is due to increased glutaminase expression in MYC-induced tumours and increased GDH and glutaminase expression in ErbB2-induced tumours.

The catabolism of glutamate into αKG can be performed by GDH or an aminotransferase reaction. Given that the production of alanine, aspartate and serine was greater in MYC-induced tumours compared to the ErbB2-induced tumours (Figure 3.17), and the RNA expression of GDH was higher in ErbB2-induced tumours, this suggests that ErbB2-induced tumours favour GDH to perform this reaction, whereas MYC-induced tumours use aminotransferases instead. This could be because MYC-induced tumours have greater requirement for the synthesis of these amino acids, which could contribute to the production of proteins, nucleotides and other amino acids. A recent paper by Coloff et al. (2016) demonstrated that proliferative mammary epithelial cells catabolise more glutamine via transaminases, whereas more quiescent cells had lower transaminase expression and higher GDH expression resulting in decreased amino acid synthesis (Coloff et al., 2016). This suggests that some of the metabolic adaptations observed in the MYC-induced tumours are common to a fast growth phenotype of the mammary gland.

A - Relative RNA expression
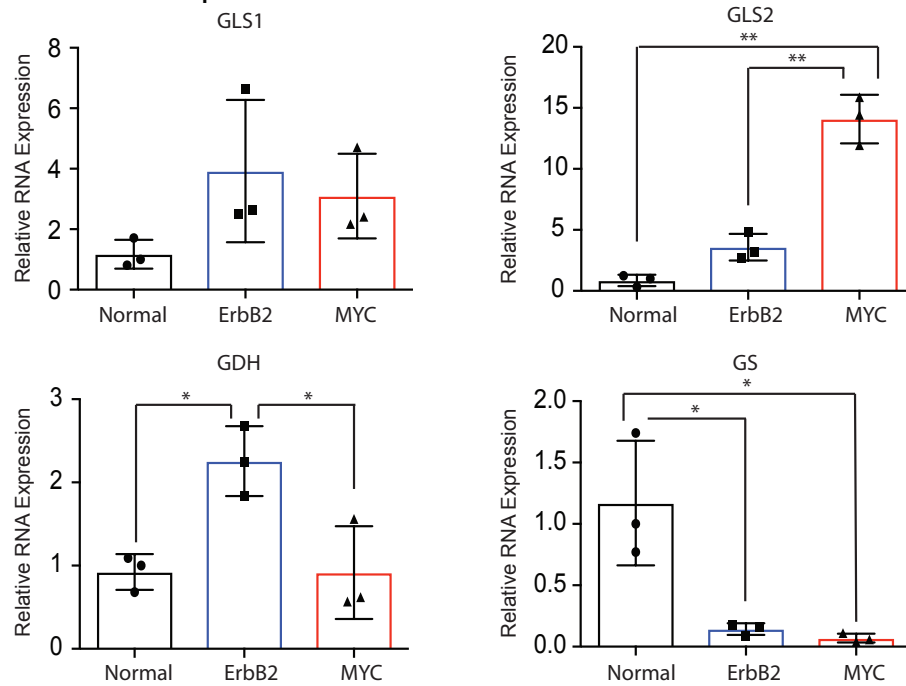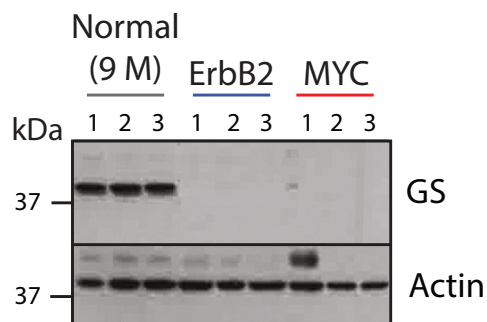
Figure 3-19 The expression of glutaminolysis genes shifts to favour glutamine catabolism in both ErbB2 and MYC-induced tumours

A – Relative RNA expression of Gls1, Gls2, GDH and GS in normal mammary gland (Normal) and ErbB2 and MYC-induced tumours (ErbB2/MYC). RNA expression is shown relative to normal mammary gland tissue. Replicates are three different tissues taken from three different mice per group. Error bars denote standard deviation.
One way ANOVA with Tukey's multiple comparisons test, *P < 0.01, **P < 0.001,
B – GS protein expression in in normal mammary gland tissue from 9 month (9 M) old mice and ErbB2 and MYC-induced mammary gland tumours (ErbB2/MYC). Biological triplicates are shown (tissues from three different mice per group).

3.9 ASCT2 expression and N-linked glycosylation is increased in MYC-induced tumours, compared to ErbB2-induced tumours, increasing its localisation to the plasma membrane

As MYC-induced tumours demonstrated increased glutamine catabolism into the TCA cycle and amino acids compared to ErbB2-induced tumours, the expression of different glutamine transporters in MYC and ErbB2-induced tumours was studied. It was believed that identifying any differences in glutamine transporters between the two tumours, might identify potential therapeutic targets against MYC-induced tumours. There are 14 different mammalian glutamine transporters (Bhutia and Ganapathy, 2016), so initially two: ASCT2 and SNAT2, were studied due to their previously described roles in different tumour models (Bode et al., 2002; Fuchs et al., 2004; Kim et al., 2013; Jeon et al., 2015; Broer et al., 2016; Van Geldermalsen et al., 2016). ASCT2 has been demonstrated to be a transcriptional target of MYC (Wise et al., 2008).
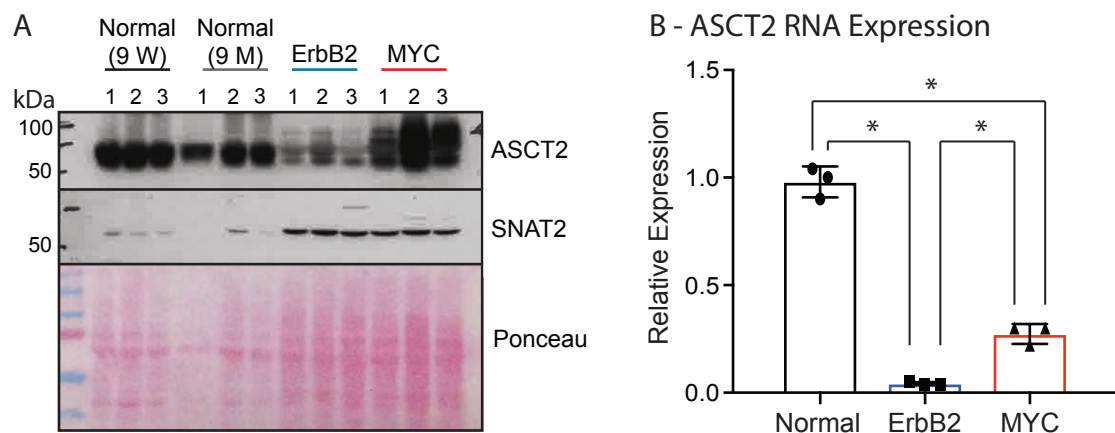
Figure 3-20 Expression of glutamine transporters in ErbB2 and MYC-induced mammary gland tumours

A – Protein expression of ASCT2 and SNAT2 in normal mammary gland tissue from 9 week (9 W) and 9 month (9 M) old mice and ErbB2 and MYC-induced mammary gland tumours (ErbB2/MYC). Biological triplicates are shown (tissues from three different mice per group).
B – ASCT2 RNA expression in normal mammary gland mice and ErbB2 and MYC-induced mammary gland tumours (ErbB2/MYC). Replicates are tissues from three different mice per group.
* One way ANOVA with Tukey's multiple comparisons test, $P < 0.01$, Error bars denote standard deviation.

The expression of SNAT2 increased to a similar level in both ErbB2 and MYC-induced tumours compared to normal mammary gland tissue (Figure 3.20). Intriguingly, while MYC-induced tumours had higher levels of ASCT2 mRNA than ErbB2-induced tumours, they still expressed roughly 70% less than the normal mammary gland tissue (Figure 3.20). At the same time, ASCT2 protein expression was higher in MYC-induced tumours compared to normal mammary gland tissue and decreased in ErbB2-induced tumours. Interestingly, the pattern of the bands on the western blot also changed between normal mammary gland tissue and MYC-induced tumours. The smeared band between 50-75 kDa seen in the normal mammary gland spread up to 100 kDa in the MYC-induced tumours. The antibody used to detect ASCT2, detects both the endogenous form of the protein at 55 kDa and the glycosylated form of the protein as a smear >55 kDa (Biotechnology, 2017). The increased smear seen in Figure 3.20 suggests that not only is ASCT2 protein expression higher in MYC-induced mammary gland tumours, but also that this protein has altered glycosylation patterns compared to that expressed in normal mammary gland tissue. Glycosylated proteins can run as a smear on western blots due to the variable patterns of glycosylation causing different increases in molecular weight. Thus, a smear at a higher molecular weight can suggest increased glycan branching in the glycosylation structure.

It has previously been demonstrated that N-linked glycosylation of ASCT2 is required to increase the stability of the protein, which enables it to be expressed at the plasma membrane (Console et al., 2015). Therefore, the increased protein levels and N-glycosylation of ASCT2 in MYC-induced tumours compared to normal mammary gland and ErbB2-induced tumours can be responsible for the increased glutamine catabolism in these tumours. In order to confirm that ASCT2 is N-glycosylated in MYC-induced tumours and the normal mammary gland, protein lysates from normal mammary gland tissue and ErbB2 and MYC-induced tumours were treated with PNGase F: an asparagine amidase that specifically cleaves the internal glycoside bonds of glycoproteins, unless the core GlcNAc contains an $\alpha(1-3)$ Fucose as shown in Figure 3.21A. This cleavage results in the loss of the glycan from the deaminated protein. Thus, if ASCT2 is N-glycosylated, the pattern of bands seen via western blot should change

after PNGase F treatment from a smeared pattern to the emergence of the endogenous protein band.
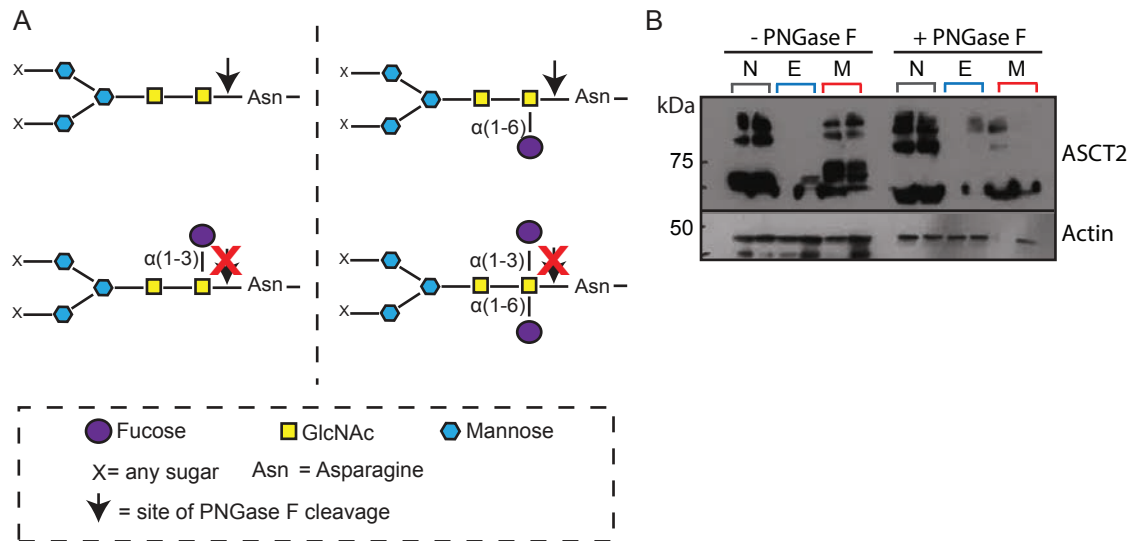
Figure 3-21 ASCT2 expression after PNGase F treatment in ErbB2 and MYC-induced mammary gland tumours

A – Diagram demonstrating the specificity of PNGase F. Image adapted from New England Biolabs, product data sheet: P0704L (2017). PNGase F specifically removes certain N-linked glycans from proteins as it cleaves between GlcNAc and the asparagine residue (top left). PNGase F can cleave when an α(1-6) Fucose is on the core GlcNAc (top right), but cannot cleave when an α(1-3) Fucose is on the core GlcNAc (bottom two).
B – Protein expression of ASCT2 in normal mammary gland tissue (N), ErbB2-induced mammary gland tumour (E) and MYC-induced mammary gland tumour (M) before and after 6 hours PNGase F treatment (activity: $\geq$192 units/mL).
Biological duplicates are shown (tissues from two different mice per group).

After 6 hours PNGase F treatment, the pattern of ASCT2 expression in MYC-induced mammary gland tumours appeared to change from a smear to a single band of about 50 kDa (Figure 3.21B). While the low loading of one of the MYC-induced mammary gland tumour samples makes it difficult to determine any changes in protein smearing in this sample, the other MYC-induced tumour sample changes from having a smear between 50-75 kDa and a higher smear above 75 kDa in the untreated sample to no longer having smeared ASCT2 after PNGase F treatment. This indicates that ASCT2 is N-glycosylated in MYC-induced tumours in a manner that can be recognised and cleaved by PNGase F, although this needs to be confirmed in other replicates.

Interestingly, the smear seen in the normal mammary gland tissue did not disappear after PNGase F treatment. This suggests that the glycosylation present on ASCT2 in normal mammary gland tissue cannot be cleaved by PNGase F treatment in the same way as the MYC-induced mammary gland tumours. In Figure 3.20, the smeared protein bands seen in the normal mammary gland samples and the MYC-induced tumour samples are also different sizes, where the MYC-induced tumours produce a bigger smear. This again suggests that the pattern of ASCT2 N-glycosylation is different between the normal and tumour samples. To identify if the pattern of N-glycosylation is different between normal mammary gland tissue and MYC-induced mammary gland tumours, a proteomics mass-spectrometry method could be used to study the branch patterns of the glycosylation on both tissue types.

As previously described by Console et al. (2015), N-glycosylation of ASCT2 stabilises the protein's expression, enabling it to localise to the plasma membrane (Console et al., 2015). When the localisation of ASCT2 in ErbB2 and MYC-induced tumours was compared, increased N-glycosylation of ASCT2 in MYC-induced tumours, demonstrated in Figure 3.20B, correlated with its increased localisation at the plasma membrane (Figure 3.22). Similarly, low ASCT2 protein expression and N-glycosylation in ErbB2-induced mammary gland tumours, shown in Figure 3.20, correlated to mostly cytoplasmic localisation of ASCT2. Interestingly, normal mammary gland tissue produced a smeared protein band, which was smaller than that produced from MYC-induced mammary gland tissues. ASCT2 was localised to the plasma membrane of adipocytes, with lower, more cytoplasmic expression within the epithelial cells of the ducts (images are representative of 5 samples from 5 different mice). As ASCT2 expression appears to be lower in the epithelial mammary gland cells, which are the cells the tumours derive from (Ahmed et al., 2002; Taneja et al., 2009), this suggests that in the MYC-induced tumour model, these cells increase ASCT2 expression and N-glycosylation when they become tumorigenic.

However, while the expression of ASCT2 appears to be low in the mammary epithelial cells, it is highly expressed and localised at the plasma membrane in the adipose cells, which make up a greater proportion of the mammary gland. Despite this, the metabolic

profile of the mammary gland, which in this study was an average of both the adipose and epithelial cells, demonstrates less glutamine catabolism than the MYC-induced tumours. This lower glutamine catabolism into the TCA cycle and amino acids in the adipose cells of the mammary gland is likely to be due to the specialised metabolic characteristics of these cells, as adipose cells synthesise and store lipids, and thus, the glutamine imported by ASCT2 in these cells is likely to be catabolised into triglycerides and lipids (Yoo et al., 2008), opposed to TCA cycle intermediates and amino acids.
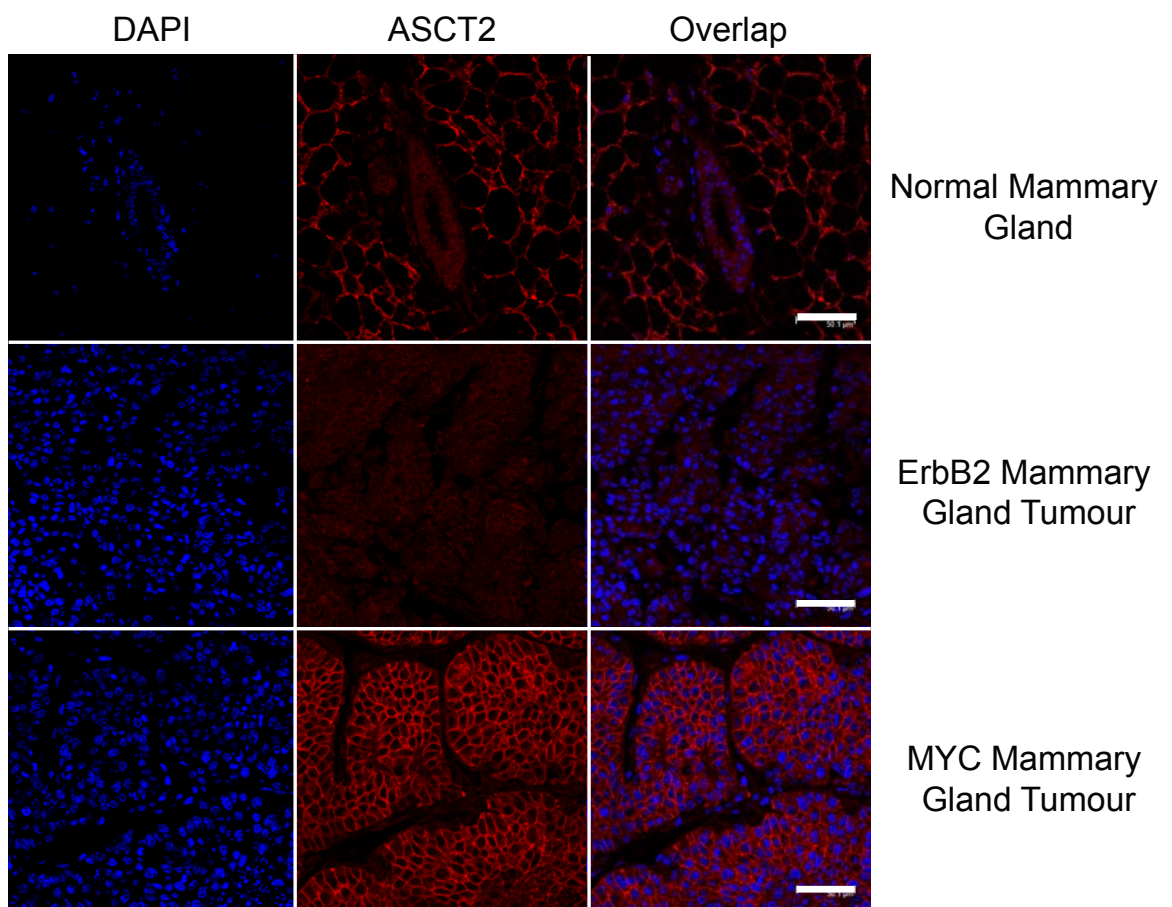
Figure 3-22 ASCT2 localises to the plasma membrane in MYC-induced mammary gland tumours

ASCT2 (red) and DAPI (blue) staining of normal mammary gland tissue (9 months), and ErbB2 and MYC-induced mammary gland tumours. Scale bar: 50 µM. Images representative of 5 different tissue samples from 5 different mice.

3.10 Overall glycosylation is altered in ErbB2 and MYC-induced mammary gland tumours

Figure 3.20 demonstrated that ASCT2 protein expression and N-glycosylation increases in MYC-induced tumours compared to ErbB2-induced tumours. The pattern of N-glycosylation also appears to be different compared to the normal mammary gland. This was confirmed by PNGase F treatment (Figure 3.21), which only affected the glycosylation pattern of ASCT2 in the MYC-induced tumours. Plasma membrane localisation of ASCT2 requires both protein expression and N-glycosylation (Console et al., 2015), and thus, its increased expression and N-glycosylation in MYC-induced tumours could be due to changes at either or both stages. Identifying if overall glycosylation is increased in MYC-induced tumours should help elucidate if this change in N-glycosylation is ASCT2 specific or common to several proteins in MYC-induced tumours. This may help understand more about how ASCT2 is regulated in MYC-induced tumours.

Many tumours exhibit aberrant overall glycosylation, resulting in widespread changes in protein activity (Pinho and Reis, 2015). Glycoproteins contain one or more glycan, covalently attached to the polypeptide backbone through either a nitrogen (N) or oxygen (O) linkage, known as N and O-linked glycans. Both N- and O-linked glycosylation require the final product of the hexosamine biosynthesis pathway (HBP), UDP-GlcNAc to attach N- and O-glycans to specific amino acids in the polypeptide backbone. The HBP requires both glucose and glutamine to produce UDP-GlcNAc (Figure 3.23).
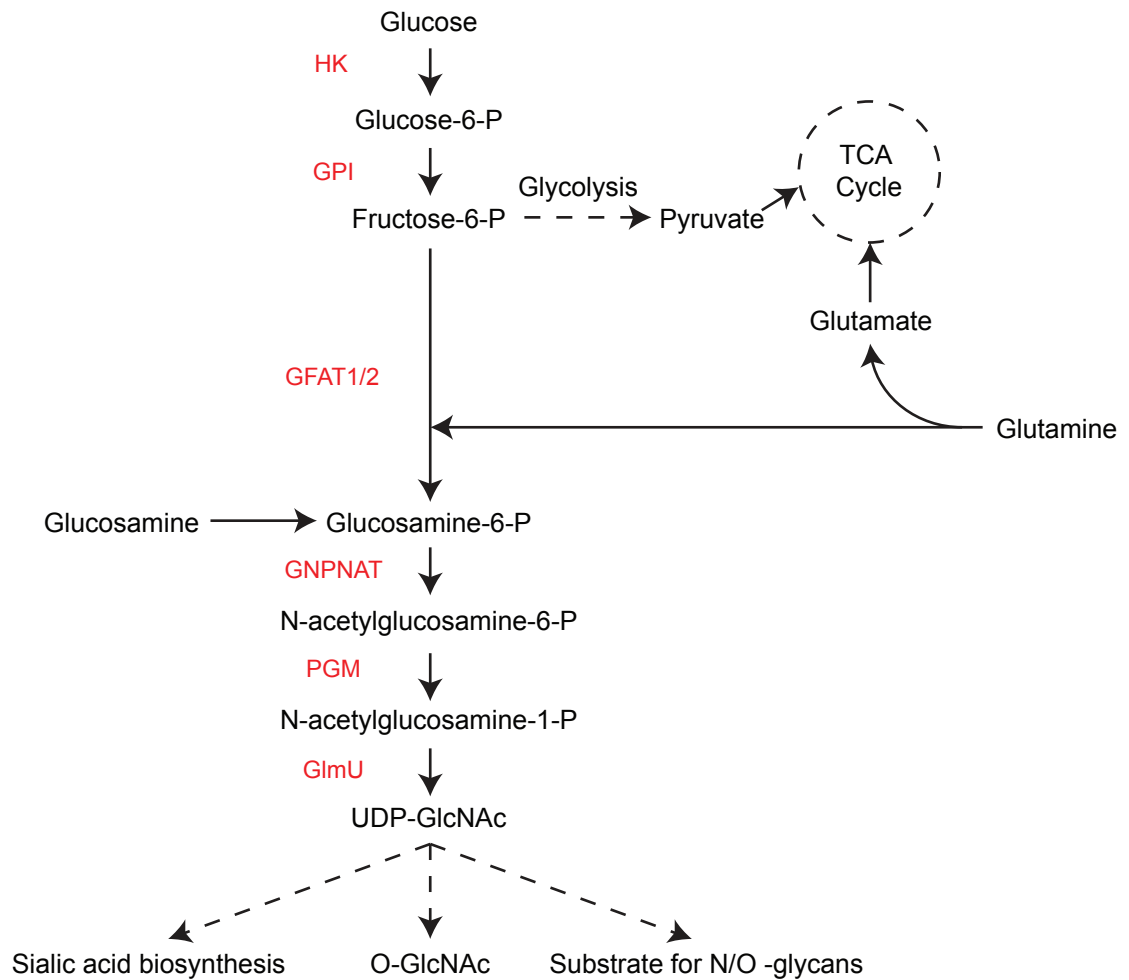
Figure 3-23 The Hexosamine Biosynthesis Pathway

Both glucose and glutamine are required to fuel the Hexosamine Biosynthesis pathway (HBP), which produces the intermediates required for O- and N-linked glycosylation. Fructose-6-P, from glycolysis, and glutamine are converted to Glc-6-P by GFAT1/2. They are subsequently N-acetylated by GNPNAT and linked to UDP by GlmU to generate UDP-GlcNAc, which is utilised for protein glycosylation.
HK – Hexokinase, GPI – Glucose-6-phosphate Isomerase, GFAT1/1 – Glutamine-Fructose 6-phosphate aminotransferase, GNPNAT – Glucosamine 6-phospate N-acetyltransferase, PGM – phosphoacetlyglucosamine mutase, GlmU – UDP-N-acetylglucosamine pyrophosphorylase,
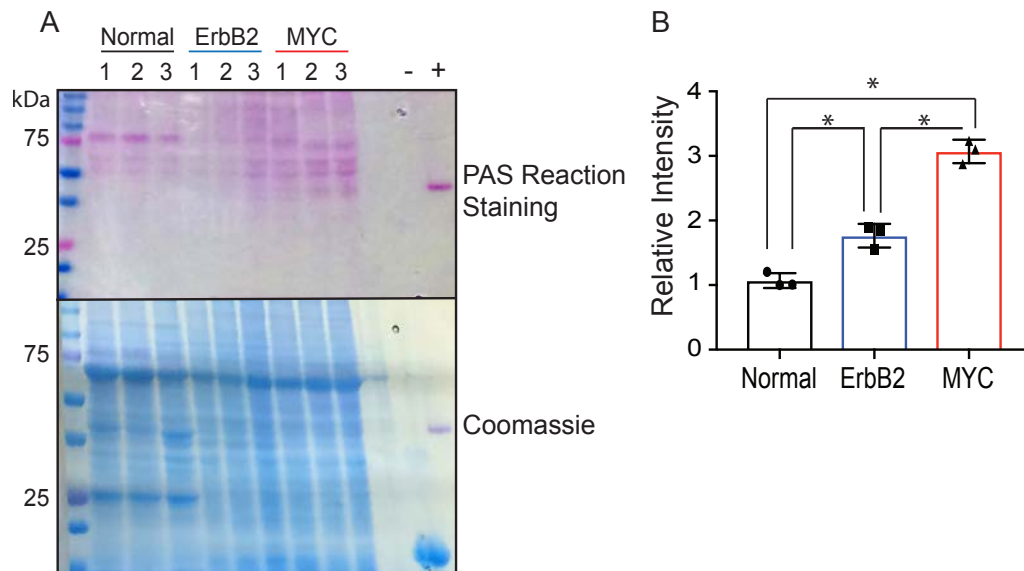
Figure 3-24 Periodic-Acid Schiff reaction staining for glycoproteins in ErbB2 and MYC-induced mammary gland tumours

A – PAS staining of protein lysates from normal mammary gland (9 months), and ErbB2 and MYC-induced mammary gland tumours, run on a 10% denaturing gel. Coomassie staining to show total protein loaded. Biological triplicates are shown (tissues from three different mice per group). Negative control (-): soybean trypsin inhibitor, Positive control (+): horseradish peroxidase.
B – Quantification of total PAS staining in each column normalised to coomassie staining. The intensity of each column was quantified using ImageJ software.
* One way ANOVA with Tukey's multiple comparisons test, $P < 0.01$, Error bars denote standard deviation.

To identify if the changes in ASCT2 N-glycosylation in MYC-induced tumours were specific to ASCT2 or the result of an overall increase in glycosylation in these tumours, the overall glycosylation levels of the tumours were studied. Overall glycosylation is detected using a Periodic Acid-Schiff reaction (PAS), which stains polysaccharides, glycolipids, mucins and glycoproteins. In this reaction, Periodic acid oxidises the vicinal diols in sugars to create a pair of aldehydes at the free ends of a broken monosaccharide ring. These aldehydes then react with Schiff reagent, staining the glycans magenta. In Figure 3.24, the overall glycosylation of protein from normal mammary gland and ErbB2 and MYC-induced tumours was compared. In order to quantify the PAS-staining (Figure 3.24B), the intensity of the whole column was normalised to the intensity of coomassie staining. Sample intensity was quantified using ImageJ. PAS-staining showed that overall glycosylation changes between normal mammary gland tissue and both tumour types, where more bands appear and the overall

intensity increases. However, the amount of overall glycosylation is higher in MYC-induced tumours compared to ErbB2-induced tumours, suggesting that the changes in ASCT2 glycosylation could be due to an overall increase in glycosylation in these tumours.

Given the increase in total glycosylation in MYC-induced tumours compared to ErbB2-induced tumours (Figure 3.24), I then wanted to identify if this was due to changes in specifically N-linked glycosylation. As O- and N-linked glycosylation use UDP-GlcNAc produced from the HBP, identifying if both types of glycosylation or just N-linked are increased might indicate whether the changes in glycosylation occur during the HBP. This would help identify more about how ASCT2 N-glycosylation is regulated in MYC-induced tumours. At present, there are limited detection methods to identify specifically N-glycosylation. Although, a MALDI imaging mass spectrometry profiling technique for the identification of the spatial distribution of N-glycans has recently been developed (Powers et al., 2014), which compares global changes in N-glycosylation.

Instead, the levels of O-linked glycosylation were studied in both tumour types. This can be done using an antibody that detects O-linked N-acetylglucosamine (O-GlcNAc). The overall expression of O-GlcNAc increased to a similar level in both ErbB2 and MYC-induced tumours compared to normal mammary gland tissue (Figure 3.25). Because overall glycosylation increased more in MYC-induced tumours compared to ErbB2-induced tumours, but O-glycosylation increased by a similar amount, it can be concluded that other types of glycosylation are changing more in MYC-induced tumours. To confirm this, a mass spectrometry method could be used, or a range of N-glycosylated proteins could be studied to see if their glycosylation consistently increases in MYC-induced tumours compared to ErbB2-induced tumours.

The difference in the pattern of protein smearing between normal mammary gland tissue and MYC-induced tumours (Figure 3.20) and their different sensitivities to PNGase F treatment (Figure 3.21), suggests that the difference in ASCT2 N-glycosylation occurs at the point of glycan transfer. Because the smears are different

lengths, this could suggest that the glycan branching is different, which could be caused by different glycosyltransferase activity or different substrate availability. Glycan structures can be resolved by mass spectrometry (ESI and MALDI) (Morelle and Michalski, 2007; Powers et al., 2014; Yang et al., 2017). It would be interesting to compare the glycan structure of ASCT2 N-glycosylation between normal mammary gland tissue and MYC-induced tumours as this might indicate differences in glycosyltransferase activity between the two tissues, as different glycosyltransferases produce different glycan structures (Pinho and Reis, 2015; Ashkani and Naidoo, 2016; Venkitachalam et al., 2016). There are currently over 240 known human glycosyltransferase sequences identified, split into 42 distinct families (Breton et al., 2006). A number of glycosyltransferases are altered in cancer (Cheung and Dennis, 2007; Ashkani and Naidoo, 2016; Venkitachalam et al., 2016). However, none of these enzymes has been described as a MYC target gene.

While identifying the specific mechanism regulating the changes in glycosylation observed in MYC-induced tumours might enable new potential therapeutic targets to be identified, it is outside the scope of this project. Instead, I decided to focus on the requirement for ASCT2 in MYC-induced tumours and how the transporter is regulated by specific oncogenes and glutamine metabolism.
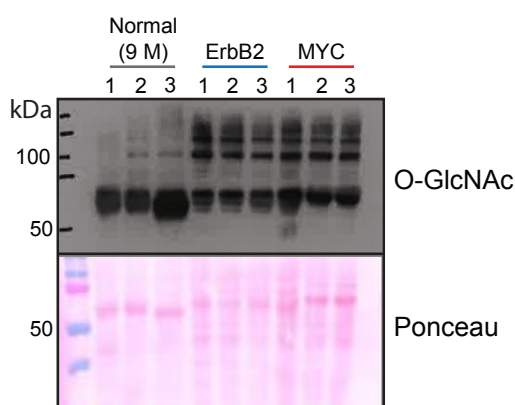
Figure 3-25 O-GlcNAc expression in normal mammary gland and ErbB2 and MYC-induced tumours

O-GlcNAc expression in normal mammary gland tissue from 9 month (9 M) old mice and ErbB2 and MYC-induced mammary gland tumours (ErbB2/MYC).
Biological triplicates are shown (tissues from three different mice per group).

3.11 Chapter 3 Summary

The initial aim of this project was to determine if different oncogenic drivers differently affect the metabolic profiles of mammary gland tumours. To do this, two different models of mammary gland tumorigenesis, MMTV-ErbB2 and MMTV-MYC, were used. These tumours were shown to express ERα, indicating that they are luminal tumours. Both tumours were also shown to express MYC, although MYC was localised to the nucleus in MYC-induced tumours and the cytoplasm in ErbB2-induced tumours, suggesting that its activity is different between the tumour types. Despite growing at the same rate, the different oncogenes produced tumours that appear physically different. While the MYC-induced tumours showed greater histological heterogeneity than the ErbB2-induced tumours, their metabolic profiles did not demonstrate this level of variability. This demonstrates that the metabolic requirements and adaptations of the tumours are more universal between tumours driven by the same oncogene than their structure.

Stable isotope labelling of the normal mammary gland, ErbB2-induced tumours and MYC-induced tumours revealed metabolic differences between both tumours and the normal mammary gland and between the two tumour types, as summarised in Figure 3.26. This confirmed that metabolic changes in tumours are determined by the initiating genetic event

$^{13}C_6$-glucose labelling demonstrated that both ErbB2 and MYC-induced tumours have greater catabolism of glucose into lactate and the TCA cycle than the normal mammary gland. This increased catabolism was similar between the two tumour types. However, while both tumours demonstrated increased catabolism of glutamine into the TCA cycle and amino acids compared to normal mammary gland tissue, the catabolism of glutamine was greater in MYC-induced tumours compared to ErbB2-induced tumours, especially into proline and aspartate. The RNA expression of the genes involved in glutaminolysis, suggest that the changes in glutamine metabolism in these tumours are partly due to increased GDH and glutaminase expression in ErbB2-induced tumours and increased glutaminase expression in MYC-induced tumours.
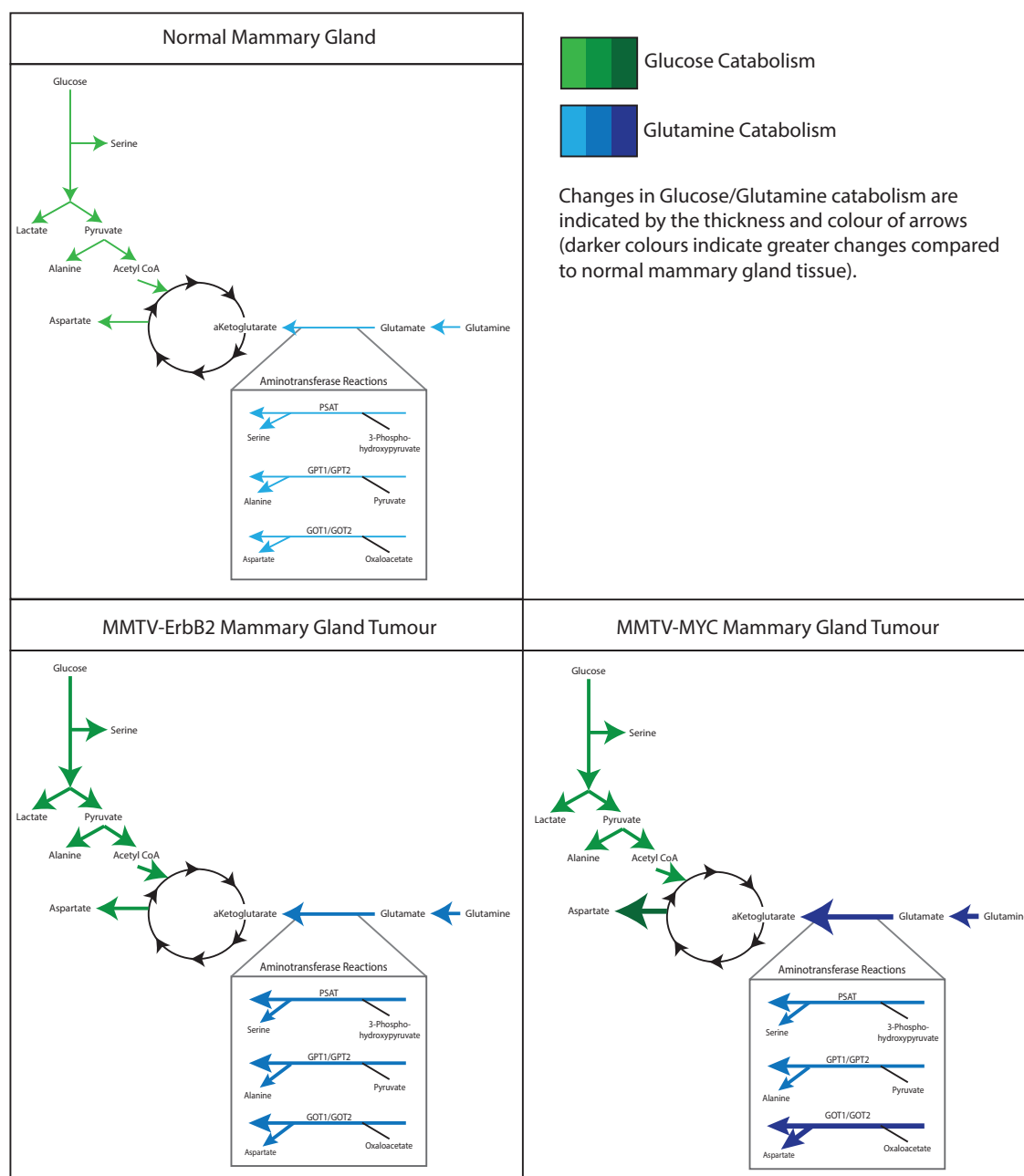
Figure 3-26 Summary of metabolic differences observed between normal mammary gland tissue and ErbB2 and MYC-induced mammary gland tumours

Summary diagrams of the changes in glucose and glutamine catabolism observed with $^{13}C_6$-glucose and $^{13}C_5$-glutamine labelling. Increased catabolism compared to the normal mammary gland is indicated by both the thickness and colour of the arrow (darker colours indicate greater changes).

Due to the increased glutamine catabolism observed in MYC-induced tumours compared to ErbB2-induced tumours, the expression of two glutamine transporters, previously described to be altered in cancer, was studied. The expression and N-glycosylation of the glutamine transporter, ASCT2 was higher in MYC-induced tumours compared to ErbB2-induced tumours, promoting the localisation of the transporter at the plasma membrane. The overall glycosylation was higher in the MYC-induced tumours compared to ErbB2-induced tumours and the normal mammary gland.

The next chapter investigates whether the difference in glutamine catabolism in MYC-induced tumours compared to ErbB2-induced tumours results in increased glutamine dependency. By identifying the requirement for ASCT2 in MYC-induced tumour cells, the potential for ASCT2-inhibition as a cancer therapeutic can be identified.

Chapter 4.   ASCT2 expression is required in MYC-induced mammary gland tumour cells

4.1 Introduction

Changes in glutamine metabolism have been observed in many cancers, resulting in increased glutamine dependency (Wang et al., 2010; Son et al., 2013; Gross et al., 2014; Xiang et al., 2015). These changes may include changes in the expression of glutaminase (Perez-Gomez et al., 2005; Gao et al., 2009; Van Den Heuvel et al., 2012; Qie et al., 2014) or glutamine synthetase (Bott et al., 2015; Tardito et al., 2015; Yang et al., 2016), as well as changes in aminotransferase activity (Thornburg et al., 2008; Locasale et al., 2011; Son et al., 2013; Dey et al., 2017) and glutathione synthesis (Jin et al., 2015; Zheng et al., 2015). In many cases targeting these changes in glutamine metabolism appears effective against tumour cells (Wang et al., 2010; Son et al., 2013; Gross et al., 2014; Xiang et al., 2015).

The data in Chapter 3 demonstrated that MYC-induced tumours have greater catabolism of glutamine into the TCA cycle and amino acids than ErbB2-induced tumours. The protein expression and N-glycosylation of the glutamine transporter, ASCT2 is higher in the MYC-induced tumours compared to ErbB2-induced tumours, promoting localisation of the transporter to the plasma membrane. The requirement for ASCT2 has previously been demonstrated in triple-negative breast cancer, lung cancer and myeloma xenografts (Bolzoni et al., 2016; Hudson et al., 2016; Van Geldermalsen et al., 2016), and ASCT2 expression showed high correlation with MYC expression in TNBC. As MMTV-MYC tumours express the estrogen receptor (ER) (Figure 3.7), determining whether their increased ASCT2 expression and N-glycosylation corresponds to increased ASCT2 requirement, will expand our understanding of ASCT2-dependent breast cancer.

Given the previously observed difference in glutamine catabolism and ASCT2 expression in Chapter 3, this chapter aims to investigate whether these tumour models demonstrate the same requirement for glutamine, glutamine uptake and specifically the

glutamine transporter, ASCT2. This should determine the suitability of inhibiting glutamine metabolism and ASCT2 as a therapeutic strategy against either MYC or ErbB2-induced mammary gland tumours.

4.2 Chapter 4 Aims

- Create an *in vitro* cell culture model of ErbB2 and MYC-induced tumours,
- Determine whether glutamine uptake occurs at the same rate in ErbB2 and MYC-induced tumour cells,
- Determine whether ErbB2 and MYC-induced tumour cells require glutamine and glutamine uptake,
- Determine the requirement for ASCT2 in cells isolated from MMTV-MYC and MMTV-ErbB2 tumours,

4.3   Isolated tumour cells maintain their *in vivo* metabolic phenotypes

Chapter 3 demonstrated that MYC-induced tumours catabolise more glutamine into the TCA cycle and amino acids than ErbB2-induced tumours. In order to investigate these differences in glutamine metabolism further, an *in vitro* model was developed. This would enable mechanistic questions that are difficult to investigate *in vivo* to be studied. Tumour cells were isolated using an adapted version of the protocol described by DeRose et al. (2013). It was important that experiments using isolated tumour cell lines were repeated using several different lines per tumour type, isolated from different mice, in order to represent tumour heterogeneity. Cell line experiments were also repeated on multiple days.
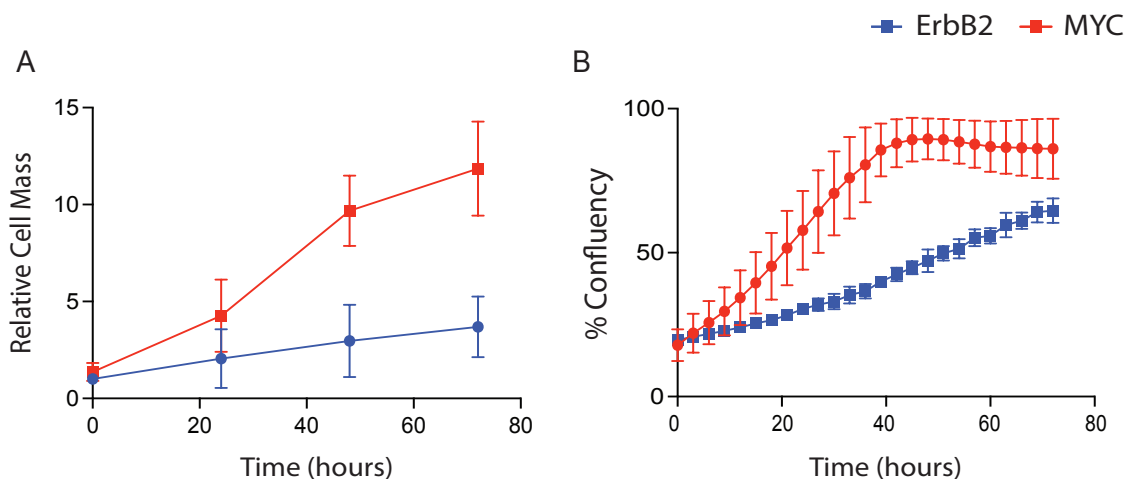
Figure 4-1 Comparative growth rates of isolated ErbB2 and MYC-induced mammary gland tumour cells *in vitro*

A – Relative cell mass, quantified by crystal violet staining, of isolated ErbB2 and MYC-induced mammary gland tumour cells, plated in 2 mM glutamine MMEC media. Cell mass was normalised to ErbB2-induced cells at 0 hours. 3 different cell lines from 3 different mice were used per group. ANCOVA $P < 0.0028$
B – Percent confluency, quantified by incucyte FLR imaging system, of isolated ErbB2 and MYC-induced mammary gland tumour cells, plated in MMEC media. 3 different cell lines from 3 different mice were used per group. ANCOVA $P < 0.0001$, Error bars denote standard deviation.

The tumour cells isolated from the different tumours grew at significantly different rates in the cell culture media used, where isolated MYC-induced tumour cells grew approximately 5 times faster than cells isolated from ErbB2-induced tumours (Figure 4.1). The significant difference in the growth rate of isolated tumour cells together with the comparable growth of the two types of tumours (Figure 3.10), may indicate that MYC-induced tumours have significantly higher levels of cells undergoing cell death.

Consistent with the ASCT2 localisation in the two tumour types, ASCT2 was localised to the plasma membrane in isolated MYC-induced tumours cells and was not observed in ErbB2-induced tumour cells (Figure 4.2, images representative of at least three different cell lines per tumour type), demonstrating that the localisation of ASCT2 is not affected by the cell isolation procedure or adherent cell culture conditions. This confirms the suitability of the isolated tumour cell model to study the requirement and regulation of ASCT2 in these cells.
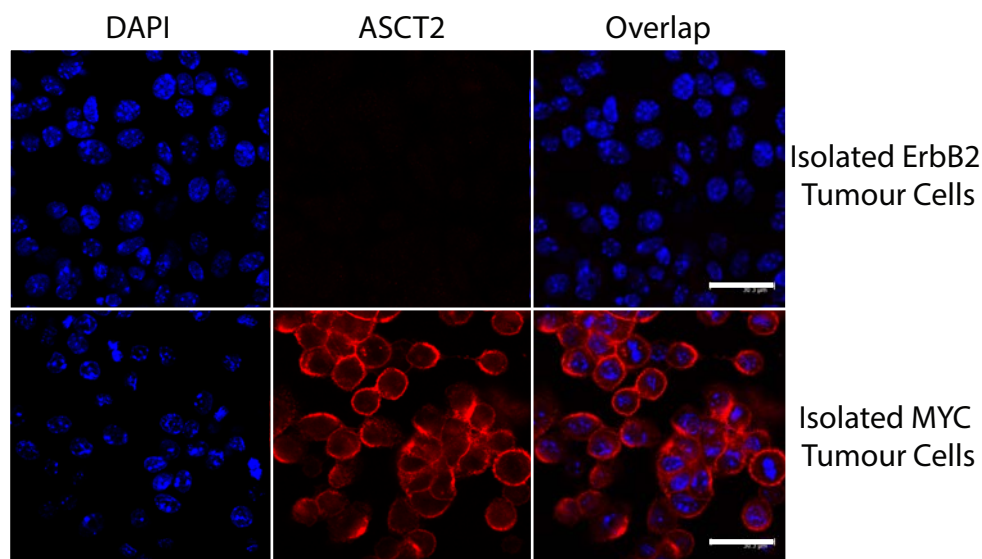
Figure 4-2 Isolated ErbB2 and MYC-induced mammary gland tumour cells maintain their *in vivo* localisation of ASCT2

ASCT2 (red) and DAPI (blue) staining of cells isolated from ErbB2 and MYC-induced mammary gland tumours and cultured in MMEC media in adherent culture for over 14 days. Scale bar: 30 μM.
Images representative of 3 different cell lines from 3 different mice.
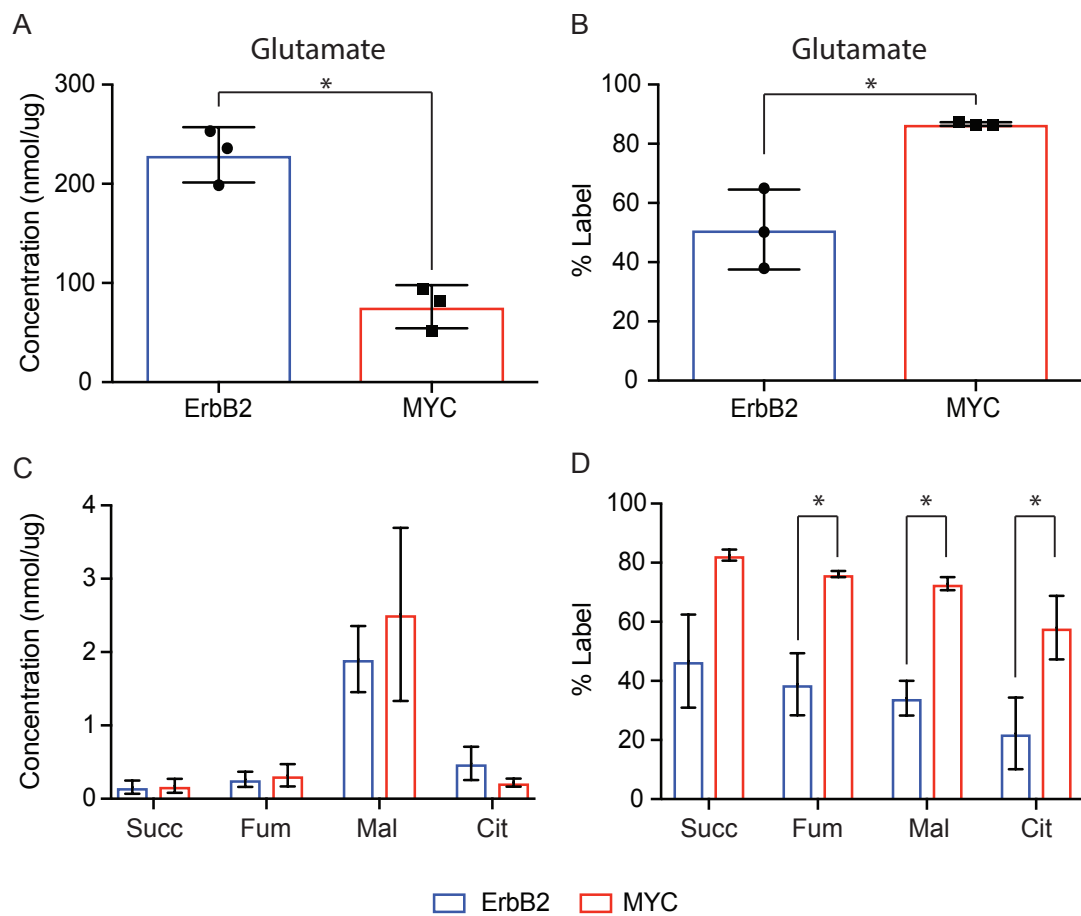
Figure 4-3 Isolated MYC-induced tumour cells maintain the increased flux of glutamine into the TCA cycle compared to isolated ErbB2-induced tumour cells *in vitro*

Tumour cells, incubated with $^{13}C_5$-glutamine for one hour, were analysed by GC-MS.
A – Total concentration of glutamate, expressed as nmol of glutamate per µg of cell protein.
B – Percent ^{13}C labelling from $^{13}C_5$-glutamine in glutamate (sum of all isotopomers except M+0).
C – Total concentration of succinate (Succ), Fumarate (Fum), Malate (Mal) and Citrate (Cit) expressed as nmol of metabolite per µg of cell protein.
D – Percent ^{13}C labelling from $^{13}C_5$-glutamine into TCA cycle intermediates (sum of all isotopomers except M+0).
Replicates are three different cell lines isolated from three different mice per group.
* Unpaired t-test $P < 0.05$, Error bars denote standard deviation.
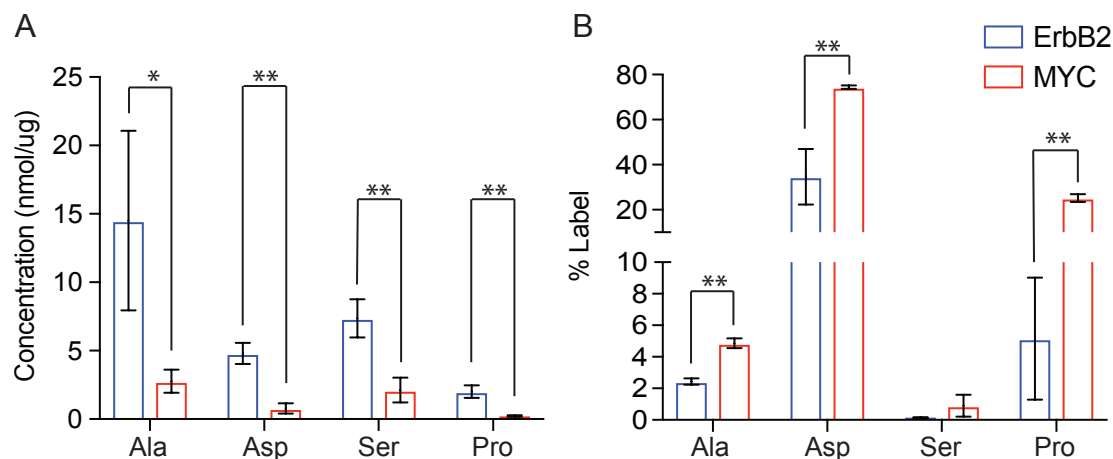
Figure 4-4 Isolated MYC-induced tumour cells demonstrate increased flux of glutamine into amino acids compared to isolated ErbB2-induced tumour cells *in vitro*

The concentration (A) and percent ^{13}C labelling (B) of alanine (Ala), aspartate (Asp), serine (Ser) and proline (Pro) after one hour [13]C$_5$-glutamine treatment in isolated ErbB2 and MYC-induced mammary gland tumour cells. Total concentration (A) is expressed as nmol metabolite per μg of cell protein. Percent ^{13}C labelling (B) from [13]C$_5$-glutamine is the sum of all isotopomers except M+0.
Replicates are three different cell lines isolated from three different mice per group.
Unpaired t-test * P < 0.05, ** P < 0.01, Error bars denote standard deviation.

The metabolic profiles of the isolated tumour cells were compared to determine whether they maintained the metabolic features observed within the tumours. The isolated tumour cells were incubated for 24 hours with [13]C$_5$-glutamine and their metabolite profiles were detected using GC-MS. While isolated MYC-induced tumour cells had a lower concentration of glutamate than isolated ErbB2-induced tumour cells, a greater proportion of this glutamate was labelled from [13]C$_5$-glutamine (Figure 4.3). The concentration of the TCA cycle intermediates was fairly similar between the two cell types. The percent labelling from [13]C$_5$-glutamine into the TCA cycle intermediates was almost double in the isolated MYC-induced tumour cells compared to the isolated ErbB2-induced cells, demonstrating that in these culture conditions, MYC-induced tumour cell lines have greater catabolism of glutamine into the TCA cycle than ErbB2-induced cells, which is consistent with the *in vivo* models.

However, when the concentration of glutamine-derived amino acids was quantified, these showed several differences compared to the transgenic tumours. In the isolated

MYC-induced tumours cells, the concentrations of alanine, aspartate, serine and proline were all significantly lower than those in ErbB2-induced cell lines (Figure 4.4), whereas in the transgenic models, the concentrations of these amino acids were similar between the two tumour types (Figure 3.17). However, the percent labelling of alanine, aspartate and proline from $^{13}C_5$-glutamine was greater in both the MYC-induced tumour cells and tumours. Overall, this demonstrates that the change from the *in vivo* tumour microenvironment to an *in vitro* cell culture system changes the intracellular concentrations of amino acids. This could be due to increased amino acid export or altered amino acid production. Muir et al. (2017) recently described how the concentration of cystine in cell culture media affects glutamate export from the cells (Muir et al., 2017). However, the requirement for glutamine to fuel the TCA cycle and amino acid synthesis remains greater in MYC-induced tumour cells compared to ErbB2-induced cells. Thus, it is important to recognise that while this *in vitro* cell culture model is useful for elucidating answers to mechanistic questions, the data collected cannot fully reflect the *in vivo* system.

4.4 MYC-induced tumour cells consume more glutamine than ErbB2-induced tumour cells

Given that the localisation of ASCT2 at the plasma membrane is greater in MYC-induced tumours than in ErbB2-induced tumours, the rate of glutamine uptake was compared between the two cell types. Isolated tumour cells were cultured in MMEC media for 24 hours. Media samples were collected at 0, 4, 8 and 24 hours. Glutamine measurements were performed by 1D-NMR. Glutamine cycles non-enzymatically with pyroglutamic acid in aqueous solutions, acidic and alkaline solutions and at high temperatures, and so some degradation occurs during the sample preparation for both GC-MS and NMR analysis. However, increased glutamine degradation has been shown to occur during the ionisation stage of mass spectrometry (Purwaha et al., 2014). As this process does not occur during 1D-NMR, this technique allows more accurate quantification of glutamine concentration within the sample. To account for the different number of cells at each time point, as the isolated tumour cells grow at different rates (Figure 4.1), glutamine uptake was normalised to cell counts taken at

each time point. This experiment showed that the rate of glutamine uptake from the media was greater in MYC-induced tumour cells compared to ErbB2-induced tumour cells (Figure 4.5). Therefore, despite some differences in the metabolic profiles of the isolated tumour cells compared to the *in vivo* tumours, the difference in glutamine catabolism between the two tumours, as well as their different localisation of ASCT2 remained in the isolated cell system. This demonstrates that this system can act as a good proxy to evaluate the requirement for ASCT2 and the mechanism of its regulation in both tumour types.
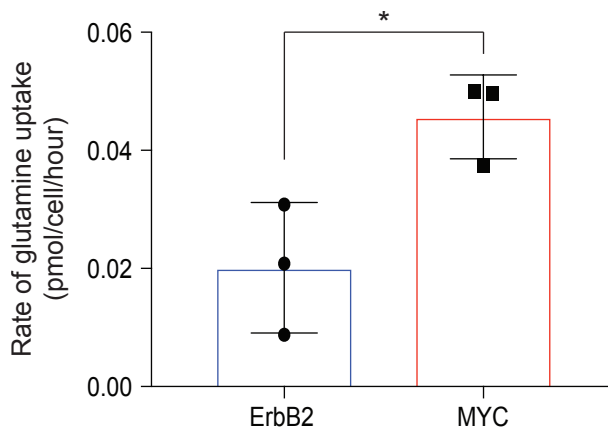
Figure 4-5 The rate of glutamine uptake is higher in MYC-induced tumour cells compared to ErbB2-induced tumour cells

The rate of glutamine uptake from the media by isolated ErbB2 and MYC-induced tumour cells from the cell media. Glutamine concentration was measured using 1D-NMR. Rate is expressed as pmol of glutamine per cell per hour. Replicates are three different cell lines isolated from three different mice per group.
Unpaired t-test * $P < 0.05$. Error bars denote standard deviation.

4.5 MYC-induced tumour cells require glutamine and the glutamine transporter ASCT2

The metabolic profiling of ErbB2 and MYC-induced mammary gland tumours in Chapter 3 revealed that MYC-induced tumours catabolise more glutamine than ErbB2-induced tumours. This glutamine was used as a carbon source to fuel the TCA cycle and was also used as a carbon and nitrogen source to produce alanine, aspartate and proline. The utilisation of glutamine for other pathways, such as glutathione synthesis, in these tumours still remains to be evaluated. Nevertheless, because glutamine is used for several different functions in these tumours, inhibiting glutamine uptake by targeting the source at the transporter may prove more effective than targeting the enzymes required for specific pathways.
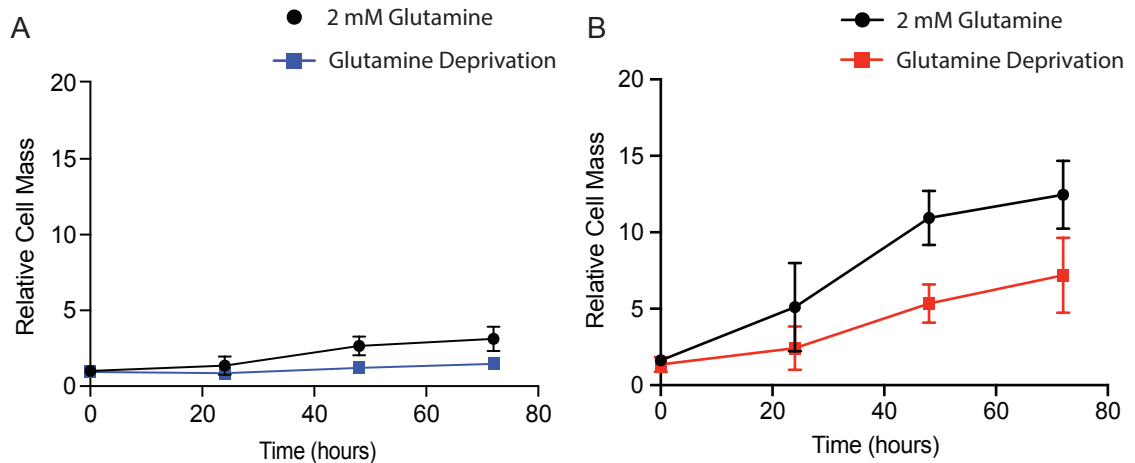
Figure 4-6 Glutamine deprivation decreases the cell mass of isolated ErbB2 and MYC-induced mammary gland tumour cells

Isolated ErbB2 (A) and MYC (B) -induced tumour cells were treated with and without 2 mM glutamine for 72 hours. Cell mass was quantified by crystal violet staining. Results were normalised to ErbB2-induced cells in 2 mM glutamine MMEC media at 0 hours. Replicates are three different cell lines isolated from three different mice per group. ANCOVA: MYC $P < 0.05$, ErbB2 $P < 0.05$, Error bars denote standard deviation.

In order to evaluate if the differential utilisation of glutamine by the two types of tumours reflects their differential dependence on glutamine availability and glutamine catabolism, isolated cells from ErbB2 and MYC-induced tumours were deprived of glutamine for 72 hours. Both tumour cell types showed decreased cell mass when deprived of glutamine compared to cells grown in 2 mM glutamine (Figure 4.6). However, the effect was much more pronounced in MYC-induced tumour cells. These results suggest that targeting glutamine metabolism in both tumour types could be an effective therapeutic strategy.

As MYC-induced tumours take up and catabolise more glutamine than ErbB2-induced tumours, I then wanted to determine whether MYC-induced tumour cells were more dependent on glutamine uptake and specifically glutamine uptake by ASCT2. This would indicate whether inhibiting glutamine transporters, such as ASCT2 in MYC-induced tumours would be a suitable therapeutic strategy. To do this, the amino-acid transporter inhibitor, γ-L-Glutamyl-p-nitroanilide (GPNA) was used. GPNA is a glutamine mimic that binds to the active site of glutamine transporters to competitively inhibit transporter activity (Esslinger et al., 2005). It was originally believed that GPNA was specific to ASCT2, as it was demonstrated to bind through specific hydrogen bonding and a lipophilic binding interaction to the active site of ASCT2 (Esslinger et al., 2005). However, GPNA does not meet all of the steric requirements to bind exclusively to ASCT2 (Esslinger et al., 2005). Recently, Broer et al. (2016) demonstrated that GPNA treatment decreased glutamine uptake by a range of different glutamine transporters, confirming that GPNA targets other glutamine transporters (Broer et al., 2016). Likewise, Chiu et al. (2017) showed that GPNA inhibits multiple sodium-dependent amino acid transporters, and thus, also affects leucine transport (Chiu et al., 2017).
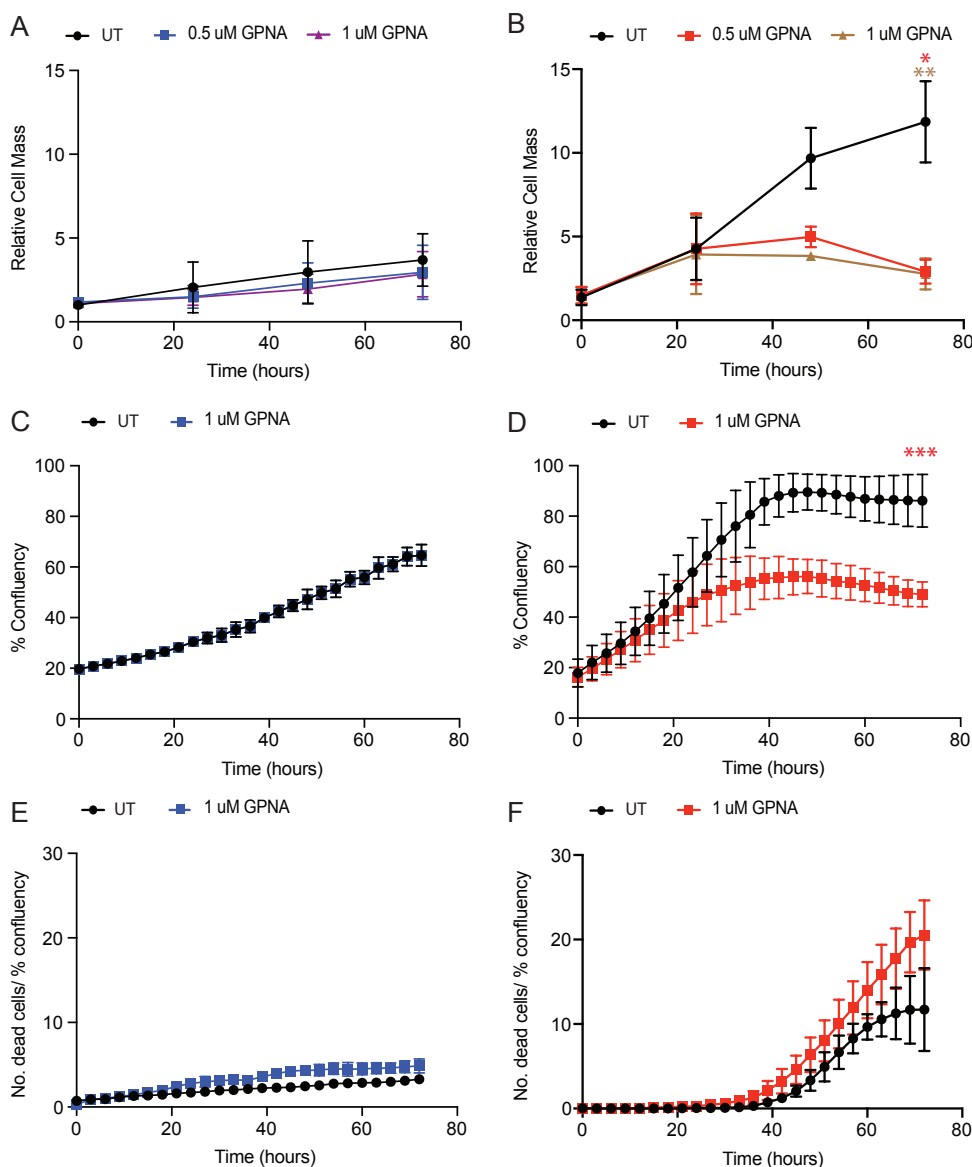
Figure 4-7 Isolated MYC-induced tumour cells are sensitive to 1 μM GPNA treatment

A + B - Isolated ErbB2 (A) and MYC (B) -induced tumour cells were treated with 0.5 μM and 1 μM GPNA for 72 hours. Cell mass was quantified by crystal violet staining. Results were normalised to untreated ErbB2-induced tumour cells at 0 hours.

C + D – Isolated ErbB2 (C) and MYC (D) -induced tumour cells were treated with 1 μM GPNA for 72 hours. Percent confluency was quantified by incucyte FLR imaging system.

E + F – Isolated ErbB2 (E) and MYC (F) -induced tumour cells were treated with 1 μM GPNA for 72 hours. Dying cells were detected with NucView 488 Caspase 3 substrate using the incucyte FLR imaging system. The number of dying cells is shown normalised to percent confluency.

UT indicates untreated cells. Replicates are three different cell lines isolated from three different mice per group.

ANCOVA: *P < 0.05, **P < 0.01, ***P < 0.0001, brown stars indicate significance between untreated cells and 0.5 μM GPNA, red stars indicate significance between untreated cells and 1 μM GPNA, Error bars denote standard deviation, the error bars in C and E are smaller than the points.

GPNA treatment significantly decreased the cell mass and percent confluency of MYC-induced tumour cells (Figure 4.7). The decrease in confluency of these cells correlated to an increase in the proportion of dying cells. However, the effect was significantly lower when ErbB2-induced cells were treated with GPNA. The slight increase in cell death observed with GPNA treatment in ErbB2-induced tumour cells, corresponds to their low sensitivity to glutamine deprivation (Figure 4.6).

As GPNA could be targeting many different amino acid transporters, and thus, the uptake of different amino acids, the effect of GPNA on the rate of glutamine uptake in both cell types was determined. Where GPNA did not alter the rate of glutamine uptake by ErbB2-induced tumour cells, it decreased the rate of glutamine uptake in MYC-induced tumour cells (Figure 4.8). Likewise, the intracellular glutamine concentration in ErbB2-induced tumour cells did not change after 24 hours GPNA treatment, whereas it decreased in MYC-induced tumour cells. This demonstrates that GPNA inhibits some of the glutamine transporters expressed in MYC-induced tumour cells.
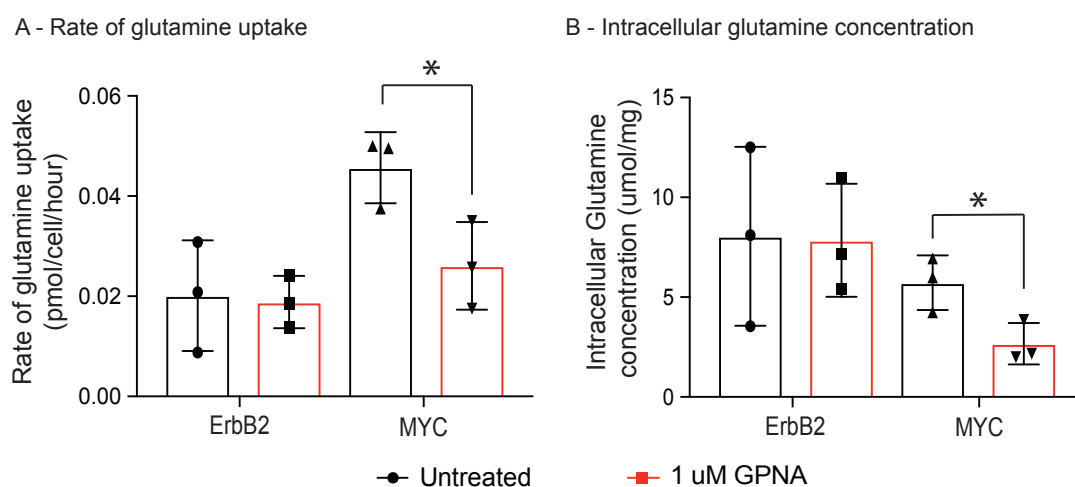
Figure 4-8 1 μM GPNA treatment decreases the rate of glutamine uptake and intracellular glutamine concentration in MYC-induced tumour cells

A – The rate of glutamine uptake from the media of ErbB2 and MYC –induced tumour cells treated with 1 μM GPNA for 24 hours. Media samples were analysed by 1D-NMR and normalised to cell number.
B – Intracellular glutamine concentration of ErbB2 and MYC-induced tumour cells after 24 hours 1 μM GPNA treatment. Cell samples were analysed by 1D-NMR and normalised to protein concentration at each time point.
Replicates are three different cell lines isolated from three different mice per group.
Unpaired t-test * P < 0.05, Error bars denote standard deviation.

In order to determine the effect of inhibiting amino acid transporters on downstream glutamine metabolism in MYC-induced tumour cells, the metabolic profile of cells treated with GPNA and $^{13}C_5$-glutamine was determined. Cells were treated continuously with 1 μM GPNA for 24 hours, but were only treated with $^{13}C_5$-glutamine for one hour before each time point. This was done so that the activity of the glutamine transporters at each time point could be assessed as this would be reflected by any changes in the percent labelling observed.

During this time, no effect of the GPNA treatment was observed on the concentration or percent labelling of succinate, fumarate and malate in the isolated ErbB2-induced tumour cells (Figure 4.9). However, this treatment decreased the total concentration of these TCA cycle intermediates in isolated MYC-induced tumour cells. The percent labelling of succinate, fumarate and malate from $^{13}C_5$-glutamine remained high after GPNA treatment in the MYC-induced tumour cells, suggesting that even though less of these intermediates were produced, the majority of these intermediates were still produced from glutamine. This confirms that MYC-induced tumour cells require glutamine uptake to contribute to the TCA cycle. It also suggests that other metabolic pathways do not compensate for decreased glutamine uptake, during this time frame. Although, labelling experiments using different isotopically labelled metabolites would be required to confirm this. The catabolism of $^{13}C_5$-glutamine into the TCA cycle also demonstrates that glutamine can still enter the cells in the presence of GPNA. This suggests that other glutamine transporters, not effected by GPNA, are active in these cells.
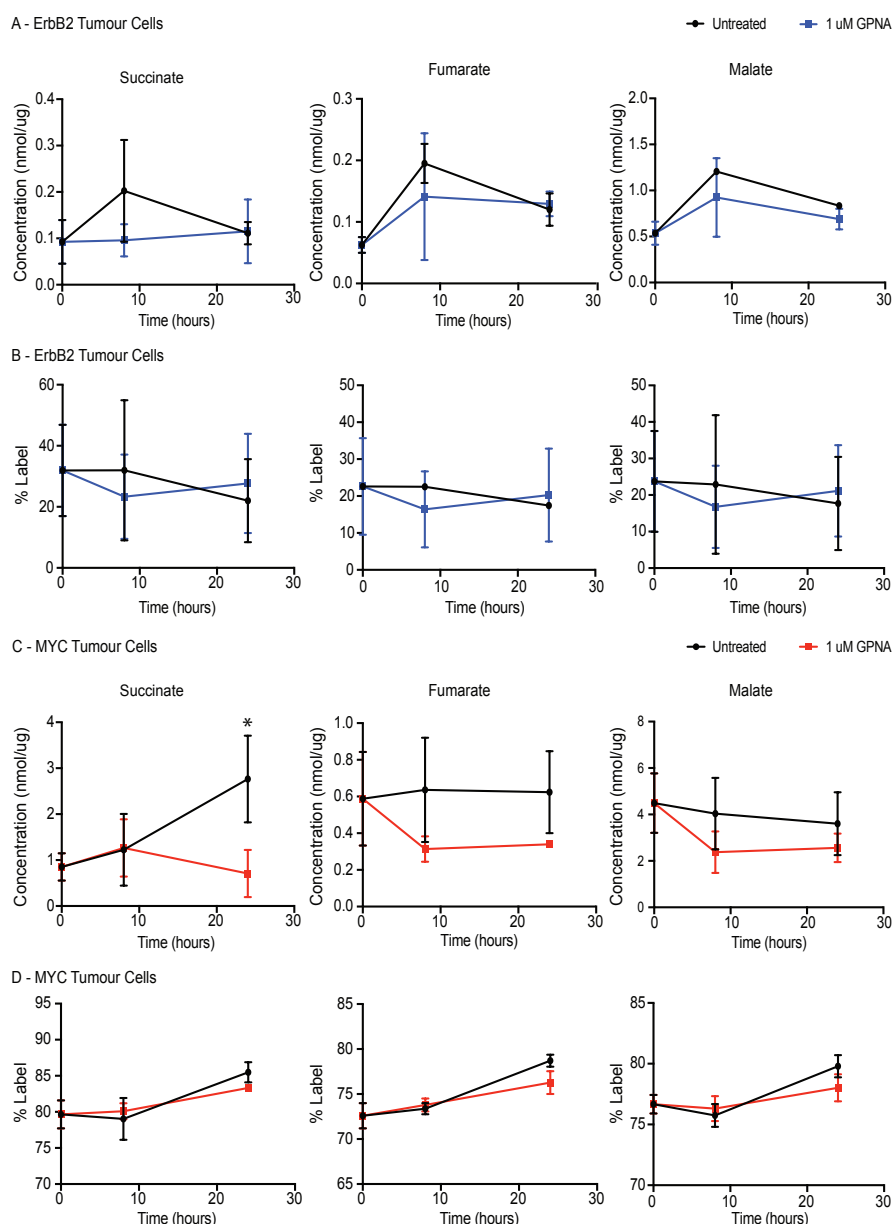
Figure 4-9 GPNA treatment decreases glutamine catabolism into the TCA cycle

Isolated ErbB2 and MYC-induced mammary gland tumour cells were incubated with 1 uM GPNA for 24 hours and $^{13}C_5$-glutamine for the final hour. Cell samples were analysed by GC-MS.

A – The concentration of Succinate, Fumarate and Malate in ErbB2-induced tumour cells.

B – Percent ^{13}C labelling from $^{13}C_5$-glutamine (sum of all isotopomers except M+0) in TCA cycle intermediates in ErbB2-induced tumour cells.

C – The concentration of Succinate, Fumarate and Malate in MYC-induced tumour cells.

D – Percent ^{13}C labelling from $^{13}C_5$-glutamine (sum of all isotopomers except M+0) in TCA cycle intermediates in MYC-induced tumour cells.

Total concentration is expressed as nmol metabolite per μg of cell protein.

Replicates are three different cell lines isolated from three different mice per group.

Unpaired t-test * $P < 0.05$. Error bars denote standard deviation. Some error bars are smaller than the data points.

148

In order to confirm that MYC-induced tumour cells require ASCT2, isolated tumour cells were treated with an siRNA against ASCT2. This would confirm whether the sensitivity of MYC-induced tumour cells to the inhibition of glutamine uptake, was partly due to ASCT2 inhibition, indicating whether ASCT2 would be a suitable therapeutic target against MYC-induced mammary gland tumorigenesis. Even the slight knockdown of ASCT2 demonstrated in Figure 4.10, caused a significant decrease in the cell mass of MYC-induced tumour cells, confirming that ASCT2 expression is required by isolated MYC-induced cells. siRNA treatment against ASCT2 did not affect the cell mass of isolated ErbB2-induced tumour cells.
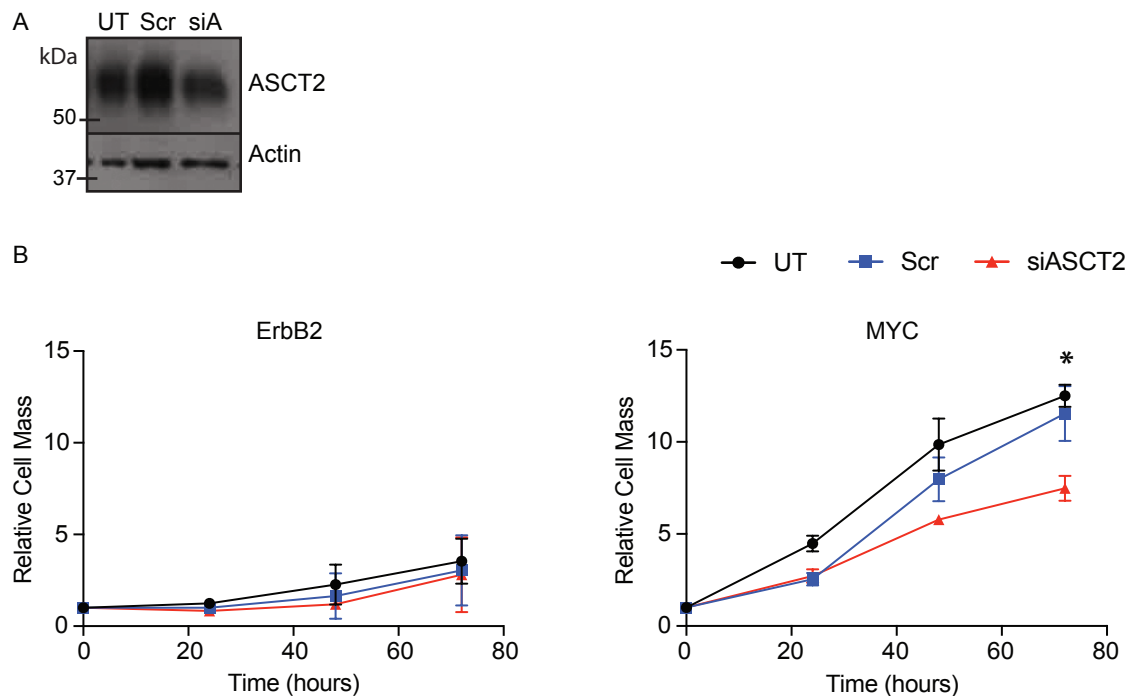
Figure 4-10 The relative cell mass of isolated MYC-induced mammary gland tumour cells decreases after 72 hours siASCT2 treatment

Isolated ErbB2 and MYC-induced tumour cells were treated with scrambled control (Scr) or siASCT2 (siA) for 72 hours. Untreated cells are indicated UT.
A – ASCT2 protein expression in MYC-induced tumour cells.
B – Cell mass was quantified by crystal violet staining. Results were normalised to untreated ErbB2-induced tumour cells at 0 hours.
Replicates are three different cell lines isolated from three different mice per group. ANCOVA * $P < 0.05$. Error bars denote standard deviation, some of the error bars in B are smaller than the points.

While these results demonstrate that ASCT2 is required by isolated MYC-induced tumour cells, they do not confirm if it is required in an *in vivo* setting. This could be done using an inducible shRNA against ASCT2 enabling the expression of ASCT2 to be manipulated *in vivo*. ASCT2 could be switched off once the tumour, generated by the injection of tumour cells into the mammary fat pad, has started to develop to determine if ASCT2 is required for tumour maintenance. This would mimic a therapeutic treatment against ASCT2.

Previously, ASCT2 was shown to be required *in vivo* for human triple negative breast cancer (TNBC) xenografts (Van Geldermalsen et al., 2016). TNBC tends to be the subtype of breast cancer with the greatest MYC overexpression (Fallah et al., 2017). However, MYC overexpression is not exclusive to this subtype (Green et al., 2016), and these results demonstrate the requirement for ASCT2 in a MYC-induced tumour model with high ER expression (Figure 3.7). Thus, it is crucial to determine how ASCT2 is regulated in breast cancer so that any therapeutic strategies can be targeted specifically to the tumours most responsive to ASCT2 inhibition.

4.6 Chapter 4 Summary

In order to answer mechanistic questions regarding the requirement and regulation of altered glutamine metabolism in mammary gland tumours, an *in vitro* cell culture model using isolated ErbB2 and MYC-induced tumour cells grown in adherent culture was developed. $^{13}C_5$-glutamine labelling revealed that isolated MYC-induced tumour cells maintained their increased catabolism of glutamine into the TCA cycle and amino acids compared to ErbB2-induced tumour cells. Isolated MYC-induced tumour cells also maintained their *in vivo* localisation of ASCT2 at the plasma membrane.

Increased glutamine uptake was observed in MYC-induced tumour cells compared to ErbB2-induced tumour cells. While both cell types were dependent on glutamine, MYC-induced tumour cells were also dependent on amino acid transport. Treatment with the wide-range amino acid transporter inhibitor, GPNA, induced cell death in MYC-induced tumour cells and decreased glutamine uptake, the intracellular concentration of glutamine and glutamine catabolism into the TCA cycle. Inhibiting ASCT2 expression using RNAi, demonstrated that ASCT2 is required for MYC-induced tumour cells. This suggests that ASCT2 could be a good therapeutic target against specifically MYC-induced mammary gland tumours. However, this still needs to be confirmed *in vivo*. The next two chapters study the regulation of ASCT2 in both ErbB2 and MYC-induced mammary gland tumour cells, in order to identify the mechanism of regulation of ASCT2 in both types of tumours. As MYC-induced tumours are ER+ (Chapter 3.7), this suggests that high ASCT2 expression is not a feature of TNBC alone, and thus, it is important to understand more about the regulation of the transporter so that the tumours that will respond well to ASCT2 inhibition can be identified.

Chapter 5. Regulation of ASCT2 transcription, N-glycosylation and localisation by MYC, mutant KRas and mutant ErbB2,

5.1 Introduction

The results in Chapter 4 support the work of van Geldermalsen et al. (2016) to suggest that inhibiting ASCT2 would be a good therapeutic strategy against breast cancer and specifically in tumours with high MYC activity (Van Geldermalsen et al., 2016). However, current ASCT2 inhibitors that act as glutamine mimics were shown to target other amino acid transporters as well (Broer et al., 2016; Chiu et al., 2017). By understanding more about the regulation of ASCT2 expression and N-glycosylation, more specific therapeutic strategies could be developed that prevent the expression or N-glycosylation of ASCT2. Likewise, in order to treat patients with a therapy against ASCT2, the patients most likely to respond need to be carefully selected. By understanding more about how ASCT2 is regulated, specific biomarkers can be identified that will allow precise identification of patients with ASCT2-dependent tumours.

ASCT2 needs to be both expressed and N-glycosylated in order to be active at the plasma membrane for the transport of amino acids (Console et al., 2015). ASCT2 expression is regulated by several factors, including the oncogenes, EGFR (Lu et al., 2016; Tao et al., 2017) and MYC (Wise et al., 2008), and the tumour suppressor genes, miR-137 (Dong et al., 2017) and Rb (Reynolds et al., 2014). ASCT2 expression has also been shown to be regulated in response to changing cellular stresses, including the ER-stress response (Jeon et al., 2015; Ren et al., 2015). Glutamine itself has also been shown to regulate the promoter of ASCT2 (Bungard and Mcgivan, 2004). However, the regulation of N-glycosylation in general remains poorly understood and the mechanism of the N-glycosylation of ASCT2 has yet to be described. Thus, while MYC can regulate ASCT2 gene expression, it has not been described whether MYC also regulates the N-glycosylation of ASCT2. Furthermore, MMTV-MYC tumours gain Ras mutations in order to become fully tumorigenic (D'cruz et al., 2001), which can also be

responsible for the increased expression and N-glycosylation of ASCT2 in MYC-induced tumours. While the expression of ASCT2 is not induced in ErbB2-induced tumours, another member of the ErbB family, EGFR, was demonstrated to interact with ASCT2 to increase its expression at the plasma membrane (Lu et al., 2016). Therefore, it should be evaluated whether ErbB2 affects ASCT2 expression and N-glycosylation, and thus, whether ASCT2 expression is inhibited in ErbB2-induced tumours by other factors.

5.2   Chapter 5 aims

- Determine whether ASCT2 expression is MYC-dependent in MYC-induced mammary gland tumour cells,
- Determine if ASCT2 can be expressed and N-glycosylated in ErbB2-induced tumour cells,
- Determine whether ectopic expression of ErbB2 affects ASCT2 expression and localisation,
- Evaluate the relationship between MYC and ASCT2 expression in human PDX samples.

5.3   The regulation of ASCT2 in MYC-induced tumour cells

5.3.1   MYC is required for ASCT2 expression in isolated MMTV-MYC mammary gland tumour cells

As ASCT2 has previously been described as a MYC transcriptional target (Wise et al., 2008), I first wanted to confirm that MYC expression was required for ASCT2 expression in MYC-induced tumour cells. To do this, an siRNA against MYC (siMYC) was used to knock down MYC expression. Figure 5.1 confirms that after 72 hours, siMYC treatment decreases MYC RNA and protein expression in MYC-induced tumour cells. The level of MYC knockdown shown in Figure 5.1, resulted in a significant decrease in ASCT2 RNA (Figure 5.2A) and N-glycosylated protein levels in MYC-induced tumour cells (Figure 5.2B). Consistently, the levels of ASCT2 at the plasma membrane were also decreased (Figure 5.2C). However, as N-glycosylation requires protein expression first, this experiment cannot distinguish between the regulation of ASCT2 expression and any changes in N-glycosylation.

5.3.2   Ectopic expression of MYC is sufficient to induce ASCT2 expression, N-glycosylation and membrane localisation

Genetic instability is a common feature of many tumours, where tumours acquire several mutations as they develop. MMTV-MYC tumours gain Ras mutations in order to become fully tumorigenic (D'cruz et al., 2001). Therefore, I then evaluated the effect of each of these two lesions on ASCT2. To do this, I ectopically expressed human MYC and a mutant form of human KRas G12V in immortalised mouse mammary epithelial cells (iMMECs). KRas G12V models one of the KRas mutations frequently observed in breast cancer (Myers et al., 2016). iMMECs are created by the ectopic expression of dominant negative p53 and E1a in primary mammary epithelial cells. Despite this loss of p53 activity, MMECs immortalised in this way are not believed to be transformed as they do not form tumours in mice when injected into the mammary fat pad (Karantza-Wadsworth et al., 2007), and thus, provide a genetically-defined control system. The increased expression of each of the genes was confirmed by qPCR (Figure 5.3).
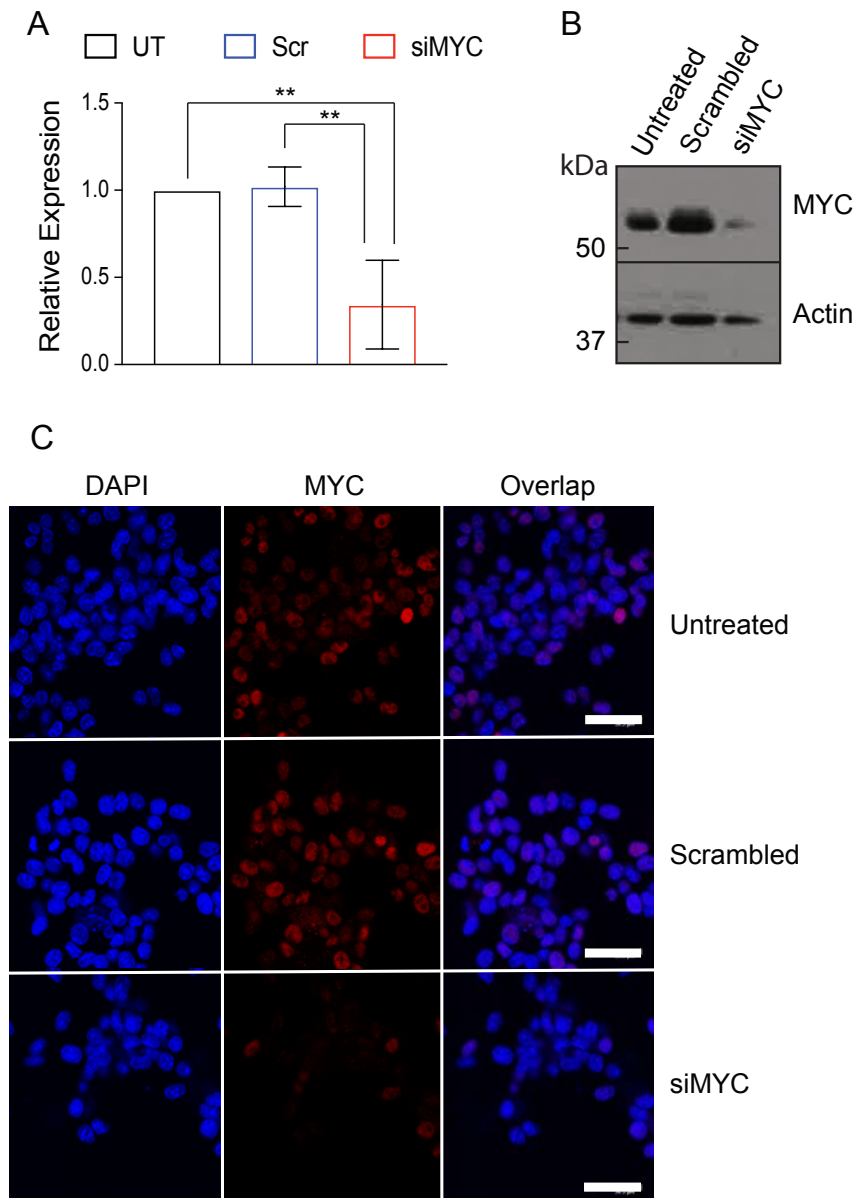
Figure 5-1 siMYC treatment decreases MYC RNA and protein expression in isolated

MYC-induced tumour cells

A – MYC RNA expression in isolated MYC-induced tumour cells, which were either untreated (UT), treated with a scrambled control (Scr) or treated with siMYC for 72 hours. Expression is shown relative to untreated cells. One way ANOVA with Tukey's multiple comparisons test, **$P < 0.001$. Error bars denote standard deviation. Replicates are cells isolated from three different mice per group.
B – MYC protein expression in isolated MYC-induced tumour cells, which were either untreated, treated with a scrambled control or treated with siMYC for 72 hours. n = 3.
C – MYC protein (red) and DAPI (blue) localisation in isolated MYC-induced tumour cells, which were either untreated, treated with a scrambled control or treated with siMYC for 72 hours. Scale bar: 30 μM. Images representative of 3 cells lines isolated from tumours from 3 different mice.
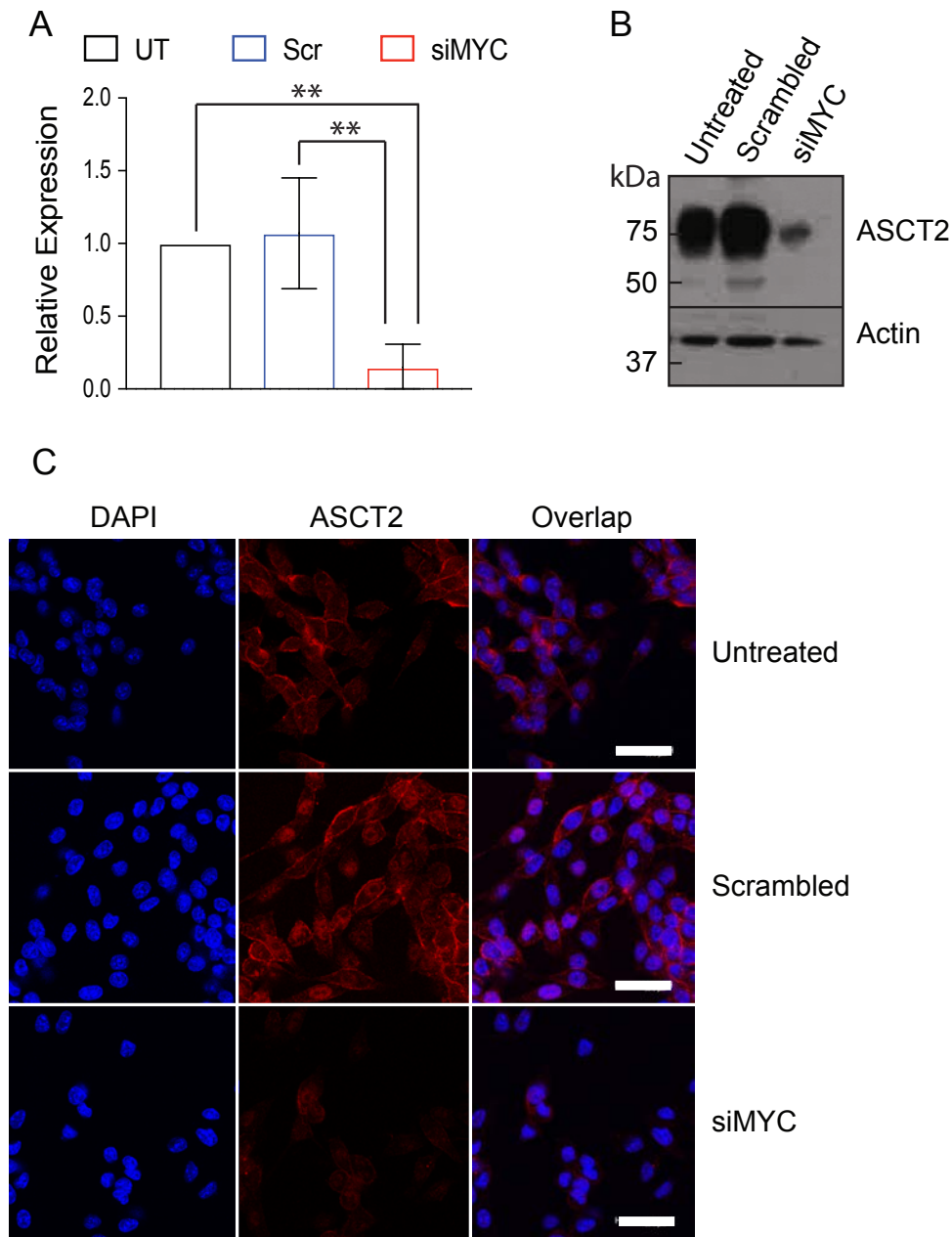
Figure 5-2 siMYC treatment decreases ASCT2 RNA and protein expression in isolated MYC-induced tumour cells

A – ASCT2 RNA expression in isolated MYC-induced tumour cells, which were either untreated (UT), treated with a scrambled control (Scr) or treated with siMYC for 72 hours. Expression is shown relative to untreated cells. One way ANOVA with Tukey's multiple comparisons test, *P < 0.01, **P < 0.001, Error bars denote standard deviation. Replicates are cells isolated from 3 different mice per group.

B – ASCT2 protein expression in isolated MYC-induced tumour cells, which were either untreated, treated with a scrambled control or treated with siMYC for 72 hours. n = 3.

C – ASCT2 protein (red) and DAPI (blue) localisation in isolated MYC-induced tumour cells, which were either untreated, treated with a scrambled control or treated with siMYC for 72 hours. Scale bar: 30 μM. Images representative of 3 cells lines isolated from tumours from 3 different mice.
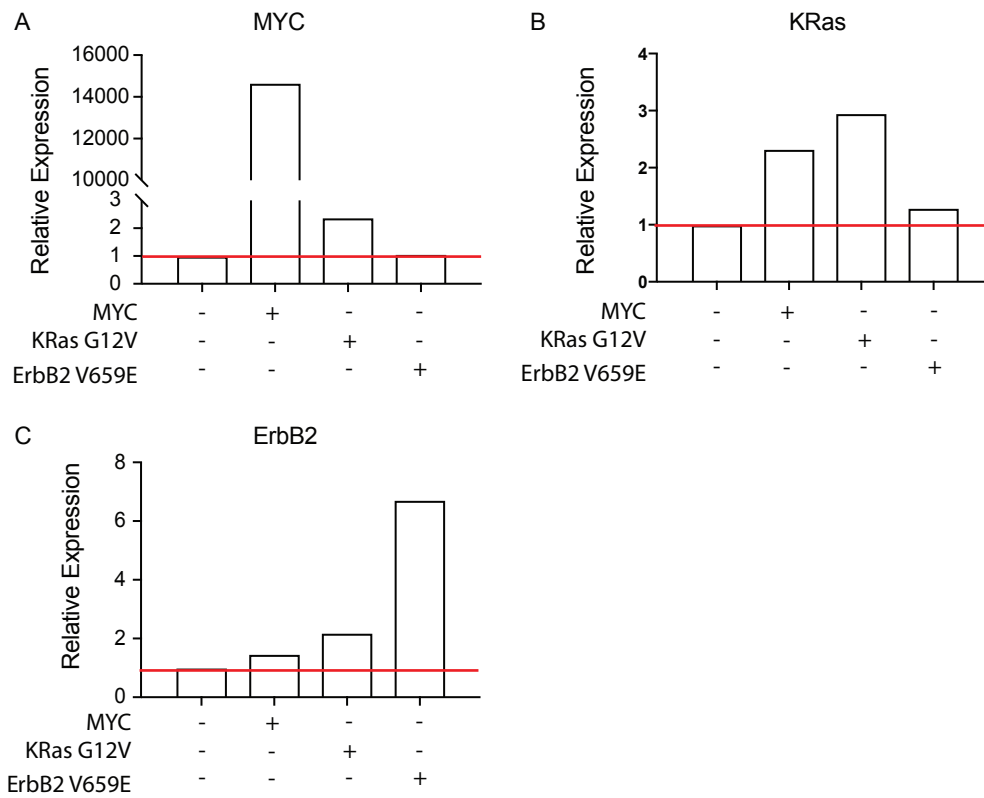
Figure 5-3 Creation of iMMEC lines with added MYC, KRAS G12V and ErbB2 V659E oncogenes

Relative MYC (A), KRas (B) and ErbB2 (C) RNA expression in iMMECs with added oncogenes. Expression is shown relative to iMMECs with nothing added. n = 1.

To ensure that the ectopically expressed MYC was acting as a transcription factor, MYC localisation to the nucleus was confirmed in the cells with MYC expression (Figure 5.4). The nuclear localisation of MYC also increased in cells with added KRas G12V. This demonstrates that KRas G12V expression increases MYC expression and activity in these cells, which is consistent with the stabilisation of MYC protein by the Ras pathway (Tsai et al., 2012). The antibody used here detects both the mouse and human form of the protein, and so can detect the increase in endogenous MYC expression, whereas it could not be detected using the human-specific Taqman probe.
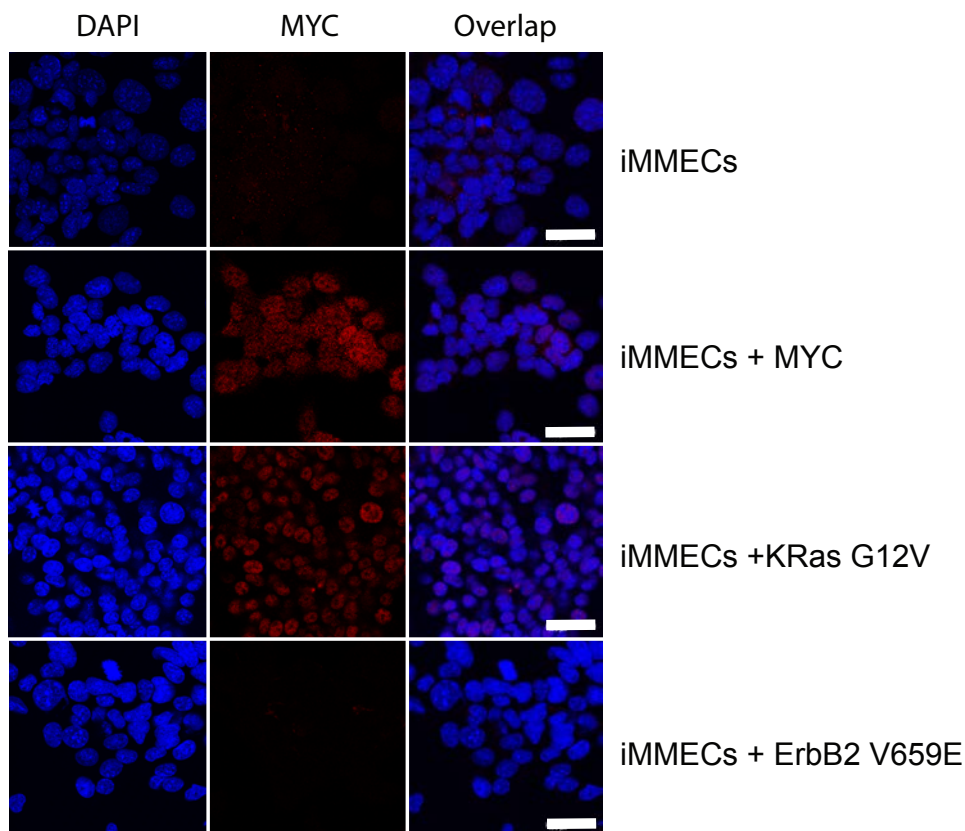
Figure 5-4 MYC localisation in iMMEC lines with added MYC, KRAS G12V and ErbB2 V659E oncogenes

MYC protein (red) and DAPI (blue) localisation in iMMECs with added oncogenes. Scale bar: 30 µM. n = 1.

Changes in ASCT2 RNA expression were detected in relation to the expression in iMMECs with no added oncogenes (Figure 5.5A). Expression of MYC and KRas G12V were sufficient to increase ASCT2 RNA expression and the levels of N-glycosylated ASCT2 (Figure 5.5B) and also, induced ASCT2 localisation at the plasma membrane (Figure 5.5C). The ectopic expression of MYC and KRas G12V was repeated using freshly isolated MMECs, to remove any additional effects that immortalisation might have on ASCT2 expression and localisation (Figures 5.6-8). Because non-immortalised mammary epithelial cells senesce within 7-10 days (Degenhardt and White, 2006), there is not a control cell line without the addition of any oncogenes, and so for the RNA expression data the values are shown relative to either the MMECs with ectopic KRas G12V expression (Figure 5.6A) or with ectopic MYC expression (Figure 5.6B and C). As observed using iMMECs, ectopic expression of MYC and mutant KRas resulted in ASCT2 protein expression, N-glycosylation and localisation to the plasma membrane (Figure 5.8). This confirms that the expression and localisation of ASCT2 observed in the iMMECs in response to ectopic MYC and mutant KRas expression was not the result of the immortalised background.
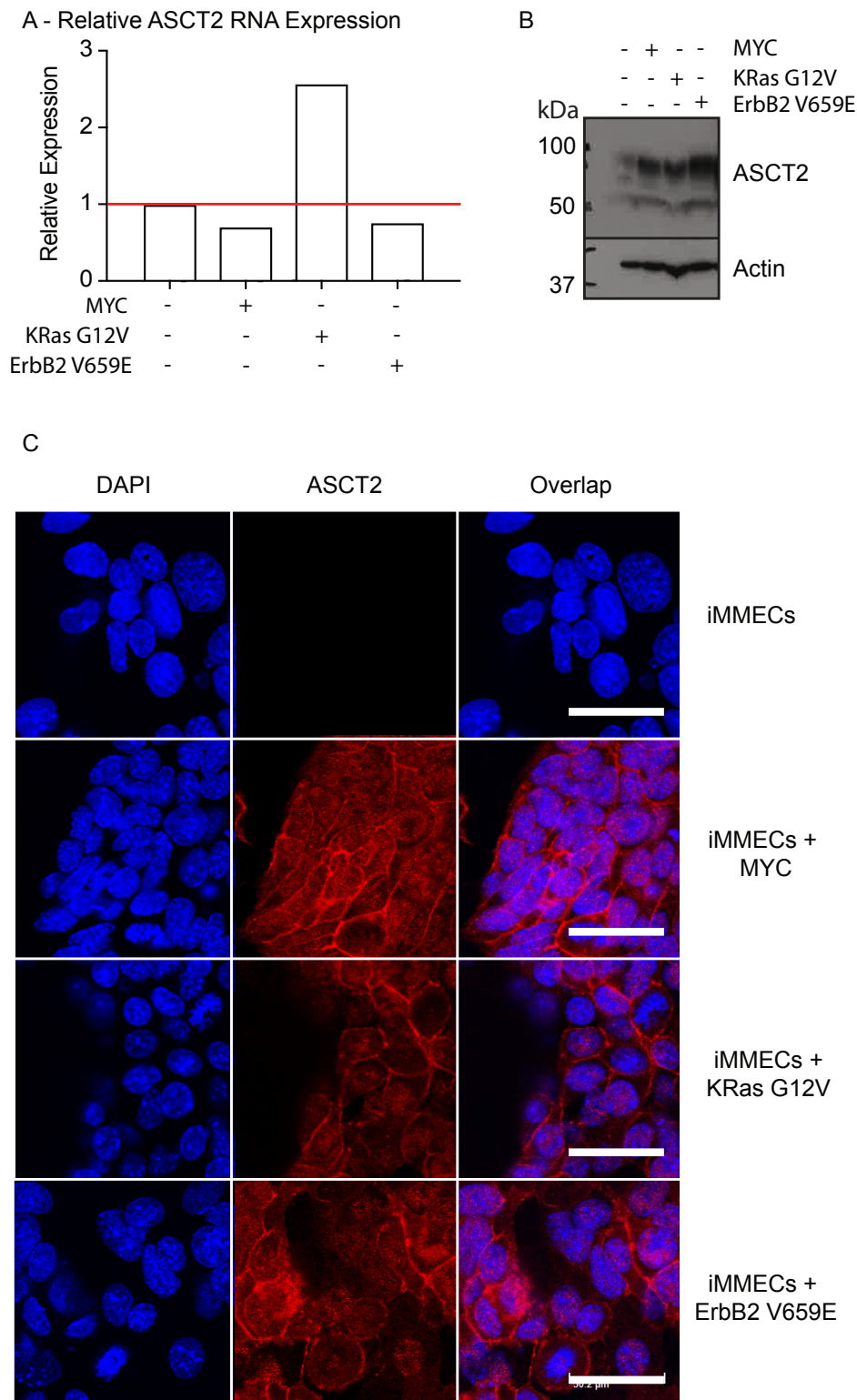
Figure 5-5 ASCT2 RNA and protein expression and membrane localisation in iMMECs

with added oncogenes

A – Relative ASCT2 RNA expression in iMMECs with added oncogenes. Expression is shown relative to iMMECs with nothing added. n = 1.
B – ASCT2 protein expression in iMMECs with added oncogenes. n = 1.
C – ASCT2 protein (red) and DAPI (blue) localisation in iMMECs with added oncogenes. Scale bar: 30 µM. n = 1.
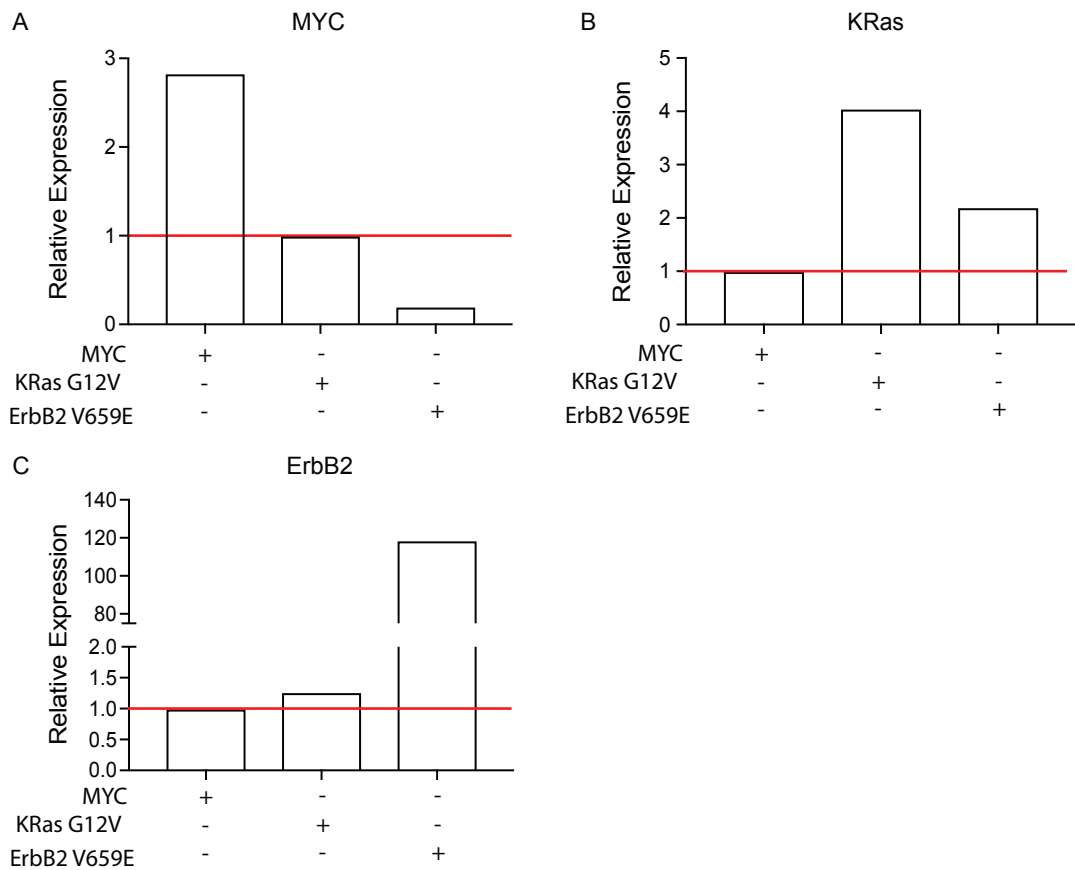
Figure 5-6 Creation of MMEC lines with added MYC, KRAS and ErbB2 oncogenes

A, B + C – Relative MYC (A), KRAS (B) and ErbB2 (C) RNA expression in MMECs with added oncogenes (MYC, KRAS and ErbB2). Expression is shown relative to MMECs + KRas G12V (A) or MMECs + MYC (B + C). n = 1.
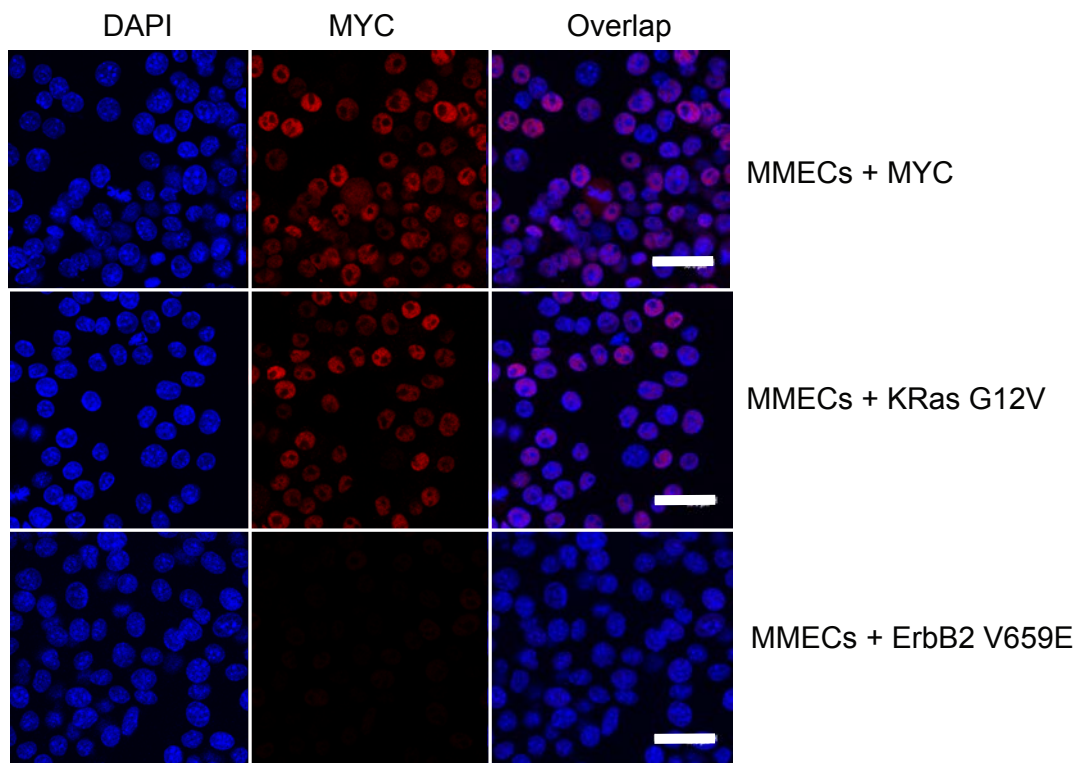
Figure 5-7 MYC localisation in MMECs with added oncogenes

MYC protein (red) and DAPI (blue) localisation in MMECs with added oncogenes. Scale bar: 30 µM. n = 1.
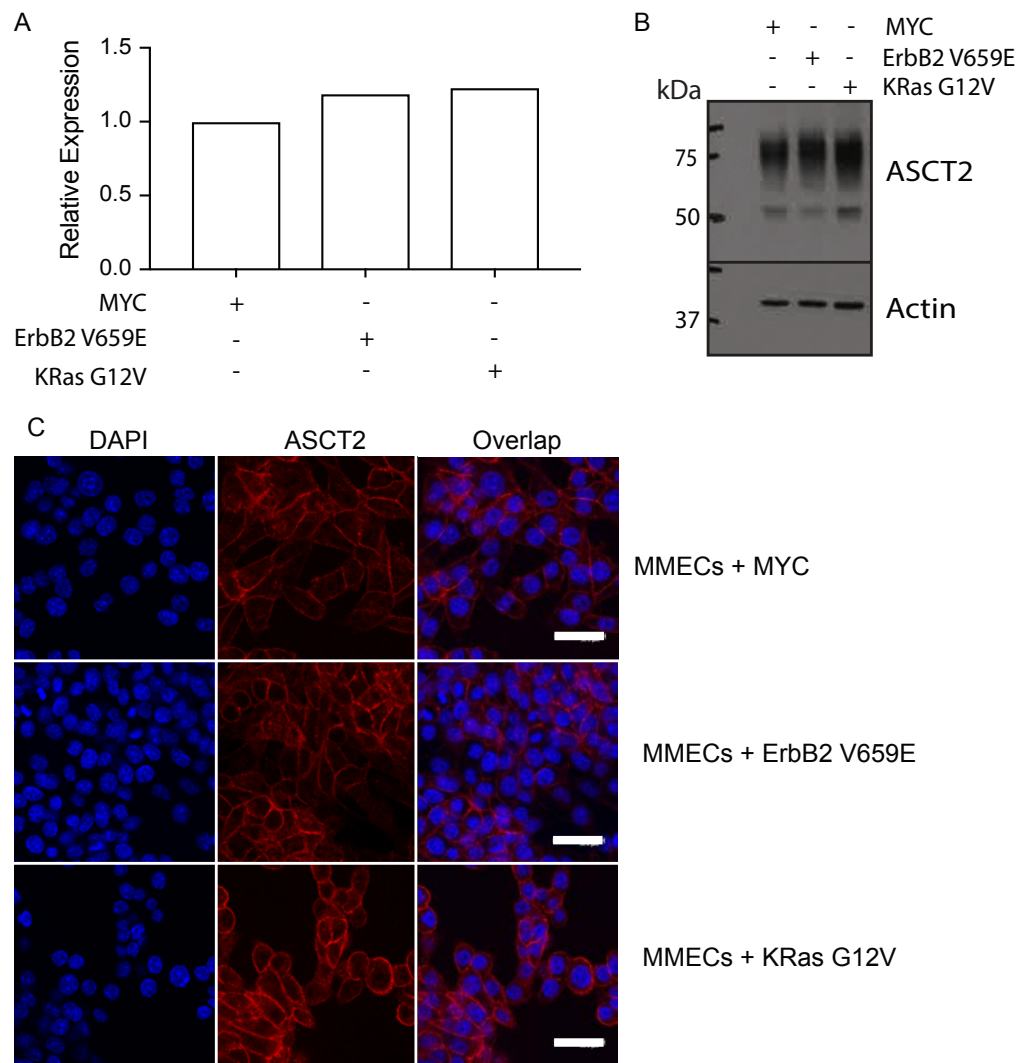
Figure 5-8 ASCT2 RNA and protein expression and membrane localisation in MMECs

with added oncogenes

A – Relative ASCT2 RNA expression in MMECs with added oncogenes. Expression is shown relative to MMECs + MYC. n = 1.
B – ASCT2 protein expression in MMECs with added oncogenes. n = 1.
C – ASCT2 protein (red) and DAPI (blue) localisation in MMECs with added oncogenes. Scale bar: 30 µM. n = 1.

The increased ASCT2 expression and N-glycosylation in iMMECs and MMECs with ectopic KRas G12V expression could be due to downstream stabilisation of MYC regulating ASCT2. To further evaluate if KRas G12V can affect ASCT2 regulation independently from MYC, ablating MYC expression in the cells with ectopic expression of KRas G12V will have to be performed.

These experiments show that MYC is required and sufficient for ASCT2 expression in MYC-induced tumour cells. As MYC regulates ASCT2 transcription, and protein expression is required before N-glycosylation can occur; these experiments cannot determine if MYC actively regulates ASCT2 N-glycosylation or whether increased N-glycosylation is the result of an increase in ASCT2 protein concentration. To address these questions, ASCT2 can be ectopically expressed in ErbB2 or primary mammary epithelial cells to evaluate whether increasing the protein levels of ASCT2 is sufficient to induce its N-glycosylation and membrane localisation. If ectopic overexpression of ASCT2 is sufficient to induce its N-glycosylation, this suggests that the expression and activity of glycosylase enzymes required is MYC-independent. If MYC proves to be required for ASCT2 N-glycosylation, the expression levels of glycosylase enzymes in cells with and without MYC could be studied. Given the large number of glycosylase enzymes (Breton et al., 2006), a high throughput transcriptomics method, such as RNAseq (Mortazavi et al., 2008; Wilhelm et al., 2008), would be appropriate to study all of the enzymes at once. If the expression of any glycosylases is altered with increased MYC activity, these enzymes could then be knocked out in MYC overexpressing mammary epithelial cells and in the isolated tumour cell lines to determine if they are required for the N-glycosylation of ASCT2.

5.4 Regulation of ASCT2 expression, N-glycosylation and localisation in ErbB2-induced tumours

Since another member of the ErbB family, EGFR, was recently demonstrated to interact with ASCT2 to increase its localisation at the plasma membrane (Lu et al., 2016) and ASCT2 RNA expression, but not N-glycosylation and membrane localisation are observed in ErbB2-induced tumours, I hypothesised that ASCT2 expression and/or N-glycosylation might be inhibited in ErbB2-induced tumours. To evaluate if this is indeed the case, I first tested if ErbB2-induced tumour cells have the ability to express ASCT2. To do this, I evaluated if ectopic expression and activation of MYC can induce ASCT2 expression and membrane localisation in isolated ErbB2-induced tumour cells. ErbB2-induced tumour cells were transduced with an inducible MYC construct, pBabe-MYCER. In this system MYC is fused with the estrogen receptor (ER) binding domain and its activity is induced by 4-hydroxytamoxifen, 4OHT, which causes the ER and the attached MYC to translocate to the nucleus (Eilers et al., 1989). Transduction with the plasmid carrying only ER, pBabe-ER, was used as a control.

Isolated ErbB2-induced tumour cells with ectopic expression of MYCER, both with or without 4OHT, had increased levels of MYC in the nucleus (Figure 5.9). The nuclear expression of MYC in the absence of 4OHT indicates that the activation of ER is not tightly regulated in this system. MYCER expression induced ASCT2 protein expression, N-glycosylation and plasma membrane localisation in ErbB2-induced tumour cells, regardless of 4OHT treatment (Figure 5.10). The ability of ErbB2-induced tumour cells to upregulate ASCT2 expression and N-glycosylation in response to ectopic expression of MYC confirms that the ASCT2 gene is not mutated in these cells and that it can be expressed and N-glycosylated. Similarly, it suggests that ErbB2-induced tumour cells have all the intermediates required for ASCT2 expression and N-glycosylation.

A - ErbB2 tumour cells + pBabe-ER

B - ErbB2 tumour cells + pBabe-MYCER
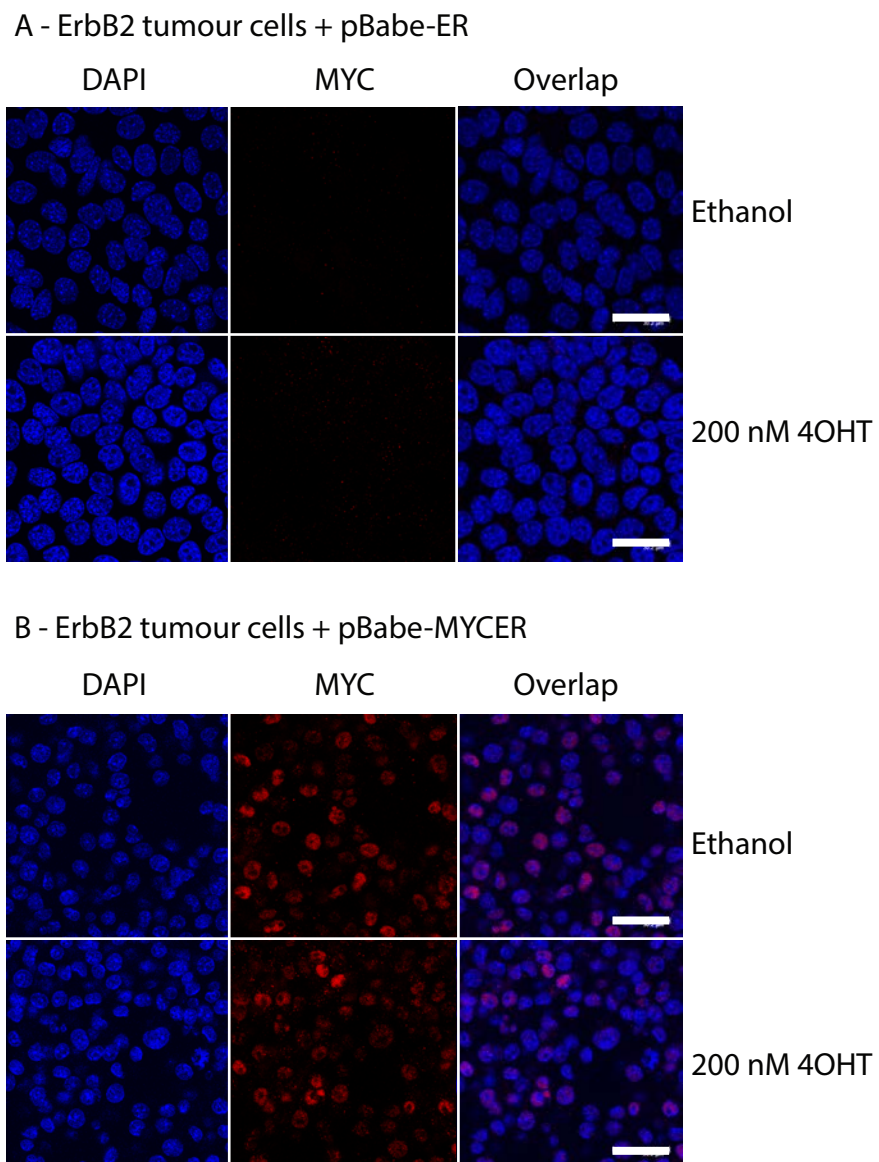
Figure 5-9 MYC localisation in the nucleus increases in isolated ErbB2-induced tumour cell lines with added pBabe-MYCER

MYC (red) and DAPI (blue) localisation in ErbB2-tumour cells with either pBabe-ER (A) or pBabe-MYCER (B), after 24 hours treatment with 200 nM 4-hydroxytamoxifen (4OHT) or ethanol vehicle control. Scale bar: 30 µM. Images representative of 3 cell lines isolated from tumours from 3 different mice.
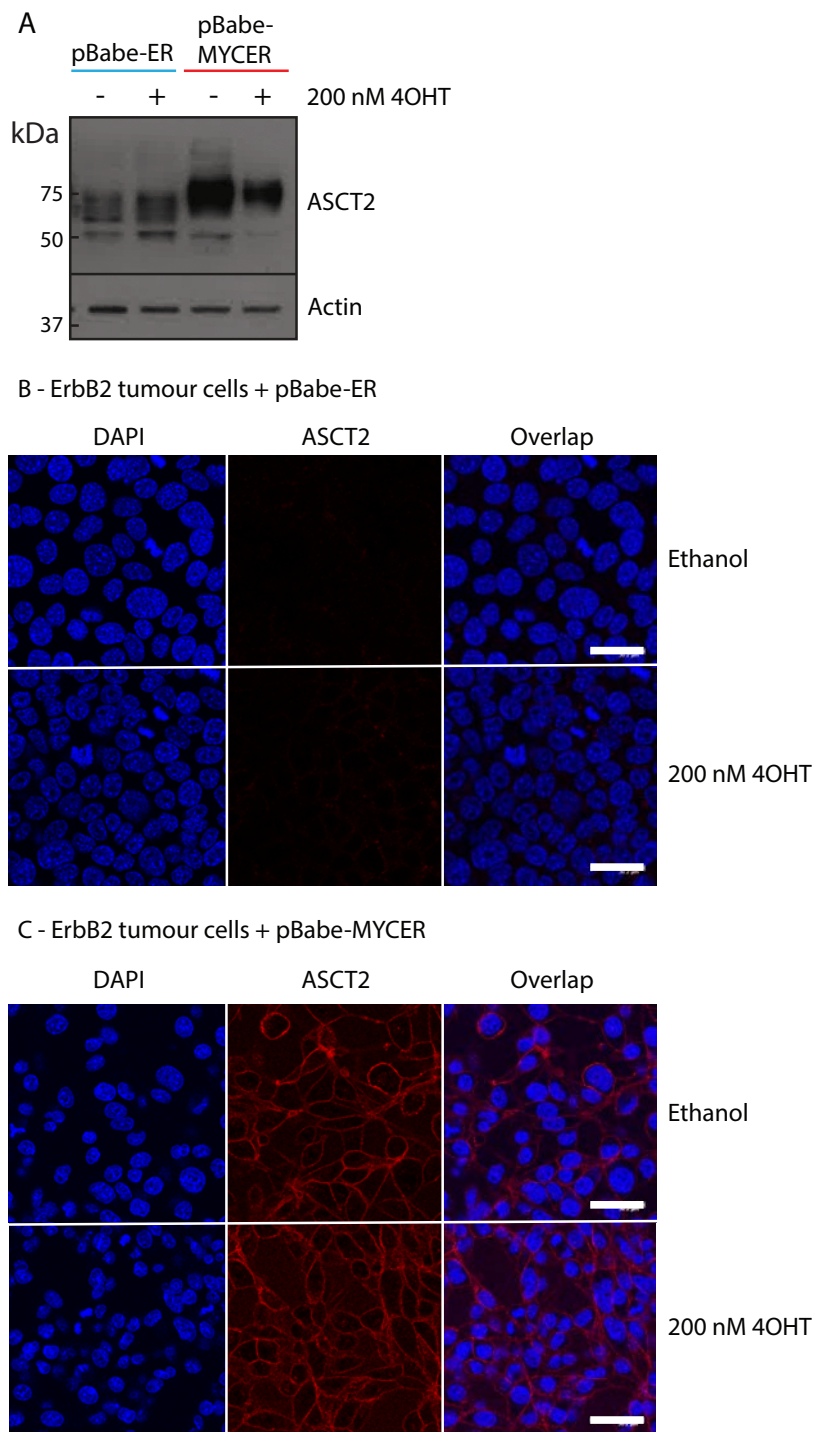
Figure 5-10 pBabe-MYCER increases ASCT2 expression and localisation at the plasma membrane in ErbB2-induced tumour cells

ASCT2 protein (A) and membrane localisation (B + C) in ErbB2-induced tumour cells with either pBabe-ER (B) or pBabe-MYCER (C), after 24 hours treatment with 200 nM 4-hydroxytamoxifen (4OHT) or ethanol vehicle control. Scale bar: 30 µM. Images representative of 3 cell lines isolated from tumours from 3 different mice.

I next tested if ectopic expression of mutant ErbB2 affects ASCT2 expression, N-glycosylation and membrane localisation. To do this, I ectopically expressed a mutant form of human ErbB2 V659E in iMMECs. The ErbB2 V659E mutant used here is constitutively active, and so models the mutant ErbB2 expressed in MMTV-ErbB2 tumours. ErbB2 expression was confirmed by qPCR (Figure 5.3). Similar to ErbB2 tumours and isolated tumour cells, ectopic expression of ErbB2 V659E did not induce nuclear localisation of MYC (Figure 5.4). Ectopic expression of ErbB2 V659E did not increase ASCT2 mRNA levels (Figure 5.5A). However, surprisingly, it increased the levels of N-glycosylated ASCT2 protein (Figure 5.5B) and induced its localisation at the plasma membrane (Figure 5.5C). The results were confirmed by the ectopic expression of ErbB2 V659E in freshly isolated MMECs (Figure 5.6-8). These results suggest that ectopic expression of ErbB2 V659E regulates ASCT2 at a post-transcriptional level, either by regulating the protein stability or the glycosylation machinery.

Despite the ability of ectopic ErbB2 expression to induce the N-glycosylation and membrane localisation of ASCT2 in mammary epithelial cells, this differs from the results observed in MMTV-ErbB2 tumour cells, where ASCT2 expression is low and there is little N-glycosylation and almost no ASCT2 located at the plasma membrane. This difference between the two systems could be due to a number of reasons.

First, this difference could be due to different expression levels of the mutant ErbB2 as the gene is under the control of different promoters in each system. Secondly, despite both mutations causing the constitutive activity of ErbB2, the mutant forms of ErbB2 used in each system were different. This different mutation might affect how ErbB2 affects ASCT2. EGFR was shown to physically interact with ASCT2 in order to promote the membrane localisation of the transporter (Lu et al., 2016). It could be that ErbB2 also interacts with the protein and increases its stability and membrane localisation, as observed with ectopic ErbB2 expression in MMECS. Thus, the different mutations might affect the ability of the ErbB2 to interact with ASCT2 in different ways. Finally, tumours are known to have high levels of genetic instability and thus, the genetic background of the MMTV-ErbB2 tumours is likely to have a higher frequency

of genetic alterations than the iMMEC cell lines. Thus, ASCT2 protein expression and/or N-glycosylation might be inhibited by one of these additional mutations in the ErbB2-induced tumours, resulting in the low ASCT2 expression levels in these tumours.

5.5 High MYC expression correlates with high levels of ASCT2 expression in PDX tumours

In order to understand how the data collected using mouse models of mammary gland tumorigenesis translate into a human setting, a panel of patient-derived xenograft (PDX) samples were tested. The samples used for this screen were kindly provided by Carlos Caldas at the Cancer Research UK Cambridge Institute. PDXs have proved to be a valuable tool to study human breast cancer samples in a physiologically relevant tumour microenvironment that mimics the oxygen and hormone levels found in the patient's primary tumour site. Implanted tumour tissues have been shown to maintain the genetic and epigenetic abnormalities found in the patient (DeRose et al., 2011; Bruna et al., 2016), and as a result, PDX models exhibit similar responses to anti-cancer agents as observed in the patient who provided the tumour sample (Izumchenko et al., 2017).

The samples were divided by their ERα and HER2 status to determine whether high ASCT2 expression was associated with one of the current subtypes of breast cancer used clinically. Some samples expressing each receptor were run on each gel (Figure 5.11). The progesterone receptor (PR) status and clinical subtype of these tumours is unknown. The expression and glycosylation of ASCT2 was present in both ERα+ and HER2+ tumours as well as in receptor-negative tumours, suggesting that ASCT2 expression is not exclusive to a particular subtype. This confirms the recent findings of Bernhardt et al. (2017), who recently demonstrated that ASCT2 expression does not correlate to a particular subtype of breast cancer (Bernhardt et al., 2017).

ASCT2 expression and N-glycosylation was present in every tumour with high MYC expression. However, ASCT2 expression was not limited to tumours with high MYC expression, demonstrating that other factors regulate ASCT2 in breast cancer as well,

and that the absence of MYC does not necessarily indicate absence of N-glycosylated ASCT2.

Van Geldermalsen et al. (2016) demonstrated ASCT2 localisation at the plasma membrane in the luminal breast cancer cell line, MCF-7 and in the TNBC cell line, HCC1806 (Van Geldermalsen et al., 2016). However, while both cell lines expressed ASCT2 at the plasma membrane, only the TNBC line was sensitive to GPNA treatment, suggesting that N-glycosylation and plasma membrane localisation of ASCT2 do not necessarily indicate that cells are dependent on the transporter and would be sensitive to its inhibition. Further studies to determine the requirement for ASCT2 in cells expressing ASCT2 at the plasma membrane need to be performed to determine which additional features of the cells result in ASCT2 dependency.

Based on the different patterns of protein smearing in different samples, the patterns of ASCT2 glycosylation varied between tumours. This too did not appear to be specific to different receptor expression or MYC expression. It would be interesting to determine how different ASCT2 glycosylation affects its membrane localisation and subsequent glutamine uptake in these tumours, as this could determine whether the tumours would be sensitive to ASCT2 inhibition.
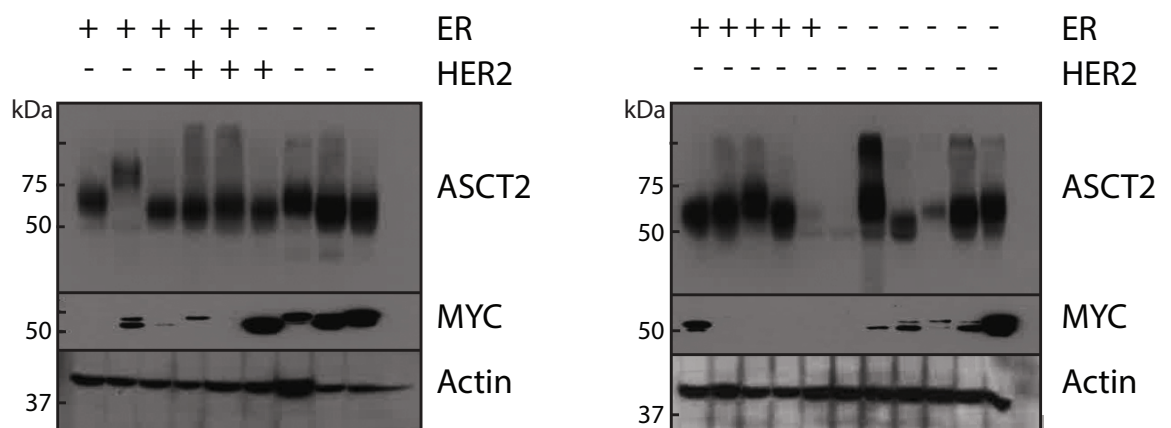
Figure 5-11 ASCT2 and MYC protein expression in human PDX samples

ASCT2 and MYC protein expression in human PDX samples after serial transplantation in mice.

5.6   Chapter 5 Summary

In order to develop new therapeutic strategies against ASCT2-dependent mammary gland tumours, a greater understanding of the regulation of the transporter is required. This will not only help to identify patients with ASCT2-dependent tumours, but might also elucidate new targets that inhibit ASCT2 without targeting the transporter itself, as current compounds targeting ASCT2 inhibit other amino acid transporters as well (Broer et al., 2016; Chiu et al., 2017). Thus, by understanding more about how ASCT2 is N-glycosylated, compounds targeting glycosylase enzymes could be developed that might prove effective at increasing ASCT2 degradation.

In this chapter, the regulation of ASCT2 in tumours induced by specific oncogenes was investigated. MYC was demonstrated to be required and sufficient for ASCT2 expression, N-glycosylation and membrane localisation in both mammary epithelial cells and mammary gland tumour cells.

Although ASCT2 N-glycosylation and membrane localisation was not observed in ErbB2 V664D-induced tumours, ectopic expression of ErbB2 V659E in primary mammary epithelial cells resulted in ASCT2 N-glycosylation and membrane localisation, which was through a MYC-independent mechanism. This result suggests that while ectopic ErbB2 V659E expression can result in ASCT2 membrane localisation, in ErbB2-induced tumours, other factors are active that prevent either the expression or N-glycosylation of the transporter.

In order to successfully target ASCT2-dependent tumours, ASCT2 vulnerability needs to be identified in human patients. To determine how the results from the mouse models of mammary gland tumours relate to human breast tumours, a panel of human PDX samples were tested. ASCT2 expression and N-glycosylation was observed in all tumours with high MYC expression. However, ASCT2 expression was also observed in tumours with low MYC expression and tumours with each type of ERα and HER2 expression. As the expression and plasma membrane localisation of ASCT2 have been shown to not always determine cell sensitivity to ASCT2 inhibition (Van Geldermalsen

et al., 2016), tumour biopsies have to be tested for membrane localisation of ASCT2 and then biopsy-derived cell cultures can be tested for their sensitivity to ASCT2 inhibition.

Chapter 6. Regulation of ASCT2 N-glycosylation and localisation by glutamine metabolism

6.1 Introduction

The membrane localisation of ASCT2 has been shown to depend on the N-linked glycosylation of the protein (Console et al., 2015). UDP-GlcNAc, a key intermediate required for both O-linked and N-linked glycosylation of proteins, including ASCT2, is produced through the hexosamine biosynthesis pathway (HBP). Both glucose and glutamine are required to fuel the HBP, where glucoseamine-fructose-6-phosphate aminotransferase, GFAT, transfers the amino group from glutamine onto the glycolytic intermediate, glucose-6-phosphate to produce glucoseamine-6-phosphate. This is the rate-limiting step of this process, controlling the flux of both glucose and glutamine into the HBP. Salvage pathways are known that divert GlcNAc into the HBP bypassing GFAT enzymes.

Glucose starvation and inhibition of glucose catabolism inhibits the HBP, preventing the glycosylation of ASCT2 (Polet et al., 2016). Whereas increasing glutamine concentrations have been shown to increase HBP activity (Abdel Rahman et al., 2013). GFAT1 expression is regulated by the concentration of the glutamine catabolite, αKG, where decreased αKG decreases GFAT1 expression (Moloughney et al., 2016), demonstrating strict regulation of GFAT1 and the HBP by downstream intermediates of glutamine metabolism (Moloughney et al., 2016). Thus, in order for ASCT2 to be N-glycosylated, and localised to the plasma membrane, cells require both glucose and glutamine.

Glutamine has also been shown to regulate the promoter of ASCT2 in hepatocellular carcinoma cells (Bungard and Mcgivan, 2004), suggesting that glutamine could regulate both the expression and N-glycosylation of ASCT2. In this chapter, I first evaluated whether the increased expression, N-glycosylation and membrane localisation of ASCT2 in MYC-induced tumour cells is glutamine-dependent. I then evaluated if the intracellular glutamine concentration can be a limiting factor for ASCT2 regulation in

ErbB2-induced tumour cells. By understanding more about how ASCT2 is regulated by glutamine and how this regulation interacts with the regulation by oncogenes; we can identify new regulatory mechanisms that reveal how cell metabolism adapts to the changing tumour microenvironment. This could enable us to predict how tumours will respond to therapies targeting metabolic pathways, revealing compensatory resistance mechanisms and potential new targets for combination therapies.

6.2   Chapter 6 Aim

- Determine whether glutamine regulates the expression and/or N-glycosylation of ASCT2 in isolated mammary gland tumour cell lines,

6.3 Glutamine is required for ASCT2 N-glycosylation in MYC-induced tumour cells

Glutamine is required for N-glycosylation through the HBP. This could form part of a positive feedback loop, where a high glutamine supply increases HBP activity, and thus, increases ASCT2 stability and activity, enabling greater glutamine uptake. As well as stabilising ASCT2 protein through N-glycosylation, glutamine has also been shown to regulate the promoter of ASCT2 (Bungard and Mcgivan, 2004). In the study by Bungard and McGiven (2004), a firefly luciferase gene was placed under the control of the promoter of ASCT2, and luciferase activity increased in the presence of glutamine. Understanding how ASCT2 is regulated by glutamine will elucidate more about the interaction between the tumour microenvironment and the regulation of cell metabolism. In order to find out whether ASCT2 can be regulated by glutamine, isolated tumour cells were cultured with and without glutamine, to determine if glutamine deprivation decreases ASCT2 expression and N-glycosylation in MYC-induced tumour cells.
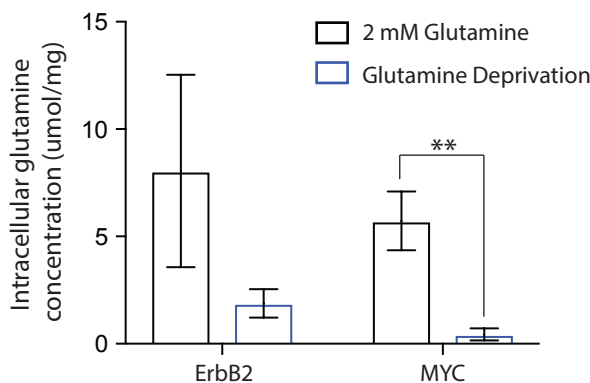
Figure 6-1 Glutamine deprivation decreases the intracellular glutamine concentration of MYC-induced tumour cells

Intracellular glutamine concentration of ErbB2 and MYC-induced tumour cells cultured in 2 mM glutamine or complete glutamine deprivation for 24 hours. Glutamine concentration, measured by 1D NMR, is expressed as µmol glutamine per mg dried protein. Replicates are three different cell lines isolated from three different mice per group. Unpaired t-test: **$P < 0.005$. Error bars denote standard deviation.

Complete glutamine deprivation for 24 hours decreased the levels of intracellular glutamine in both cell types (Figure 6.1) and caused the loss of ASCT2 from the plasma membrane in MYC-induced tumour cells (Figure 6.2). Glutamine deprivation did not affect ASCT2 localisation in ErbB2-induced tumour cells. Interestingly, ASCT2 RNA expression increased slightly during glutamine deprivation in both cell lines, suggesting that the loss of N-glycosylated ASCT2 protein was due to the lack of N-glycosylation and not due to a decrease in RNA expression. Given that glutamine is required for N-glycosylation through the HBP, this suggests that in glutamine deprived conditions, there is insufficient glutamine for N-glycosylation, and thus, ASCT2 is no longer N-glycosylated and so is rapidly degraded. Our results demonstrate that in MYC-induced mammary gland tumour cells, glutamine regulates ASCT2 glycosylation and stabilisation, rather than transcription. While the findings of Bungard and McGiven demonstrated that glutamine activated the promoter of ASCT2 in hepatocellular carcinoma cells (Bungard and Mcgivan, 2004); glutamine deprivation can also trigger an endoplasmic reticulum stress (ER-stress) response (Chen et al., 2014), which has also been shown to regulate ASCT2 expression through increased ATF4 activity (Qing et al., 2012). The latter could be a mechanism how ASCT2 RNA is upregulated in ErbB2 and MYC-induced mammary gland tumour cells in response to glutamine deprivation.
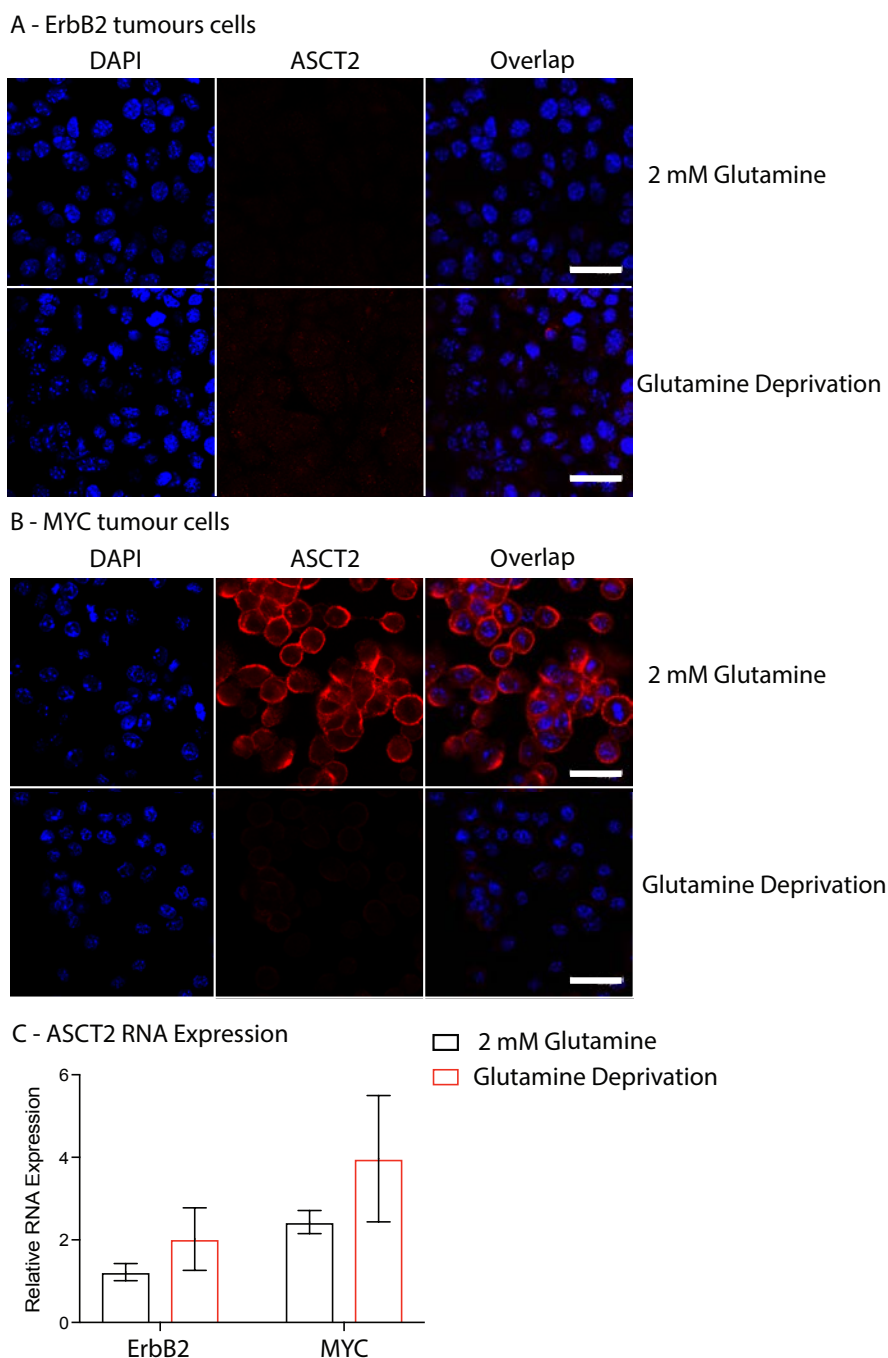
Figure 6-2 Glutamine deprivation decreases ASCT2 membrane localisation but not RNA expression in MYC-induced tumour cells

A + B – ASCT2 (red) and DAPI (blue) localisation in isolated ErbB2 (A) and MYC (B) –induced tumour cells cultured in 2 mM glutamine or complete glutamine deprivation for 24 hours. Scale bar: 30 µM. Images representative of three different cell lines isolated from three different mice per group.

C – ASCT2 RNA expression in ErbB2 and MYC-induced tumour cells cultured in 2 mM glutamine media or complete glutamine deprivation for 24 hours. RNA expression is shown relative to untreated ErbB2-induced cells. Replicates are three different cell lines isolated from three different mice per group. Error bars denote standard deviation.

6.4 Gls1 inhibition increases ASCT2 N-glycosylation and localisation at the plasma membrane in ErbB2-induced tumour cells

It has been shown that inhibiting Gls1 increases the intracellular glutamine concentration in cells (Yuneva et al., 2012). Therefore, to probe if a low intracellular concentration of glutamine in ErbB2-induced tumour cells can be a limiting factor for ASCT2 N-glycosylation, isolated tumour cells were treated with BPTES, an allosteric Gls1 inhibitor.

To evaluate if BPTES treatment increased the intracellular concentration of glutamine, this was measured by 1D-NMR (Figure 6.3). The concentration of glutamine in ErbB2-induced cells remained fairly constant after BPTES treatment and decreased slightly in MYC-induced tumour cells. This was unexpected as it disagrees with previous work, where BPTES treatment increased intracellular glutamine concentration (Yuneva et al., 2012). This suggests that glutamine catabolism by alternative pathways may be faster with BPTES treatment, as there is no build-up of surplus glutamine when Gls1 is inhibited.
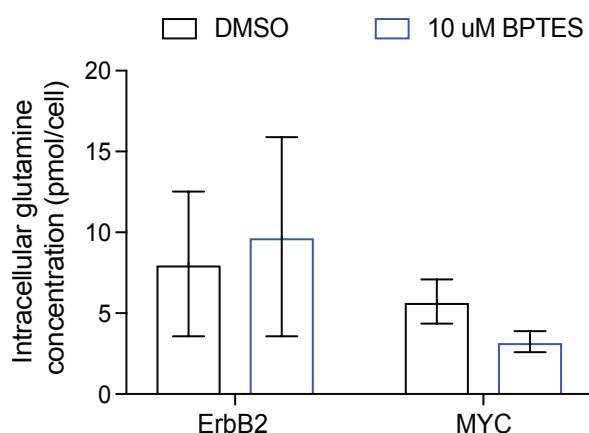
Figure 6-3 10 μM BPTES treatment does not change the intracellular glutamine concentration in ErbB2 and MYC-induced tumour cells

The intracellular glutamine concentration of ErbB2 and MYC-induced tumour cells treated with 10 μM BPTES for 24 hours. Glutamine concentration, measured by 1D NMR, is normalised cell number. Replicates are three different cell lines isolated from three different mice per group. Error bars denote standard deviation.

As BPTES treatment did not cause an increase in intracellular glutamine concentration, to confirm that BPTES treatment was inhibiting Gls1 activity, I evaluated the catabolism of glutamine into glutamate and the TCA cycle. To do this, isolated tumour cells were treated with BPTES and $^{13}C_5$-glutamine, and analysed by GC-MS (Figure 6.4).
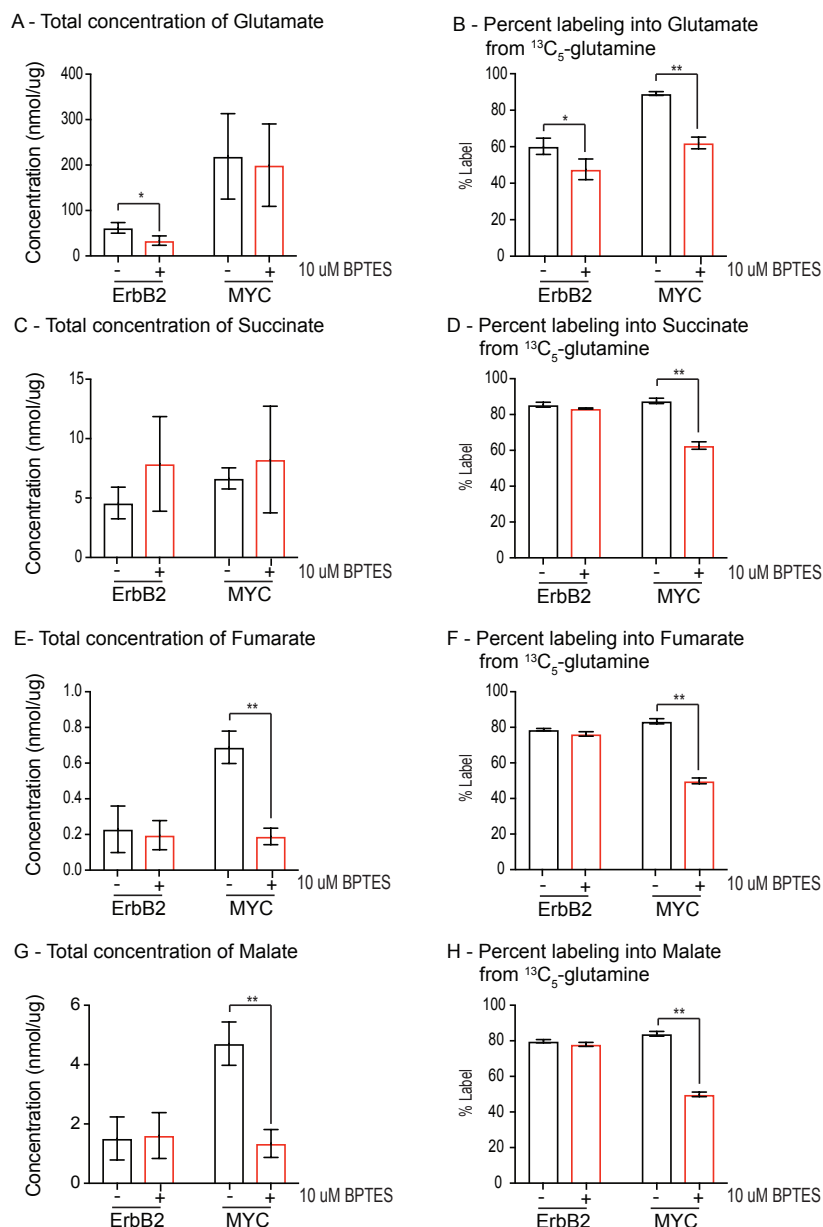
Figure 6-4 10 µM BPTES treatment decreases $^{13}C_5$-glutamine flux into the TCA cycle in MYC but not ErbB2-induced tumour cells

Isolated ErbB2 and MYC-induced tumour cells were treated with 10 µM BPTES and incubated with $^{13}C_5$-glutamine for 24 hours. Cell samples were analysed by GC-MS.
A & B – The concentration and percent ^{13}C labelling from $^{13}C_5$-glutamine (sum of all isotopomers except M+0) in glutamate in ErbB2 and MYC-induced tumour cells.
C & D – The concentration and percent ^{13}C labelling from $^{13}C_5$-glutamine (sum of all isotopomers except M+0) in succinate in ErbB2 and MYC-induced tumour cells.
E & F – The concentration and percent ^{13}C labelling from $^{13}C_5$-glutamine (sum of all isotopomers except M+0) in fumarate in ErbB2 and MYC-induced tumour cells.
G & H – The concentration and percent ^{13}C labelling from $^{13}C_5$-glutamine (sum of all isotopomers except M+0) in malate in ErbB2 and MYC-induced tumour cells.
Total concentration is expressed as nmol metabolite per µg of cell protein.
Replicates are three different cell lines isolated from three different mice per group.
Unpaired t-test * P < 0.05, ** P < 0.001, Error bars denote standard deviation.

The percent ^{13}C-labelling from ^{13}C$_5$-glutamine into glutamate decreased in MYC-induced tumour cells (Figure 6.4). However, the concentration of glutamate remained the same after BPTES treatment. The decrease in percent labelling suggests that less glutamate is being produced from glutamine, confirming Gls1 inhibition by BPTES in these cells. Decreased ^{13}C-labelling from ^{13}C$_5$-glutamine into the TCA cycle intermediates was also observed in MYC-induced tumour cells (Figure 6.4). However, while the concentration of glutamate remained the same, the concentration of fumarate and malate decreased in MYC-induced tumour cells after BPTES treatment.

The concentration and percent labelling of ^{13}C$_5$-glutamine into the glutamine-derived amino acids, alanine, aspartate, proline and serine was also studied to determine how other downstream products of glutamine catabolism were affected by BPTES treatment (Figure 6.5). Consistent with the decrease in fumarate and malate concentrations and percent enrichment from ^{13}C$_5$-glutamine, the concentration and percent enrichment of alanine and aspartate decreased in MYC-induced tumour cells after BPTES treatment. Whereas, serine and proline followed the trend of glutamate where the percent enrichment from ^{13}C$_5$-glutamine decreased with the total concentration remaining constant. This difference in the changing concentration of glutamate and its downstream metabolites could suggest compartmentalisation of glutamine and glutamate within these cells, where different pools are utilised for different pathways (Zielke et al., 2002).

Although, in ErbB2-induced cells the total concentration of glutamate as well as the percent enrichment from ^{13}C$_5$-glutamine decreased upon BPTES treatment, it did not affect the concentration or the percent ^{13}C-labelling of the TCA cycle metabolites. BPTES treatment also did not affect either the concentration or percent enrichment of glutamine-derived amino acids, suggesting that Gls1 plays a much less significant role in supporting glutamine catabolism in ErbB2-induced cells than in MYC-induced cells.
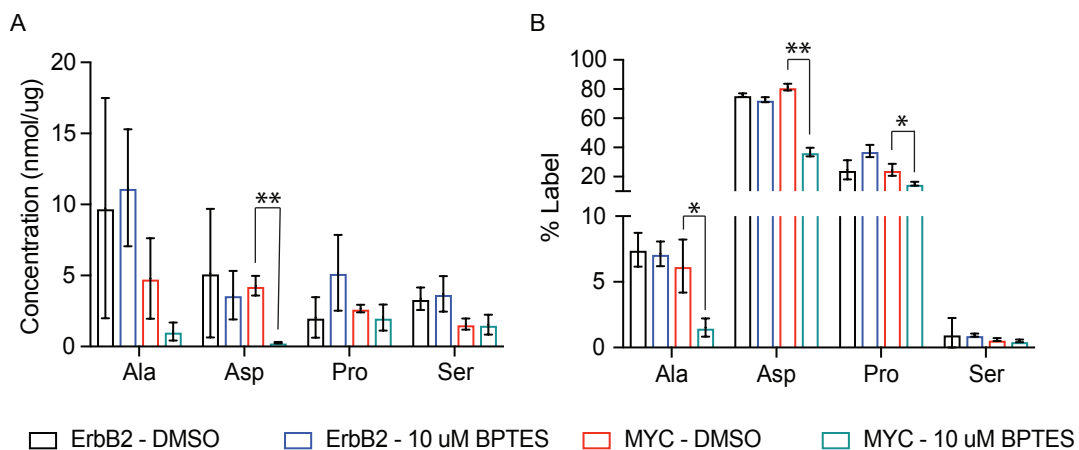
Figure 6-5 10 µM BPTES treatment decreases glutamine catabolism into amino acids in MYC but not ErbB2-induced tumour cells

Isolated ErbB2 and MYC-induced mammary gland tumour cells were treated with 10 µM BPTES and incubated with $^{13}C_5$-glutamine for 24 hours. Cell samples were analysed by GC-MS.

A – The concentration of alanine (Ala), aspartate (Asp), proline (Pro) and serine (Ser) in ErbB2 and MYC-induced tumour cells. Total concentration is expressed as nmol metabolite per µg of cell protein.

B – Percent ^{13}C labelling from $^{13}C_5$-glutamine (sum of all isotopomers except M+0) in alanine, aspartate, proline and serine in ErbB2 and MYC-induced tumour cells. Replicates are three different cell lines isolated from three different mice per group. Unpaired t-test * $P < 0.05$, ** $P < 0.001$, Error bars denote standard deviation.

To determine if BPTES treatment affected ASCT2 expression or N-glycosylation, the RNA expression, protein expression and localisation of ASCT2 was studied after 24 hours of BPTES treatment in both types of isolated tumour cells (Figure 6.6). BPTES treatment slightly increased the RNA expression of the transporter in both cell lines. The protein expression of ASCT2 decreased slightly in MYC-induced tumour cells after BPTES treatment, but the ASCT2 protein detected was still N-glycosylated and localised to the plasma membrane.

A recent study by Moloughney et al. (2016) demonstrated that a decrease in αKG levels from glutamine catabolism, decreased the expression of GFAT1, the rate limiting enzyme of the HBP (Moloughney et al., 2016). Thus, in MYC-induced tumour cells, decreased glutamine catabolism into the TCA cycle through BPTES treatment (Figure 6.4), could result in decreased αKG, inhibiting GFAT1 expression and thus, decreasing overall glycosylation. This would result in the observed decrease in ASCT2 expression as non-glycosylated ASCT2 is less stable and rapidly degraded (Console et al., 2015). The decrease in ASCT2 protein expression could cause the observed decrease in intracellular glutamine concentration (Figure 6.3) as less glutamine could be taken up.

Where BPTES treatment decreased ASCT2 protein expression in MYC-induced tumour cells, it increased ASCT2 protein expression and N-glycosylation in ErbB2-induced tumour cells (Figure 6.6), which resulted in more ASCT2 localised to the plasma membrane (Figure 6.6C). These results were confirmed by inhibiting Gls1 expression using RNAi. ErbB2 and MYC-induced tumour cells were treated with either a scrambled control siRNA or an siRNA against Gls1 (siGLS1) for 72 hours. Knockdown of Gls1 RNA expression with siGLS1 compared to untreated cells or those treated with the scrambled control was confirmed in Figure 6.7. Knockdown of Gls1 by siGLS1 slightly increased ASCT2 RNA expression in both ErbB2 and MYC-induced tumour cells, as observed with BPTES treatment. Gls1 knockdown also increased the localisation of ASCT2 to the plasma membrane in ErbB2-induced tumour cells, whereas it did not affect ASCT2 localisation in MYC-induced tumour cells.
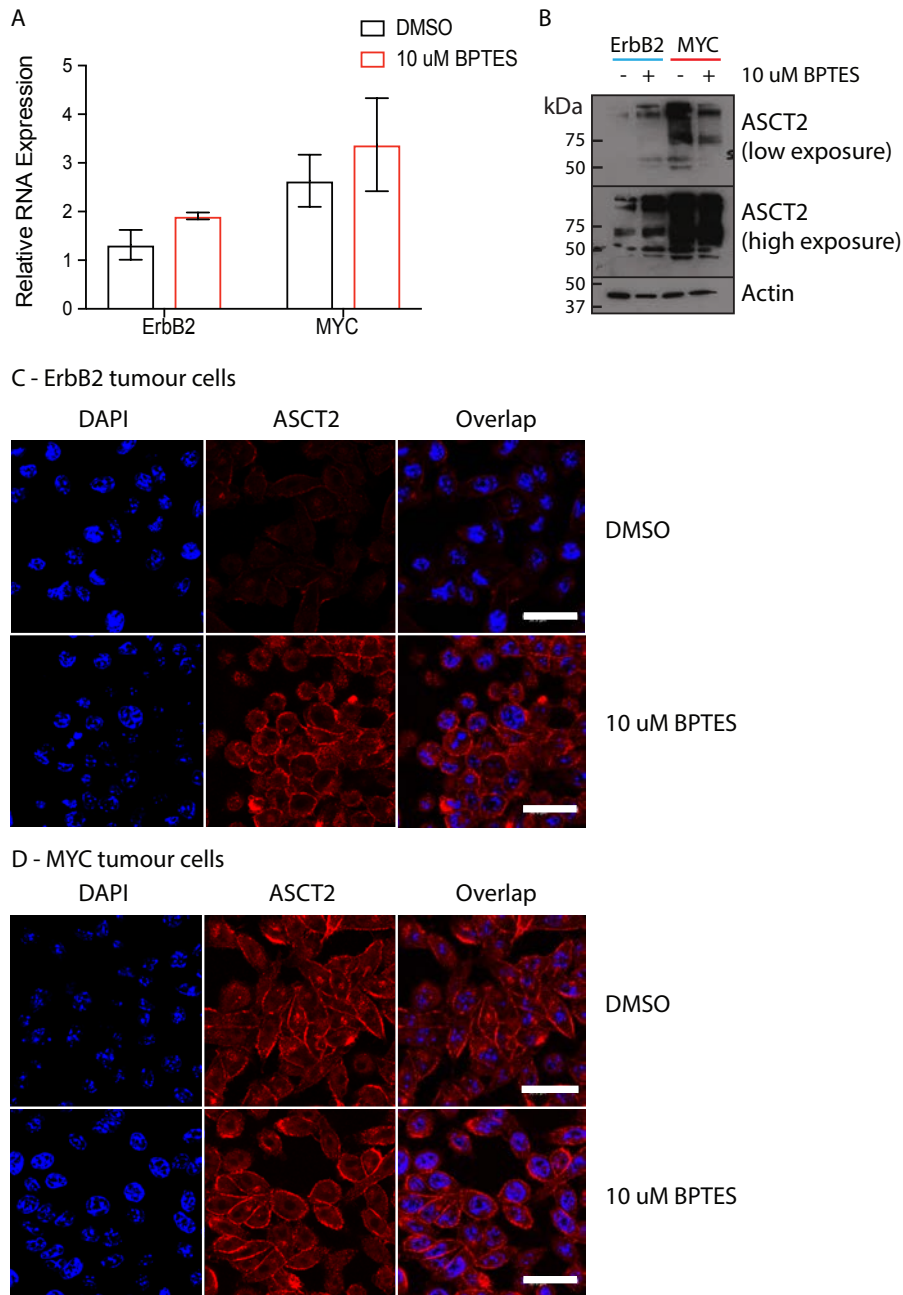
Figure 6-6 10 µM BPTES treatment increases ASCT2 expression in ErbB2-induced tumour cells

A – ASCT2 RNA expression in ErbB2 and MYC-induced tumour cells after 10 µM BPTES treatment for 24 hours. RNA expression is shown relative to untreated ErbB2 cells. Replicates are three different cell lines isolated from three different mice per group. Error bars denote standard deviation.

B – ASCT2 protein expression in ErbB2 and MYC-induced tumour cells after 10 µM BPTES treatment for 24 hours.

C + D – ASCT2 (red) and DAPI (blue) localisation in ErbB2 (C) and MYC (D) - induced tumour cells after 10 µM BPTES treatment for 24 hours. Scale bar: 30 µM. Images representative of 3 biological replicates (cells isolated from 3 different mice).
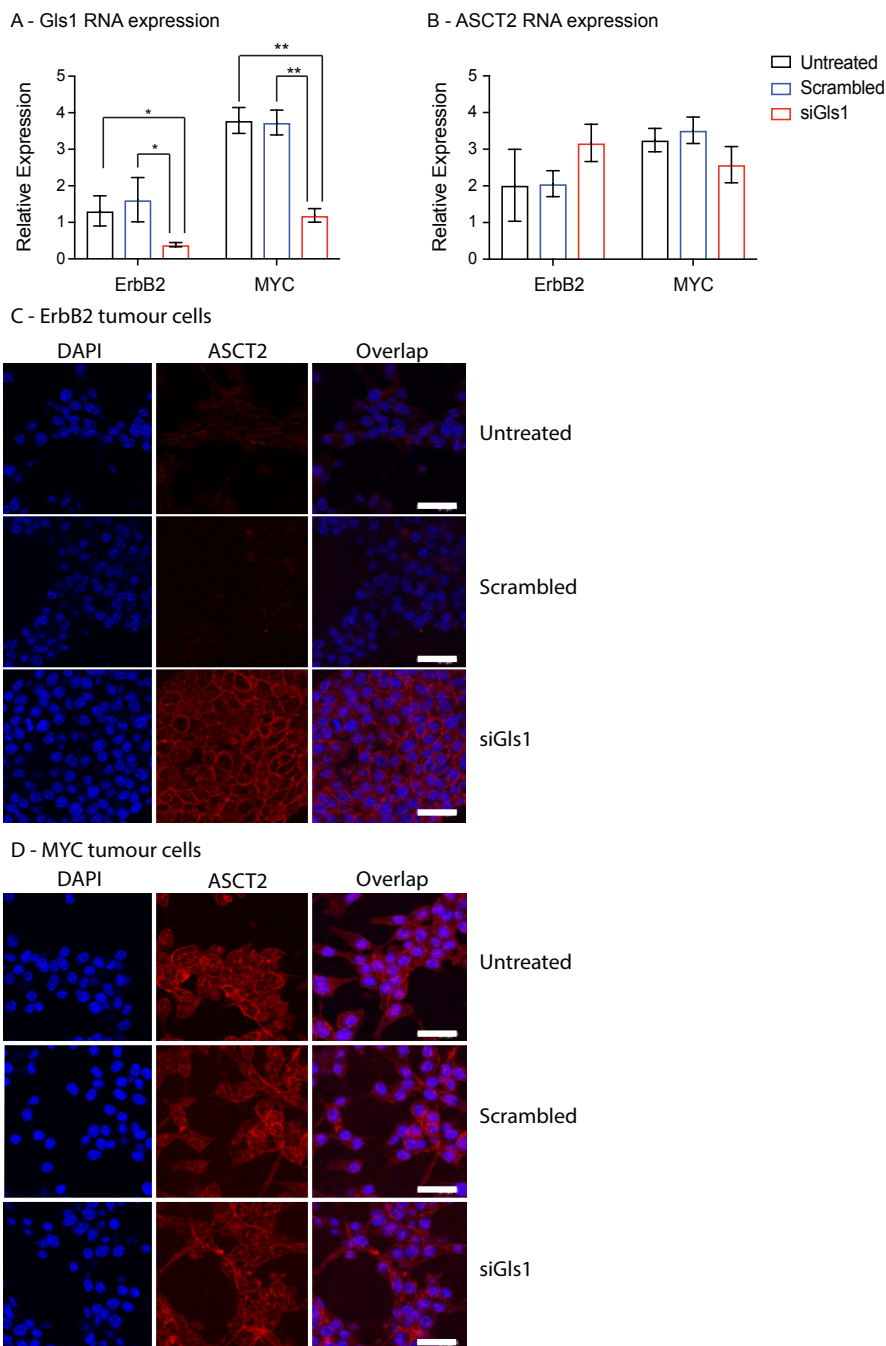
Figure 6-7 siGls1 treatment increases the localisation of ASCT2 to the plasma membrane

in ErbB2-induced tumour cells

A – Relative Gls1 RNA expression in ErbB2 and MYC-induced tumour cells after 72 hours treatment with either scrambled control siRNA or siGls1.

B – Relative ASCT2 RNA expression in ErbB2 and MYC-induced tumour cells after 72 hours treatment with either scrambled control siRNA or siGls1.

C + D – Localisation of ASCT2 (red) and DAPI (blue) in ErbB2 and MYC-induced tumour cells after 72 hours treatment with either scrambled control siRNA or siGls1. Scale bar: 30 µM. Images representative of 3 biological replicates (cells isolated from 3 different mice).

Replicates are three different cell lines isolated from three different mice per group. One way ANOVA with Tukey's multiple comparisons test, *P < 0.01, **P < 0.001, Error bars denote standard deviation.

The increase in ASCT2 mRNA levels in both types of tumour cells after Gls1 inhibition could be due to an ER-stress response, which has previously been shown to increase ASCT2 expression (Qing et al., 2012). In ErbB2-induced cells, this increase in ASCT2 levels may be sufficient for increased protein glycosylation, stabilisation and membrane localisation. Under these conditions, there would have been sufficient glutamine for the N-glycosylation of ASCT2, stabilising the protein and allowing its localisation at the plasma membrane. This supports the findings in Chapter 5, where ectopic expression of MYC in ErbB2-induced tumour cells increased the expression, N-glycosylation and plasma membrane localisation of ASCT2. This suggests that once the RNA expression of ASCT2 is increased in ErbB2-induced tumour cells, whether through ectopic MYC expression or ER-stress induced by Gls1 inhibition, provided the cells have sufficient glutamine for the HBP, these cells have all the downstream intermediates required for ASCT2 N-glycosylation. Despite a likely induction of ER-stress during glutamine deprivation (Qing et al., 2012), the protein expression and N-glycosylation of ASCT2 could not increase under these conditions, as there was no glutamine to fuel the HBP.

6.5   Summary

Glutamine was previously shown to regulate ASCT2 promoter activity (Bungard and Mcgivan, 2004). Likewise, glutamine is required for the HBP, which produces the precursors required for glycosylation and increasing glutamine concentrations have been shown to increase HBP activity (Abdel Rahman et al., 2013). Thus, glutamine could regulate ASCT2 at both the expression and glycosylation level. To test whether glutamine regulates ASCT2 expression or N-glycosylation in these tumour cell lines, ErbB2 and MYC-induced tumour cells were deprived of glutamine. Complete glutamine deprivation increased ASCT2 RNA expression, but decreased ASCT2 protein expression and localisation at the plasma membrane. This suggests that in the absence of glutamine, ASCT2 is no longer N-glycosylated and thus, the protein is degraded. This is most likely because there is insufficient glutamine to fuel the HBP. As glutamine deprivation induces ER-stress (Chen et al., 2014), which has previously been shown to upregulate ASCT2 expression (Qing et al., 2012), it is likely that the increase

in ASCT2 RNA expression observed here during glutamine deprivation is due to an alternative mechanism of ASCT2 regulation, such as those induced by ER-stress.

Gls1 inhibition by BPTES has previously been shown to increase intracellular glutamine concentrations (Yuneva et al., 2012), and thus, BPTES was used to determine if changes in intracellular glutamine metabolism altered ASCT2 expression or N-glycosylation in either ErbB2 or MYC-induced tumour cells. Gls1 inhibition by BPTES or Gls1 knockdown increased ASCT2 RNA expression in both ErbB2 and MYC-induced tumour cells. This increase in ASCT2 RNA expression with Gls1 inhibition is likely to be due to a secondary mechanism, such as ER-stress that is known to be activated during glutamine deprivation and increase ASCT2 expression (Qing et al., 2012). In MYC-induced tumour cells, inhibition of glutaminolysis by Gls1 inhibition, decreased ASCT2 protein expression, which, given that the RNA expression increased, suggests that N-glycosylation of ASCT2 was decreased. As decreased glutamine catabolism has been shown to decrease GFAT1 expression through decreased αKG levels (Moloughney et al., 2016), this suggests that inhibition of glutaminolysis in these cells could have resulted in decreased GFAT1 expression resulting in decreased glycosylation.

Interestingly, Gls1 inhibition had a different effect on ASCT2 protein expression in ErbB2-induced tumour cells, where ASCT2 protein expression, N-glycosylation and localisation to the plasma membrane increased. This is likely to be due to a separate mechanism of ASCT2 regulation to that observed in Chapter 5 where ectopic mutant ErbB2 expression in MMECs also increased ASCT2 expression and plasma membrane localisation. The increased ASCT2 RNA expression observed in ErbB2-induced tumour cells after Gls1 inhibition is likely to be due to an ER-stress response induced by Gls1 inhibition. This increase in ASCT2 RNA expression might be sufficient to increase the subsequent protein expression and N-glycosylation of ASCT2, as in these cells there is sufficient glutamine for downstream N-glycosylation to stabilise the protein.

These results demonstrate the ability of glutamine metabolism to adapt to the intracellular and extracellular environment. As the RNA expression and protein stability

of ASCT2 can be regulated by glutamine and downstream glutamine catabolism, this could enable tumours to adapt directly to changes in the microenvironment and their altered metabolic needs. While it is known that some amino acid transporters such as LAT1 are not regulated in the same manner (Yanagida et al., 2001), identifying whether other amino acid transporters show the same ability to adapt to the intracellular and extracellular conditions of the cell would enable the identification of potential compensatory mechanisms that might arise when ASCT2 is inhibited.

Chapter 7.   Discussion

7.1   Targeting metabolism as a therapeutic strategy against cancer

Tumour cells rewire their metabolic networks so that they can simultaneously increase the production of both energy and biosynthetic intermediates in order to maintain the increased proliferation associated with cancer. This observation led to further studies to understand more about these altered metabolic pathways and how they are regulated, with the aim of identifying new therapeutic strategies against cancer. While this has led to the development of new treatments, such as the use of asparaginase to treat acute lymphoblastic leukaemia (Gutierrez et al., 2006), the factors that determine metabolic changes and tumour dependency remain to be elucidated in many tumour types.

Differences in the metabolic phenotypes of different tumours have been described in several models, where the tissue of tumour origin, the tumour subtype and the genetic background have been shown to affect the overall metabolic phenotype (Wise et al., 2008; Yuneva et al., 2012; Kim et al., 2013; Kerr et al., 2016). By understanding more about what determines tumour metabolism and the particular metabolic features that tumours depend on, new therapeutic targets against cancer can be identified. Due to the high levels of plasticity within cellular metabolism, a full understanding of the tumour in context with its microenvironment is required.

Different metabolic profiles have been observed between the different subtypes of breast cancer. Where the glycolytic and glutaminolytic flux of HER2+ and triple negative breast cancers tends to increase, glutamine catabolism decreases and glycolytic flux tends to be context dependent in ER+ breast cancer (Ogrodzinski et al., 2017). However, the regulation of these metabolic changes remains to be fully defined and could result in breast cancer being defined by specific genetic alterations opposed to their molecular subtype.

In order to determine if different genetic drivers produce tumours with different metabolic profiles, two models of mammary gland tumorigenesis were compared. It was important that this initial comparison was performed *in vivo*, as previous studies

189

have shown that tumour metabolism varies when cells are grown *in vitro*, as the nutrient supply and interactions with the surrounding microenvironment change (Davidson et al., 2016; Muir et al., 2017). The oncogenes chosen were the ErbB2 and MYC oncogenes, as these have high prevalence within breast cancer (Slamon et al., 1989; Deming et al., 2000), are known to alter metabolic genes (Yoon et al., 2007; Wise et al., 2008; Zhao et al., 2009; Anso et al., 2013; Qie et al., 2014; Camarda et al., 2017) and tumours with high expression of these genes often become resistant to current therapeutic strategies (Pohlmann et al., 2009; Miller et al., 2011; Horiuchi et al., 2012).

7.1.1 Different genetic drivers produce tumours with different metabolic profiles in mammary gland tumours

Stable isotope labelling of MMTV-ErbB2 and MMTV-MYC tumours revealed that while both tumours have a similar increased rate of glucose catabolism compared to normal mammary gland tissue, their glutamine catabolism is different. MYC-induced tumours were shown to catabolise more glutamine into the TCA cycle and amino acids than ErbB2-induced tumours. While different breast cancer subtypes have been shown to have different metabolic phenotypes (Kim et al., 2013; Kim et al., 2015; Ogrodzinski et al., 2017), the specific genetic alterations regulating these changes are yet to be fully described. As both oncogenes were under the control of the MMTV promoter, this promoter would have been activated in the same cell of origin, at the same stage of mammary gland development in the same environmental conditions, confirming that these metabolic changes are a result of the different oncogenic drivers. However, MYC and ErbB2 can regulate the components of the tumour microenvironment, including angiogenesis, stromal and immune cells in different ways, which could contribute to the different metabolic profiles of these tumours. The full extent of how different genetic changes alter tumour metabolism remains to be determined.

The catabolism of glucose into the TCA cycle and the expression of the glycolytic enzymes HK1 and HK2 increased to a similar level in both types of tumours compared to the normal mammary gland. While the requirement for HK2 in ErbB2-induced mammary gland tumours has been demonstrated (Patra et al., 2013), its requirement in

MYC-induced tumours has yet to be described. The synthesis of the amino acids: alanine, aspartate, proline and serine also increased in both types of tumours compared to the normal mammary gland tissue; although the catabolism of glutamine into these amino acids was greater in MYC-induced tumours, compared to ErbB2-induced tumours. This suggests these tumours may require the activity of different aminotransferase enzymes. Further work into the requirement for the different enzymes involved in the synthesis of these amino acids in these two types of tumours might reveal new therapeutic targets against either tumour.

7.1.2   Glutamine addiction as a therapeutic strategy

Cells isolated from both ErbB2 and MYC-induced mammary gland tumours were dependent on glutamine; although, the effect was much more pronounced in MYC-induced tumour cells. This suggests that targeting glutamine metabolism could be a potential therapeutic strategy against both types of tumour. However, while both tumours increased the catabolism of glutamine into the TCA cycle and amino acids compared to the normal mammary gland, this was achieved through the upregulation of different enzymes. Where both tumour types had slightly increased Gls1 RNA expression in comparison with normal mammary gland, MYC was previously shown to increase Gls1 expression on a post-transcriptional level (Gao et al., 2009). Thus, to make a final conclusion about the enzymes responsible for increased glutamine catabolism in the two tumour types, their protein expression needs to be evaluated. Nevertheless, the different expression of glutaminolytic enzymes between the two tumour models suggests that identifying the specific metabolic changes causing the metabolic differences between each tumour type and normal tissues is vital to identify specific therapeutic targets.

The MYC oncogene regulates a number of metabolic enzymes involved in glutamine metabolism, including Gls1 (Gao et al., 2009), Gls2 (Xiao et al., 2015) and GS (Bott et al., 2015), and increased glutamine catabolism has been observed in a number of MYC-driven tumour models (Yuneva et al., 2012; Anderton et al., 2017). Knockdown and inhibition of Gls1 and Gls2 have been shown to be an effective therapeutic approach

against MYC-driven hepatocellular carcinoma (Xiang et al., 2015) and glioblastoma (Xiao et al., 2015) respectively. Gls1 inhibition has also been shown to decrease tumour cell proliferation and tumour growth in triple negative breast cancer cells (Gross et al., 2014). However, MYC was shown to have opposing roles in glutamine metabolism in breast cancer. Where glutamine uptake was shown to be required for the initiation and progression of TNBC xenografts (Van Geldermalsen et al., 2016), Bott et al. (2015) found that MYC promoted glutamine synthetase expression in human breast cancer cell lines (Bott et al., 2015). However, MYC knockdown in these cell lines effected the expression of Gls1 and GS differently dependent on the line, suggesting that the mutational background of the tumour, opposed to the expression of MYC alone affects the overall metabolic phenotype (Bott et al., 2015). Here, MYC-induced mammary gland tumours demonstrated increased glutamine catabolism, high RNA expression of Gls1 and Gls2 and decreased RNA and protein expression of GS compared to the normal mammary gland. Unpublished results from our laboratory demonstrate that the knockout of Gls1 in MMTV-MYC tumours increases tumour latency, but does not prevent tumour development. Thus, I compared the expression of different glutamine transporters between the tumours and normal mammary gland, as targeting glutamine catabolism at the source of glutamine entry might prove a more effective therapeutic strategy than targeting a downstream glutamine catabolising pathway.

7.2 Glutamine transporters as therapeutic targets

Given the number of altered pathways that require glutamine in tumours, it is unsurprising that the increased expression and requirement for a number of glutamine transporters was demonstrated for different tumours (Gupta et al., 2006; Wang et al., 2013; Namikawa et al., 2014; Nikkuni et al., 2015; Shimizu et al., 2015; Barollo et al., 2016; Honjo et al., 2016). The whole-body knockout of ASCT2, whose increased expression and N-glycosylation is associated with increased glutamine catabolism in MYC-induced tumours, does not have an observable phenotype (Masle-Farquhar et al., 2017), whereas knockdown of the protein decreases breast cancer, myeloma and lung cancer xenograft growth *in vivo* (Hassanein et al., 2015; Bolzoni et al., 2016; Van Geldermalsen et al., 2016).

A recent study by Davidson et al. demonstrated that while K-Ras driven lung tumour cells were dependent on Gls1 activity *in vitro*, the same effect was not observed in *in vivo* mouse models (Davidson et al., 2016), suggesting that glutamine metabolism may be perturbed by the tumour cells' microenvironment, casting doubts on the relevance of targeting glutamine metabolism in patients. However, ^{18}F-fluoroglutamine PET imaging in human patients revealed increased glutamine uptake in a number of tumours (Hassanein et al., 2016), including in breast cancer (Zhou et al., 2017). While this does not confirm that human tumours are dependent on glutamine uptake, it does demonstrate that these tumours consume more glutamine and thus, further studies into the requirement for glutamine in human tumours may demonstrate the suitability of targeting glutamine transporters in human tissues.

Our present and previous *in vitro* results demonstrate that metabolic changes, including increased glutamine catabolism and sensitivity towards targeting glutamine catabolism, are oncogene-specific (Yuneva et al., 2012; Camarda et al., 2017). This is why one cannot expect the results from one tumour model to be projected to all other cases and is why the present work is so important identifying the relationship between a specific oncogene and sensitivity to inhibiting glutamine catabolism.

7.2.1   ASCT2 inhibition as a therapeutic strategy against cancer

Targeting ASCT2 as a therapeutic strategy against cancer has been the focus of several recent studies. Knockdown of ASCT2 expression by shRNA has been shown to be effective against both tumour initiation and progression *in vivo* using a human TNBC cell line (Van Geldermalsen et al., 2016). Knockdown of ASCT2 by shRNA has also been shown to be effective against human myeloma and small cell lung cancer xenografts *in vivo* (Hassanein et al., 2015; Bolzoni et al., 2016), and human hepatoma and prostate cancer cells *in vitro* (Fuchs et al., 2004; Wang et al., 2015). These studies support the idea that preventing glutamine uptake in tumours dependent on downstream glutamine catabolism is an effective therapeutic approach.

The expression, N-glycosylation and plasma membrane localisation of the glutamine transporter, ASCT2 was higher in MYC-induced tumours compared to ErbB2-induced tumours. This correlated to increased glutamine catabolism into the TCA cycle and amino acids in these tumours, and increased glutamine consumption in cells isolated from MYC-induced tumours. Knockdown of ASCT2 expression using RNA interference, decreased the relative cell mass of isolated MYC-induced tumour cells, suggesting that these cells are dependent on ASCT2. These results suggest that targeting ASCT2 could be a good therapeutic approach in cancers with high MYC expression and/or activity. As the whole-body knockout of ASCT2 did not display any observable phenotypes, this suggests that targeting tumours with a specific ASCT2 inhibitor should cause limited side effects (Masle-Farquhar et al., 2017). However, to confirm the requirement for ASCT2 in MYC-induced mammary gland tumours, studies where the transporter is knocked down *in vivo* need to be performed.

Previous studies have described the upregulation of other glutamine transporters, LAT1 (Polet et al., 2016) and SNAT1 (Broer et al., 2016), when ASCT2 was inhibited. It is unknown how other amino acid transporters responded in this study to the decrease in ASCT2 expression, and so this could be studied further to predict any compensatory mechanisms the tumours might develop against ASCT2 inhibition. These studies suggested a combinatorial approach where multiple transporters could be simultaneously inhibited to overcome these resistance mechanisms. Combination therapies can be designed to increase the specificity of the treatment by targeting transporter combinations not frequently observed in normal tissues. They can also reduce the development of drug resistance against the therapy (Bayat Mokhtari et al., 2017).

Overall, our studies support the work of others to strengthen the evidence supporting the suitability of inhibiting ASCT2 to prevent glutamine uptake as a good therapeutic approach against breast cancer. In a previous study the requirement for ASCT2 was linked to triple-negative breast cancer cells (Van Geldermalsen et al., 2016), whereas our study demonstrates a direct connection between MYC and the increased expression

and requirement of ASCT2. This suggests that MYC-overexpression could be a good biomarker for tumours that might be sensitive to ASCT2 inhibition.

Given the number of different tumours observed to express ASCT2 (Huang et al., 2014; Kim et al., 2014; Namikawa et al., 2014; Shimizu et al., 2014; Hassanein et al., 2015; Liu et al., 2015; Ren et al., 2015; Bolzoni et al., 2016; Hudson et al., 2016; Sun et al., 2016; Van Geldermalsen et al., 2016; Marshall et al., 2017; Toda et al., 2017), the development of a specific ASCT2 inhibitor could potentially be used to target several different tumour types. However, the development of a specific ASCT2 inhibitor remains to be achieved. Compounds that act as glutamine mimics to competitively inhibit the active site of ASCT2, such as GPNA, have been shown to inhibit other transporters due to the similarity of their active sites (Broer et al., 2016; Chiu et al., 2017). Current work is being done to modify the existing backbone of GPNA in order to make the compound more specific (Colas et al., 2015; Schulte et al., 2015; Schulte et al., 2016). Likewise, alternative approaches using monoclonal antibodies are being developed to inhibit ASCT2 (Suzuki et al., 2017). A synthetic polymer has recently been described that binds to cells with a high density of ASCT2 at the plasma membrane (Yamada et al., 2017). It is believed that such polymers could be exploited to specifically deliver inhibitory compounds to cancer cells.

7.2.2   The regulation of ASCT2 in cancer

While current work focuses on developing more specific compounds to inhibit ASCT2 directly, understanding more about how ASCT2 is regulated might enable the development of therapeutic strategies that indirectly inhibit ASCT2 by targeting part of its regulatory mechanism. This was demonstrated by Jeon et al. (2015), who found that treating the tumours of MMTV-PyMT mice with Paclitaxel decreased tumour growth by increasing RNF5-mediated ubiquitination and degradation of ACST2 (Jeon et al., 2015). Thus, by understanding more about how ASCT2 is regulated, new therapeutic strategies against the transporter can be developed.

ASCT2 has multiples stages of regulation, where it must be both expressed and N-glycosylated before it is active at the plasma membrane (Console et al., 2015). In this work, I have confirmed the previous finding of Wise et al. (2008), that ASCT2 expression is regulated by the MYC oncogene. This contributes to a number of changes induced by MYC that promote glutamine catabolism in tumours (Wise et al., 2008). However, it still remains to be elucidated if increased ASCT2 N-glycosylation in MYC-induced mammary gland tumours is actively promoted by MYC or is the result of increased gene and protein expression of ASCT2.

MYC is not the only oncogene that regulates ASCT2 expression. For instance, ASCT2 forms a complex with the epithelial growth factor receptor, EGFR, which promotes its localisation to the plasma membrane (Lu et al., 2016). Likewise, the tumour suppressor genes, miRNA-137 (Dong et al., 2017) and Rb (Reynolds et al., 2014) also regulate ASCT2 expression, as do the kinases, SGK1-3 and protein kinase B (Palmada et al., 2005). These studies focus on ASCT2 expression levels, opposed to the post-translational modification of the protein. This study found that the ectopic expression of mutant ErbB2 V659E induces ASCT2 protein but not gene expression in isolated mammary epithelial cells. This increased protein expression was also associated with increased N-glycosylation and membrane localisation of ASCT2. Despite being downstream of ErbB2 signalling, MYC localisation in the nucleus did not occur in ErbB2-expressing cells, suggesting that ASCT2 protein expression was regulated in a MYC-independent manner.

Despite the increase in ASCT2 expression with the ectopic expression of mutant ErbB2 in mammary epithelial cells, the expression of a different ErbB2 mutant that results in the same constitutive activity of ErbB2 in *in vivo* tumours, in the MMTV-ErbB2 tumour model, resulted in low levels of N-glycosylated ASCT2. This difference in the ability of mutant ErbB2 to induce ASCT2 expression could be due to differences in the expression levels of the mutant ErbB2 in each model, as they were under the control of different promotors. Furthermore, while both of the mutant forms of ErbB2 produced constitutively active proteins, the mutants in each experiment were different and thus, can have different abilities to regulate ASCT2. Finally, this difference in the ability of

mutant ErbB2 to induce ASCT2 protein expression and N-glycosylation could be due to the mutational background of the tumour, which might activate pathways that inhibit ErbB2-induced ASCT2 expression.

In this study, a panel of patient derived xenografts (PDXs) was tested to determine the correlation between ASCT2 status, MYC and the existing breast cancer subtypes. High MYC expression was associated with ASCT2 expression in tumours, but not every tumour with high ASCT2 expression also had high MYC expression. The expression of ER and HER2 did not correlate to ASCT2 expression or N-glycosylation, suggesting that the expression and N-glycosylation of ASCT2 does not correlate to an existing subtype of breast cancer.

The study by van Geldermalsen et al. (2016) demonstrates that not all cells with ASCT2 localisation at the plasma membrane are sensitive to amino acid transporter inhibition by GPNA (Van Geldermalsen et al., 2016). This suggests that not all tumours that express ASCT2 are dependent on its activity. Thus, work needs to be done to identify which features of tumours make them dependent on glutamine uptake by ASCT2. One possibility is that the tumours that are not sensitive to ASCT2 inhibition express other glutamine transporters that can compensate for the lost ASCT2 activity.

In the panel of different PDXs, the samples demonstrated different patterns of N-glycosylation of ASCT2. This is similar to the results observed in the study by van Geldermalsen et al. (2016), which also demonstrates different N-glycosylation of ASCT2 in human breast cancer cell lines (Van Geldermalsen et al., 2016). While the sites of N-glycosylation in ASCT2 have been described (Console et al., 2015), the exact pattern of N-glycosylation has yet to be determined. Different patterns of glycosylation could have different effects on the transporter. This was observed with the glycosylation patterns of the EGFR, where a more branched pattern of glycosylation increased the latency of the receptor at the plasma membrane (Lajoie et al., 2007). Thus, identifying the different patterns of N-glycosylation observed on ASCT2 in tumours could determine if a particular glycosylation pattern is required by those tumours dependent on ASCT2.

Different glycosyltransferase enzymes are known to produce different patterns of glycosylation. By identifying the pattern of N-glycosylation in tumours known to require ASCT2 activity, the glycosyltransferases involved could be identified. Further studies into the requirement for these specific glycosyltransferases might reveal which ones are required for ASCT2 N-glycosylation and tumour survival. Little is known about specific glycosyltransferases in cancer. In melanoma cells, overexpression of GnT-III, the glycosyltransferase that adds a bi-secting GlcNAc to inhibit further elongation of glycan branches, suppressed lung metastasis in mice (Yoshimura et al., 1995). Whereas downregulation of GnT-V, the glycosyltransferase responsible for the increased expression of complex β1,6-branched N-linked glycans, which are frequently observed in cancer (Asada et al., 1997), decreases tumour growth and metastasis in mouse mammary carcinoma cells (Seberger and Chaney, 1999). Thus, identification of the glycosyltransferases that regulate ASCT2 N-glycosylation could identify new therapeutic strategies to indirectly inhibit ASCT2. Given the vast number of substrates glycosylated by specific glycosyltransferases, inhibiting specific glycosyltransferases could cause a number of off-target effects on normal tissues. Thus, work needs to be done to identify those specifically upregulated in tumours to define a suitable therapeutic window.

7.2.3   The regulation of ASCT2 by glutamine metabolism

Previously, the promoter of ASCT2 was shown to be regulated by glutamine (Bungard and Mcgivan, 2004). Likewise, glutamine is required for the hexosamine biosynthesis pathway (HBP), which produces the precursors required for N-glycosylation (Abdel Rahman et al., 2013). Thus, glutamine could regulate both the expression and N-glycosylation of ASCT2 in tumours. Here, glutamine deprivation studies in cells isolated from MYC-induced tumours revealed that glutamine is required for ASCT2 N-glycosylation, but that ASCT2 RNA expression increases in the absence of glutamine, possibly through a mechanism induced by ER-stress (Ren et al., 2015), which is known to be activated during glutamine deprivation (Qing et al., 2012).

The work presented here supports the findings of Moloughney et al. (2016), who demonstrated that the HBP is regulated by downstream glutamine catabolism, as the levels of the glutamine catabolite αKG, regulate the expression of the rate-limiting enzyme of the HBP, GFAT1 (Moloughney et al., 2016). When Gls1 was inhibited in MYC-induced tumour cells inhibiting glutamine catabolism into the TCA cycle, the protein expression of ASCT2 decreased, despite an increase in ASCT2 RNA expression in MYC-induced tumour cells. This suggests that decreased glutamine catabolism to the TCA cycle, decreases ASCT2 N-glycosylation and protein stability. This could be due to decreased GFAT1 expression caused by the decrease in αKG, resulting in decreased HBP activity. This result suggests an interesting feedback loop where ASCT2 can be regulated by the availability of glutamine. This suggests that tumour cells can adapt their metabolic pathways to changes in nutrient availability. The high level of plasticity within metabolism could make targeting tumour metabolism difficult, as therapeutic strategies without compensatory pathways need to be identified.

As previously described, the metabolic profiles of tumours are dependent on their genetic background and here, tumour cells driven by different oncogenes were shown to respond to metabolic manipulation in different ways. When Gls1 was inhibited in ErbB2-induced tumour cells, the gene expression, N-glycosylation and plasma membrane localisation of ASCT2 increased. The gene expression and N-glycosylation of ASCT2 was also shown to increase in ErbB2-induced tumour cells with ectopic expression of MYC. This suggests that increased gene expression of ASCT2 may be sufficient to promote its N-glycosylation, stabilisation and membrane localisation in ErbB2-induced tumour cells. It is likely that during Gls1 inhibition, the RNA expression of ASCT2 increases due to an ER-stress response, as this has previously been shown to increase ASCT2 expression during glutamine deprivation (Qing et al., 2012). Together these results suggest that the low expression of ASCT2 in the MMTV-ErbB2 model may be due to its insufficient RNA expression. ErbB2 V664D may also be capable of promoting the N-glycosylation of ASCT2 as ErbB2 V659E does.

7.3 Lessons for future metabolomics studies

During this study, some important lessons were observed that can be applied to future metabolomics studies.

7.3.1 The difference between *in vivo* and *in vitro* metabolism

In this study, an *in vitro* cell culture model of the *in vivo* tumours initially profiled was required to enable mechanistic questions that are difficult to study *in vivo* to be studied. Comparing the metabolic profile of MYC and ErbB2-induced tumour cells *in vivo* and *in vitro* revealed differences in the relative amino acid concentrations in these different conditions.

The tumour microenvironment is highly complex, where tumour cells interact with stromal and immune cells. Symbiotic relationships between tumour cells and stromal, immune or other tumour cells have been demonstrated, where tumour cells take up the nutrients secreted by their neighbouring cells in order to fuel their metabolic requirements (Sonveaux et al., 2008; Chang et al., 2015; Brand et al., 2016; Yang et al., 2016). Targeting the metabolic interactions between tumour cells and cancer associated fibroblasts has been shown to be effective against ovarian cancer (Yang et al., 2016). This suggests a high level of plasticity in tumour metabolism that enables tumour cells to adapt to their changing microenvironment.

The *in vitro* cell culture environment is considerably different, where cells are grown in adherent monolayers, limiting their interactions with other tumour cells, and in the absence of infiltrating immune and stromal cells. The cell culture medium contains non-physiological levels of nutrients, including glucose, glutamine and other amino acids. Thus, the metabolic requirements of tumour cells grown in cell culture are different to those grown *in vivo*. This was demonstrated by Davidson et al. (2016), who observed differences in glutamine metabolism in lung cancer cells grown *in vitro* compared to the same cells *in vivo* (Davidson et al., 2016).

While metabolic differences between cells grown *in vitro* and *in vivo* are likely to be observed, it is interesting that certain features such as the increased catabolism of glutamine into the TCA cycle were maintained in MYC-induced tumour cells. This suggests that key metabolic features induced by changes in the genetic background of the tumour can be maintained when tumour cells are isolated. However, it is important to note that while the activity of key metabolic pathways may be retained when tumour cells are grown *in vitro*, the cells may not respond in the same way to inhibition of metabolic pathways. A recent study by Muir et al. (2017), demonstrated that the amino acid rich cell culture media frequently used can modify a tumour cell's requirement for glutamine, where many cell lines that depend on glutamine catabolism *in vitro* rely on it less to proliferate *in vivo* (Muir et al., 2017). This is due to non-physiological levels of extracellular cystine in the media, which activates the SLC7A11 (xCT) glutamate/cystine antiporter, increasing glutamate secretion from cells. However, increased catabolism of glutamine into the TCA cycle was observed both *in vitro* and *in vivo* in MYC-induced tumour cells, suggesting that the requirement for glutamine catabolism in these tumours is not an artefact of *in vitro* cell culture.

7.3.2   Tumour size alters the metabolic profile of the tumour

As tumours grow, regions appear that are further from blood vessels and thus, receive fewer nutrients and oxygen. This creates areas of hypoxia and necrosis within tumours. This heterogeneity is likely to produce different regions within tumours with different metabolic profiles, which can be identified using mass-spectrometry imaging (MSI) techniques (Randall et al., 2016; Tillner et al., 2017). In this study, the metabolic profiles of MMTV-ErbB2 tumours were compared between tumours of different sizes, revealing that bigger tumours have a higher total concentration of lactate and TCA cycle intermediates as well as higher levels of these metabolites derived from both glucose and glutamine. These differences could be caused by changes in the mutational profiles of the tumour cells as the tumours develop. They could also be caused by changes in the proliferative and metastatic potential of the tumour cells in bigger tumours compared to smaller tumours. Thus, this study highlights that tumour metabolism changes as the tumours grow, and so, studying the metabolic profiles of tumours as they develop could

reveal which metabolic pathways are utilised at different stages. This would identify enzymes and metabolites that are required for either tumour initiation or tumour progression, revealing when therapeutic inhibition against specific enzymes would be most effective against tumorigenesis.

7.3.3   The normal mammary gland is a complex tissue

The normal mammary gland is a complex tissue, which consists of several different cell types, including epithelial and adipose cells. The mammary gland also goes through multiple stages of rapid growth and development, during puberty, estrous, pregnancy and lactation. During these stages, epithelial ducts branch and elongate, altering the proportion of adipose to epithelial cells. In this study, the metabolic phenotype of the mammary gland taken at two different ages was compared in order to determine whether the metabolic profile of the mammary gland changed with different stages of development. The catabolism of glucose into lactate, the TCA cycle and serine increased in the mammary gland from the older mice, demonstrating that the metabolic profile of the mammary gland changes as the mice get older. This demonstrates that studying the changing metabolic profile of the mammary gland at different stages of development will not only increase our understanding of this complex tissue, but will also identify metabolic changes associated with a fast growth phenotype in the mammary gland and by comparison to mammary gland tumours, identify the metabolic changes acquired as the tumour develops.

For the metabolomics analysis of the mammary gland performed here, the whole tissue was ground and so the metabolomics data presented reflects an average across the whole tissue. However, this ignores the different metabolic profiles of the different cell types in this tissue. The importance of considering these different cell types was highlighted when the localisation of ASCT2 in the normal mammary gland was studied. The mammary epithelial cells had low expression levels of ASCT2 at the plasma membrane. As these are the cells the tumours in the MMTV-MYC mice derive from, this demonstrated that as these cells become tumorigenic, they increase their expression of ASCT2. However, the adipose cells had high levels of ASCT2 localised at their

plasma membrane. Despite the high expression of ASCT2 in the normal mammary gland, the catabolism of glutamine into the TCA cycle and amino acids was higher in the MYC-induced tumours compared to the normal mammary gland, which was an average across the whole tissue. Adipose cells are likely to have very different metabolic profiles compared to epithelial cells, as these cells are designed to store energy in the form of lipids. Thus, while both adipose cells and MYC-induced tumour cells take up glutamine, due to their plasma membrane localisation of ASCT2, glutamine is likely to be catabolised into lipids in the adipose cells opposed to the TCA cycle and amino acids.

By using newly developed mass spectrometry imaging (MSI) techniques (Randall et al., 2016; Tillner et al., 2017), the metabolic profiles of the individual cells *in situ* can be studied, and thus, the individual metabolic profiles of the epithelial and adipose cells can be described. This will enable the metabolic profiles of the tumour cells to be compared directly to their cell of origin, opposed to an average of the whole tissue. As all organs consist of multiple cell types, these studies should be expanded to other tissues to fully identify how different cell types interact both in normal tissues and as different tumours develop.

Similarly, as different regions of tumours have different oxygen and nutrient supplies, the metabolic profile of the tumour is not homogeneous across the tissue (Ito et al., 2011; Carmona-Fontaine et al., 2017). Not only are there regions of hypoxia and necrosis, but in some cases specific nutrient deprivation can affect signalling as well. For example, regions of glutamine deprivation can result in histone hypermethylation due to decreased TET protein activity caused by the decrease in αKG (Ito et al., 2011). Applying MSI techniques to tumours will identify how heterogeneous tumours are and reveal metabolic profiles that are common across the whole tumour, compared to those which are only altered in certain regions. This can help dictate the design of new therapeutic strategies as it will reveal which pathways are required for the whole tumour, and thus, are the most likely to halt tumour progression when inhibited. This will also reveal any metabolic symbiosis between interacting tumour cells, as well as between tumour cells and infiltrating stromal or immune cells.

7.4   Conclusion and future directions

This study confirms that the metabolic phenotypes of mammary gland tumours depend on the genetic driver, which has previously been observed in many other tissues and in different subtypes of breast cancer (Wise et al., 2008; Yuneva et al., 2012; Kim et al., 2013; Kerr et al., 2016). The comparison of the two tumour types revealed common metabolic features such as the increased catabolism of glucose into the TCA cycle compared to the normal mammary gland, and differences in metabolic pathways, where MYC-induced tumours catabolise more glutamine into the TCA cycle and amino acids than the ErbB2-induced tumours. This large scale metabolic profiling revealed a number of pathways that were altered in these tumours, suggesting that further work into the enzymes required for these pathways might reveal new therapeutic strategies against mammary gland tumorigenesis.

Here, I demonstrate that not only does the expression of the glutamine transporter, ASCT2 increase in MYC-induced tumours, but that its N-glycosylation increases as well. This N-glycosylation is required to increase the stability of the protein (Console et al., 2015), increasing its localisation at the plasma membrane and thus, increasing its ability to transport glutamine. My results also demonstrate that MYC is required and sufficient to induce ASCT2 gene expression. However, it remains to be elucidated if the N-glycosylation of ASCT2 in MYC-induced tumours is the result of high levels of

protein expression or whether the glycosylation step is being actively regulated by MYC.

Isolated MYC-induced tumour cells were sensitive to decreased ASCT2 expression, demonstrating that ASCT2 could be a plausible therapeutic target in tumours with high MYC activity (Van Geldermalsen et al., 2016). However, this needs to be confirmed by inhibiting ASCT2 expression in MYC-induced tumours *in vivo*.

Using a panel of human patient derived xenograft samples (PDX), I demonstrated that MYC is a good biomarker for ASCT2 expression and N-glycosylation. However, MYC is not expressed in all tumour samples with high ASCT2 expression and N-glycosylation. As the study of van Geldermalsen et al. (2016) demonstrates, plasma membrane localisation of ASCT2 does not necessarily indicate sensitivity to sodium-dependent amino acid transporter inhibition (Van Geldermalsen et al., 2016), which could be due to the expression of other amino acid transporters that can compensate for the inhibited transporters. Thus, more work needs to be done to identify the additional features required to make cells dependent on ASCT2 activity.

The design of specific compounds that inhibit ASCT2 has been hindered by the similarity of the active sites of glutamine transporters, resulting in non-specific amino acid transporter inhibition (Broer et al., 2016; Chiu et al., 2017). Understanding more about how ASCT2 is regulated, either through specific oncogenes, glutamine metabolism or N-glycosylation could reveal new ways to inhibit ASCT2 activity.

This project also demonstrated that the metabolic profiles of both the normal mammary gland and tumours change as these tissues develop. Identifying the mechanisms behind these changes should help to understand the metabolic functions and interactions between different cells within the normal mammary gland and tumours. This in turn would help to understand the mechanisms of metabolic remodelling and will help develop different therapeutic strategies to target the specific stage of tumour development they will be most effective against.

Reference List

Abdel Rahman, A. M., Ryczko, M., Pawling, J. and Dennis, J. W. (2013) Probing the hexosamine biosynthetic pathway in human tumor cells by multitargeted tandem mass spectrometry. *ACS Chem Biol* **8**(9): 2053-2062.10.1021/cb4004173

Ahmad, S., Gupta, S., Kumar, R., Varshney, G. C. and Raghava, G. P. (2014) Herceptin resistance database for understanding mechanism of resistance in breast cancer patients. *Sci Rep* **4**.10.1038/srep04483

Ahmed, F., Wyckoff, J., Lin, E. Y., Wang, W., Wang, Y., Hennighausen, L., Miyazaki, J.-I., Jones, J., Pollard, J. W., Condeelis, J. S. and Segall, J. E. (2002) GFP Expression in the Mammary Gland for Imaging of Mammary Tumor Cells in Transgenic Mice. *Cancer Research* **62**: 7166-7169

Airley, R., Loncaster, J., Davidson, S., Bromley, M., Roberts, S., Patterson, A., Hunter, R., Stratford, I. and West, C. (2001) Glucose transporter glut-1 expression correlates with tumor hypoxia and predicts metastasis-free survival in advanced carcinoma of the cervix. *Clin Cancer Res* **7**: 928-934

Alvarez, J. V., Belka, G. K., Pan, T. C., Chen, C. C., Blankemeyer, E., Alavi, A., Karp, J. S. and Chodosh, L. A. (2014) Oncogene pathway activation in mammary tumors dictates FDG-PET uptake. *Cancer Res* **74**(24): 7583-7598.10.1158/0008-5472.CAN-14-1235

Amati, B. and Land, H. (1994) Myc—Max—Mad: a transcription factor network controlling cell cycle progression, differentiation and death. *Current Opinion in Genetics & Development* **4**(1): 102-108.10.1016/0959-437x(94)90098-1

Anderton, B., Camarda, R., Balakrishnan, S., Balakrishnan, A., Kohnz, R. A., Lim, L., Evason, K. J., Momcilovic, O., Kruttwig, K., Huang, Q., Xu, G., Nomura, D. K. and Goga, A. (2017) MYC-driven inhibition of the glutamate-cysteine ligase promotes glutathione depletion in liver cancer. *EMBO Rep* **18**(4): 569-585.10.15252/embr.201643068

Andrechek, E. R., Cardiff, R. D., Chang, J. T., Gatza, M. L., Acharya, C. R., Potti, A. and Nevins, J. R. (2009) Genetic heterogeneity of Myc-induced mammary tumors reflecting diverse phenotypes including metastatic potential. *Proc Natl Acad Sci U S A* **106**(38): 16387-16392.10.1073/pnas.0901250106

Anso, E., Mullen, A. R., Felsher, D. W., Mates, J. M., Deberardinis, R. J. and Chandel, N. S. (2013) Metabolic changes in cancer cells upon suppression of Myc. *Cancer and Metabolism* **1**(7)

Asada, M., Furukawa, K., Segawa, K., Endo, T. and Kobata, A. (1997) Increased expression of highly branched N‑glycans at cell surface is correlated with the malignant phenotypes of mouse tumor cells. *Cancer Res* **57**: 1073-1080

Ashkani, J. and Naidoo, K. J. (2016) Glycosyltransferase Gene Expression Profiles Classify Cancer Types and Propose Prognostic Subtypes. *Sci Rep* **6**: 26451.10.1038/srep26451

Aupperlee, M. D., Leipprandt, J. R., Bennett, J. M., Schwartz, R. C. and Haslam, S. Z. (2013) Amphiregulin mediates progesterone-induced mammary ductal development during puberty. *Breast Cancer Res* **15**(3).10.1186/bcr3431

Avissar, N. E., Sax, H. C. and Toia, L. (2008) In human entrocytes, GLN transport and ASCT2 surface expression induced by short-term EGF are MAPK, PI3K, and Rho-dependent. *Dig Dis Sci* **53**(8): 2113-2125.10.1007/s10620-007-0120-y

Babu, E., Bhutia, Y. D., Ramachandran, S., Gnanaprakasam, J. P., Prasad, P. D., Thangaraju, M. and Ganapathy, V. (2015) Deletion of the amino acid transporter Slc6a14 suppresses tumour growth in spontaneous mouse models of breast cancer. *Biochem J* **469**(1): 17-23.10.1042/BJ20150437

Bak, L. K., Waagepetersen, H. S., Melo, T. M., Schousboe, A. and Sonnewald, U. (2007) Complex glutamate labeling from [U-13C]glucose or [U-13C]lactate in co-cultures of cerebellar neurons and astrocytes. *Neurochem Res* **32**: 671-680.10.1007/s11064-006-9161-4

Barollo, S., Bertazza, L., Watutantrige-Fernando, S., Censi, S., Cavedon, E., Galuppini, F., Pennelli, G., Fassina, A., Citton, M., Rubin, B., Pezzani, R., Benna, C., Opocher, G., Iacobone, M. and Mian, C. (2016) Overexpression of L-Type Amino Acid Transporter 1 (LAT1) and 2 (LAT2): Novel Markers of Neuroendocrine Tumors. *PLoS One* **11**(5).10.1371/journal.pone.0156044

Bayat Mokhtari, R., Homayouni, T. S., Baluch, N., Morgatskaya, E., Kumar, S., Das, B. and Yeger, H. (2017) Combination therapy in combating cancer. *Oncotarget* **8**(23): 38022-38043.10.18632/oncotarget.16723

Bernhardt, S., Bayerlova, M., Vetter, M., Wachter, A., Mitra, D., Hanf, V., Lantzsch, T., Uleer, C., Peschel, S., John, J., Buchmann, J., Weigert, E., Burrig, K. F., Thomssen, C., Korf, U., Beissbarth, T., Wiemann, S. and Kantelhardt, E. J. (2017) Proteomic profiling of breast cancer metabolism identifies SHMT2 and ASCT2 as prognostic factors. *Breast Cancer Res* **19**(1): 112-126.10.1186/s13058-017-0905-7

Bhutia, Y. D., Babu, E., Ramachandran, S. and Ganapathy, V. (2015) Amino Acid transporters in cancer and their relevance to "glutamine addiction": novel targets for the design of a new class of anticancer drugs. *Cancer Res* **75**(9): 1782-1788.10.1158/0008-5472.CAN-14-3745

Bhutia, Y. D. and Ganapathy, V. (2016) Glutamine transporters in mammalian cells and their functions in physiology and cance. *Biochim Biophys Acta* **1863**(10): 2531-2539.0.1016/j.bbamcr.2015.12.017

Biotechnology, S. C. (2017). "Data Sheets ASCT2 (H-52)." from https://datasheets.scbt.com/sc-99002.pdf.

Birsoy, K., Wang, T., Chen, W. W., Freinkman, E., Abu-Remaileh, M. and Sabatini, D. M. (2015) An Essential Role of the Mitochondrial Electron Transport Chain in Cell Proliferation Is to Enable Aspartate Synthesis. *Cell* **162**(3): 540-551.10.1016/j.cell.2015.07.016

Board, M., Humm, S. and Newsholme, E. A. (1990) Maximum activitiesofkeyenzymes ofglycolysis,glutaminolysis, pentose phosphate pathway and tricarboxylic acid cycle in normal, neoplastic and suppressed cells. *Biochem J* **265**: 503-509

Bode, B. P., Fuchs, B. C., Hurley, B. P., Conroy, J. L., Suetterlin, J. E., Tanabe, K. K., Rhoads, D. B., Abcouwer, S. F. and Souba, W. W. (2002) Molecular and functional analysis of glutamine uptake in human hepatoma and liver-derived cells. *Am J Physiol Gastrointest Liver Physiol* **283**: 1062-1073

Boehmer, C., Okur, F., Setiawan, I., Bröer, S. and Lang, F. (2003) Properties and regulation of glutamine transporter SN1 by protein kinases SGK and PKB. *Biochemical and Biophysical Research Communications* **306**(1): 156-162.10.1016/s0006-291x(03)00921-5

Bolzoni, M., Chiu, M., Accardi, F., Vescovini, R., Airoldi, I., Storti, P., Todoerti, K., Agnelli, L., Missale, G., Andreoli, R., Bianchi, M. G., Allegri, M., Barilli, A., Nicolini, F., Cavalli, A., Costa, F., Marchica, V., Toscani, D., Mancini, C., Martella, E., Dall'asta, V., Donofrio, G., Aversa, F., Bussolati, O. and Giuliani, N. (2016) Dependence on glutamine uptake and glutamine addiction characterize myeloma cells: a new attractive target. *Blood* **128**(5): 667-679.10.1182/blood-2016-01-690743

Boros, L., Brackett, D. and Harrigan, G. (2003) Metabolic biomarker and kinase drug target discovery in cancer using stable isotope-based dynamic metabolic profiling (SIDMAP). *Curr Cancer Drug Targets.* **3**: 447-455

Bott, A. J., Peng, I. C., Fan, Y., Faubert, B., Zhao, L., Li, J., Neidler, S., Sun, Y., Jaber, N., Krokowski, D., Lu, W., Pan, J. A., Powers, S., Rabinowitz, J., Hatzoglou, M., Murphy, D. J., Jones, R., Wu, S., Girnun, G. and Zong, W. X. (2015) Oncogenic Myc Induces Expression of Glutamine Synthetase through Promoter Demethylation. *Cell Metab* **22**(6): 1068-1077.10.1016/j.cmet.2015.09.025

Brand, A., Singer, K., Koehl, G. E., Kolitzus, M., Schoenhammer, G., Thiel, A., Matos, C., Bruss, C., Klobuch, S., Peter, K., Kastenberger, M., Bogdan, C., Schleicher, U., Mackensen, A., Ullrich, E., Fichtner-Feigl, S., Kesselring, R., Mack, M., Ritter, U., Schmid, M., Blank, C., Dettmer, K., Oefner, P. J., Hoffmann, P., Walenta, S., Geissler, E. K., Pouyssegur, J., Villunger, A., Steven, A., Seliger, B., Schreml, S., Haferkamp, S., Kohl, E., Karrer, S., Berneburg, M., Herr, W., Mueller-Klieser, W., Renner, K. and Kreutz, M. (2016) LDHA-Associated Lactic Acid Production Blunts Tumor Immunosurveillance by T and NK Cells. *Cell Metab* **24**(5): 657-671.10.1016/j.cmet.2016.08.011

Bratasz, A., Pandian, R. P., Deng, Y., Petryakov, S., Grecula, J. C., Gupta, N. and Kuppusamy, P. (2007) In vivo imaging of changes in tumor oxygenation during growth and after treatment. *Magn Reson Med* **57**(5): 950-959.10.1002/mrm.21212

Breton, C., Snajdrova, L., Jeanneau, C., Koca, J. and Imberty, A. (2006) Structures and mechanisms of glycosyltransferases. *Glycobiology* **16**(2): 29-37.10.1093/glycob/cwj016

Broer, A., Rahimi, F. and Broer, S. (2016) Deletion of Amino Acid Transporter ASCT2 (SLC1A5) Reveals an Essential Role for Transporters SNAT1 (SLC38A1) and SNAT2 (SLC38A2) to Sustain Glutaminolysis in Cancer Cells. *J Biol Chem* **291**(25): 13194-13205.10.1074/jbc.M115.700534

Bruna, A., Rueda, O. M., Greenwood, W., Batra, A. S., Callari, M., Batra, R. N., Pogrebniak, K., Sandoval, J., Cassidy, J. W., Tufegdzic-Vidakovic, A., Sammut, S. J., Jones, L., Provenzano, E., Baird, R., Eirew, P., Hadfield, J., Eldridge, M., Mclaren-Douglas, A., Barthorpe, A., Lightfoot, H., O'connor, M. J., Gray, J., Cortes, J., Baselga, J., Marangoni, E., Welm, A. L., Aparicio, S., Serra, V., Garnett, M. J. and Caldas, C. (2016) A Biobank of Breast Cancer Explants with Preserved Intra-tumor Heterogeneity to Screen Anticancer Compounds. *Cell* **167**(1): 260-274.10.1016/j.cell.2016.08.041

Buckhaults, P., Chen, L., Fregien, N. and Pierce, M. (1997) Transcriptional Regulation ofN-Acetylglucosaminyltransferase V by thesrcOncogene. *Journal of Biological Chemistry* **272**(31): 19575-19581.10.1074/jbc.272.31.19575

Bungard, C. I. and Mcgivan, J. D. (2004) Glutamine availability up-regulates expression of the amino acid transporter protein ASCT2 in HepG2 cells and stimulates the ASCT2 promoter. *Biochem J* **382**(1): 27-32.10.1042/BJ20040487

Calithera-Biosciences (2017). "Glutaminase Inhibitor CB-839." from https://www.calithera.com/programs/cb-839/.

Camarda, R., Williams, J. and Goga, A. (2017) In vivo Reprogramming of Cancer Metabolism by MYC. *Front Cell Dev Biol* **5**.10.3389/fcell.2017.00035

Camarda, R., Zhou, A. Y., Kohnz, R. A., Balakrishnan, S., Mahieu, C., Anderton, B., Eyob, H., Kajimura, S., Tward, A., Krings, G., Nomura, D. K. and Goga, A. (2016) Inhibition of fatty acid oxidation as a therapy for MYC-overexpressing triple-negative breast cancer. *Nat Med* **22**(4): 427-432.10.1038/nm.4055

Cancer Genome Atlas, N. (2012) Comprehensive molecular portraits of human breast tumours. *Nature* **490**(7418): 61-70.10.1038/nature11412

Cancer Research Uk (2017). "Breast Cancer Survival." 2017, from http://about-cancer.cancerresearchuk.org/about-cancer/breast-cancer/survival.

Cancer Research Uk (2017). "Cancer Incidence for all cancers combined." 2017, from http://www.cancerresearchuk.org/health-professional/cancer-statistics/incidence/all-cancers-combined.

Cancer Research Uk (2017). "Cancer mortality for all cancers combined." from http://www.cancerresearchuk.org/health-professional/cancer-statistics/mortality/all-cancers-combined.

Cardiff, R. D. and Wellings, S. R. (1999) The comparative pathology of human and mouse mammary glands. *journal of mammary gland biology and neoplasia* **4**(1): 105-122

Carmona-Fontaine, C., Deforet, M., Akkari, L., Thompson, C. B., Joyce, J. A. and Xavier, J. B. (2017) Metabolic origins of spatial organization in the tumor microenvironment. *Proc Natl Acad Sci U S A* **114**(11): 2934-2939.10.1073/pnas.1700600114

Cen, H., Mao, F., Aronchik, I., Fuentes, R. J. and Firestone, G. L. (2008) DEVD-NucView488: a novel class of enzyme substrates for real-time detection of caspase-3 activity in live cells. *FASEB J* **22**(7): 2243-2252.10.1096/fj.07-099234

Chaneton, B., Hillmann, P., Zheng, L., Martin, A. C., Maddocks, O. D., Chokkathukalam, A., Coyle, J. E., Jankevics, A., Holding, F. P., Vousden, K. H., Frezza, C., O'reilly, M. and Gottlieb, E. (2012) Serine is a natural ligand and allosteric activator of pyruvate kinase M2. *Nature* **491**(7424): 458-462.10.1038/nature11540

Chang, C. H., Qiu, J., O'sullivan, D., Buck, M. D., Noguchi, T., Curtis, J. D., Chen, Q., Gindin, M., Gubin, M. M., Van Der Windt, G. J., Tonc, E., Schreiber, R. D., Pearce, E. J. and Pearce, E. L. (2015) Metabolic Competition in the Tumor Microenvironment Is a Driver of Cancer Progression. *Cell* **162**(6): 1229-1241.10.1016/j.cell.2015.08.016

Chen, R., Zou, Y., Mao, D., Sun, D., Gao, G., Shi, J., Liu, X., Zhu, C., Yang, M., Ye, W., Hao, Q., Li, R. and Yu, L. (2014) The general amino acid control pathway regulates mTOR and autophagy during serum/glutamine starvation. *J Cell Biol* **206**(2): 173-182.10.1083/jcb.201403009

Chen, Z., Wang, Y., Warden, C. and Chen, S. (2015) Cross-talk between ER and HER2 regulates c-MYC-mediated glutamine metabolism in aromatase inhibitor resistant breast cancer cells. *J Steroid Biochem Mol Biol* **149**: 118-127.10.1016/j.jsbmb.2015.02.004

Cheong, H., Lindsten, T., Wu, J., Lu, C. and Thompson, C. B. (2011) Ammonia-induced autophagy is independent of ULK1/ULK2 kinases. *Proc Natl Acad Sci U S A* **108**(27): 11121-11126.10.1073/pnas.1107969108

Cheung, P. and Dennis, J. W. (2007) Mgat5 and Pten interact to regulate cell growth and polarity. *Glycobiology* **17**(7): 767-773.10.1093/glycob/cwm037

Chiu, M., Sabino, C., Taurino, G., Bianchi, M. G., Andreoli, R., Giuliani, N. and Bussolati, O. (2017) GPNA inhibits the sodium-independent transport system L for neutral amino acids. *Amino Acids*.10.1007/s00726-017-2436-z

Choi, J., Credit, K., Henderson, K., Deverkadra, R., He, Z., Wiig, H., Vanpelt, H. and Flessner, M. F. (2006) Intraperitoneal immunotherapy for metastatic ovarian carcinoma: Resistance of intratumoral collagen to antibody penetration. *Clin Cancer Res* **12**(6): 1906-1912.10.1158/1078-0432.CCR-05-2141

Clarke, R., Liu, M. C., Bouker, K. B., Gu, Z., Lee, R. Y., Zhu, Y., Skaar, T. C., Gomez, B., O'brien, K., Wang, Y. and Hilakivi-Clarke, L. A. (2003) Antiestrogen resistance in breast cancer and the role of estrogen receptor signaling. *Oncogene* **22**(47): 7316-7339.10.1038/sj.onc.1206937

Clem, B., Telang, S., Clem, A., Yalcin, A., Meier, J., Simmons, A., Rasku, M. A., Arumugam, S., Dean, W. L., Eaton, J., Lane, A., Trent, J. O. and Chesney, J. (2008) Small-molecule inhibition of 6-phosphofructo-2-kinase activity suppresses glycolytic flux and tumor growth. *Mol Cancer Ther* **7**(1): 110-120.10.1158/1535-7163.MCT-07-0482

Colas, C., Grewer, C., Otte, N. J., Gameiro, A., Albers, T., Singh, K., Shere, H., Bonomi, M., Holst, J. and Schlessinger, A. (2015) Ligand Discovery for the Alanine-Serine-Cysteine Transporter (ASCT2, SLC1A5) from Homology Modeling and Virtual Screening. *PLoS Comput Biol* **11**(10).10.1371/journal.pcbi.1004477

Colegio, O. R., Chu, N. Q., Szabo, A. L., Chu, T., Rhebergen, A. M., Jairam, V., Cyrus, N., Brokowski, C. E., Eisenbarth, S. C., Phillips, G. M., Cline, G. W., Phillips, A. J. and Medzhitov, R. (2014) Functional polarization of tumour-associated macrophages by tumour-derived lactic acid. *Nature* **513**(7519): 559-563.10.1038/nature13490

Coloff, J. L., Murphy, J. P., Braun, C. R., Harris, I. S., Shelton, L. M., Kami, K., Gygi, S. P., Selfors, L. M. and Brugge, J. S. (2016) Differential Glutamate Metabolism in Proliferating and Quiescent Mammary Epithelial Cells. *Cell Metab* **23**(5): 867-880.10.1016/j.cmet.2016.03.016

Console, L., Scalise, M., Tarmakova, Z., Coe, I. R. and Indiveri, C. (2015) N-linked glycosylation of human SLC1A5 (ASCT2) transporter is critical for trafficking to membrane. *Biochim Biophys Acta* **1853**(7): 1636-1645.10.1016/j.bbamcr.2015.03.017

Cormerais, Y., Giuliano, S., Lefloch, R., Front, B., Durivault, J., Tambutte, E., Massard, P. A., De La Ballina, L. R., Endou, H., Wempe, M. F., Palacin, M., Parks, S. K. and Pouyssegur, J. (2016) Genetic Disruption of the Multifunctional CD98/LAT1 Complex Demonstrates the Key Role of Essential Amino Acid Transport in the Control of mTORC1 and Tumor Growth. *Cancer Res* **76**(15): 4481-4492.10.1158/0008-5472.CAN-15-3376

Crespo, J. L., Powers, T., Fowler, B. and Hall, M. N. (2002) The TOR-controlled transcription activators GLN3, RTG1, and RTG3 are regulated in response to

intracellular levels of glutamine. *Proc Natl Acad Sci U S A* **99**(10): 6784-6789.10.1073/pnas.102687599

Csibi, A., Fendt, S. M., Li, C., Poulogiannis, G., Choo, A. Y., Chapski, D. J., Jeong, S. M., Dempsey, J. M., Parkhitko, A., Morrison, T., Henske, E. P., Haigis, M. C., Cantley, L. C., Stephanopoulos, G., Yu, J. and Blenis, J. (2013) The mTORC1 pathway stimulates glutamine metabolism and cell proliferation by repressing SIRT4. *Cell* **153**(4): 840-854.10.1016/j.cell.2013.04.023

Csibi, A., Lee, G., Yoon, S. O., Tong, H., Ilter, D., Elia, I., Fendt, S. M., Roberts, T. M. and Blenis, J. (2014) The mTORC1/S6K1 pathway regulates glutamine metabolism through the eIF4B-dependent control of c-Myc translation. *Curr Biol* **24**(19): 2274-2280.10.1016/j.cub.2014.08.007

D'cruz, C., Gunther, E., Boxer, R., Hartman, J., Sintasath, L., Moody, S., Cox, J., Ha, S., Belka, G., Golant, A., Cardiff, R. and Chodosh, L. (2001) c-MYC induces mammary tumorigenesis by means of a preferred pathway involving spontaneous Kras2 mutations. *Nature Medicine* **7**(2)

Dai, C., Whitesell, L., Rogers, A. B. and Lindquist, S. (2007) Heat shock factor 1 is a powerful multifaceted modifier of carcinogenesis. *Cell* **130**(6): 1005-1018.10.1016/j.cell.2007.07.020

David, C. J., Chen, M., Assanah, M., Canoll, P. and Manley, J. L. (2010) HnRNP proteins controlled by c-Myc deregulate pyruvate kinase mRNA splicing in cancer. *Nature* **463**(7279): 364-368.10.1038/nature08697

Davidson, S. M., Papagiannakopoulos, T., Olenchock, B. A., Heyman, J. E., Keibler, M. A., Luengo, A., Bauer, M. R., Jha, A. K., O'brien, J. P., Pierce, K. A., Gui, D. Y., Sullivan, L. B., Wasylenko, T. M., Subbaraj, L., Chin, C. R., Stephanopolous, G., Mott, B. T., Jacks, T., Clish, C. B. and Vander Heiden, M. G. (2016) Environment Impacts the Metabolic Dependencies of Ras-Driven Non-Small Cell Lung Cancer. *Cell Metab* **23**(3): 517-528.10.1016/j.cmet.2016.01.007

Deberardinis, R. J., Mancuso, A., Daikhin, E., Nissim, I., Yudkoff, M., Wehrli, S. and Thompson, C. B. (2007) Beyond aerobic glycolysis: transformed cells can engage in glutamine metabolism that exceeds the requirement for protein and nucleotide synthesis. *Proc Natl Acad Sci U S A* **104**(49): 19345-19350.10.1073/pnas.0709747104

Degenhardt, K. and White, E. (2006) A mouse model system to genetically dissect the molecular mechanisms regulating tumorigenesis. *Clin Cancer Res* **12**(18): 5298-5304.10.1158/1078-0432.CCR-06-0439

Deming, S. L., Nass, S. J., Dickson, R. B. and Trock, B. J. (2000) C-myc amplification in breast cancer: a meta-analysis of its occurrence and prognostic relevance. *Br J Cancer* **83**(12): 1688-1695.10.1054/bjoc.2000.1522

Derose, Y. S., Gligorich, K. M., Wang, G., Georgelas, A., Bowman, P., Courdy, S. J., Welm, A. L. and Welm, B. E. (2013) Patient-derived models of human breast cancer: protocols for in vitro and in vivo applications in tumor biology and translational medicine. *Curr Protoc Pharmacol* **Chapter 14**.10.1002/0471141755.ph1423s60

Derose, Y. S., Wang, G., Lin, Y. C., Bernard, P. S., Buys, S. S., Ebbert, M. T., Factor, R., Matsen, C., Milash, B. A., Nelson, E., Neumayer, L., Randall, R. L., Stijleman, I. J., Welm, B. E. and Welm, A. L. (2011) Tumor grafts derived from women with breast cancer authentically reflect tumor pathology, growth, metastasis and disease outcomes. *Nat Med* **17**(11): 1514-1520.10.1038/nm.2454

Dey, P., Baddour, J., Muller, F., Wu, C. C., Wang, H., Liao, W. T., Lan, Z., Chen, A., Gutschner, T., Kang, Y., Fleming, J., Satani, N., Zhao, D., Achreja, A., Yang, L., Lee, J., Chang, E., Genovese, G., Viale, A., Ying, H., Draetta, G., Maitra, A., Wang, Y. A., Nagrath, D. and Depinho, R. A. (2017) Genomic deletion of malic enzyme 2 confers collateral lethality in pancreatic cancer. *Nature* **542**(7639): 119-123.10.1038/nature21052

Donald, S. P., Sun, X. Y., Hu, C. A., Yu, J., Mei, J. M., Valle, D. and Phang, J. M. (2001) Proline oxidase, encoded by p53-induced gene-6, catalyzes the generation of proline-dependent reactive oxygen species. *Cancer Res* **61**(5): 1810-1815

Dong, J., Xiao, D., Zhao, Z., Ren, P., Li, C., Hu, Y., Shi, J., Su, H., Wang, L., Liu, H., Li, B., Gao, P. and Qing, G. (2017) Epigenetic silencing of microRNA-137 enhances ASCT2 expression and tumor glutamine metabolism. *Oncogenesis* **6**(7).10.1038/oncsis.2017.59

Duan, F., Jia, D., Zhao, J., Wu, W., Min, L., Song, S., Wu, H., Wang, L., Wang, H., Ruan, Y. and Gu, J. (2016) Loss of GFAT1 promotes epithelial-to-mesenchymal transition and predicts unfavorable prognosis in gastric cancer. *Oncotarget* **7**(25): 38427-38439.10.18632/oncotarget.9538

Duran, R. V., Oppliger, W., Robitaille, A. M., Heiserich, L., Skendaj, R., Gottlieb, E. and Hall, M. N. (2012) Glutaminolysis activates Rag-mTORC1 signaling. *Mol Cell* **47**(3): 349-358.10.1016/j.molcel.2012.05.043

Eilers, M., Picard, D., Yamamoto, K. R. and Bishop, J. M. (1989) Chimaeras of myc oncoprotein and steroid receptors cause hormone-dependent transformation of cells. *Nature* **340**(6228): 66-68.10.1038/340066a0

Elgadi, K., Meguid, R., Qian, M., Souba, W. and Abcouwer, S. (1999) Cloning and analysis of unique human glutaminase isoforms generated by tissue-specific alternative splicing. . *Physiol Genomics* **1**: 51-62

Esslinger, C. S., Cybulski, K. A. and Rhoderick, J. F. (2005) Ngamma-aryl glutamine analogues as probes of the ASCT2 neutral amino acid transporter binding site. *Bioorg Med Chem* **13**(4): 1111-1118.10.1016/j.bmc.2004.11.028

Fallah, Y., Brundage, J., Allegakoen, P. and Shajahan-Haq, A. N. (2017) MYC-Driven Pathways in Breast Cancer Subtypes. *Biomolecules* **7**(3).10.3390/biom7030053

Fan, T. W., Lane, A. N., Higashi, R. M., Bousamra, M., 2nd, Kloecker, G. and Miller, D. M. (2009) Metabolic profiling identifies lung tumor responsiveness to erlotinib. *Exp Mol Pathol* **87**(1): 83-86.10.1016/j.yexmp.2009.04.004

Fan, T. W., Lane, A. N., Higashi, R. M. and Yan, J. (2011) Stable isotope resolved metabolomics of lung cancer in a SCID mouse model. *Metabolomics* **7**(2): 257-269.10.1007/s11306-010-0249-0

Fendt, S. M., Bell, E. L., Keibler, M. A., Olenchock, B. A., Mayers, J. R., Wasylenko, T. M., Vokes, N. I., Guarente, L., Vander Heiden, M. G. and Stephanopoulos, G. (2013) Reductive glutamine metabolism is a function of the alpha-ketoglutarate to citrate ratio in cells. *Nat Commun* **4**.10.1038/ncomms3236

Fiaschi, T., Marini, A., Giannoni, E., Taddei, M. L., Gandellini, P., De Donatis, A., Lanciotti, M., Serni, S., Cirri, P. and Chiarugi, P. (2012) Reciprocal metabolic reprogramming through lactate shuttle coordinately influences tumor-stroma interplay. *Cancer Res* **72**(19): 5130-5140.10.1158/0008-5472.CAN-12-1949

Fuchs, B. C. and Bode, B. P. (2005) Amino acid transporters ASCT2 and LAT1 in cancer: partners in crime? *Semin Cancer Biol* **15**(4): 254-266.10.1016/j.semcancer.2005.04.005

Fuchs, B. C., Perez, J. C., Suetterlin, J. E., Chaudhry, J. E. and Bode, B. P. (2004) Inducible antisense RNA targeting amino acid transporter ATB0/ASCT2 elicits apoptosis in human hepatoma cells. *Am J Physiol Gastrointest Liver Physiol*: 467-478

Fukumura, D., Xu, L., Chen, Y., Gohongi, T., Seed, B. and Jain, R. K. (2001) Hypoxia and Acidosis Independently Up-Regulate Vascular Endothelial Growth Factor Transcription in Brain Tumors in Vivo. *Cancer Research*: 6020-6024

Gaglio, D., Metallo, C. M., Gameiro, P. A., Hiller, K., Danna, L. S., Balestrieri, C., Alberghina, L., Stephanopoulos, G. and Chiaradonna, F. (2011) Oncogenic K-Ras decouples glucose and glutamine metabolism to support cancer cell growth. *Mol Syst Biol* **7**: 523.10.1038/msb.2011.56

Galmozzi, E., Casalini, P., Iorio, M. V., Casati, B., Olgiati, C. and Menard, S. (2004) HER2 signaling enhances 5'UTR-mediated translation of c-Myc mRNA. *J Cell Physiol* **200**(1): 82-88.10.1002/jcp.20012

Gao, P., Tchernyshyov, I., Chang, T. C., Lee, Y. S., Kita, K., Ochi, T., Zeller, K. I., De Marzo, A. M., Van Eyk, J. E., Mendell, J. T. and Dang, C. V. (2009) c-Myc suppression of miR-23a/b enhances mitochondrial glutaminase expression and glutamine metabolism. *Nature* **458**(7239): 762-765.10.1038/nature07823

Gatza, M. L., Lucas, J. E., Barry, W. T., Kim, J. W., Wang, Q., Crawford, M. D., Datto, M. B., Kelley, M., Mathey-Prevot, B., Potti, A. and Nevins, J. R. (2010) A pathway-based classification of human breast cancer. *Proc Natl Acad Sci U S A* **107**(15): 6994-6999.10.1073/pnas.0912708107

Gershon, T. R., Crowther, A. J., Tikunov, A., Garcia, I., Annis, R., Yuan, H., Miller, C. R., Macdonald, J., Olson, J. and Deshmukh, M. (2013) Hexokinase-2-mediated aerobic glycolysis is integral to cerebellar neurogenesis and pathogenesis of medulloblastoma. *Cancer Metab* **1**(1).10.1186/2049-3002-1-2

Gill, D. J., Chia, J., Senewiratne, J. and Bard, F. (2010) Regulation of O-glycosylation through Golgi-to-ER relocation of initiation enzymes. *J Cell Biol* **189**(5): 843-858.10.1083/jcb.201003055

Gottlob, K., Majewski, N., Kennedy, S., Kandel, E., Robey, R. B. and Hay, N. (2001) Inhibition of early apoptotic events by Akt/PKB is dependent on the first committed step of glycolysis and mitochondrial hexokinase. *Genes Dev* **15**(11): 1406-1418.10.1101/gad.889901

Grassi, I., Nanni, C., Allegri, V., Morigi, J. J., Montini, G. C., Castellucci, P. and Fanti, S. (2012) The clinical use of PET with 11C-acetate. *American Journal of Nuclear Medicine and Molecular Imaging* **2**(1): 33-47

Graven, K. K., Bellur, D., Klahn, B. D., Lowrey, S. L. and Amberger, E. (2003) HIF-2α regulates glyceraldehyde-3-phosphate dehydrogenase expression in endothelial cells. *Biochimica et Biophysica Acta (BBA) - Gene Structure and Expression* **1626**: 10-18.10.1016/s0167-4781(03)00049-6

Green, A. R., Aleskandarany, M. A., Agarwal, D., Elsheikh, S., Nolan, C. C., Diez-Rodriguez, M., Macmillan, R. D., Ball, G. R., Caldas, C., Madhusudan, S., Ellis, I. O. and Rakha, E. A. (2016) MYC functions are specific in biological subtypes of breast cancer and confers resistance to endocrine therapy in luminal tumours. *Br J Cancer* **114**(8): 917-928.10.1038/bjc.2016.46

Grewer, C. and Grabsch, E. (2004) New inhibitors for the neutral amino acid transporter ASCT2 reveal its Na+-dependent anion leak. *J Physiol* **557**(3): 747-759.10.1113/jphysiol.2004.062521

Gross, M. I., Demo, S. D., Dennison, J. B., Chen, L., Chernov-Rogan, T., Goyal, B., Janes, J. R., Laidig, G. J., Lewis, E. R., Li, J., Mackinnon, A. L., Parlati, F., Rodriguez, M. L., Shwonek, P. J., Sjogren, E. B., Stanton, T. F., Wang, T., Yang, J., Zhao, F. and Bennett, M. K. (2014) Antitumor activity of the glutaminase inhibitor CB-839 in triple-negative breast cancer. *Mol Cancer Ther* **13**(4): 890-901.10.1158/1535-7163.MCT-13-0870

Groves, A. M., Win, T., Haim, S. B. and Ell, P. J. (2007) Non-[18F]FDG PET in clinical oncology. *The Lancet Oncology* **8**(9): 822-830.10.1016/s1470-2045(07)70274-7

Gupta, N., Prasad, P. D., Ghamande, S., Moore-Martin, P., Herdman, A. V., Martindale, R. G., Podolsky, R., Mager, S., Ganapathy, M. E. and Ganapathy, V. (2006) Up-regulation of the amino acid transporter ATB(0,+) (SLC6A14) in carcinoma of the cervix. *Gynecol Oncol* **100**(1): 8-13.10.1016/j.ygyno.2005.08.016

Gusterson, B. A., Gullick, W. J., Venter, D. J., Powles, T. J., Elliott, C., Ashley, S., Tidy, A. and Harrison, S. (1987) Immunohistochemical localization of c-erbB-2 in human breast carcinomas. *Molecular and Cellular Probes* **1**(4): 383-391.10.1016/0890-8508(87)90019-3

Gutierrez, J. A., Pan, Y. X., Koroniak, L., Hiratake, J., Kilberg, M. S. and Richards, N. G. (2006) An inhibitor of human asparagine synthetase suppresses proliferation of an L-asparaginase-resistant leukemia cell line. *Chem Biol* **13**(12): 1339-1347.10.1016/j.chembiol.2006.10.010

Hagiwara, A., Cornu, M., Cybulski, N., Polak, P., Betz, C., Trapani, F., Terracciano, L., Heim, M. H., Ruegg, M. A. and Hall, M. N. (2012) Hepatic mTORC2 activates glycolysis and lipogenesis through Akt, glucokinase, and SREBP1c. *Cell Metab* **15**(5): 725-738.10.1016/j.cmet.2012.03.015

Hahn, W. C., Dessain, S. K., Brooks, M. W., King, J. E., Elenbaas, B., Sabatini, D. M., Decaprio, J. A. and Weinberg, R. A. (2002) Enumeration of the Simian Virus 40 Early Region Elements Necessary for Human Cell Transformation. *Molecular and Cellular Biology* **22**(7): 2111-2123.10.1128/mcb.22.7.2111-2123.2002

Hanahan, D. and Folkman, J. (1996) Patterns and emerging mechanisms of the angiogenic switch during tumorigenesis. *Cell* **86**: 353-364

Harding, H. P., Zhang, Y., Zeng, H., Novoa, I., Lu, P. D., Calfon, M., Sadri, N., Yun, C., Popko, B., Paules, R., Stojdl, D. F., Bell, J. C., Hettmann, T., Leiden, J. M. and Ron, D. (2003) An Integrated Stress Response Regulates Amino Acid Metabolism and Resistance to Oxidative Stress. *Molecular Cell* **11**(3): 619-633.10.1016/s1097-2765(03)00105-9

Hassanein, M., Hight, M. R., Buck, J. R., Tantawy, M. N., Nickels, M. L., Hoeksema, M. D., Harris, B. K., Boyd, K., Massion, P. P. and Manning, H. C. (2016) Preclinical Evaluation of 4-[18F]Fluoroglutamine PET to Assess ASCT2 Expression in Lung Cancer. *Mol Imaging Biol* **18**(1): 18-23.10.1007/s11307-015-0862-4

Hassanein, M., Qian, J., Hoeksema, M. D., Wang, J., Jacobovitz, M., Ji, X., Harris, F. T., Harris, B. K., Boyd, K. L., Chen, H., Eisenberg, R. and Massion, P. P. (2015) Targeting SLC1a5-mediated glutamine dependence in non-small cell lung cancer. *Int J Cancer* **137**(7): 1587-1597.10.1002/ijc.29535

Hatano, K., Miyamoto, Y., Nonomura, N. and Kaneda, Y. (2011) Expression of gangliosides, GD1a, and sialyl paragloboside is regulated by NF-kappaB-dependent

transcriptional control of alpha2,3-sialyltransferase I, II, and VI in human castration-resistant prostate cancer cells. *Int J Cancer* **129**(8): 1838-1847.10.1002/ijc.25860

Helmlinger, G., Yuan, F., Dellian, M. and Jain, R. K. (1997) Interstitial pH and pO2 gradients in solid tumors in vivo: High-resolution measurements reveal a lack of correlation. *Nature Medicine* **3**(2): 177-182.10.1038/nm0297-177

Hommes, F. A. and Wilmink, C. W. (1968) Developmental Changes of Glycolytic Enzymes in Rat Brain, Liver and Skeletal Muscle. *Neonatology* **13**(3): 181-193.10.1159/000240145

Honjo, H., Kaira, K., Miyazaki, T., Yokobori, T., Kanai, Y., Nagamori, S., Oyama, T., Asao, T. and Kuwano, H. (2016) Clinicopathological significance of LAT1 and ASCT2 in patients with surgically resected esophageal squamous cell carcinoma. *J Surg Oncol* **113**(4): 381-389.10.1002/jso.24160

Horiuchi, D., Kusdra, L., Huskey, N. E., Chandriani, S., Lenburg, M. E., Gonzalez-Angulo, A. M., Creasman, K. J., Bazarov, A. V., Smyth, J. W., Davis, S. E., Yaswen, P., Mills, G. B., Esserman, L. J. and Goga, A. (2012) MYC pathway activation in triple-negative breast cancer is synthetic lethal with CDK inhibition. *J Exp Med* **209**(4): 679-696.10.1084/jem.20111512

Huang, F., Zhao, Y., Zhao, J., Wu, S., Jiang, Y., Ma, H. and Zhang, T. (2014) Upregulated SLC1A5 promotes cell growth and survival in colorectal cancer. *International Journal of Clinical & Experimental Pathology* **7**(9): 6006-6014

Hudson, C. D., Savadelis, A., Nagaraj, A. B., Joseph, P., Avril, S., Difeo, A. and Avril, N. (2016) Altered glutamine metabolism in platinum resistant ovarian cancer. *Oncotarget* **7**(27): 41637-41649.10.18632/oncotarget.9317

Hui, S., Ghergurovich, J. M., Morscher, R. J., Jang, C., Teng, X., Lu, W., Esparza, L. A., Reya, T., Le, Z., Yanxiang Guo, J., White, E. and Rabinowitz, J. D. (2017) Glucose feeds the TCA cycle via circulating lactate. *Nature* **551**(7678): 115-118.10.1038/nature24057

Hutchinson, L. (2010) Breast cancer: challenges, controversies, breakthroughs. *Nat Rev Clin Oncol* **7**(12): 669-670.10.1038/nrclinonc.2010.192

Hutchison, G. J., Valentine, H. R., Loncaster, J. A., Davidson, S. E., Hunter, R. D., Roberts, S. A., Harris, A. L., Stratford, I. J., Price, P. M. and West, C. M. (2004) Hypoxia-inducible factor 1alpha expression as an intrinsic marker of hypoxia: correlation with tumor oxygen, pimonidazole measurements, and outcome in locally advanced carcinoma of the cervix. *Clin Cancer Res* **10**(24): 8405-8412.10.1158/1078-0432.CCR-03-0135

Hynes, N. E. and Lane, H. A. (2001) Myc and Mammary Cancer: Myc is a Downstream Effector of the ErbB2 Receptor Tyrosine Kinase. *journal of mammary gland biology and neoplasia* **6**(1): 141-150

Ito, S., Shen, L., Dai, Q., Wu, S. C., Collins, L. B., Swenberg, J. A., He, C. and Zhang, Y. (2011) Tet proteins can convert 5-methylcytosine to 5-formylcytosine and 5-carboxylcytosine. *Science* **333**(6047): 1300-1303.10.1126/science.1210597

Izumchenko, E., Paz, K., Ciznadija, D., Sloma, I., Katz, A., Vasquez-Dunddel, D., Ben-Zvi, I., Stebbing, J., Mcguire, W., Harris, W., Maki, R., Gaya, A., Bedi, A., Zacharoulis, S., Ravi, R., Wexler, L. H., Hoque, M. O., Rodriguez-Galindo, C., Pass, H., Peled, N., Davies, A., Morris, R., Hidalgo, M. and Sidransky, D. (2017) Patient-derived xenografts effectively capture responses to oncology therapy in a heterogeneous cohort of patients with solid tumors. *Ann Oncol* **28**(10): 2595-2605.10.1093/annonc/mdx416

Jakeman, L. B., Armanini, M., Phillips, H. S. and Ferrara, N. (1993) Developmental expression of binding sites and messenger ribonucleic acid for vascular endothelial growth factor suggests a role for this protein in vasculogenesis and angiogenesis. *Endocrinology* **133**(2): 848-859.10.1210/endo.133.2.7688292

Jean, J. C., Rich, C. B. and Joyce-Brady, M. (2006) Hypoxia results in an HIF-1-dependent induction of brain-specific aldolase C in lung epithelial cells. *Am J Physiol Lung Cell Mol Physiol* **291**(5): 950-956.10.1152/ajplung.00087.2006

Jeon, Y. J., Khelifa, S., Ratnikov, B., Scott, D. A., Feng, Y., Parisi, F., Ruller, C., Lau, E., Kim, H., Brill, L. M., Jiang, T., Rimm, D. L., Cardiff, R. D., Mills, G. B., Smith, J. W., Osterman, A. L., Kluger, Y. and Ronai, Z. A. (2015) Regulation of glutamine carrier proteins by RNF5 determines breast cancer response to ER stress-inducing chemotherapies. *Cancer Cell* **27**(3): 354-369.10.1016/j.ccell.2015.02.006

Jin, L., Li, D., Alesi, G. N., Fan, J., Kang, H. B., Lu, Z., Boggon, T. J., Jin, P., Yi, H., Wright, E. R., Duong, D., Seyfried, N. T., Egnatchik, R., Deberardinis, R. J., Magliocca, K. R., He, C., Arellano, M. L., Khoury, H. J., Shin, D. M., Khuri, F. R. and Kang, S. (2015) Glutamate dehydrogenase 1 signals through antioxidant glutathione peroxidase 1 to regulate redox homeostasis and tumor growth. *Cancer Cell* **27**(2): 257-270.10.1016/j.ccell.2014.12.006

Kaira, K., Arakawa, K., Shimizu, K., Oriuchi, N., Nagamori, S., Kanai, Y., Oyama, T. and Takeyoshi, I. (2015) Relationship between CD147 and expression of amino acid transporters (LAT1 and ASCT2) in patients with pancreatic cancer. *Am J Transl Res.* **7**(2): 356-363

Kaira, K., Oriuchi, N., Imai, H., Shimizu, K., Yanagitani, N., Sunaga, N., Hisada, T., Tanaka, S., Ishizuka, T., Kanai, Y., Endou, H., Nakajima, T. and Mori, M. (2008) Prognostic significance of L-type amino acid transporter 1 expression in resectable stage I-III nonsmall cell lung cancer. *Br J Cancer* **98**(4): 742-748.10.1038/sj.bjc.6604235

Karantza-Wadsworth, V., Patel, S., Kravchuk, O., Chen, G., Mathew, R., Jin, S. and White, E. (2007) Autophagy mitigates metabolic stress and genome damage in mammary tumorigenesis. *Genes Dev* **21**(13): 1621-1635.10.1101/gad.1565707

Kasai, N., Sasakawa, A., Hosomi, K., Poh, T. W., Chua, B. L., Yong, W. P., So, J., Chan, S. L., Soong, R., Kono, K., Ishii, T. and Yamano, K. (2017) Anti-tumor efficacy evaluation of a novel monoclonal antibody targeting neutral amino acid transporter ASCT2 using patient-derived xenograft mouse models of gastric cancer. *American Journal of Translational Research* **9**(7): 3399-3410

Katherine Sellers, M. P. F., Michael Bousamra Ii, Stephen P. Slone, Richard M. Higashi, Donald M. Miller, Yali Wang, Jun Yan, Mariia O. Yuneva, Rahul Deshpande, Andrew N. Lane and Teresa W.-M. Fan (2015) Pyruvate carboxylase is critical for non–small-cell lung cancer proliferation. *J Clin Invest.*10.1172/JCI79188 10.1172/JCI72873DS1

Kato, Y., Ozawa, S., Tsukuda, M., Kubota, E., Miyazaki, K., St-Pierre, Y. and Hata, R. (2007) Acidic extracellular pH increases calcium influx-triggered phospholipase D activity along with acidic sphingomyelinase activation to induce matrix metalloproteinase-9 expression in mouse metastatic melanoma. *FEBS J* **274**(12): 3171-3183.10.1111/j.1742-4658.2007.05848.x

Kerr, E. M., Gaude, E., Turrell, F. K., Frezza, C. and Martins, C. P. (2016) Mutant Kras copy number defines metabolic reprogramming and therapeutic susceptibilities. *Nature* **531**(7592): 110-113.10.1038/nature16967

Kim, J. W., Gao, P., Liu, Y. C., Semenza, G. L. and Dang, C. V. (2007) Hypoxia-inducible factor 1 and dysregulated c-Myc cooperatively induce vascular endothelial growth factor and metabolic switches hexokinase 2 and pyruvate dehydrogenase kinase 1. *Mol Cell Biol* **27**(21): 7381-7393.10.1128/MCB.00440-07

Kim, J. W., Zeller, K. I., Wang, Y., Jegga, A. G., Aronow, B. J., O'donnell, K. A. and Dang, C. V. (2004) Evaluation of myc E-box phylogenetic footprints in glycolytic genes by chromatin immunoprecipitation assays. *Mol Cell Biol* **24**(13): 5923-5936.10.1128/MCB.24.13.5923-5936.2004

Kim, M.-J., Kim, D.-H., Jung, W.-H. and Koo, J.-S. (2014) Expression of metabolism-related proteins in triple-negative breast cancer. *International Journal of Clinical & Experimental Pathology*

Kim, S., Kim, D. H., Jung, W. H. and Koo, J. S. (2013) Expression of glutamine metabolism-related proteins according to molecular subtype of breast cancer. *Endocr Relat Cancer* **20**(3): 339-348.10.1530/ERC-12-0398

Kim, S., Lee, Y. and Koo, J. S. (2015) Differential expression of lipid metabolism-related proteins in different breast cancer subtypes. *PLoS One* **10**(3).10.1371/journal.pone.0119473

Kim, S. K., Jung, W. H. and Koo, J. S. (2014) Differential expression of enzymes associated with serine/glycine metabolism in different breast cancer subtypes. *PLoS One* **9**(6).10.1371/journal.pone.0101004

Klos, K. S., Wyszomierski, S. L., Sun, M., Tan, M., Zhou, X., Li, P., Yang, W., Yin, G., Hittelman, W. N. and Yu, D. (2006) ErbB2 increases vascular endothelial growth factor protein synthesis via activation of mammalian target of rapamycin/p70S6K leading to increased angiogenesis and spontaneous metastasis of human breast cancer cells. *Cancer Res* **66**(4): 2028-2037.10.1158/0008-5472.CAN-04-4559

Krall, A. S., Xu, S., Graeber, T. G., Braas, D. and Christofk, H. R. (2016) Asparagine promotes cancer cell proliferation through use as an amino acid exchange factor. *Nat Commun* **7**.10.1038/ncomms11457

Kress, S., Stein, A., Maurer, P., Weber, B., Reichert, J., Buchmann, A., Huppert, P. and Schwarz, M. (1998) Expression of hypoxia-inducible genes in tumor cells. *J Cancer Res Clin Oncol* **124**(6): 315-320

Kumamoto, K., Goto, Y., Sekikawa, K., Takenoshita, S., Ishida, N., Kawakita, M. and Kannagi, R. (2001) Increased expression of UDP-galactose transporter messenger RNA in human colon cancer tissues and its implication in synthesis of Thomsen-Friedenreich antigen and sialyl Lewis A/X determinants. *Cancer Res* **61**: 4620-4627

Lacey, J. and Wilmore, D. (1990) Is glutamine a conditionally essential amino acid? *Nutr Rev* **48**: 297-309

Lajoie, P., Partridge, E. A., Guay, G., Goetz, J. G., Pawling, J., Lagana, A., Joshi, B., Dennis, J. W. and Nabi, I. R. (2007) Plasma membrane domain organization regulates EGFR signaling in tumor cells. *J Cell Biol* **179**(2): 341-356.10.1083/jcb.200611106

Lampson, B. L., Pershing, N. L., Prinz, J. A., Lacsina, J. R., Marzluff, W. F., Nicchitta, C. V., Macalpine, D. M. and Counter, C. M. (2013) Rare codons regulate KRas oncogenesis. *Curr Biol* **23**(1): 70-75.10.1016/j.cub.2012.11.031

Lanning, N. J., Castle, J. P., Singh, S. J., Leon, A. N., Tovar, E. A., Sanghera, A., Mackeigan, J. P., Filipp, F. V. and Graveel, C. R. (2017) Metabolic profiling of triple-negative breast cancer cells reveals metabolic vulnerabilities. *Cancer Metab* **5**.10.1186/s40170-017-0168-x

Le, A., Cooper, C. R., Gouw, A. M., Dinavahi, R., Maitra, A., Deck, L. M., Royer, R. E., Vander Jagt, D. L., Semenza, G. L. and Dang, C. V. (2010) Inhibition of lactate dehydrogenase A induces oxidative stress and inhibits tumor progression. *Proc Natl Acad Sci U S A* **107**(5): 2037-2042.10.1073/pnas.0914433107

Le, A., Lane, A. N., Hamaker, M., Bose, S., Gouw, A., Barbi, J., Tsukamoto, T., Rojas, C. J., Slusher, B. S., Zhang, H., Zimmerman, L. J., Liebler, D. C., Slebos, R. J., Lorkiewicz, P. K., Higashi, R. M., Fan, T. W. and Dang, C. V. (2012) Glucose-independent glutamine metabolism via TCA cycling for proliferation and survival in B cells. *Cell Metab* **15**(1): 110-121.10.1016/j.cmet.2011.12.009

Li, L., Shao, M., Peng, P., Yang, C., Song, S., Duan, F., Jia, D., Zhang, M., Zhao, J., Zhao, R., Wu, W., Wang, L., Li, C., Wu, H., Zhang, J., Wu, X., Ruan, Y. and Gu, J. (2017) High expression of GFAT1 predicts unfavorable prognosis in patients with hepatocellular carcinoma. *Oncotarget* **8**(12): 19205-19217.10.18632/oncotarget.15164

Li, Y. M., Pan, Y., Wei, Y., Cheng, X., Zhou, B. P., Tan, M., Zhou, X., Xia, W., Hortobagyi, G. N., Yu, D. and Hung, M. C. (2004) Upregulation of CXCR4 is essential for HER2-mediated tumor metastasis. *Cancer Cell* **6**(5): 459-469.10.1016/j.ccr.2004.09.027

Liao, D. J. and Dickson, R. B. (2000) c-MYC in breast cancer. *Endocrine-Related Cancer* **7**: 143-164

Liberti, M. V. and Locasale, J. W. (2016) The Warburg Effect: How Does it Benefit Cancer Cells? *Trends Biochem Sci* **41**(3): 211-218.10.1016/j.tibs.2015.12.001

Liou, G. Y. and Storz, P. (2010) Reactive oxygen species in cancer. *Free Radic Res* **44**(5): 479-496.10.3109/10715761003667554

Liu, W., Le, A., Hancock, C., Lane, A. N., Dang, C. V., Fan, T. W. and Phang, J. M. (2012) Reprogramming of proline and glutamine metabolism contributes to the proliferative and metabolic responses regulated by oncogenic transcription factor c-MYC. *Proc Natl Acad Sci U S A* **109**(23): 8983-8988.10.1073/pnas.1203244109

Liu, Y., Yang, L., An, H., Chang, Y., Zhang, W., Zhu, Y., Xu, L. and Xu, J. (2015) High expression of Solute Carrier Family 1, member 5 (SLC1A5) is associated with poor prognosis in clear-cell renal cell carcinoma. *Sci Rep* **5**.10.1038/srep16954

Locasale, J. W., Grassian, A. R., Melman, T., Lyssiotis, C. A., Mattaini, K. R., Bass, A. J., Heffron, G., Metallo, C. M., Muranen, T., Sharfi, H., Sasaki, A. T., Anastasiou, D., Mullarky, E., Vokes, N. I., Sasaki, M., Beroukhim, R., Stephanopoulos, G., Ligon, A. H., Meyerson, M., Richardson, A. L., Chin, L., Wagner, G., Asara, J. M., Brugge, J. S., Cantley, L. C. and Vander Heiden, M. G. (2011) Phosphoglycerate dehydrogenase diverts glycolytic flux and contributes to oncogenesis. *Nat Genet* **43**(9): 869-874.10.1038/ng.890

Lu, H., Li, X., Lu, Y., Qiu, S. and Fan, Z. (2016) ASCT2 (SLC1A5) is an EGFR-associated protein that can be co-targeted by cetuximab to sensitize cancer cells to ROS-induced apoptosis. *Cancer Lett* **381**(1): 23-30.10.1016/j.canlet.2016.07.020

Lucena, M. C., Carvalho-Cruz, P., Donadio, J. L., Oliveira, I. A., De Queiroz, R. M., Marinho-Carvalho, M. M., Sola-Penna, M., De Paula, I. F., Gondim, K. C., Mccomb, M. E., Costello, C. E., Whelan, S. A., Todeschini, A. R. and Dias, W. B. (2016) Epithelial Mesenchymal Transition Induces Aberrant Glycosylation through Hexosamine Biosynthetic Pathway Activation. *J Biol Chem* **291**(25): 12917-12929.10.1074/jbc.M116.729236

Luque-Cabal, M., Garcia-Teijido, P., Fernandez-Perez, Y., Sanchez-Lorenzo, L. and Palacio-Vazquez, I. (2016) Mechanisms Behind the Resistance to Trastuzumab in HER2-Amplified Breast Cancer and Strategies to Overcome It. *Clin Med Insights Oncol* **10**(1): 21-30.10.4137/CMO.S34537

Maclennan, M. B., Anderson, B. M. and Ma, D. W. (2011) Differential mammary gland development in FVB and C57Bl/6 mice: implications for breast cancer research. *Nutrients* **3**(11): 929-936.10.3390/nu3110929

Maddocks, O. D. K., Athineos, D., Cheung, E. C., Lee, P., Zhang, T., Van Den Broek, N. J. F., Mackay, G. M., Labuschagne, C. F., Gay, D., Kruiswijk, F., Blagih, J., Vincent, D. F., Campbell, K. J., Ceteci, F., Sansom, O. J., Blyth, K. and Vousden, K. H. (2017) Modulating the therapeutic response of tumours to dietary serine and glycine starvation. *Nature* **544**(7650): 372-376.10.1038/nature22056

Makrides, V., Bauer, R., Weber, W., Wester, H. J., Fischer, S., Hinz, R., Huggel, K., Opfermann, T., Herzau, M., Ganapathy, V., Verrey, F. and Brust, P. (2007) Preferred transport of O-(2-[18F]fluoroethyl)-D-tyrosine (D-FET) into the porcine brain. *Brain Res* **1147**: 25-33.10.1016/j.brainres.2007.02.008

Marshall, A. D., Van Geldermalsen, M., Otte, N. J., Lum, T., Vellozzi, M., Thoeng, A., Pang, A., Nagarajah, R., Zhang, B., Wang, Q., Anderson, L., Rasko, J. E. J. and Holst, J. (2017) ASCT2 regulates glutamine uptake and cell growth in endometrial carcinoma. *Oncogenesis* **6**(7).10.1038/oncsis.2017.70

Martin-Rufian, M., Tosina, M., Campos-Sandoval, J. A., Manzanares, E., Lobo, C., Segura, J. A., Alonso, F. J., Mates, J. M. and Marquez, J. (2012) Mammalian glutaminase Gls2 gene encodes two functional alternative transcripts by a surrogate promoter usage mechanism. *PLoS One* **7**(6).10.1371/journal.pone.0038380

Mashimo, T., Pichumani, K., Vemireddy, V., Hatanpaa, K. J., Singh, D. K., Sirasanagandla, S., Nannepaga, S., Piccirillo, S. G., Kovacs, Z., Foong, C., Huang, Z., Barnett, S., Mickey, B. E., Deberardinis, R. J., Tu, B. P., Maher, E. A. and Bachoo, R. M. (2014) Acetate is a bioenergetic substrate for human glioblastoma and brain metastases. *Cell* **159**(7): 1603-1614.10.1016/j.cell.2014.11.025

Masle-Farquhar, E., Broer, A., Yabas, M., Enders, A. and Broer, S. (2017) ASCT2 (SLC1A5)-Deficient Mice Have Normal B-Cell Development, Proliferation, and Antibody Production. *Front Immunol* **8**.10.3389/fimmu.2017.00549

Masui, K., Tanaka, K., Akhavan, D., Babic, I., Gini, B., Matsutani, T., Iwanami, A., Liu, F., Villa, G. R., Gu, Y., Campos, C., Zhu, S., Yang, H., Yong, W. H., Cloughesy, T. F., Mellinghoff, I. K., Cavenee, W. K., Shaw, R. J. and Mischel, P. S. (2013) mTOR complex 2 controls glycolytic metabolism in glioblastoma through FoxO acetylation and upregulation of c-Myc. *Cell Metab* **18**(5): 726-739.10.1016/j.cmet.2013.09.013

Mayer, A., Wree, A., Hockel, M., Leo, C., Pilch, H. and Vaupel, P. (2004) Lack of correlation between expression of HIF-1alpha protein and oxygenation status in

identical tissue areas of squamous cell carcinomas of the uterine cervix. *Cancer Res* **64**(16): 5876-5881.10.1158/0008-5472.CAN-03-3566

Mcguirk, S., Gravel, S. P., Deblois, G., Papadopoli, D. J., Faubert, B., Wegner, A., Hiller, K., Avizonis, D., Akavia, U. D., Jones, R. G., Giguere, V. and St-Pierre, J. (2013) PGC-1alpha supports glutamine metabolism in breast cancer. *Cancer Metab* **1**(1).10.1186/2049-3002-1-22

Menezes, M. E., Das, S. K., Emdad, L., Windle, J. J., Wang, X. Y., Sarkar, D. and Fisher, P. B. (2014) Genetically engineered mice as experimental tools to dissect the critical events in breast cancer. *Adv Cancer Res* **121**: 331-382.10.1016/B978-0-12-800249-0.00008-1

Metallo, C. M., Gameiro, P. A., Bell, E. L., Mattaini, K. R., Yang, J., Hiller, K., Jewell, C. M., Johnson, Z. R., Irvine, D. J., Guarente, L., Kelleher, J. K., Vander Heiden, M. G., Iliopoulos, O. and Stephanopoulos, G. (2011) Reductive glutamine metabolism by IDH1 mediates lipogenesis under hypoxia. *Nature* **481**(7381): 380-384.10.1038/nature10602

Mezquita, P., Parghi, S. S., Brandvold, K. A. and Ruddell, A. (2005) Myc regulates VEGF production in B cells by stimulating initiation of VEGF mRNA translation. *Oncogene* **24**(5): 889-901.10.1038/sj.onc.1208251

Miccheli, A., Tomassini, A., Puccetti, C., Valerio, M., Peluso, G., Tuccillo, F., Calvani, M., Manetti, C. and Conti, F. (2006) Metabolic profiling by 13C-NMR spectroscopy: [1,2-13C2]glucose reveals a heterogeneous metabolism in human leukemia T cells. *Biochimie* **88**(5): 437-448.10.1016/j.biochi.2005.10.004

Miller, T. W., Balko, J. M., Ghazoui, Z., Dunbier, A., Anderson, H., Dowsett, M., Gonzalez-Angulo, A. M., Mills, G. B., Miller, W. R., Wu, H., Shyr, Y. and Arteaga, C. L. (2011) A gene expression signature from human breast cancer cells with acquired hormone independence identifies MYC as a mediator of antiestrogen resistance. *Clin Cancer Res* **17**(7): 2024-2034.10.1158/1078-0432.CCR-10-2567

Milman, L. S. and Yurowitzki, Y. G. (1967) The control of glycolysis in early embryogenesis. *Biochimica et Biophysica Acta (BBA) - General Subjects* **148**(2): 362-371.10.1016/0304-4165(67)90132-8

Minchenko, O., Opentanova, I., Minchenko, D., Ogura, T. and Esumi, H. (2004) Hypoxia induces transcription of 6-phosphofructo-2-kinase/fructose-2,6-biphosphatase-4 gene via hypoxia-inducible factor-1alpha activation. *FEBS Lett* **576**(2): 14-20.10.1016/j.febslet.2004.08.053

Miyamoto, S., Murphy, A. N. and Brown, J. H. (2008) Akt mediates mitochondrial protection in cardiomyocytes through phosphorylation of mitochondrial hexokinase-II. *Cell Death Differ* **15**(3): 521-529.10.1038/sj.cdd.4402285

Moja, L., Tagliabue, L., Balduzzi, S., Parmelli, E., Pistotti, V., Guarneri, V. and D'amico, R. (2012) Trastuzumab containing regimens for early breast cancer. *Cochrane Database Syst Rev* (4).10.1002/14651858.CD006243.pub2

Moloughney, J. G., Kim, P. K., Vega-Cotto, N. M., Wu, C. C., Zhang, S., Adlam, M., Lynch, T., Chou, P. C., Rabinowitz, J. D., Werlen, G. and Jacinto, E. (2016) mTORC2 Responds to Glutamine Catabolite Levels to Modulate the Hexosamine Biosynthesis Enzyme GFAT1. *Mol Cell* **63**(5): 811-826.10.1016/j.molcel.2016.07.015

Moreadith, R. W. and Lehninger, A. L. (1984) The Pathways of Glutamate and Glutamine Oxidation by Tumor Cell Mitochondria. *Journal of Biological Chemistry* **259**(10): 6216-6221

Morelle, W. and Michalski, J. C. (2007) Analysis of protein glycosylation by mass spectrometry. *Nat Protoc* **2**(7): 1585-1602.10.1038/nprot.2007.227

Morrish, F., Isern, N., Sadilek, M., Jeffrey, M. and Hockenbery, D. M. (2009) c-Myc activates multiple metabolic networks to generate substrates for cell-cycle entry. *Oncogene* **28**(27): 2485-2491.10.1038/onc.2009.112

Mortazavi, A., Williams, B. A., Mccue, K., Schaeffer, L. and Wold, B. (2008) Mapping and quantifying mammalian transcriptomes by RNA-Seq. *Nat Methods* **5**(7): 621-628.10.1038/nmeth.1226

Motulsky, H. J. and Brown, R. E. (2006) Detecting outliers when fitting data with nonlinear regression - a new method based on robust nonlinear regression and the false discovery rate. *BMC Bioinformatics* **7**: 123.10.1186/1471-2105-7-123

Muir, A., Danai, L. V., Gui, D. Y., Waingarten, C. Y., Lewis, C. A. and Vander Heiden, M. G. (2017) Environmental cystine drives glutamine anaplerosis and sensitizes cancer cells to glutaminase inhibition. *Elife* **6**.10.7554/eLife.27713

Mullen, A. R., Wheaton, W. W., Jin, E. S., Chen, P. H., Sullivan, L. B., Cheng, T., Yang, Y., Linehan, W. M., Chandel, N. S. and Deberardinis, R. J. (2011) Reductive carboxylation supports growth in tumour cells with defective mitochondria. *Nature* **481**(7381): 385-388.10.1038/nature10642

Myers, M. B., Banda, M., Mckim, K. L., Wang, Y., Powell, M. J. and Parsons, B. L. (2016) Breast Cancer Heterogeneity Examined by High-Sensitivity Quantification of PIK3CA, KRAS, HRAS, and BRAF Mutations in Normal Breast and Ductal Carcinomas. *Neoplasia* **18**(4): 253-263.10.1016/j.neo.2016.03.002

Nair, R., Roden, D. L., Teo, W. S., Mcfarland, A., Junankar, S., Ye, S., Nguyen, A., Yang, J., Nikolic, I., Hui, M., Morey, A., Shah, J., Pfefferle, A. D., Usary, J., Selinger, C., Baker, L. A., Armstrong, N., Cowley, M. J., Naylor, M. J., Ormandy, C. J., Lakhani, S. R., Herschkowitz, J. I., Perou, C. M., Kaplan, W., O'toole, S. A. and Swarbrick, A. (2014) c-Myc and Her2 cooperate to drive a stem-like phenotype with poor prognosis in breast cancer. *Oncogene* **33**(30): 3992-4002.10.1038/onc.2013.368

Nair, R. N., Mishra, J. K., Li, F., Tortosa, M., Yang, C., Doherty, J. R., Cameron, M., Cleveland, J. L., Roush, W. R. and Bannister, T. D. (2016) Exploiting the co-reliance of tumours upon transport of amino acids and lactate: Gln and Tyr conjugates of MCT1 inhibitors. *Medchemcomm* **7**(5): 900-905.10.1039/C5MD00579E

Namikawa, M., Kakizaki, S., Kaira, K., Tojima, H., Yamazaki, Y., Horiguchi, N., Sato, K., Oriuchi, N., Tominaga, H., Sunose, Y., Nagamori, S., Kanai, Y., Oyama, T., Takeyoshi, I. and Yamada, M. (2014) Expression of amino acid transporters (LAT1, ASCT2 and xCT) as clinical significance in hepatocellular carcinoma. *Hepatol Res* **45**(9): 1014-1022.10.1111/hepr.12431

Naviaux, R., Costanzi, E., Haas, M. and Verma, I. (1996) The pCL vector system: rapid production of helper-free, high-titer, recombinant retroviruses. *Journal of Virology* **70**(8): 5701-5705

Nicklin, P., Bergman, P., Zhang, B., Triantafellow, E., Wang, H., Nyfeler, B., Yang, H., Hild, M., Kung, C., Wilson, C., Myer, V. E., Mackeigan, J. P., Porter, J. A., Wang, Y. K., Cantley, L. C., Finan, P. M. and Murphy, L. O. (2009) Bidirectional transport of amino acids regulates mTOR and autophagy. *Cell* **136**(3): 521-534.10.1016/j.cell.2008.11.044

Nikkuni, O., Kaira, K., Toyoda, M., Shino, M., Sakakura, K., Takahashi, K., Tominaga, H., Oriuchi, N., Suzuki, M., Iijima, M., Asao, T., Nishiyama, M., Nagamori, S., Kanai, Y., Oyama, T. and Chikamatsu, K. (2015) Expression of Amino Acid Transporters (LAT1 and ASCT2) in Patients with Stage III/IV Laryngeal Squamous Cell Carcinoma. *Pathol Oncol Res* **21**(4): 1175-1181.10.1007/s12253-015-9954-3

Noguchi, Y., James, J. H., Fischer, J. E. and Hasselgren, P.-O. (1996) Increased Glutamine Consumption in Small Intestine Epithelial Cells during Sepsis in Rats. *The American Journal of Surgery* **173**: 199-205

Ogrodzinski, M. P., Bernard, J. J. and Lunt, S. Y. (2017) Deciphering metabolic rewiring in breast cancer subtypes. *Translational Research* **189**: 106-122.10.1016/j.trsl.2017.07.004

Olalla, L., Gutierrez, A., Campos, J. A., Khan, Z. U., Alonso, F. J., Segura, J. A., Marquez, J. and Aledo, J. C. (2002) Nuclear localization of L-type glutaminase in mammalian brain. *J Biol Chem* **277**(41): 38939-38944.10.1074/jbc.C200373200

Ono, M., Oka, S., Okudaira, H., Nakanishi, T., Mizokami, A., Kobayashi, M., Schuster, D. M., Goodman, M. M., Shirakami, Y. and Kawai, K. (2015) [(14)C]Fluciclovine (alias anti-[(14)C]FACBC) uptake and ASCT2 expression in castration-resistant prostate cancer cells. *Nucl Med Biol* **42**(11): 887-892.10.1016/j.nucmedbio.2015.07.005

Otten, A. D., Sanders, M. M. and Mcknight, G. S. (1988) The MMTV LTR promoter is induced by progesterone and dihydrotestosterone but not by estrogen. *Mol Endocrinol* **2**(2): 143-147.10.1210/mend-2-2-143

Palmada, M., Speil, A., Jeyaraj, S., Bohmer, C. and Lang, F. (2005) The serine/threonine kinases SGK1, 3 and PKB stimulate the amino acid transporter ASCT2. *Biochem Biophys Res Commun* **331**(1): 272-277.10.1016/j.bbrc.2005.03.159

Park, K., Kwak, K., Kim, J., Lim, S. and Han, S. (2005) c-myc amplification is associated with HER2 amplification and closely linked with cell proliferation in tissue microarray of nonselected breast cancers. *Hum Pathol* **36**(6): 634-639.10.1016/j.humpath.2005.04.016

Parker, J. S., Mullins, M., Cheang, M. C., Leung, S., Voduc, D., Vickery, T., Davies, S., Fauron, C., He, X., Hu, Z., Quackenbush, J. F., Stijleman, I. J., Palazzo, J., Marron, J. S., Nobel, A. B., Mardis, E., Nielsen, T. O., Ellis, M. J., Perou, C. M. and Bernard, P. S. (2009) Supervised risk predictor of breast cancer based on intrinsic subtypes. *J Clin Oncol* **27**(8): 1160-1167.10.1200/JCO.2008.18.1370

Patra, K. C., Wang, Q., Bhaskar, P. T., Miller, L., Wang, Z., Wheaton, W., Chandel, N., Laakso, M., Muller, W. J., Allen, E. L., Jha, A. K., Smolen, G. A., Clasquin, M. F., Robey, R. B. and Hay, N. (2013) Hexokinase 2 is required for tumor initiation and maintenance and its systemic deletion is therapeutic in mouse models of cancer. *Cancer Cell* **24**(2): 213-228.10.1016/j.ccr.2013.06.014

Pavlides, S., Whitaker-Menezes, D., Castello-Cros, R., Flomenberg, N., Witkiewicz, A. K., Frank, P. G., Casimiro, M. C., Wang, C., Fortina, P., Addya, S., Pestell, R. G., Martinez-Outschoorn, U. E., Sotgia, F. and Lisanti, M. P. (2009) The reverse Warburg effect: aerobic glycolysis in cancer associated fibroblasts and the tumor stroma. *Cell Cycle* **8**(23): 3984-4001.10.4161/cc.8.23.10238

Peng, T., Golub, T. R. and Sabatini, D. M. (2002) The Immunosuppressant Rapamycin Mimics a Starvation-Like Signal Distinct from Amino Acid and Glucose Deprivation. *Molecular and Cellular Biology* **22**(15): 5575-5584.10.1128/mcb.22.15.5575-5584.2002

Penheiter, A. R., Erdogan, S., Murphy, S. J., Hart, S. N., Felipe Lima, J., Rakhshan Rohakhtar, F., O'brien, D. R., Bamlet, W. R., Wuertz, R. E., Smyrk, T. C., Couch, F. J., Vasmatzis, G., Bender, C. E. and Carlson, S. K. (2015) Transcriptomic and Immunohistochemical Profiling of SLC6A14 in Pancreatic Ductal Adenocarcinoma. *Biomed Res Int*.10.1155/2015/593572

Perez-Escuredo, J., Dadhich, R. K., Dhup, S., Cacace, A., Van Hee, V. F., De Saedeleer, C. J., Sboarina, M., Rodriguez, F., Fontenille, M. J., Brisson, L., Porporato, P. E. and Sonveaux, P. (2016) Lactate promotes glutamine uptake and metabolism in oxidative cancer cells. *Cell Cycle* **15**(1): 72-83.10.1080/15384101.2015.1120930

Perez-Gomez, C., Campos-Sandoval, J. A., Alonso, F. J., Segura, J. A., Manzanares, E., Ruiz-Sanchez, P., Gonzalez, M. E., Marquez, J. and Mates, J. M. (2005) Co-expression of glutaminase K and L isoenzymes in human tumour cells. *Biochem J* **386**(Pt 3): 535-542.10.1042/BJ20040996

Perez-Gomez, C., Campos-Sandoval, J. A., Alonso, F. J., Segura, J. A., Manzanares, E., Ruiz-Sanchez, P., Gonzalez, M. E., Marquez, J. and Mates, J. M. (2005) Co-expression of glutaminase K and L isoenzymes in human tumour cells. *Biochem J* **386**: 535-542

Petronini, P. C., Urbani, S., Alfieri, R., Borchetti, A. F. and Cuidotti, C. C. (1996) Cell Susceptibility to Apoptosis by Glutamine Deprivation and Rescue: Survival and Apoptotic Death in Cultured Lymphoma-Leukemia Cell Lines. *journal of cellular physiology* **169**: 175-185

Pinho, S. S. and Reis, C. A. (2015) Glycosylation in cancer: mechanisms and clinical implications. *Nat Rev Cancer* **15**(9): 540-555.10.1038/nrc3982

Pohlmann, P. R., Mayer, I. A. and Mernaugh, R. (2009) Resistance to Trastuzumab in Breast Cancer. *Clin Cancer Res* **15**(24): 7479-7491.10.1158/1078-0432.CCR-09-0636

Polet, F., Martherus, R., Corbet, C., Pinto, A. and Feron, O. (2016) Inhibition of glucose metabolism prevents glycosylation of the glutamine transporter ASCT2 and promotes compensatory LAT1 upregulation in leukemia cells. *Oncotarget* **7**(29): 46371-46383.10.18632/oncotarget.10131

Poncet, N., Mitchell, F. E., Ibrahim, A. F., Mcguire, V. A., English, G., Arthur, J. S., Shi, Y. B. and Taylor, P. M. (2014) The catalytic subunit of the system L1 amino acid transporter (slc7a5) facilitates nutrient signalling in mouse skeletal muscle. *PLoS One* **9**(2).10.1371/journal.pone.0089547

Possemato, R., Marks, K. M., Shaul, Y. D., Pacold, M. E., Kim, D., Birsoy, K., Sethumadhavan, S., Woo, H. K., Jang, H. G., Jha, A. K., Chen, W. W., Barrett, F. G., Stransky, N., Tsun, Z. Y., Cowley, G. S., Barretina, J., Kalaany, N. Y., Hsu, P. P., Ottina, K., Chan, A. M., Yuan, B., Garraway, L. A., Root, D. E., Mino-Kenudson, M., Brachtel, E. F., Driggers, E. M. and Sabatini, D. M. (2011) Functional genomics reveal that the serine synthesis pathway is essential in breast cancer. *Nature* **476**(7360): 346-350.10.1038/nature10350

Powers, T. W., Neely, B. A., Shao, Y., Tang, H., Troyer, D. A., Mehta, A. S., Haab, B. B. and Drake, R. R. (2014) MALDI imaging mass spectrometry profiling of N-glycans in formalin-fixed paraffin embedded clinical tissue blocks and tissue microarrays. *PLoS One* **9**(9).10.1371/journal.pone.0106255

Purwaha, P., Silva, L. P., Hawke, D. H., Weinstein, J. N. and Lorenzi, P. L. (2014) An artifact in LC-MS/MS measurement of glutamine and glutamic acid: in-source cyclization to pyroglutamic acid. *Anal Chem* **86**(12): 5633-5637.10.1021/ac501451v

Qie, S., Chu, C., Li, W., Wang, C. and Sang, N. (2014) ErbB2 activation upregulates glutaminase 1 expression which promotes breast cancer cell proliferation. *J Cell Biochem* **115**(3): 498-509.10.1002/jcb.24684

Qing, G., Li, B., Vu, A., Skuli, N., Walton, Z. E., Liu, X., Mayes, P. A., Wise, D. R., Thompson, C. B., Maris, J. M., Hogarty, M. D. and Simon, M. C. (2012) ATF4 regulates MYC-mediated neuroblastoma cell death upon glutamine deprivation. *Cancer Cell* **22**(5): 631-644.10.1016/j.ccr.2012.09.021

Randall, E. C., Race, A. M., Cooper, H. J. and Bunch, J. (2016) MALDI Imaging of Liquid Extraction Surface Analysis Sampled Tissue. *Anal Chem* **88**(17): 8433-8440.10.1021/acs.analchem.5b04281

Reitzer, L. J., Wice, B. M. and Kennell, D. (1978) Evidence That Glutamine, Not Sugar, Is the Major Energy Source for Cultured HeLa Cells. *Journal of Biological Chemistry* **254**(8): 2669-2676

Ren, P., Yue, M., Xiao, D., Xiu, R., Gan, L., Liu, H. and Qing, G. (2015) ATF4 and N-Myc coordinate glutamine metabolism in MYCN-amplified neuroblastoma cells through ASCT2 activation. *J Pathol* **235**(1): 90-100.10.1002/path.4429

Reynolds, M. R., Lane, A. N., Robertson, B., Kemp, S., Liu, Y., Hill, B. G., Dean, D. C. and Clem, B. F. (2014) Control of glutamine metabolism by the tumor suppressor Rb. *Oncogene* **33**(5): 556-566.10.1038/onc.2012.635

Rosario, F. J., Kanai, Y., Powell, T. L. and Jansson, T. (2013) Mammalian target of rapamycin signalling modulates amino acid uptake by regulating transporter cell surface abundance in primary human trophoblast cells. *J Physiol* **591**(3): 609-625.10.1113/jphysiol.2012.238014

Samuelson, A. V. and Lowe, S. W. (1997) Selective induction of p53 and chemosensitivity in RB-deficient cells by E1A mutants unable to bind the RB-related proteins. *PNAS* **94**: 12094-12099

Sangaletti, S., Chiodoni, C., Tripodo, C. and Colombo, M. P. (2017) The good and bad of targeting cancer-associated extracellular matrix. *Curr Opin Pharmacol* **35**: 75-82.10.1016/j.coph.2017.06.003

Sato, M., Kawana, K., Adachi, K., Fujimoto, A., Taguchi, A., Fujikawa, T., Yoshida, M., Nakamura, H., Nishida, H., Inoue, T., Ogishima, J., Eguchi, S., Yamashita, A., Tomio, K., Arimoto, T., Wada-Hiraike, O., Oda, K., Nagamatsu, T., Osuga, Y. and Fujii, T. (2017) Low uptake of fluorodeoxyglucose in positron emission tomography/computed tomography in ovarian clear cell carcinoma may reflect glutaminolysis of its cancer stem cell-like properties. *Oncol Rep* **37**(3): 1883-1888.10.3892/or.2017.5398

Schulte, M. L., Dawson, E. S., Saleh, S. A., Cuthbertson, M. L. and Manning, H. C. (2015) 2-Substituted Ngamma-glutamylanilides as novel probes of ASCT2 with improved potency. *Bioorg Med Chem Lett* **25**(1): 113-116.10.1016/j.bmcl.2014.10.098

Schulte, M. L., Hight, M. R., Ayers, G. D., Liu, Q., Shyr, Y., Washington, M. K. and Manning, H. C. (2017) Non-Invasive Glutamine PET Reflects Pharmacological Inhibition of BRAFV600E In Vivo. *Mol Imaging Biol* **19**(3): 421-428.10.1007/s11307-016-1008-z

Schulte, M. L., Khodadadi, A. B., Cuthbertson, M. L., Smith, J. A. and Manning, H. C. (2016) 2-Amino-4-bis(aryloxybenzyl)aminobutanoic acids: A novel scaffold for inhibition of ASCT2-mediated glutamine transport. *Bioorg Med Chem Lett* **26**(3): 1044-1047.10.1016/j.bmcl.2015.12.031

Seberger, P. J. and Chaney, W. G. (1999) Control of metastasis by Asn-linked, β1–6 branched oligosaccharides in mouse mammary cancer cells. *Glycobiology* **9**(3): 235-241

Shain, A. H., Yeh, I., Kovalyshyn, I., Sriharan, A., Talevich, E., Gagnon, A., Dummer, R., North, J., Pincus, L., Ruben, B., Rickaby, W., D'arrigo, C., Robson, A. and Bastian, B. C. (2015) The Genetic Evolution of Melanoma from Precursor Lesions. *N Engl J Med* **373**(20): 1926-1936.10.1056/NEJMoa1502583

Shajahan-Haq, A. N., Cook, K. L., Schwartz-Roberts, J. L., Eltayeb, A. E., Demas, D. M., Warri, A. M., Facey, C. O., Hilakivi-Clarke, L. A. and Clarke, R. (2014) MYC regulates the unfolded protein response and glucose and glutamine uptake in endocrine resistant breast cancer. *Mol Cancer* **13**(239).10.1186/1476-4598-13-239

Sharma, P. (2016) Biology and Management of Patients With Triple-Negative Breast Cancer. *Oncologist* **21**(9): 1050-1062.10.1634/theoncologist.2016-0067

Shestov, A. A., Liu, X., Ser, Z., Cluntun, A. A., Hung, Y. P., Huang, L., Kim, D., Le, A., Yellen, G., Albeck, J. G. and Locasale, J. W. (2014) Quantitative determinants of aerobic glycolysis identify flux through the enzyme GAPDH as a limiting step. *Elife* **3**.10.7554/eLife.03342

Shim, H., Dolde, C., Lewis, B. C., Wu, C.-S., Dang, G., Jungmann, R. A., Dalla-Favera, R. and Dang, C. V. (1997) c-Myc transactivation of LDH-A: Implications for tumor metabolism and growth. *Proc Natl Acad Sci U S A* **94**: 6658-6663

Shimizu, A., Kaira, K., Kato, M., Yasuda, M., Takahashi, A., Tominaga, H., Oriuchi, N., Nagamori, S., Kanai, Y., Oyama, T., Asao, T. and Ishikawa, O. (2015) Prognostic significance of L-type amino acid transporter 1 (LAT1) expression in cutaneous melanoma. *Melanoma Res* **25**(5): 399-405.10.1097/CMR.0000000000000181

Shimizu, K., Kaira, K., Tomizawa, Y., Sunaga, N., Kawashima, O., Oriuchi, N., Tominaga, H., Nagamori, S., Kanai, Y., Yamada, M., Oyama, T. and Takeyoshi, I.

(2014) ASC amino-acid transporter 2 (ASCT2) as a novel prognostic marker in non-small cell lung cancer. *Br J Cancer* **110**(8): 2030-2039.10.1038/bjc.2014.88

Shweiki, D., Itin, A., Neufeld, G., Gitay-Goren, H. and Keshet, E. (1993) Patterns of expression of vascular endothelial growth factor (VEGF) and VEGF receptors in mice suggest a role in hormonally regulated angiogenesis. *J Clin Invest* **91**(5): 2235-2243.10.1172/JCI116450

Singh, K., Tanui, R., Gameiro, A., Eisenberg, G., Colas, C., Schlessinger, A. and Grewer, C. (2017) Structure activity relationships of benzylproline-derived inhibitors of the glutamine transporter ASCT2. *Bioorg Med Chem Lett* **27**(3): 398-402.10.1016/j.bmcl.2016.12.063

Slamon, D., Godolphin, W., Jones, L., Holt, J., Wong, S., Keith, D., Levin, W., Stuart, S., Udove, J., Ullrich, A. and Et, A. (1989) Studies of the HER-2/neu proto-oncogene in human breast and ovarian cancer. *Science* **244**(4905): 707-712.10.1126/science.2470152

Smith, B., Schafer, X. L., Ambeskovic, A., Spencer, C. M., Land, H. and Munger, J. (2016) Addiction to Coupling of the Warburg Effect with Glutamine Catabolism in Cancer Cells. *Cell Rep* **17**(3): 821-836.10.1016/j.celrep.2016.09.045

Son, J., Lyssiotis, C. A., Ying, H., Wang, X., Hua, S., Ligorio, M., Perera, R. M., Ferrone, C. R., Mullarky, E., Shyh-Chang, N., Kang, Y., Fleming, J. B., Bardeesy, N., Asara, J. M., Haigis, M. C., Depinho, R. A., Cantley, L. C. and Kimmelman, A. C. (2013) Glutamine supports pancreatic cancer growth through a KRAS-regulated metabolic pathway. *Nature* **496**(7443): 101-105.10.1038/nature12040

Sonveaux, P., Vegran, F., Schroeder, T., Wergin, M. C., Verrax, J., Rabbani, Z. N., De Saedeleer, C. J., Kennedy, K. M., Diepart, C., Jordan, B. F., Kelley, M. J., Gallez, B., Wahl, M. L., Feron, O. and Dewhirst, M. W. (2008) Targeting lactate-fueled respiration selectively kills hypoxic tumor cells in mice. *J Clin Invest* **118**(12): 3930-3942.10.1172/JCI36843

Sorlie, T., Tibshirani, R., Parker, J., Hastie, T., Marron, J. S., Nobel, A., Deng, S., Johnsen, H., Pesich, R., Geisler, S., Demeter, J., Perou, C. M., Lonning, P. E., Brown, P. O., Borresen-Dale, A. L. and Botstein, D. (2003) Repeated observation of breast tumor subtypes in independent gene expression data sets. *Proc Natl Acad Sci U S A* **100**(14): 8418-8423.10.1073/pnas.0932692100

Squires, H., Pandor, A., Thokala, P., Stevens, J. W., Kaltenthaler, E., Clowes, M., Coleman, R. and Wyld, L. (2017) Pertuzumab for the Neoadjuvant Treatment of Early-Stage HER2-Positive Breast Cancer: An Evidence Review Group Perspective of a NICE Single Technology Appraisal. *Pharmacoeconomics*.10.1007/s40273-017-0556-7

Stefania, R., Tei, L., Barge, A., Geninatti Crich, S., Szabo, I., Cabella, C., Cravotto, G. and Aime, S. (2009) Tuning glutamine binding modes in Gd-DOTA-based probes for

an improved MRI visualization of tumor cells. *Chemistry* **15**(1): 76-85.10.1002/chem.200801567

Still, E. R. and Yuneva, M. O. (2017) Hopefully devoted to Q: targeting glutamine addiction in cancer. *Br J Cancer* **116**(11): 1375-1381.10.1038/bjc.2017.113

Stowell, S. R., Ju, T. and Cummings, R. D. (2015) Protein glycosylation in cancer. *Annu Rev Pathol* **10**: 473-510.10.1146/annurev-pathol-012414-040438

Sun, H. W., Yu, X. J., Wu, W. C., Chen, J., Shi, M., Zheng, L. and Xu, J. (2016) GLUT1 and ASCT2 as Predictors for Prognosis of Hepatocellular Carcinoma. *PLoS One* **11**(12): e0168907.10.1371/journal.pone.0168907

Sun, R. C. and Denko, N. C. (2014) Hypoxic regulation of glutamine metabolism through HIF1 and SIAH2 supports lipid synthesis that is necessary for tumor growth. *Cell Metab* **19**(2): 285-292.10.1016/j.cmet.2013.11.022

Sun, W. Y., Kim, H. M., Jung, W. H. and Koo, J. S. (2016) Expression of serine/glycine metabolism-related proteins is different according to the thyroid cancer subtype. *J Transl Med* **14**(1).10.1186/s12967-016-0915-8

Suzuki, M., Toki, H., Furuya, A. and Ando, H. (2017) Establishment of monoclonal antibodies against cell surface domains of ASCT2/SLC1A5 and their inhibition of glutamine-dependent tumor cell growth. *Biochem Biophys Res Commun* **482**(4): 651-657.10.1016/j.bbrc.2016.11.089

Svenneby, G. and Torgner, I. A. (1987) Localization and function of glutamine synthetase and glutaminase. *Biochem Soc Trans* **15**(2): 213-215.10.1042/bst0150213

Taneja, P., Frazier, D. P., Kendig, R. D., Maglic, D., Sugiyama, T., Kai, F., Taneja, N. K. and Inoue, K. (2009) MMTV mouse models and the diagnostic values of MMTV-like sequences in human breast cancer. *Expert Rev Mol Diagn* **9**(5): 423-440.10.1586/erm.09.31

Tao, X., Lu, Y., Qiu, S., Wang, Y., Qin, J. and Fan, Z. (2017) AP1G1 is involved in cetuximab-mediated downregulation of ASCT2-EGFR complex and sensitization of human head and neck squamous cell carcinoma cells to ROS-induced apoptosis. *Cancer Lett* **408**(33-42).10.1016/j.canlet.2017.08.012

Tardito, S., Oudin, A., Ahmed, S. U., Fack, F., Keunen, O., Zheng, L., Miletic, H., Sakariassen, P. O., Weinstock, A., Wagner, A., Lindsay, S. L., Hock, A. K., Barnett, S. C., Ruppin, E., Morkve, S. H., Lund-Johansen, M., Chalmers, A. J., Bjerkvig, R., Niclou, S. P. and Gottlieb, E. (2015) Glutamine synthetase activity fuels nucleotide biosynthesis and supports growth of glutamine-restricted glioblastoma. *Nat Cell Biol* **17**(12): 1556-1568.10.1038/ncb3272

Thornburg, J. M., Nelson, K. K., Clem, B. F., Lane, A. N., Arumugam, S., Simmons, A., Eaton, J. W., Telang, S. and Chesney, J. (2008) Targeting aspartate aminotransferase in breast cancer. *Breast Cancer Res* **10**(5).10.1186/bcr2154

Tillner, J., Wu, V., Jones, E. A., Pringle, S. D., Karancsi, T., Dannhorn, A., Veselkov, K., Mckenzie, J. S. and Takats, Z. (2017) Faster, More Reproducible DESI-MS for Biological Tissue Imaging. *J Am Soc Mass Spectrom*.10.1007/s13361-017-1714-z

Timmerman, L. A., Holton, T., Yuneva, M., Louie, R. J., Padro, M., Daemen, A., Hu, M., Chan, D. A., Ethier, S. P., Van 'T Veer, L. J., Polyak, K., Mccormick, F. and Gray, J. W. (2013) Glutamine sensitivity analysis identifies the xCT antiporter as a common triple-negative breast tumor therapeutic target. *Cancer Cell* **24**(4): 450-465.10.1016/j.ccr.2013.08.020

Toda, K., Nishikawa, G., Iwamoto, M., Itatani, Y., Takahashi, R., Sakai, Y. and Kawada, K. (2017) Clinical Role of ASCT2 (SLC1A5) in KRAS-Mutated Colorectal Cancer. *Int J Mol Sci* **18**(8).10.3390/ijms18081632

Todorova, V. K., Kaufmann, Y., Luo, S. and Klimberg, V. S. (2011) Tamoxifen and raloxifene suppress the proliferation of estrogen receptor-negative cells through inhibition of glutamine uptake. *Cancer Chemother Pharmacol* **67**(2): 285-291.10.1007/s00280-010-1316-y

Tsai, W. B., Aiba, I., Long, Y., Lin, H. K., Feun, L., Savaraj, N. and Kuo, M. T. (2012) Activation of Ras/PI3K/ERK pathway induces c-Myc stabilization to upregulate argininosuccinate synthetase, leading to arginine deiminase resistance in melanoma cells. *Cancer Res* **72**(10): 2622-2633.10.1158/0008-5472.CAN-11-3605

Ursini-Siegel, J., Schade, B., Cardiff, R. D. and Muller, W. J. (2007) Insights from transgenic mouse models of ERBB2-induced breast cancer. *Nat Rev Cancer* **7**(5): 389-397.10.1038/nrc2127

Van Den Heuvel, A. P., Jing, J., Wooster, R. F. and Bachman, K. E. (2012) Analysis of glutamine dependency in non-small cell lung cancer: GLS1 splice variant GAC is essential for cancer cell growth. *Cancer Biol Ther* **13**(12): 1185-1194.10.4161/cbt.21348

Van Geldermalsen, M., Wang, Q., Nagarajah, R., Marshall, A. D., Thoeng, A., Gao, D., Ritchie, W., Feng, Y., Bailey, C. G., Deng, N., Harvey, K., Beith, J. M., Selinger, C. I., O'toole, S. A., Rasko, J. E. and Holst, J. (2016) ASCT2/SLC1A5 controls glutamine uptake and tumour growth in triple-negative basal-like breast cancer. *Oncogene* **35**(24): 3201-3208.10.1038/onc.2015.381

Varia, M. A., Calkins-Adams, D., Rinker, L. H., Kennedy, A. S., Novotny, D. B., Fowlerjr., W. C. and Raleigh, J. A. (1998) Pimonidazole: A Novel Hypoxia Marker for Complementary Study of Tumor Hypoxia and Cell Proliferation in Cervical Carcinoma. *Gynecologic Oncology* **71**(2): 270-277.10.1006/gyno.1998.5163

Venkitachalam, S., Revoredo, L., Varadan, V., Fecteau, R. E., Ravi, L., Lutterbaugh, J., Markowitz, S. D., Willis, J. E., Gerken, T. A. and Guda, K. (2016) Biochemical and functional characterization of glycosylation-associated mutational landscapes in colon cancer. *Sci Rep* **6**: 23642.10.1038/srep23642

Vogel, C. L., Cobleigh, M. A., Tripathy, D., Gutheil, J. C., Harris, L. N., Fehrenbacher, L., Slamon, D. J., Murphy, M., Novotny, W. F., Burchmore, M., Shak, S., Stewart, S. J. and Press, M. (2002) Efficacy and safety of trastuzumab as a single agent in first-line treatment of HER2-overexpressing metastatic breast cancer. *J Clin Oncol* **20**(3): 719-726.10.1200/JCO.2002.20.3.719

Vu, T. and Claret, F. X. (2012) Trastuzumab: updated mechanisms of action and resistance in breast cancer. *Front Oncol* **2**.10.3389/fonc.2012.00062

Wagner, K.-U., Ward, T., Ward, T., Davis, B., Wiseman, R. and Hennighausen, L. (2001) Spatial and temporal expression of the Cre gene under the control of the MMTV-LTR in different lines of transgenic mice. *Transgenic Research* **10**(6): 545-553.10.1023/a:1013063514007

Wang, C., Mayer, J. A., Mazumdar, A., Fertuck, K., Kim, H., Brown, M. and Brown, P. H. (2011) Estrogen induces c-myc gene expression via an upstream enhancer activated by the estrogen receptor and the AP-1 transcription factor. *Mol Endocrinol* **25**(9): 1527-1538.10.1210/me.2011-1037

Wang, J. B., Erickson, J. W., Fuji, R., Ramachandran, S., Gao, P., Dinavahi, R., Wilson, K. F., Ambrosio, A. L., Dias, S. M., Dang, C. V. and Cerione, R. A. (2010) Targeting mitochondrial glutaminase activity inhibits oncogenic transformation. *Cancer Cell* **18**(3): 207-219.10.1016/j.ccr.2010.08.009

Wang, K., Cao, F., Fang, W., Hu, Y., Chen, Y., Ding, H. and Yu, G. (2013) Activation of SNAT1/SLC38A1 in human breast cancer: correlation with p-Akt overexpression. *BMC Cancer* **13**(343).10.1186/1471-2407-13-343

Wang, Q., Beaumont, K. A., Otte, N. J., Font, J., Bailey, C. G., Van Geldermalsen, M., Sharp, D. M., Tiffen, J. C., Ryan, R. M., Jormakka, M., Haass, N. K., Rasko, J. E. and Holst, J. (2014) Targeting glutamine transport to suppress melanoma cell growth. *Int J Cancer* **135**(5): 1060-1071.10.1002/ijc.28749

Wang, Q., Hardie, R. A., Hoy, A. J., Van Geldermalsen, M., Gao, D., Fazli, L., Sadowski, M. C., Balaban, S., Schreuder, M., Nagarajah, R., Wong, J. J., Metierre, C., Pinello, N., Otte, N. J., Lehman, M. L., Gleave, M., Nelson, C. C., Bailey, C. G., Ritchie, W., Rasko, J. E. and Holst, J. (2015) Targeting ASCT2-mediated glutamine uptake blocks prostate cancer growth and tumour development. *J Pathol* **236**(3): 278-289.10.1002/path.4518

Wang, R., Dillon, C. P., Shi, L. Z., Milasta, S., Carter, R., Finkelstein, D., Mccormick, L. L., Fitzgerald, P., Chi, H., Munger, J. and Green, D. R. (2011) The transcription

factor Myc controls metabolic reprogramming upon T lymphocyte activation. *Immunity* **35**(6): 871-882.10.1016/j.immuni.2011.09.021

Wang, T., Marquardt, C. and Foker, J. (1976) Aerobic glycolysis during lymphocyte proliferation. *Nature* **261**(5562): 702-705.10.1038/261702a0

Warburg, O. (1925) The metabolism of carcinoma cells. *The Journal of cancer research*

Warburg, O., Wind, F. and Negelein, E. (1927) The metabolism of tumours in the body. *J Gen Physiol*

Wasa, M., Bode, B. P. and Souba, W. W. (1996) Adaptive regulation of amino acid transport in nutrient-deprived human hepatomas. *The American Journal of Surgery* **171**(1): 163-169.10.1016/s0002-9610(99)80093-2

Weinberg, F., Hamanaka, R., Wheaton, W. W., Weinberg, S., Joseph, J., Lopez, M., Kalyanaraman, B., Mutlu, G. M., Budinger, G. R. and Chandel, N. S. (2010) Mitochondrial metabolism and ROS generation are essential for Kras-mediated tumorigenicity. *Proc Natl Acad Sci U S A* **107**(19): 8788-8793.10.1073/pnas.1003428107

Weinstein, I. B. and Joe, A. K. (2006) Mechanisms of disease: Oncogene addiction--a rationale for molecular targeting in cancer therapy. *Nat Clin Pract Oncol* **3**(8): 448-457.10.1038/ncponc0558

Wellberg, E. A., Johnson, S., Finlay-Schultz, J., Lewis, A. S., Terrell, K. L., Sartorius, C. A., Abel, E. D., Muller, W. J. and Anderson, S. M. (2016) The glucose transporter GLUT1 is required for ErbB2-induced mammary tumorigenesis. *Breast Cancer Res* **18**(1).10.1186/s13058-016-0795-0

Wellen, K. E., Lu, C., Mancuso, A., Lemons, J. M., Ryczko, M., Dennis, J. W., Rabinowitz, J. D., Coller, H. A. and Thompson, C. B. (2010) The hexosamine biosynthetic pathway couples growth factor-induced glutamine uptake to glucose metabolism. *Genes Dev* **24**(24): 2784-2799.10.1101/gad.1985910

Wiesener, M. S., Jurgensen, J. S., Rosenberger, C., Scholze, C. K., Horstrup, J. H., Warnecke, C., Mandriota, S., Bechmann, I., Frei, U. A., Pugh, C. W., Ratcliffe, P. J., Bachmann, S., Maxwell, P. H. and Eckardt, K. U. (2003) Widespread hypoxia-inducible expression of HIF-2alpha in distinct cell populations of different organs. *FASEB J* **17**(2): 271-273.10.1096/fj.02-0445fje

Wilhelm, B. T., Marguerat, S., Watt, S., Schubert, F., Wood, V., Goodhead, I., Penkett, C. J., Rogers, J. and Bahler, J. (2008) Dynamic repertoire of a eukaryotic transcriptome surveyed at single-nucleotide resolution. *Nature* **453**(7199): 1239-1243.10.1038/nature07002

Wise, D. R., Deberardinis, R. J., Mancuso, A., Sayed, N., Zhang, X. Y., Pfeiffer, H. K., Nissim, I., Daikhin, E., Yudkoff, M., Mcmahon, S. B. and Thompson, C. B. (2008) Myc

regulates a transcriptional program that stimulates mitochondrial glutaminolysis and leads to glutamine addiction. *Proc Natl Acad Sci U S A* **105**(48): 18782-18787.10.1073/pnas.0810199105

Wise, D. R., Ward, P. S., Shay, J. E., Cross, J. R., Gruber, J. J., Sachdeva, U. M., Platt, J. M., Dematteo, R. G., Simon, M. C. and Thompson, C. B. (2011) Hypoxia promotes isocitrate dehydrogenase-dependent carboxylation of alpha-ketoglutarate to citrate to support cell growth and viability. *Proc Natl Acad Sci U S A* **108**(49): 19611-19616.10.1073/pnas.1117773108

Xiang, Y., Stine, Z. E., Xia, J., Lu, Y., O'connor, R. S., Altman, B. J., Hsieh, A. L., Gouw, A. M., Thomas, A. G., Gao, P., Sun, L., Song, L., Yan, B., Slusher, B. S., Zhuo, J., Ooi, L. L., Lee, C. G., Mancuso, A., Mccallion, A. S., Le, A., Milone, M. C., Rayport, S., Felsher, D. W. and Dang, C. V. (2015) Targeted inhibition of tumor-specific glutaminase diminishes cell-autonomous tumorigenesis. *J Clin Invest* **125**(6): 2293-2306.10.1172/JCI75836

Xiao, D., Ren, P., Su, H., Yue, M., Xiu, R., Hu, Y., Liu, H. and Qing, G. (2015) Myc promotes glutaminolysis in human neuroblastoma through direct activation of glutaminase 2. *Oncotarget* **6**(38): 40655-40666.10.18632/oncotarget.5821

Xu, D. and Hemler, M. E. (2005) Metabolic activation-related CD147-CD98 complex. *Mol Cell Proteomics* **4**(8): 1061-1071.10.1074/mcp.M400207-MCP200

Xu, J., Chen, Y. and Olopade, O. I. (2010) MYC and Breast Cancer. *Genes Cancer* **1**(6): 629-640.10.1177/1947601910378691

Xu, L., Fukumura, D. and Jain, R. K. (2002) Acidic extracellular pH induces vascular endothelial growth factor (VEGF) in human glioblastoma cells via ERK1/2 MAPK signaling pathway: mechanism of low pH-induced VEGF. *J Biol Chem* **277**(13): 11368-11374.10.1074/jbc.M108347200

Yamada, N., Honda, Y., Takemoto, H., Nomoto, T., Matsui, M., Tomoda, K., Konno, M., Ishii, H., Mori, M. and Nishiyama, N. (2017) Engineering Tumour Cell-Binding Synthetic Polymers with Sensing Dense Transporters Associated with Aberrant Glutamine Metabolism. *Sci Rep* **7**(1).10.1038/s41598-017-06438-y

Yanagida, O., Kanai, Y., Chairoungdua, A., Kim, D. K., Segawa, H., Nii, T., Cha, S. H., Matsuo, H., Fukushima, J.-I., Fukasawa, Y., Tani, Y., Taketani, Y., Uchino, H., Kim, J. Y., Inatomi, J., Okayasu, I., Miyamoto, K.-I., Takeda, E., Goya, T. and Endou, H. (2001) Human L-type amino acid transporter 1 (LAT1): characterization of function and expression in tumor cell lines. *Biochimica et Biophysica Acta (BBA) - Biomembranes* **1514**(2): 291-302.10.1016/s0005-2736(01)00384-4

Yang, C., Peng, P., Li, L., Shao, M., Zhao, J., Wang, L., Duan, F., Song, S., Wu, H., Zhang, J., Zhao, R., Jia, D., Zhang, M., Wu, W., Li, C., Rong, Y., Zhang, L., Ruan, Y. and Gu, J. (2016) High expression of GFAT1 predicts poor prognosis in patients with pancreatic cancer. *Sci Rep* **6**.10.1038/srep39044

Yang, L., Achreja, A., Yeung, T. L., Mangala, L. S., Jiang, D., Han, C., Baddour, J., Marini, J. C., Ni, J., Nakahara, R., Wahlig, S., Chiba, L., Kim, S. H., Morse, J., Pradeep, S., Nagaraja, A. S., Haemmerle, M., Kyunghee, N., Derichsweiler, M., Plackemeier, T., Mercado-Uribe, I., Lopez-Berestein, G., Moss, T., Ram, P. T., Liu, J., Lu, X., Mok, S. C., Sood, A. K. and Nagrath, D. (2016) Targeting Stromal Glutamine Synthetase in Tumors Disrupts Tumor Microenvironment-Regulated Cancer Cell Growth. *Cell Metab* **24**(5): 685-700.10.1016/j.cmet.2016.10.011

Yang, S., Hu, Y., Sokoll, L. and Zhang, H. (2017) Simultaneous quantification of N- and O-glycans using a solid-phase method. *Nat Protoc* **12**(6): 1229-1244.10.1038/nprot.2017.034

Yao, J., Maslov, K. I. and Wang, L. V. (2012) In vivo photoacoustic tomography of total blood flow and potential imaging of cancer angiogenesis and hypermetabolism. *Technol Cancer Res Treat* **11**(4): 301-307.10.7785/tcrt.2012.500278

Ying, H., Kimmelman, A. C., Lyssiotis, C. A., Hua, S., Chu, G. C., Fletcher-Sananikone, E., Locasale, J. W., Son, J., Zhang, H., Coloff, J. L., Yan, H., Wang, W., Chen, S., Viale, A., Zheng, H., Paik, J. H., Lim, C., Guimaraes, A. R., Martin, E. S., Chang, J., Hezel, A. F., Perry, S. R., Hu, J., Gan, B., Xiao, Y., Asara, J. M., Weissleder, R., Wang, Y. A., Chin, L., Cantley, L. C. and Depinho, R. A. (2012) Oncogenic Kras maintains pancreatic tumors through regulation of anabolic glucose metabolism. *Cell* **149**(3): 656-670.10.1016/j.cell.2012.01.058

Yoo, H., Antoniewicz, M. R., Stephanopoulos, G. and Kelleher, J. K. (2008) Quantifying reductive carboxylation flux of glutamine to lipid in a brown adipocyte cell line. *J Biol Chem* **283**(30): 20621-20627.10.1074/jbc.M706494200

Yoon, S., Lee, M. Y., Park, S. W., Moon, J. S., Koh, Y. K., Ahn, Y. H., Park, B. W. and Kim, K. S. (2007) Up-regulation of acetyl-CoA carboxylase alpha and fatty acid synthase by human epidermal growth factor receptor 2 at the translational level in breast cancer cells. *J Biol Chem* **282**(36): 26122-26131.10.1074/jbc.M702854200

Yoshimura, M., Nishikawa, A., Ihara, Y., Taniguchi, S. and Taniguchi, N. (1995) Suppression of lung metastasis of B16 mouse melanoma by N-acetylglucosaminyltransferase III gene transfection. *Proc Natl Acad Sci U S A* **92**: 8754-8758

Yuneva, M., Zamboni, N., Oefner, P., Sachidanandam, R. and Lazebnik, Y. (2007) Deficiency in glutamine but not glucose induces MYC-dependent apoptosis in human cells. *J Cell Biol* **178**(1): 93-105.10.1083/jcb.200703099

Yuneva, M. O., Fan, T. W., Allen, T. D., Higashi, R. M., Ferraris, D. V., Tsukamoto, T., Mates, J. M., Alonso, F. J., Wang, C., Seo, Y., Chen, X. and Bishop, J. M. (2012) The metabolic profile of tumors depends on both the responsible genetic lesion and tissue type. *Cell Metab* **15**(2): 157-170.10.1016/j.cmet.2011.12.015

Zhao, Y. H., Zhou, M., Liu, H., Ding, Y., Khong, H. T., Yu, D., Fodstad, O. and Tan, M. (2009) Upregulation of lactate dehydrogenase A by ErbB2 through heat shock factor 1 promotes breast cancer cell glycolysis and growth. *Oncogene* **28**(42): 3689-3701.10.1038/onc.2009.229

Zheng, L., Cardaci, S., Jerby, L., Mackenzie, E. D., Sciacovelli, M., Johnson, T. I., Gaude, E., King, A., Leach, J. D., Edrada-Ebel, R., Hedley, A., Morrice, N. A., Kalna, G., Blyth, K., Ruppin, E., Frezza, C. and Gottlieb, E. (2015) Fumarate induces redox-dependent senescence by modifying glutathione metabolism. *Nat Commun* **6**.10.1038/ncomms7001

Zheng, L., Zhang, W., Zhou, Y., Li, F., Wei, H. and Peng, J. (2016) Recent Advances in Understanding Amino Acid Sensing Mechanisms that Regulate mTORC1. *Int J Mol Sci* **17**(10).10.3390/ijms17101636

Zhou, R., Pantel, A. R., Li, S., Lieberman, B. P., Ploessl, K., Choi, H., Blankemeyer, E., Lee, H., Kung, H. F., Mach, R. H. and Mankoff, D. A. (2017) [(18)F](2S,4R)4-Fluoroglutamine PET Detects Glutamine Pool Size Changes in Triple-Negative Breast Cancer in Response to Glutaminase Inhibition. *Cancer Res* **77**(6): 1476-1484.10.1158/0008-5472.CAN-16-1945

Zhu, J., Xiong, G., Trinkle, C. and Xu, R. (2014) Integrated extracellular matrix signaling in mammary gland development and breast cancer progression. *Histology and histopathology.* **29**(9): 1083-1092.

Zielke, H. R., Collins, R. M., Baab, P. J., Huang, Y., Zielke, C. L. and Tildon, J. T. (2002) Compartmentation of [14C]Glutamate and [14C]Glutamine Oxidative Metabolism in the Rat Hippocampus as Determined by Microdialysis. *Journal of Neurochemistry* **71**(3): 1315-1320.10.1046/j.1471-4159.1998.71031315.x